Synthesis of Triazole-Linked Chloroquinoline Derivatives as Novel Antimalarial Agents

Lebusetsa Taleli

A Thesis submitted to the Faculty of Natural Science,

Department of Chemistry and Polymer Science

University of Stellenbosch

In partial fulfilment of the requirements for the Degree of Master of Science in Chemistry

March 2013

Declaration

I declare that the work presented in this thesis represent my own work that was carried out by myself under the supervision of Professor W.A.L van Otterlo. It is being submitted for the degree of Master of Chemistry in the University of Stellenbosch and the thesis has not been submitted previously for the academic examination towards any qualification. The thesis represents my own opinions and not necessarily those of the Stellenbosch University.

_____

March 2013

Abstract

Aminoquinolines are important class of drugs that have been used for malaria chemotherapy for centuries. However, long-term exposure to these drugs leads to extensive spread of drug resistance. As such, modified chloroquinoline derivatives are being studied as alternative antimalarial agents with the possibility to overcome drug resistance associated with chloroquine analogues.

In this study, 15 aminoquinoline derivatives that are linked by a 1,4-disubstituted 1,2,3-triazole ring to an ethyl and propyl carbon spacer with a distal amine motif were designed and synthesized as novel antimalarial agents using the Cu(I)-promoted Huisgen reaction. The compounds have been synthesized from the 7-chloro-*N*-(prop-2-yn-1-yl)quinolin-4-amine alkyne precursor and the azides of ethyl and propyl amino moieties using a 1,3-dipolar cycloaddition-coupling in the presence of CuI catalyst to obtain moderate to good yields (53 – 85%). These compounds have been characterized by the combination of NMR, ESI^+ HRMS and IR spectroscopic methods.

The antiplasmodial activity of the compounds was investigated *in vitro* against *P. falciparum* strain NF54 using chloroquine as a reference drug together with a standard antimalarial drug artesunate. Of the 15 novel chloroquinoline derivatives, 11 have demonstrated to possess promising potency by way of the inhibition concentrations less than 250 nM with the lowest being 28 nM. The observed activities have been ascribed to the overall modifications such as the introduction of a triazole linker and changing of carbon chain length as these were the variables. The compounds are accordingly under further biological investigations and only the chloroquine sensitive results are reported in this work.

Acknowledgements

I listened to Albert Einstein telling me, “Any man who can drive safely while kissing a pretty girl is simply not giving the kiss the attention it deserves.” I could have not done this work without the following contributions;

First and foremost, I thank my supervisor Professor Williem van Otterlo for his sterling guidance in this work, but most importantly for your inconvenient time schedule that you have spent reading and making the incisive comments about this thesis. These have played a significant role both in shaping the content and the presentation of my arguments in this work.

I extend my gratitude to the co-supervisors, Dr Margaret Blackie and Dr Stephen Pelly, whose efforts are highly distinguished with gratefulness. Dr Blackie, with whom the biological investigation of our target compounds have had valuable results and Dr Pelly for the important discussions that have made me learn.

The labwork would have not been better without the Group of Organic and Medicinal Chemistry. I thank everyone especially the colleagues in 2020 & 2021; Mohammed Hassam, Abu Taher, Tanya Mabank, Leandi van der Westhuizen, Ronnel Muller and Jaco de Jagger whom we have shared joy and cheerlessness.

To my family, the support and courage that I ever receive, stimulates me daily. To my friends and brothers, Tiro your hospitality and warm welcome into the Cape has been tremendous, and Kebitsamang thanks for the Chinese talents.

To Else Malherbe, Dr Jaco Brand for running my uninterrupted NMR samples, you ever tireless NMR spectra analysis has been very valuable. To Dr Marietje Stander and Hiten Fletcher, the mass spectral analysis of my samples has also been great. To Raymond and Mary, I thank you for your unfailing support in the lab.

I also thank the NRF for the financial assistance that has made this study possible, without the support this work would have been a dream. To the Stellenbosch University, I extend my

gratitude for studying with you. Thanks to the Pharmacology division of the University of Cape Town for the biological evaluation of the compounds.

Big thanks to Yahew.

Table of Contents

Chapter 3

Chapter 4

Chapter 5

Supplementary information

List of figures

List of tables

Preface

Thesis layout

This thesis is divided into five chapters. The first chapter consists of the background introduction to the impact of the disease malaria, then motivates and explains why the research question as to why synthesizing structurally novel aminoquinoline antimalarial drugs is important. The research objectives that this work is intended to achieve have been listed in this chapter.

The second chapter is a review of the previous research work in the subject research area related to antimalarial drugs and chemotherapy but leans towards the aminoquinoline drugs which are more significant in this study. The basic antimalarial biology of chloroquine analogues, an aminoquinoline derivative has been added to stress the importance of current understanding of drug resistance and developing the alternative antimalarial agents in an effort to overcome drug resistance.

The third chapter specifically discusses and analyses the successes and failures that have been encountered in the course of this work. It elaborates on the important experimental findings which which are in line with this work, mainly the chemistry of the synthetic work. The biological study performed in this work was intended to assess the potential of the synthesized compounds to inhibit the antimalarial activity and as such the discussion of antimalarial activity has been catered for in brief, and not to primarily formulate the biological reasons for the outcome.

The fourth chapter gives the summary and a conclusion of this study finding, the limitations of the methods employed, and suggests the implications based on the obtained results. Finally, the last chapter gives the detailed experimental methods as well as the spectrometric data collected during the analyses.

Numbering of captions and interpretations of spectroscopic data

Due to a variable number of figures per subtitle, the captions for figures and tables have the extended digit that displays the count of the figure or a table. The numbering of atoms in the

chemical structures is unconventional but the same numbering sequence has been maintained for the spectral references of the compounds.

Chapter 1

Brief background introduction and research objectives

1.1 Background introduction

The disease malaria is a haematozoan infection caused by sporozoites, transmitted by female *Anopheline* mosquitoes.[1] It is a pernicious and most deadly parasitic infection whose impact ranks it the second cause of death in the African continent, after HIV/AIDS related infections. In addition, it is globally a leading cause of morbidity and mortality,[2] mainly in the tropical and subtropical regions where this disease is endemic. It is now over a century since a Nobel laureate Robert Ross, in his pioneering work of malaria parasite transmission, considered malaria as a "million-murdering death"[3] and today the disease continues to wreak havoc on millions annually. In 2010, the human burden caused by malaria approximated 216 million episodes in different territories around the world with most occurrences in sub-Sahara Africa affecting children without a protective immunity.[4]

The nature of the burden caused by the disease malaria is a result of diversity in the parasite host species (*Plasmodium falciparum, P. vivax, P. malariae, and P. ovale* and *P. knowlesi*) that are responsible for the human malaria.[5-6] Among these species, *P. falciparum* is responsible for the lethal human malaria; obstruction of the blood vessels of vital organs, premature delivery of infants, and the worst problem of developing resistive genetic mutations to antimalarial drugs.[7-8] The emergence and spread of resistant parasite is a therapeutic challenge that has undermined generations of antimalarial drugs and the current grim death rate statistics could even rise higher should the resistance to the existing drugs develop further. The life-cycle of malaria causing parasites and their developmental stages are complex, each with a preferred cell-target in different hosts such as mosquitoes and humans or macaques, and thus creates a challenge in the management, control and elimination of the infection.[9]

The reason for the continued survival of the *Plasmodium* parasites against antimalarial drugs lies in their genetic adaptability. The parasites have selective advantage mechanisms over drugs which are not fully understood, but certainly the parasite undergoes sexual recombination, a process of genetic cross-over that results in the offspring having different combinations of genes from those of their parents.[10] This meiotic recombination process results in 'genetic mutations' that make parasites less sensitive to antimalarial drugs.[11] Clinical experience and experimental evidence

indicates that drugs are generally effective when first introduced; however, their efficacies are curtailed by the emergence of resistant parasites. Coupled to the ever-present problem of controlling the disease vectors, is the lack of an effective vaccine. The problem has stimulated investigators to overturn the continuously evolving resistant parasites by developing analogues of once-effective and well-established antimalarial drugs, in addition to the identification of novel drug targets.

Despite the long-standing global efforts to eliminate malaria,[12] no new classes of antimalarial drugs have been introduced into clinical practice since artemisinin combination therapy (ACT). Traditionally, antimalarial agents have been classified by the stages that are targeted by the drugs in the parasite's life-cycle, but to date the chemotherapy arsenal represents three main structural categories, namely, quinolines, antifolate and artemisinin derivatives (**figure 1.1.1**). The primary discovery of antimalarial drugs began with the alkaloids comprised of a quinoline motif. Since then, quinoline derivatives such as the aminoquinolines, quinoline-methanols, acridines and others have evolved from these initial structures. The antifolate is a different class that encompasses mostly sulfur-containing and aminopyrimidine antimalarial drugs. Finally, the artemisinin derivatives are sesquiterpene lactone endoperoxides, and currently the World Health Organisation (WHO) "gold standard" drugs of malaria therapy.

The heterocyclic compounds with a quinoline motif are versatile, with a wide range of pharmacological activities and continue to be useful for antimalarial drug discovery. They have been a cornerstone for the synthesis of active antimalarial drugs for several decades and effective antimalarial drugs such as chloroquine (CQ), mefloquine (MQ), amodiaquine (AQ), pamaquine (PamQ) and others have been developed (refer to **figure 1.1.1a**).[13] The essence of drug resistance has had a paradigm shifting effect in defining the molecular basis of antimalarial drug resistance and its relationship to therapeutic failure as guidance to design new effective antimalarial agents. The aminoquinoline moiety is the key pharmacophore on which the attachment of various ionizable amino side-chains have shown to enhance activity via increasing basicity, possible pH trapping, or as CQ resistance reversal motifs in CQ analogues.

a) Quinoline-based antimalarial agents

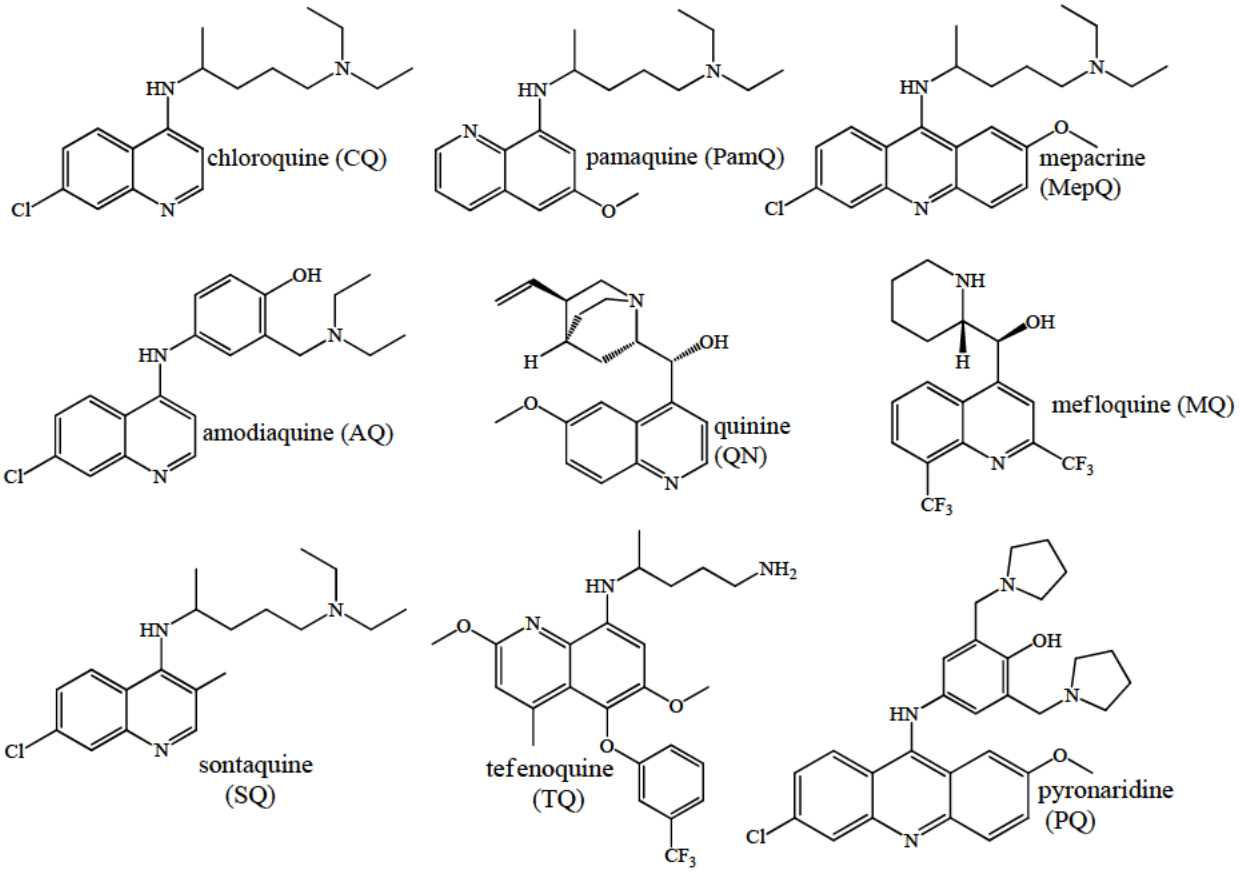

b) Antifolate antimalarial agents

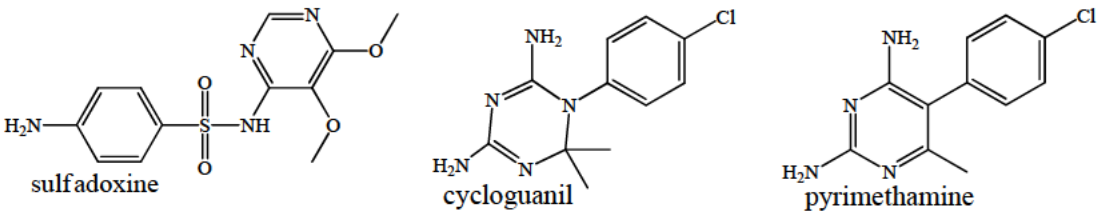

c) Sesquiterpene lactones

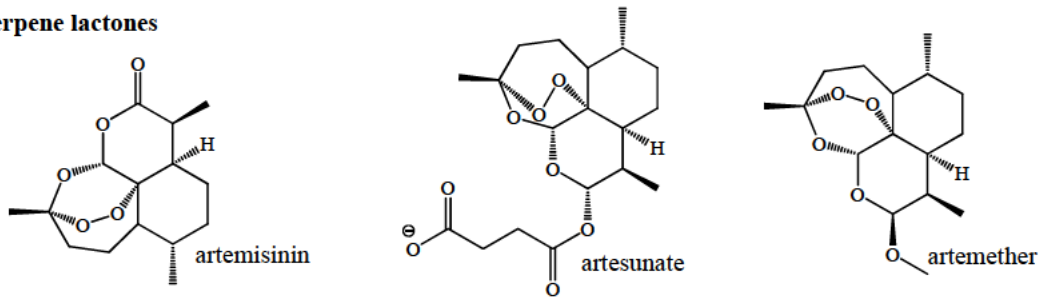

Figure 1.1.1 Three main categories of antimalarial drugs and examples thereof.

In a response to a burdensome challenge posed by malaria, the importance of generating new antimalarial drugs and maximizing therapy by improving the physicochemical properties of drugs cannot be overemphasized. A design based on the structure activity relationship (SAR) has reignited interest in discovering novel antimalarial agents by identifying discrete molecular components with recognition at a given target.[13-14] In the process, the biological activity of potent antimalarial drugs is enhanced by the addition or repositioning of functionalities on a molecular fragment. The synthetic organic chemistry of antimalarial drugs was overturned in the late 19th century after William Henry Perkin commenced to synthesise QN in 1856, but failed and the first total synthesis of quinine was accomplished almost a century later in 1944.[15] The end synthetic chemistry of QN was found to be complex for commercial use and, even to this day, has not been accomplished on an economic scale.

The addition of an alkylamine side chain functionality to quinoline scaffolds in designing aminoquinoline antimalarial drugs was a result of Paul Ehrlich's work in using haematological stains to diagnose blood diseases, including malaria itself.[16] He observed that a synthetic dye, methylene blue (**figure 1.1.2)**, was effective in staining and poisoning malaria parasites. Ehrlich's intensions to enhance stain visibility led to the preparation of methylene blue analogues with alkylamine chains, in addition, the analogues were found to possess better antimalarial activity.[16-17] On the basis of these observations, the alkylamine chain was viewed as beneficial for the antimalarial activity and thus the invention of potent antimalarial drugs were discovered through addition of alkylamine side chains on different quinoline scaffolds, most notably by the chemists at Bayer (this process is described schematically in **figure 1.1.2**).[8,16,18] Nonetheless, it was only after the 2002 unveiling of the *P. falciparum* genome in a joint global effort led by the Wellcome Trust Sanger Institute,[19] that many intricate details about *P. falciparum* drug resistance were obtained and significantly provided an opportunity to challenge therapeutic resistance with modified CQ analogues.

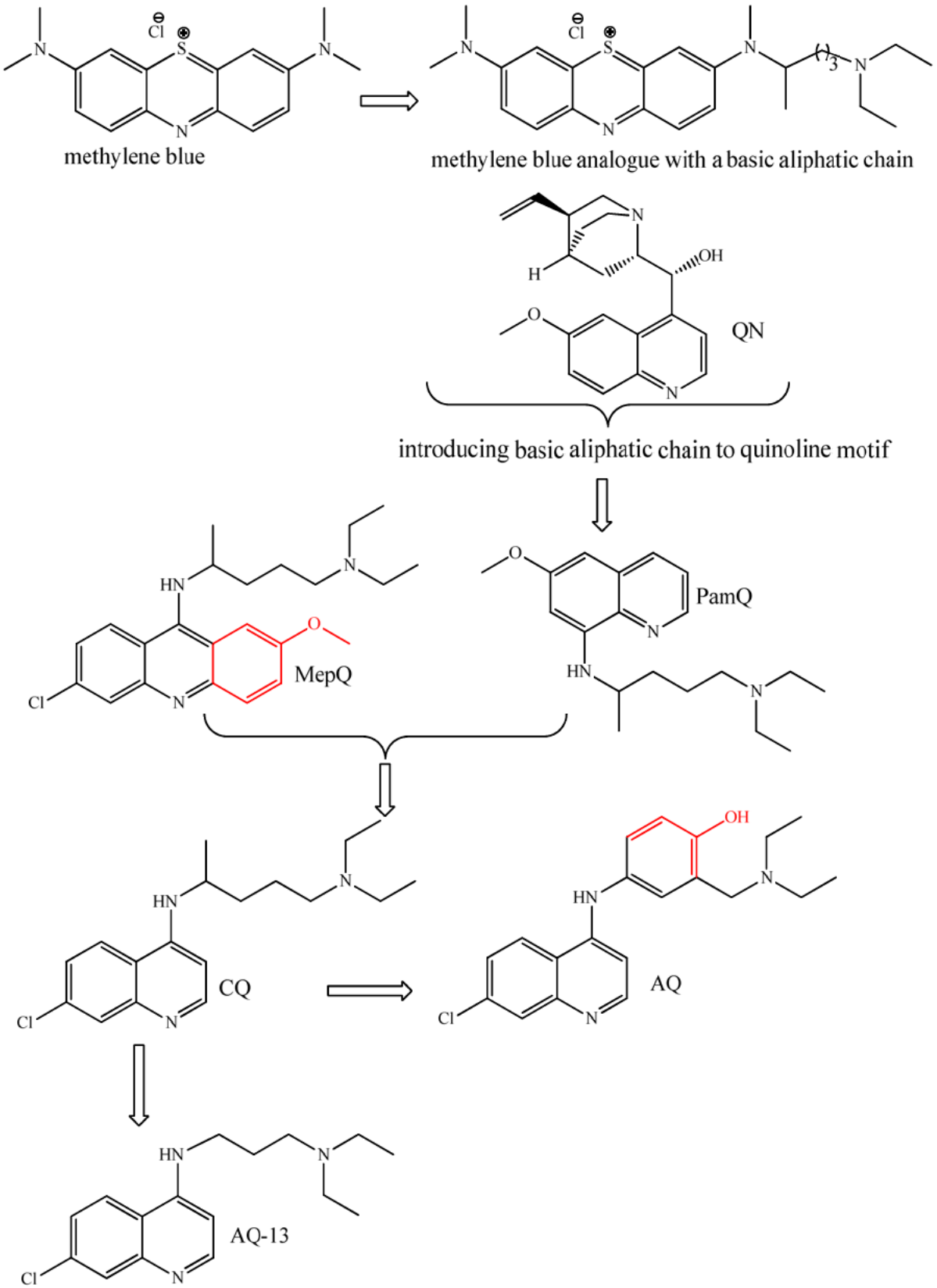

Figure 1.1.2 Historical perspective of aminoquinoline drugs discovery.

1.2 Research objectives

The structural function of quinoline antimalarial drugs remains definitively demonstrated. Recent short chain analogues of CQ have suggested chain variation as a recognition motif to overcome CQ resistance, explained in detail later in the thesis. The lateral amine functionality is another distinctive feature that has the ability to "reverse" CQ resistance. In general, modifications on the alkylamine side chain can be viewed as a feasible prospect to overcome the acquired parasite drug resistance to aminoquinoline agents. The application of click chemistry for the formation of a triazole-linked quinoline system, which possesses metabolic stability, to the lateral alkylamine chain is therefore justified. The perspectives for triazole-linked compounds stand on the threshold of the new era and the reported triazole pharmacological activity in various bioactive molecules is also remarkable.

Our particular study is intended at developing potent antimalarial agents through syntheses of new molecular entities that are structurally unrelated to CQ or AQ on the lateral side chain. Thus, we aimed at the creation of a small library of triazole-linked chloroquinoline derivatives having a short alkyl chain bearing amino functionalities and determination of the SAR for these modifications. The derivatives are characterized by an aminoquinoline ring that is linked by a 1,4-disubstituted 1,2,3-triazole to an ethyl and/or propyl spaced tertiary amino moiety (**figure 1.2.1)**. The work intends to use a Huisgen-Meldal-Sharpless reaction in creating a covalent triazole linkage of two molecular units by means of copper(I)-accelerated azide-alkyne 1,3-cycloaddition (CuAAC). This synthetic method tolerates various functionalized aminoalkyl azides to be integrated with the aminoquinoline parent compound and gives a broader structural horizon for exploring basic amines with the possibility of overcoming CQ resistance.

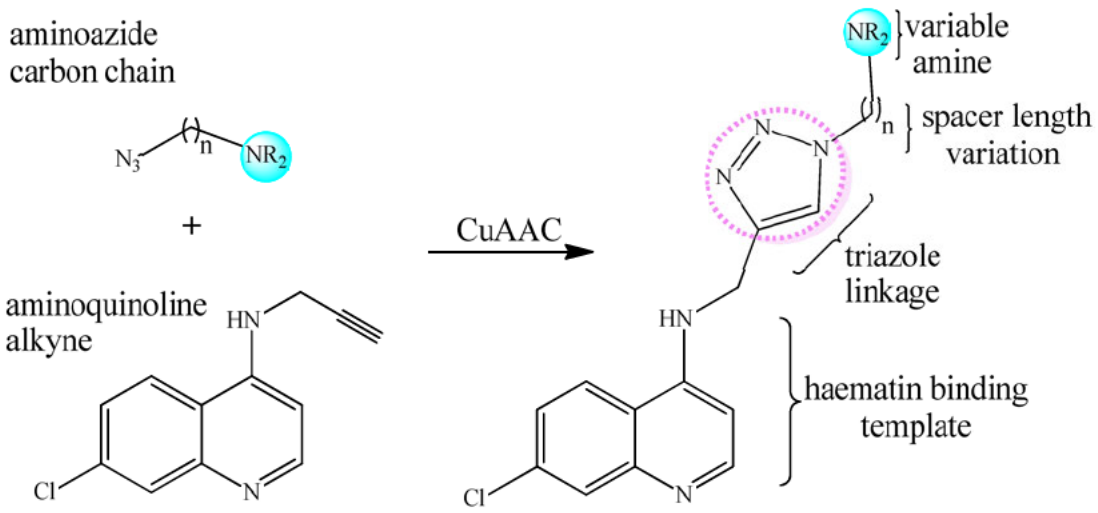

Figure 1.2.1 A representative structure for a library of triazole-linked CQ derivatives

The study explores the use of small amine functionalities such as diethylamine, metabolically stable cyclic amines (i.e. piperidinyl, pyrrolidinyl and morpholinyl)[20] and some bulkier aromatic amines. Some of the latter analogues have been demonstrated to possess the ability to inhibit the efflux transport of drugs in multi-drug resistance diseases;[21-22] as such their chemical structures are revealed in the next chapters to follow.

The following objectives for this study were therefore formulated;

- To synthesize the 7-chloro-*N*-(prop-2-yn-1-yl)quinolin-4-amine alkyne precursor, azides of ethyl amino and propyl amino moieties suitable for the triazole formation.
- To synthesize 1,4-disubstituted 1,2,3-triazole-linked chloroquinoline derivatives using the CuAAC reaction.
- To determine the antiplasmodial activity of the above synthesized compounds *in vitro* against *P. falciparum* strains.
- To compare the respective antimalarial activities to that of the conventional antimalarial drug CQ.

In the light of these objectives, the main theme of this work involves organic synthesis of the aminoquinoline alkyne, the aminoalkyl azides functionalized with a basic tertiary amine, and to

carry out the 1,3-cycloaddition of azides and alkyne promoted by CuI. The *in vitro* antimalarial activity investigations of the synthesized compounds should further assist in determining the SAR and the application of triazole moiety in the future development of antimalarial agents of chloroquinoline analogues. Should the introduction of a triazole linker be an important strategy in the modification of chloroquinoline analogues, it would follow that this moiety can critically influence pharmacologic bioavailability and potentially reverse CQ resistance. The synthesized compounds might have potent antimalarial activity, although it should not be ignored that the compounds can inhibit resistance mechanisms by some, as yet unidentified, protein interactions that are involved in the efflux of drugs by the malaria parasite.

After the short introduction provided in this section, the next chapter will give a more “in-depth” look of aminoquinoline derivatives and various strategies involved in their use as antimalarials.

Chapter 2

Literature review: Antimalarial activity of aminoquinoline derivatives, chemotherapeutic treatment of malaria and the synthesis of antimalarial agents.

2.1 Molecular mechanisms of action for CQ analogues and resistance

The exogenous supply of amino acids from haemoglobin degradation is absolutely essential for the parasite growth and survival. In the degradation process, toxic haematin moieties are generated as by-products and are removed by polymerization into an inert haemozoin.[23-25] The haem accumulation is induced by the CQ analogues that bind to haematin moieties leading to inhibition of haemozoin formation.[19] This inhibition of haematin polymerisation vitally sensitises the parasite and the antimalarial activity is subsequently manifested. Unlike other drug targets, haematin polymerisation process is non-enzymatic and the drug target remains vulnerable to drug's bioavailability.[26] The aminoquinoline target, haem-detoxification has been extensively studied, and continues to remain the most attractive area for developing 4-aminoquinoline antimalarial agents.[25,27]

CQ accumulation in the parasite's digestive vacuole (DV) might occur via ion trapping, in other words, a passive diffusion of a basic CQ across the pH gradient into the acidic vacuole or binding to active transporters such as ATP or CQ receptors.[28] In the DV, CQ becomes membrane impermeable after *di*-protonation (CQ^{2+}) and complexes with the intra-vacuolar free haematin or ferriprotoporphyrin IX (FP) receptor and thus inhibits the formation of crystalline haemozoin. The resistance of CQ is considered to be modulated by the protein membrane transporters such as P. *falciparum* CQ resistance transporters (PfCRT) or ATP-dependent P-glycoprotein homolog-I (Pgh-1) pumps which decrease drug concentration by way of drug efflux mechanisms.[29-30] In addition, biochemical data in the literature indicates that resistance to CQ is a multi-genetic phenomenon and affects drug accumulation in the parasite's food vacuole.[17,31]

The molecular mechanisms of CQ resistance have remained enigmatic and theoretical models adopting reduced drug accumulation in the DV or carrier-mediated efflux have received much attention. The present evidence reveals that CQ resistance is primarily linked to an increased drug's efflux as a result of mutations in the metabolite transporter of *P. falciparum* (PfCRT). PfCRT is a membrane localized protein in the parasite's digestive vacuole which is associated with the drug's efflux from the site of action in the parasite's DV.[32-33] The key role of PfCRT in CQ resistance is beyond dispute[34] and studies confirming the point mutations in this gene as

primary determinants of cross-resistance on various antimalarial drugs has been established.[35] The molecular mechanism of CQ mode of action and resistance mechanism is summarized in **figure 2.1.1** adapted from the literature.[28]

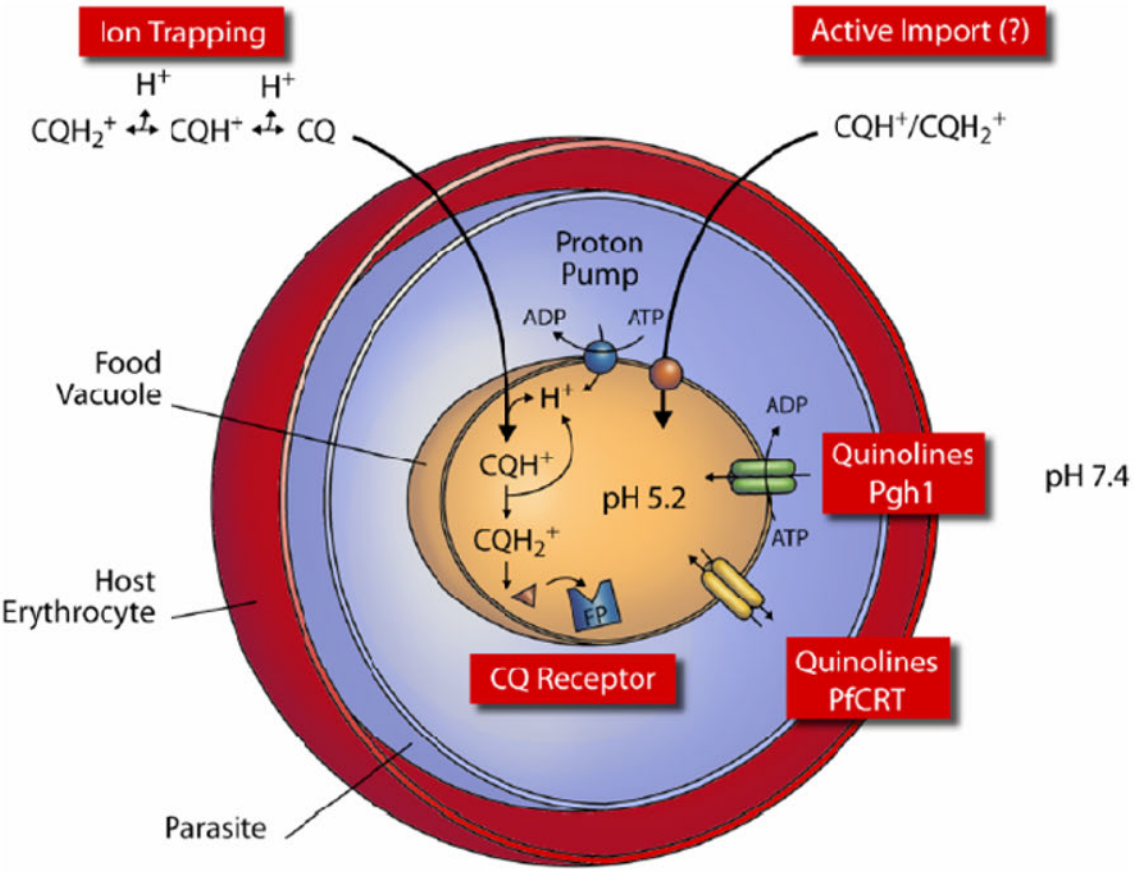

Figure 2.1.1 Proposed molecular mechanisms for CQ mode of action and resistance.[28]

2.2 Structure function relationships in CQ derivatives

The SAR of 4-aminoquinolines has been extensively elucidated in an attempt to restore antimalarial efficacy and overcome drug resistance. To this end, synthetic medicinal chemistry has developed a shortened-chain series of CQ analogues, organometallic antimalarial agents and also the hybrid antimalarial drugs, see **figure 2.2.1**. These classes of compounds have established the crucial role of the 7-chloro-4-aminoquinoline ring as well as the lateral side chain nitrogen for the antimalarial activity.[24,36] The significance of alterations on the lipophilic carbon chain of CQ

analogues has also led to new analogues with improved efficacy and compounds which do not exhibit *in vivo* cross-resistance with CQ against *P. falciparum*.[37-38]

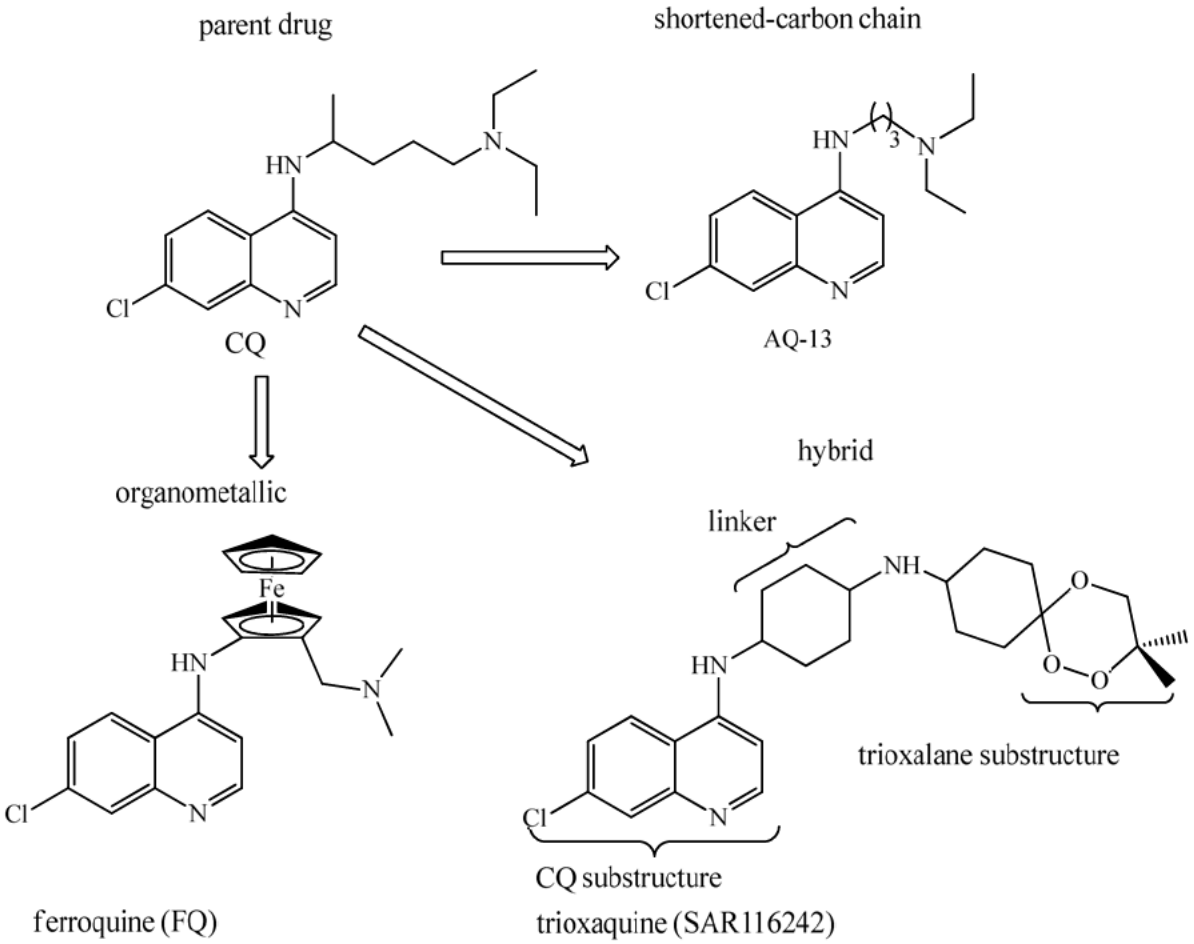

Figure 2.2.1 Shortened carbon chain series of CQ analogues that are active against CQ resistant *P. falciparum* strains.

AQ-13 (refer to above **figure 2.2.1**) is an example of a short chain 4-aminoquinoline antimalarial drug that has undergone Phase I clinical trials and progressive dose-finding Phase II (efficacy) studies which are estimated to be complete by March 2013 in Mali.[39]

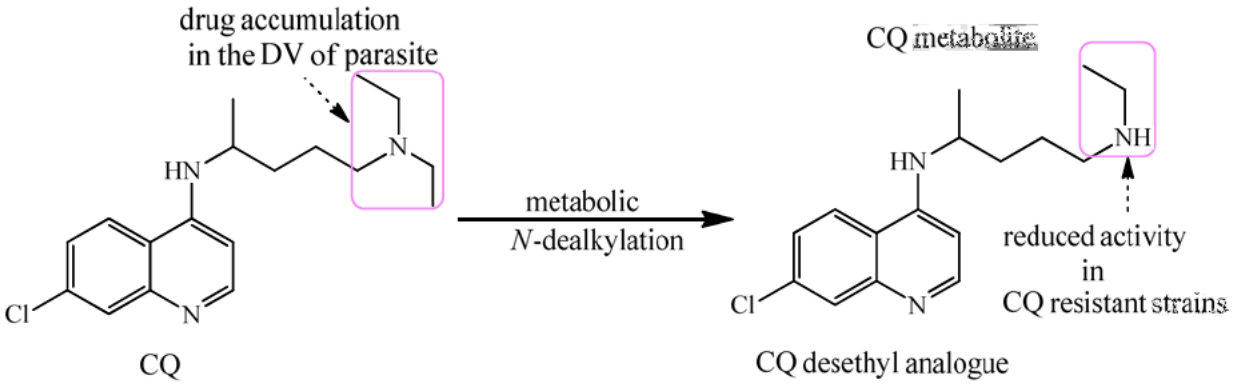

Figure 2.2.2 Metabolic *N*-dealkylation of CQ antimalarial drug.

Of note is that CQ undergoes *in vivo* metabolic *N*-dealkylation and is transformed into a CQ metabolite (refer to **figure 2.2.2**) that has the same efficacy as CQ against sensitive *P. falciparum* strains except for the reduced activity in CQ resistant strains.[40] AQ-13 has a similar metabolism to CQ but its modest activity against the MDR *P. falciparum* is believed to circumvent the parasite resistance mechanism as a result of reduced carbon chain length.[38,41] The *in vivo* *N*-dealkylation and increased plasma clearance are key problems with this CQ analogue, but the replacements of the distal diethylamine with *N*-heterocyclic structures (i.e. piperidinyl, pyrrolidinyl, and morpholinyl groups) in AQ analogues is known to result in compounds that are metabolically stable to dealkylation and increased antimalarial activity (refer to **figure 2.2.3**).[20] Of additional interest is that a large number of antimalarial drugs, for instance mefloquine and amopyroquine, having the *N*-heterocycle ring as part of their chemical structures, have potent antimalarial activity.

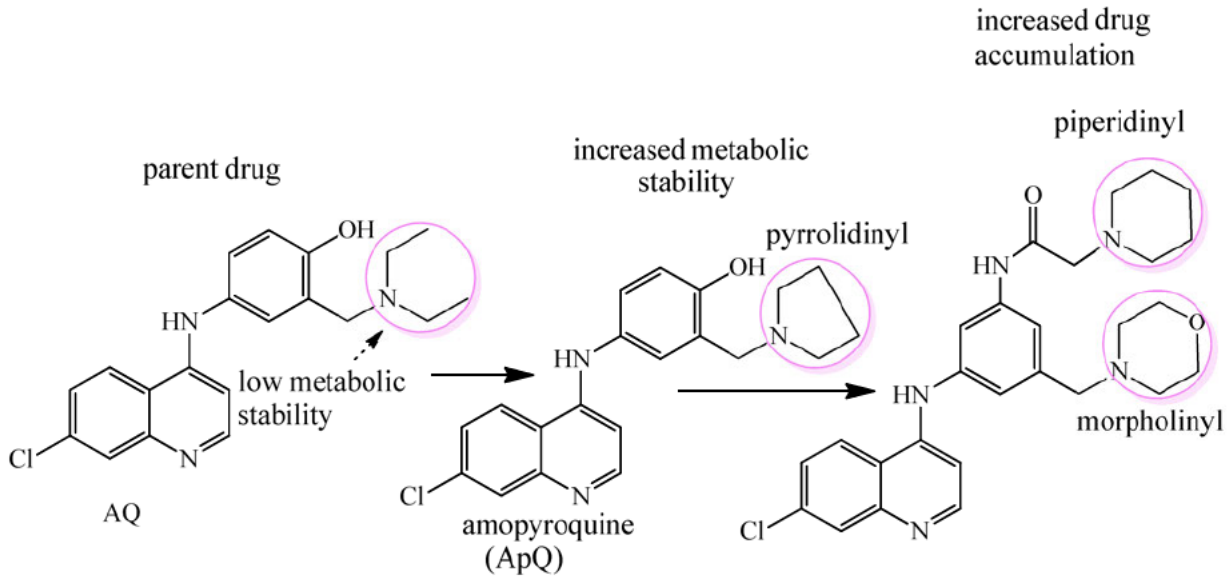

Figure 2.2.3 Increasing metabolic stability and bioavailability of CQ analogues.[27]

Another interesting rigid and more lipophilic CQ derivative is the antimalarial drug AQ with a 4-aminophenol linker joining chloroquinoline with an *N*-diethylamine short side-chain. This drug has been established as a superior alternative to CQ for the treatment of malaria infection in areas of high CQ resistance, see **figure 2.2.4**.[42] AQ has a similar profile to CQ's mechanism of action, but unfortunately, *in vivo* formation of toxic quinoneimine metabolites such as AQ metabolite 2, which is associated with liver toxicity and reduction of white blood cells, has severely restricted the clinical use of this promising candidate.[22] Metabolic *N*-dealkylation of AQ further reduced the lipid solubility and increased cross-resistance with CQ.[43-44]

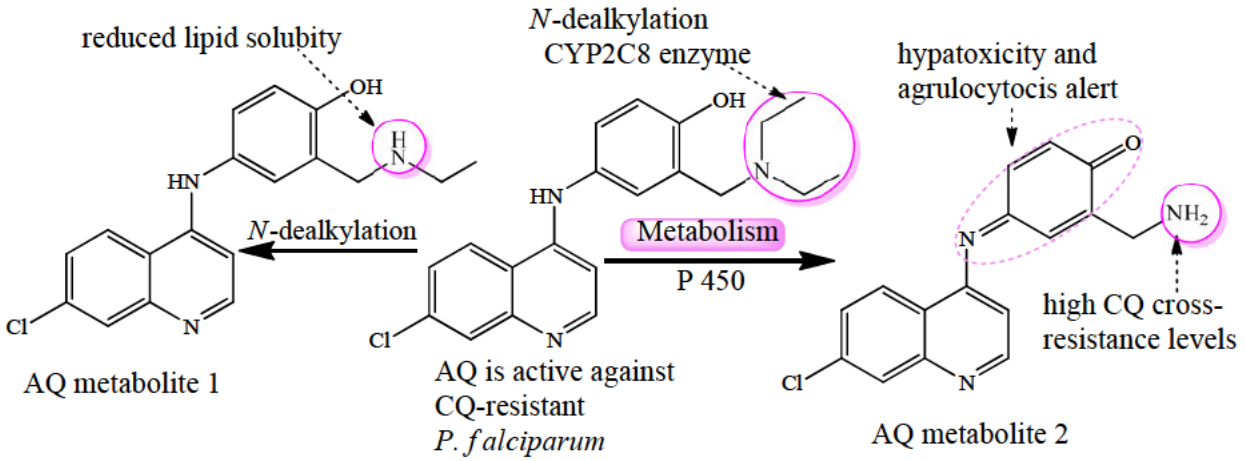

Figure 2.2.4 AQ, a CQ derivative metabolic transformation and toxicity.

From the chemistry point of view, the major limitation of the AQ drug's potential is the inherent structural toxicity of the *p*-aminophenol linker that is subsequently transformed into a reactive quinoneimine (see AQ metabolite 2 on **figure 2.2.4**). The majority of the toxic effects are associated with the formation of covalent immunogenic aryl protein conjugates known to occur with interactions with the reactive quinoneimine metabolites.[45] The isosteric replacement of the 4-aminophenol fragment with a piperazino or phenyl linker has been demonstrated to result in compounds with improved safety profile, observed during the formulation of hybrid molecules by Kumar and co-workers.[46-47] A recent study has also demonstrated that benzyl-linked CQ derivatives of 4-aminoquinoline utilised in a tandem with a reversal agent, result in the improved antimalarial activity against CQ resistant parasites and also the ability to inhibit the efflux action of PfCRT.[48] Of importance is that these latter benzyl-linked CQ analogues have been alleged to be the first reversed-CQ antimalarial agents to inhibit haemozoin formation and CQ resistance mechanisms *in vivo* (refer to structures in **figure 2.2.5**).[48-49]

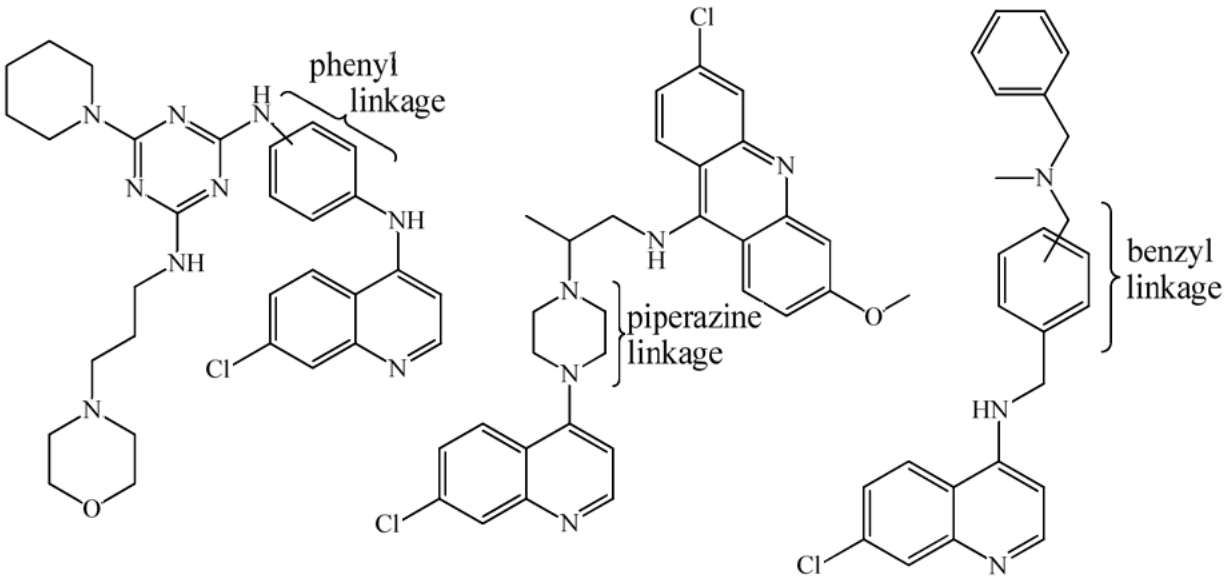

Figure 2.2.5 Linker variants in reversed CQ resistance compounds.[46-48]

2.3 Reversed CQ resistance compounds

The multi drug resistance (MDR) in CQ analogues is associated with reduced drug uptake that is caused by enhanced drug efflux but this process can be mechanistically reversed by chemosensitizers.[21] The chemosensitizers, also known as the reversal agents, have the capability of inhibiting certain lysosomal functions by disrupting accumulation-efflux mechanisms, and CQ resistance by PfCRT is thus reversible via these mechanisms.[21,50] Imipramine and verapamil (**figure 2.3.1**) are amongst the better-studied PfCRT reversal agents, but have not been embraced for clinical use because their co-administration to potentiate efficacy require unacceptably high clinical doses.[23,51] The clinical value of CQ sensitizers has also been impaired by their profound antipsychotic, antihistaminic, or cardiovascular effects.[51]

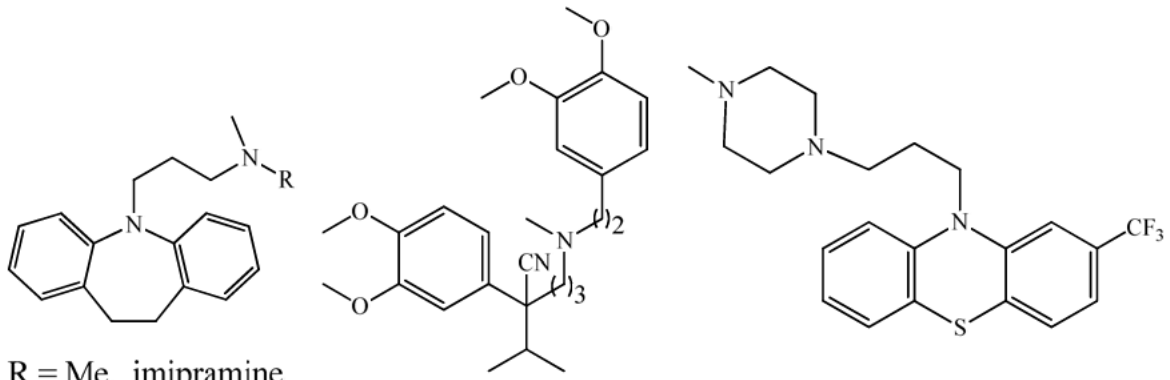

Figure 2.3.1 Some known chemosensitizers for CQ resistance reversal.

The CQ derivatives with bulkier and more lipophilic amino substitutions at the distal amino group have also been demonstrated to show remarkable efficacy against CQ resistant *P. falciparum* strains.[22] Several structurally diverse motifs that are known to aid or partially inhibit the PfCRT efflux mechanism have been identified as important components of reversal agents (in fact, some are structural analogues of reversal agents) and these are shown in **figure 2.3.2**.[52] Of interest is that these particular pharmacophores have demonstrated abilities to act as direct inhibitors of PfCRT when linked to a 7-chloroquinoline ring.[49] The primary requirement of a reversal agent is to inhibit efflux and to enhance build-up of a CQ derivative in the parasite's DV. The latter assignment to a reversal agent does not necessarily require a direct interaction with an efflux

effector, but the reversed-CQ molecule could have a lower binding to such transporters so that a reduced binding could lead to a higher drug accumulation.

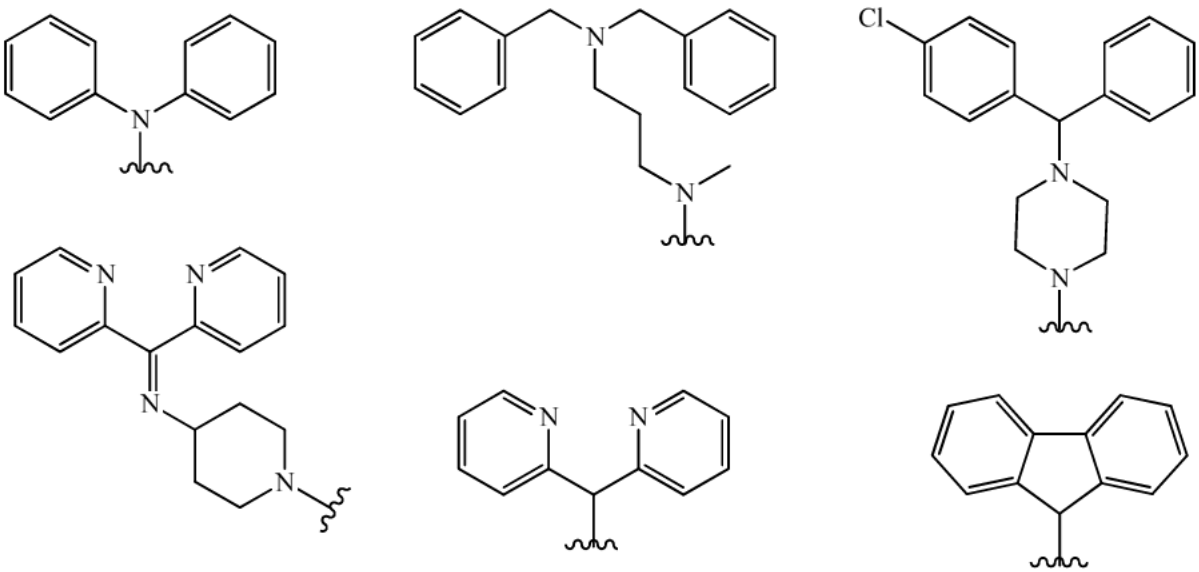

Figure 2.3.2 Structural motifs recognised as CQ reversal agents.

2.4 Chemotherapy of malaria

Humanity has possessed the tools to tackle malaria for centuries, in fact even preceding the discovery of quinoline-containing pharmacophores in 1820s and before, the causative organisms of the disease were identified.[53] Quinine (QN) and other *cinchona* alkaloids were the first active ingredients to be used against human malaria[54] which made malaria the first human disease to be controlled by a pure chemical,[53] thus chemotherapy has been a reliable option for malaria control ever since. QN, a quinoline derivative, finds application in the intravenous treatment of uncomplicated malaria although it has been recently superceded by the drug artesunate.[55-57] Due to clinical resistance, the monotherapeutic use of QN has been discontinued and a combination therapy with antibiotics such as tetracycline, doxycycline or clindamycin (see structures in **figure 2.4.1**), is now preferred for the treatment of uncomplicated malaria.[73-74]

Antimalarial drugs

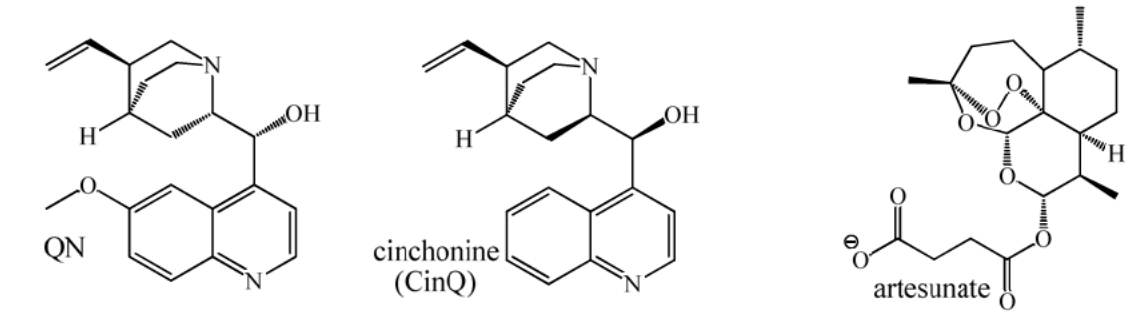

Antibiotics

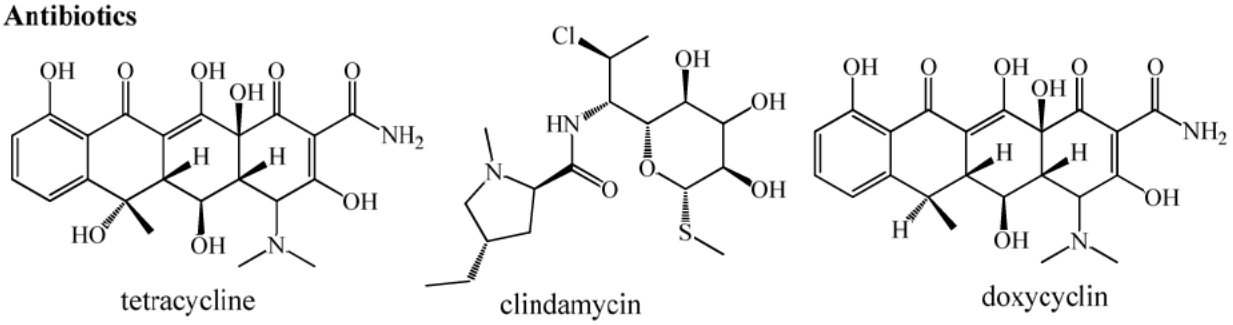

Figure 2.4.1 Antimalarial drugs and a number of antibiotics used for antimalarial combination therapy.

The initial practice of applying clinical combinations of sulfadoxine, mefloquine and pyrimethamine (see chemical structures in **figure 2.4.2**) was developed in Thailand, with the specific intention to delay the onset of resistance to mefloquine; unfortunately these combinations failed to have the desired effect.[58-59] The main reasons for the failure were the significant pharmacokinetic variations of individual drugs, such as absorption and distribution, metabolism, concentration achieved in the body, and subsequent elimination of the compounds. A pyrimethamine-sulfadoxine combination was, by then, coincidentally used in Africa (Malawi) to treat CQ resistant *P. falciparum* malaria. The rates of accelerated recoveries and reduced parasite transmission results were astonishing; however, a prolonged use this particular combination of compounds showed a decrease to 21% of the original efficacy and finally failed to prevent the emergence and spread of drug resistance.[60-61]

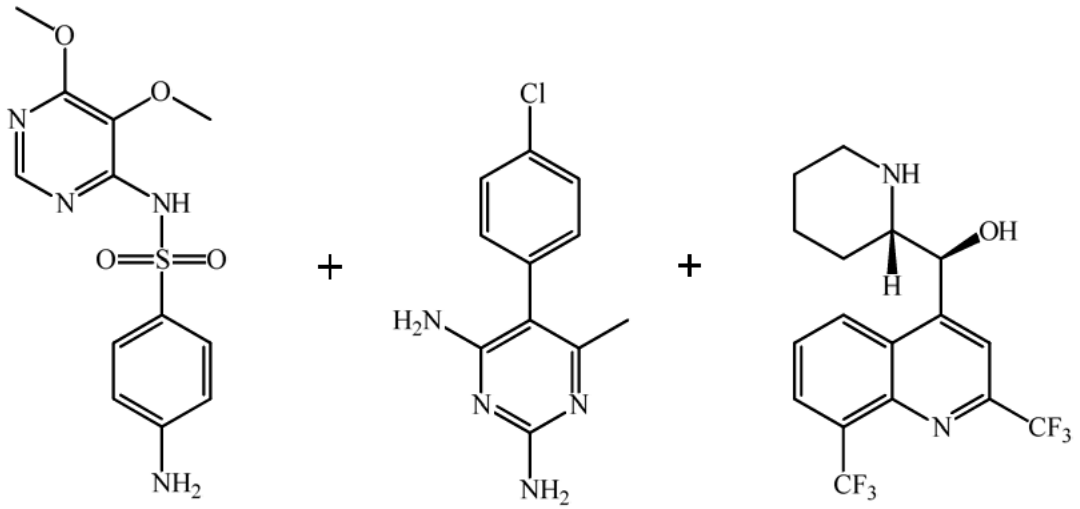

Figure 2.4.2 First triple combination antimalarial drugs employed against *P. falciparum*.

Malaria therapy advocates a simultaneous use of different classes of antimalarial drugs with unrelated targets or mechanisms of action. This approach is geared towards delaying and preventing further emergence of drug resistance or even combating MDR *P. falciparum* malaria.[62] The model underlying combination therapy is often designed to exploit synergy, shorten duration of treatment and increase patient compliance.[60] A combination of drugs is therefore anticipated to effectively exploit multiple reductions in selection risks that arise from spontaneous genetic mutations of a parasite.[60,63]

The idea of retarding resistance through combinations is a common solution to MDR and this concept was first pioneered in anti-tuberculosis therapy, later used on cancer chemotherapy, and more recently adapted to antiretroviral treatment.[64] The notion has also been adopted as a standard care of *P. falciparum* malaria following extensive combination studies by Peters and his colleagues in the mouse model *P. bergei*.[44,59] However, the current combinations lack synthetic simplicity which has prevented easy access in the Third World. In addition, their pharmacology has become a major economic disadvantage due to large and costly clinical profiling requirements (on average the current price of high quality artemisinin before combination is around US$ 450/kg).[65]

The prophylactic use of CQ has been challenged by the widespread CQ resistant strains and has been replaced by artemisinin derivatives. However, the first signs of therapeutic resistance to artemisinin are subtle and have been very difficult to analyse.[65-66] At the present moment, there is no convenient surveillance for detecting ACT resistance and the most reliable way is through rigorous clinical efficacy studies, which are very expensive and often lengthy.[67] Clinical evidence gathered from Western Cambodia has recently warned that the emerging ACT resistance against the current first-line drugs would be catastrophic to initiatives aiming at global malaria control.[66] The Southeast Asia region has, in the past, hatched ACT treatment-resistant malaria that has spread to the rest of tropical regions around the world.[65] It is therefore imperative to prime the antimalarial pipeline with novel compounds that have been made by the application of facile, reliable and quick synthetic methods.

2.5 Rationale for selecting 1,2,3-triazoles as linkers

Apart from creating benzyl- or phenyl-linked chloroquinoline derivatives in creating "reversed" CQ compounds that might exhibit similar cross-resistance susceptibility patterns to AQ, it is envisaged that a triazole moiety can be used as a scaffold to broaden structural diversity. A 1,2,3-triazole is a five-membered heterocyclic aromatic system containing three consecutive nitrogen atoms connected to two carbon atoms in a ring, as illustrated in **figure 2.5.1**. Triazoles have been known for over a century[68] and are stable to hydrolysis, as well as reductive or oxidative conditions, as a result of their aromatic stabilization. The triazole moiety is more than just a passive linker with *in vivo* metabolic stability[69] and rigidity, as it associates readily with biological targets through hydrogen bonding and dipole interactions.[70] It is also an important structural feature that has inhibition activity against cytochrome p450 enzyme and/or peptide analogue in many biological compounds.[71]

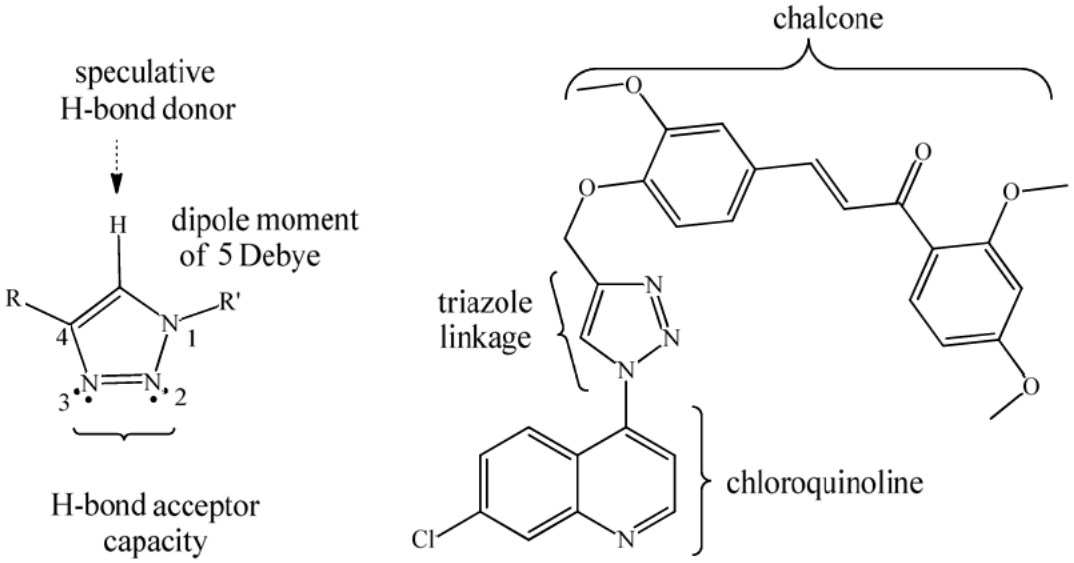

Figure 2.5.1 The 1,2,3-triazole structure and an example of a triazole-linked CQ-chalcone hybrid compound.[72]

The use of the triazole functional group as a linker has been utilised in a wide variety of biological applications.[73] A large volume of research has reviewed and disclosed the excellent biological activities such as the antibiotic,[74] anticancer,[75] antituberculosis,[76] and antiviral properties[77] associated with of the triazole-containing compounds. The pharmacological activities tailored by a triazole while acting as an effective linker of biomolecules is therefore difficult to ignore.[70,78]At the moment, there are approximately 15 triazole-bearing compounds in the "Drug Bank" and the market, mostly with antifungal activities, and a further 24 are in different clinical trial stages.[79-80] The significance of triazoles ability to effect the treatment of parasitic drug-resistant cutaneous leishmaniasis, Chaga's diseases,[81-82] and enhance the *in vitro* activity of protease inhibition against the strains of *P. falciparum* has been documented.[72,83]

The triazoles also successfully play pivotal roles as linkers and nonclassical bioisosteres of metabolically unstable groups to enhance pharmacokinetic properties of several drugs.[67-68] This means that the triazole ring can replace many functional groups of structural diversity in potent compounds to produce viable clinical candidates. It is, therefore, a suitable bioisostere of many functional groups such as pyrazoles,[84] aromatic rings,[85] amides[86] and others. The bioisosteric and linker functions offered by triazoles are more prominent in drug discovery. One of the challenges

of the malaria chemotherapy is to develop promising compounds that are innovative with chemical structures and mechanism of action.

2.6 New generation antimalarial agents

In the advent of the organic synthesis of new antimalarial drugs that are affordable, two or more 'biologically privileged' pharmacophores can be covalently joined into a single molecule by a linker.[87-88] These derivatized compounds have the potential to offer an effective way of delivering a drug with favourable synergistic pharmacological activity.[13-14] This approach can be regarded as supplementary to combinations, especially when combination has a marginal benefit that carries a significant toxicity. The formulation of "linked drugs" carries less risk of combination pharmacological interactions although inherent negative traits of individual pharmacophores is still possible.[13] This is thus a cheaper development investment in drug discovery, especially where there are difficulties in sourcing natural metabolites or when the chemistry of synthesis is complex.

Another basis for hybridization is to exploit receptor binding capabilities by using linkers that can actively enhance active transport mechanisms and drug bioavailability. This is vital with respect to designing molecules which are intended to overcome cross-resistance under metabolic conditions. The 1,2,3-triazoles linkers are logical antiplasmodials as they are lipophilic nitrogen-containing heterocycles that tend to accumulate into the DV of a parasite.[89] A critically important strategic element in generating such linkers is the reliability of the synthetic chemistry,[88] which must proceed selectively to construct chemically stable bonds in a broad range of functional groups. For this reason, Kolb, Finn and Sharpless described the ideal class of reactions with organic transformations that satisfies this criteria, namely click chemistry reactions.[90] The transformations performed with these reactions are versatile and have found applications in various fields of chemistry, materials, peptides, bioconjugation, radiolabeling of biomolecules for imaging, and importantly in the advancement of structure-based drug discovery.[85,90-91]

2.7 Click chemistry

The energetically favoured click reactions generate stable molecules by irreversibly joining suitable molecular units or pharmacophores together, predominantly by way of heteroatomic linkages.[85] Among the click reaction transformations, the 1,3-dipolar cycloadditions readily form five-membered rings at the aromatic oxidation level and this particular reaction has been shown to have had a significant impact in drug discovery.[92-93] The 1,3-cycloaddition reaction that results in the formation of triazoles was discovered by Michael[68] in 1893 and extensively studied by Dimroth in the early 1900s.[94] The scope and diversity of the reaction was elucidated mechanistically in the 1960s by Huisgen.[93,95] Azides and alkynes are energetically reactive species ($\Delta H°$ = -45 to -55 kcal/mol) that undergo a kinetically sluggish concerted cycloaddition reaction as a result of a high activation-energy barrier (*ca* 24 – 26 kcal/mol).[90,96-98] The thermal promotion of the Huisgen reaction lacks regioselectivity and as a result generates a mixture of 1,4- and 1,5-disubstituted triazoles, as depicted in **figure 2.7.1**.

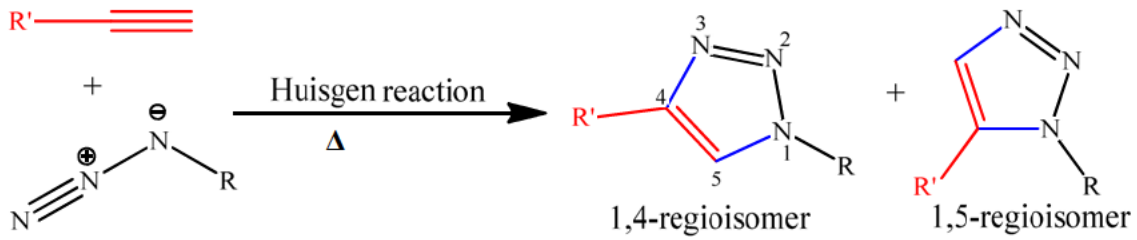

Figure 2.7.1 Triazole formation via the Huisgen 1,3-dipolar cycloaddition reaction.

The Huisgen [3 + 2] cycloaddition reaction between a terminal alkyne and an azide that results in the generation of a disubstituted 1,2,3-triazole moieties is of popular interest and a key example in the click chemistry 'area'.[93,96] The central electron deficient nitrogen of an azide dipole influences a synchronous shift of electrons during the reaction with an alkyne, thereby generating the triazole heterocycles.[93] The mesomerism of the 1,3-dipole, proposed by Pauling,[99] results in a negative charge exchange between the two ends of a dipole which compellingly explains the reactivity and formation of two isomeric triazoles in the Huisgen reaction.[93] Huisgen himself described these types of compounds as ambivalent since they displayed electrophilic and nucleophilic character in the positions 1 and 3, respectively, as shown in **figure 2.7.2**.[100]

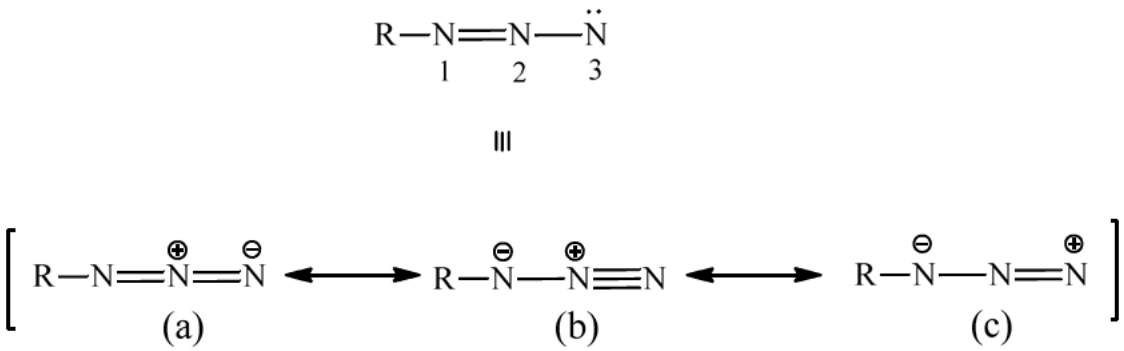

Figure 2.7.2 The 1,3-dipolar azide mesomeric structures.

2.8 Copper(I)-catalysed alkyne-azide 1,3-cycloaddition reactions

The regioselective synthesis of the triazole ring following the Huisgen reaction remained a puzzle even after Kinugasa and Hashimoto had demonstrated the application of Cu(I)-acetylides and 1,3-dipolar nitrones in the enantioselective 1,3-dipolar cycloadditions reactions.[101] The application of Cu(I)-acetylides with the 1,3-dipolar azides for the exclusive formation of 1,4-disubstituted triazoles in 1,3-dipolar cycloadditions was illustrated by independent reports of Meldal and Sharpless , see **figure 2.8.1**.[90,102] A reaction resulting in the complementary 1,5-disubstituted isomer was later reported by Fokin and Sharpless, this time using ruthenium(II)-pentamethylcyclopentadienyl (Cp*) analogues, RuAAC.[98] With the CuAAC reaction, the Cu(I) complex engages in the catalysis of terminal alkynes, while in the RuAAC reactions the ruthenium is also compatible with internal alkynes.[98,103] Among the two transformations, the CuAAC reaction has been the more important reaction, and has been extensively utilised for the customisation and linking of the functional molecules.

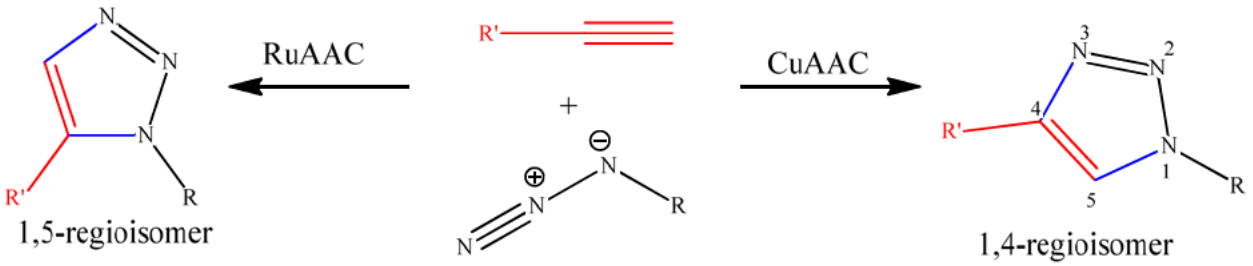

Figure 2.8.1 Regioselective transformations of the Huisgen reaction under ruthenium and copper metal catalysis.

To date, for assembling disparate molecular fragments, the CuAAC reaction has demonstrated several advantages over the uncatalyzed Huisgen reaction.[90,104] The application of copper catalyst significantly lowers the activation-energy barrier and thus accelerates the reaction rate (10^7 to 10^8 faster) at room temperature. An important feature is that Cu(I)-accelerated reaction is not affected by the steric and stereoelectronic influences of the substrates utilised.[102,105-106] A variety of experimental approaches have been effectively carried out with different Cu(I) sources, direct Cu(I) salts or the *in situ* reduction of Cu(II) salts, on a myriad substituted alkyne functional groups.[102,106-107]

A nitrogenous base or copper ligands are sometimes added to the CuAAC reaction, with the most commonly used conditions being those reported by Sharpless group.[106] Under those conditions, a catalytic Cu(II) salt and excess molar equivalents of a reducing ascorbate with the amine base additive are used to couple azides and alkynes with little or no co-solvent. The mechanism of the CuAAC reaction has been under several in-depth and ongoing investigations. According to kinetic studies and density functional theory calculations, the reaction is considered to be non-concerted in nature and proceeds in a stepwise fashion.[107-108] The key steps in the reaction are highlighted in **figure 2.8.2**. The reaction proceeds by generating the copper(I)-acetylide, which occurs via alkyne π-coordination with a copper catalyst. The alkyne reactivity is thereby enhanced via a decrease in the electron density of the sp carbon atom and subsequently the pK_a of the acetylene proton is lowered by about 10 log units.[97,109-111] The reaction has been demonstrated to follow a second order rate law in copper when catalytic quantities are used.[110] The intermediate Cu(I)-acetylide participates in a [3 + 2] dipolar cycloaddition with the azide. Due to a high potential energy barrier (*ca* 23.7 kcal/mol) of the 1,3-cycloaddition of azides to the copper(1)-acetylide, the azide is selectively activated by coordination to the acetylide-copper complex, thus forming a 6-membered metallocycle ring.[109-111] A ring contraction then follows the thermo-neutral ligand exchange, after which a triazole ring is formed by protonation and release of the copper catalyst.

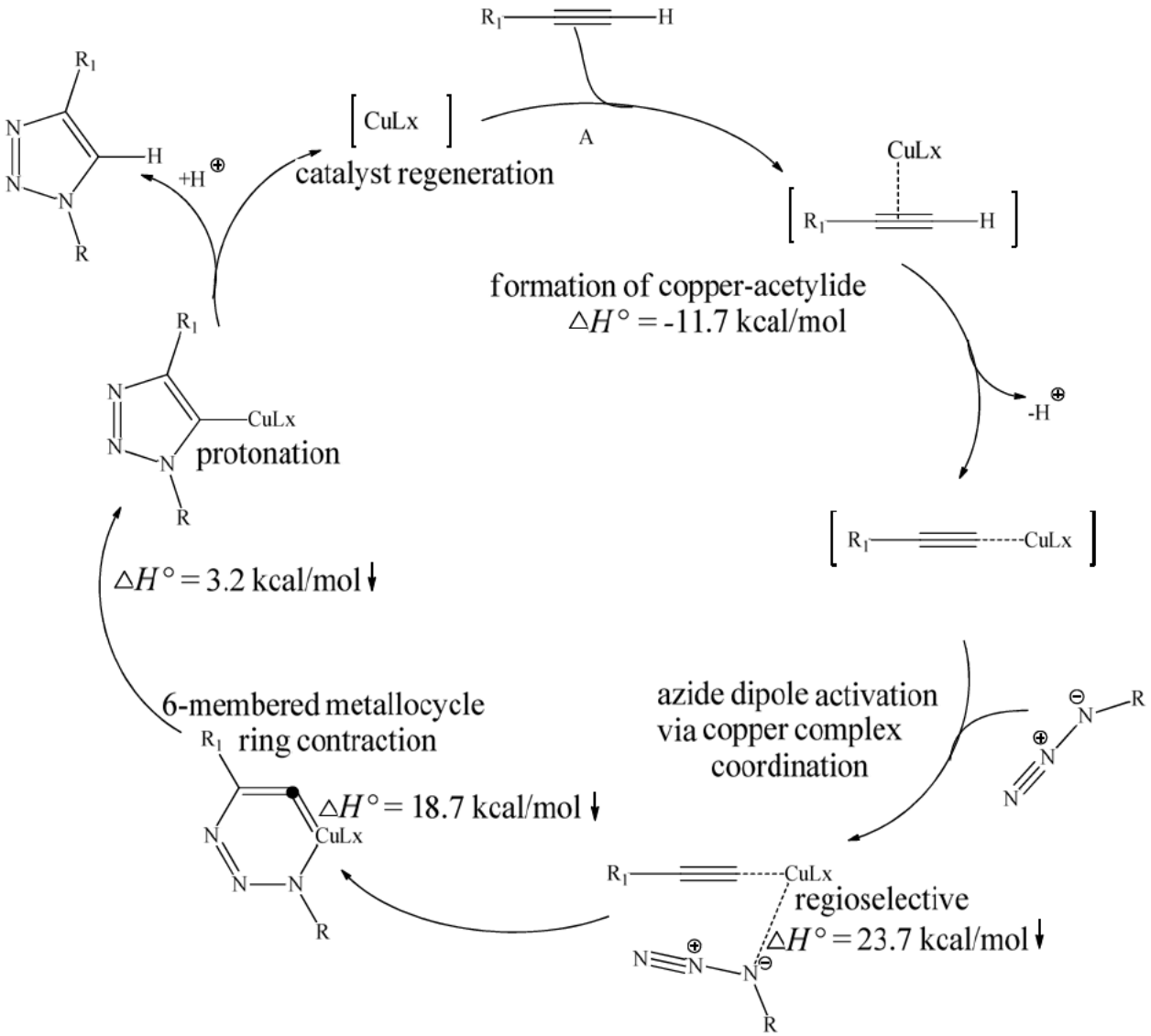

Figure 2.8.2 Stepwise CuAAC reaction between terminal azides and alkynes.[97]

Given the modular synthesis of the above reaction, it was anticipated that its deployment in developing analogues of existing antimalarial drugs might create promising compounds with the novel chemical structures coupled with a different mechanism of action to the molecular target of the aminoquinolines.

Chapter 3

Results and discussion: Synthetic methods and *in vitro* antimalarial activity

3.1 Target compounds

The chemical structures shown below represent the final test compounds that were synthesized and evaluated for antiplasmodial activity. The first set of triazole linked chloroquinoline derivatives is the small aliphatic amines followed by the aryl amines.

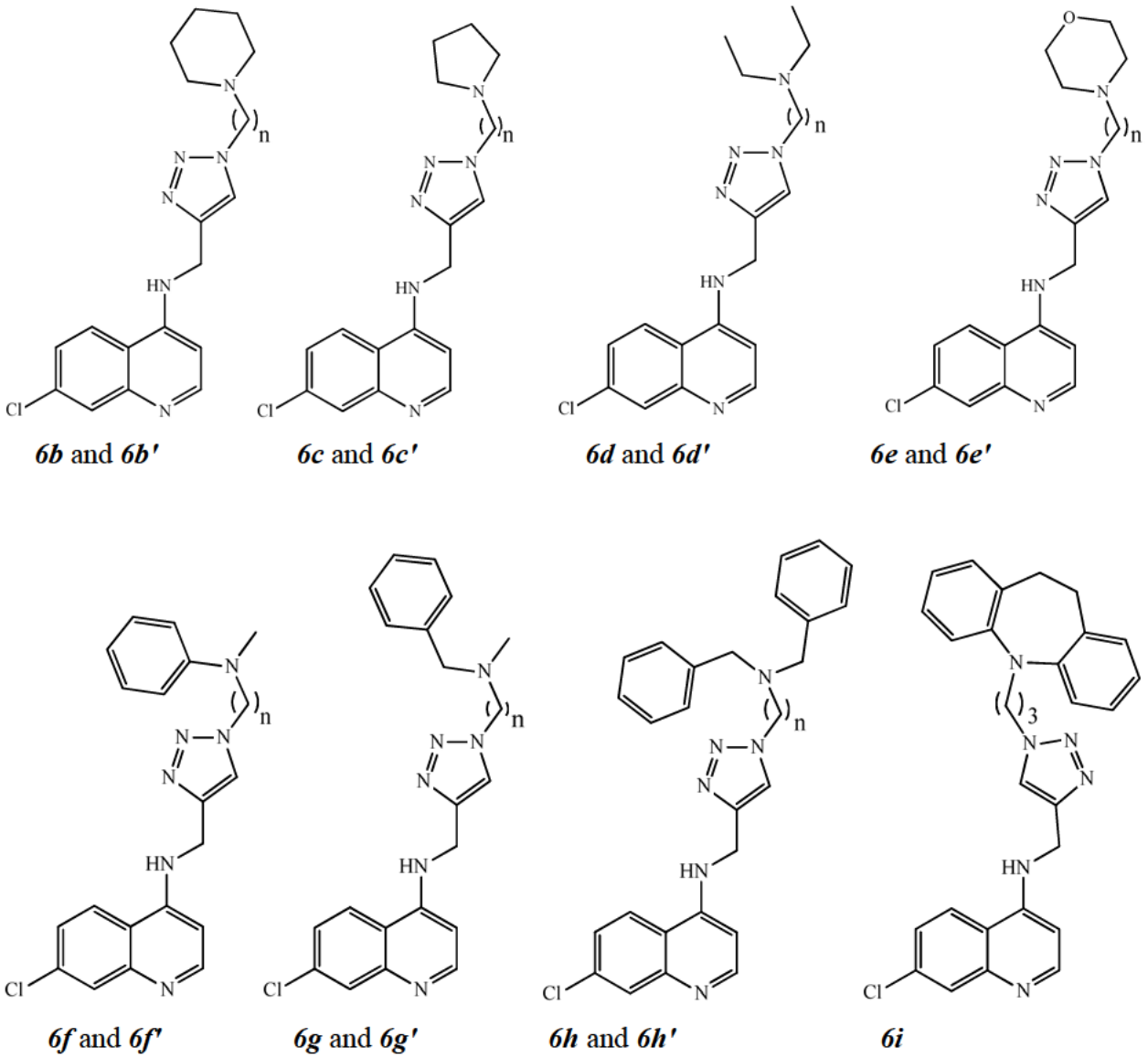

Figure 3.1.1 Triazole-linked chloroquinoline test compounds.

A carbon spacer (n) corresponds to ethyl or propyl length in the respective order.

3.2 Synthesis of the amino chloroquinoline alkyne precursor

At the onset of our investigations, the synthesis of triazole-linked chloroquinoline derivatives by means of the Huisgen-Meldal-Sharpless reaction was the key chemical transformation because of its appealing regioselective formation of 1,4-disubstituted triazole products. More precisely, the Cu(I)-catalysed 1,3-cycloaddition reactions between the aminoquinoline alkyne and azide building blocks were the central focus of synthesis that were then utilised to afford 1,4-disubstituted 1,2,3-triazole linked compounds with potential antimalarial activity.

The first step of the proposed strategy was to synthesise a terminal alkyne precursor derived from the well-known haematin-binding template, chloroquinoline. The synthesis of the key aminoquinoline alkyne precursor ***1*** was carried out via a nucleophilic *ipso* substitution on the suitably substituted 4,7-dichloroquinoline scaffold. This was achieved by using propargyl amine as a nucleophile (refer to **figure 3.2.1**). It should be noted that the chloroquinoline ring can be considered as the prototypical electron poor aromatic system. The electronegative nitrogen substituted on the ring has its aromaticity disrupted through a strong permanent dipole by the inductive polarisation that causes fractional positive charges on the α- and γ-carbon atoms of the chloroquinoline ring. Therefore, the 4,7-dichloroquinoline ring can be pictured as experiencing mesomeric electron withdrawal by the nitrogen atom, and more importantly, experiences additional inductive withdrawal from the chlorine atom at the γ-position.[112] This means that the chloroquinoline preferably undergoes nucleophilic aromatic substitution via an addition of a nucleophile at γ-carbon, followed by the elimination of chlorine atom (S_NAE).

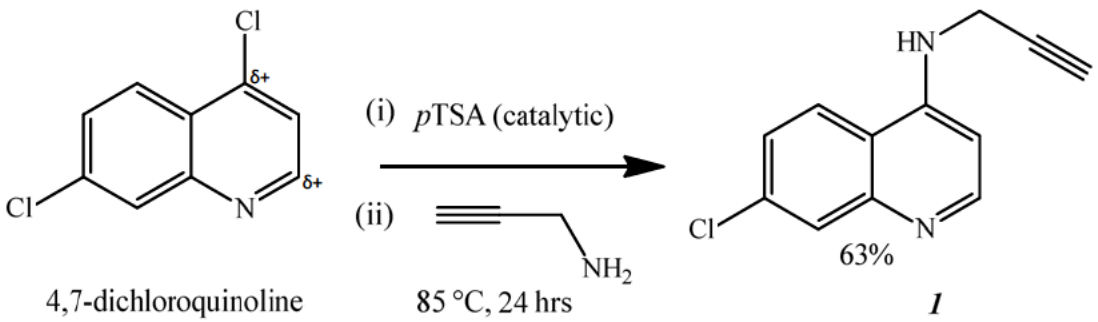

Figure 3.2.1 Synthesis of 7-chloro-*N*-(prop-2-yn-1-yl)quinolin-4-amine.

The synthesis of ***1*** has not been reported in the literature before, but the nucleophilic *ipso* substitution reactions on 4,7-dichloroquinoline ring system using non-activated primary amines have been described in established literature methods.[113-116] We therefore turned our attention to the development of this aminoquinoline alkyne precursor ***1***. A brief assessment of reagents used in these reactions show that amine nucleophiles play several additional roles, for instance, to basify and to solvate the reaction media. These methods thus predominantly make use of a large excess of amine nucleophile, up to 20 molar equivalents, to obtain moderate to good yields of the desired product (60% – 92%). It should be considered that in our case, the high price of propargyl amine (5 mL > 1,300 ZAR Sigma Aldrich) would make this atom uneconomical approach extremely costly. The described literature conditions were however attempted with the initial 2 molar equivalents of propargyl amine,[113] supplemented by another less nucleophilic base to decrease the amounts of propargyl amine required as described in the paragraphs that follow.

According to the cited experimental methods,[113-115] and others reported elsewhere, a mixture of chloroquinoline and amine is usually homogenised at 80 °C, followed by a heating at reflux or at elevated temperature, i.e. 120 – 140 °C. Similarly, in our hands, the experiments were stirred at 80 °C for 1 hour during which TLC monitoring displayed formation of the intended product. However, a follow-up reaction at 120 °C made it clear that at elevated temperature the product was undergoing decomposition into a brown solid of unknown composition (see **table 3.2.1**, entry **1**). From this observation, it was concluded that higher temperature was detrimental to the reaction. Decomposition has been demonstrated as a major problem for similar reactions and milder reaction conditions have often been considered necessary for these reactions to be successful, i.e. reactions at 85 °C rather than high temperatures.[24] In further modifications, the amounts of supplementary base was increased, but unfortunately the yields obtained were rather low (refer to **table 3.2.1**, entries **2 – 6**). In addition, it can be deduced from entry **3** from the same table that a proportional addition of excess propargyl amine, which was believed to perhaps escape from the reaction medium by vaporisation, did not have a significant impact on the reaction yield obtained and alternative conditions were thus investigated.

Table 3.2.1 The Attempted experimental conditions for *N*-alkylation of 4,7-dichloroquinoline

Nucleophile equivalents	**Base/Acid equivalents**	**Solvent**	**Temperature (°C)**	**Yield (%)**
1) 2	Et_3N (0.5)	None	80 – 120	Decomposition
2) 2	Et_3N (0.5)	None	80 – 100	11
3) 2 + 2	Et_3N (2.0)	None	80 – 85	24
4) 2	Et_3N (4.0)	None	80 – 85	17
5) 2	K_2CO_3 (3.0)	DMSO	80 – 100	Insignificant product
6) 2	K_2CO_3 (3.0) + Et_3N (2.0)	DMSO	80 – 85	Insignificant product
7) 2	*p*TSA (0.1)	MeCN	80 – 85	37
8) 2	*p*TSA (0.1)	Dioxane	80 – 85	55 – 63
9) 2	None	Dioxane	80 – 85	6

Nucleophilic substitution reactions that proceed slowly at high temperature to give low yields might be found, in polar aprotic solvents like DMSO, to proceed rapidly and give better yields. Given the reputable advantages of DMSO in promoting such reactions together with a high boiling point advantage, it was expected that the yields of ***1*** would improve, unfortunately under these conditions, the reaction was found to have hardly progressed even after 24 hours, although decomposition was not observed (see **table 3.2.1,** entries **5 – 6**).

In these type of reactions, it is known that the chlorine atom generally has poor leaving abilities when compared to other leaving groups due to strength of the C–Cl bond (D_0 ~ 79 kcal/mol).[112] In order to carry out successful nucleophilic substitutions on the ring carrying this leaving group, the *N*-heterocycle's propensity to undergo nucleophilic addition can be enhanced by inducing a formal positive charge on the ring nitrogen. Thus, *N*-oxides or *N*-quinolinium salts are established promoters of such reactions; nonetheless, *N*-oxides on quinoline can be viewed as disguised 1,3-

dipoles that will likely undergo Diels-Alder [3 + 2] cycloadditions with the alkyne of the propargyl amine, and this approach was not attempted.

A direct *N*-alkylation in the nucleophilic substitution of *N*-heterocyclic structures appears deceptively simple, but the synthetic value of this method is chiefly limited to employing a large excess of the alkylating amine. Chauhan's group[47] has demonstrated that the amination of 4,7-dichloroquinoline under *p*-toluenesulfonic acid (*p*TSA) catalysis using lower quantities of primary amine nucleophile, is viable, and such reactions have also been carried out on other substituted 4,7-dichloroquinolines using different catalytic acids such as HCl.[117] Therefore, chloroquinoline was protonated with *p*TSA which supposedly forms a more polarised *N*-chloroquinolinium intermediate. The reaction was anticipated to undergo a known S_NAE process under the strong influence of a positive formal charge on the nitrogen as graphically depicted in **figure 3.2.2**.

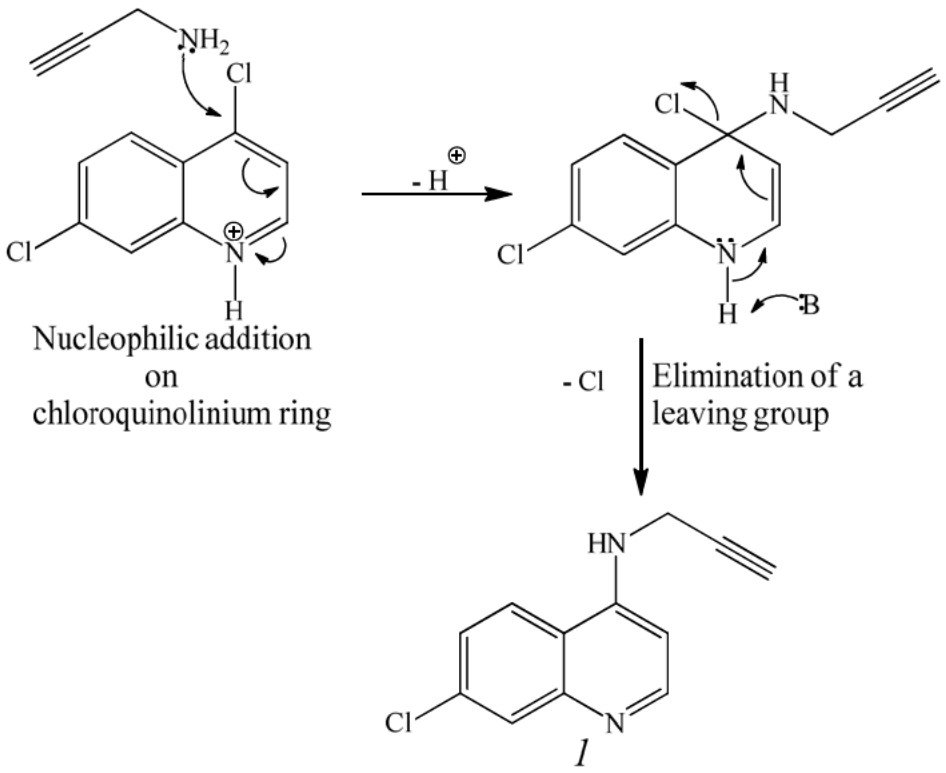

Figure 3.2.2 *p*TSA catalysed *N*-alkylation of 4,7-dichloroquinoline.

Given the impact of the heterocyclic nitrogen atom in nucleophilic substitutions on the chloroquinoline ring, *p*TSA catalysis was therefore investigated in MeCN and dioxane solvents with the intention of promoting the substitution rates (see **table 3.2.1**, entries **7** – **10**). Of significance was that a maximum yield of 63% was obtained when 1,4-dioxane was used as compared to 37% for MeCN as solvent. The importance of the *p*TSA catalysis was also investigated and a low yield of only 6% was obtained where this catalyst was omitted (refer to **table 3.2.1,** entry **9)**. Nonetheless, under acid catalysis, it appears that nucleophilic substitution on halogenated *N*-heterocycles remains the most feasible option, particularly when only utilising a single equivalent of a nucleophile, as the use of mild basic conditions with multiple equivalents of amine nucleophile were found not to be optimal.

In deuterated DMSO, the structural elucidation of compound ***1*** by ^{1}H NMR spectroscopy confirmed that the signals representing the expected aromatic signals for the chloroquinoline ring in the region 6.6 – 8.5 ppm were present (refer to **figure 3.2.3**). The doublets at 8.5 ppm and 6.5 ppm with decreased coupling constant $J_{H,H\ ortho}$ = 5.7 Hz coupling were assigned to the two protons H-2 and H-3 experiencing the mesomeric and inductive deshielding effect from the ring nitrogen, N-1 and the substituted N-4, respectively. A doublet at 8.2 ppm integrating for a single proton, was attributed to H-5 with $J_{H,H\ ortho}$= 9.0 Hz coupling to a doublet of doublets H-6, that was further coupled to a *meta* proton H-8 at 7.5 ppm with a $J_{H,H\ meta}$ = 2.2 Hz. The aromatic coupling of protons ($J_{H,H\ ortho}$ = 5 – 9 Hz between H-2 and H-3 as well as H-5 and H-6, $J_{H,H\ meta}$ = 2.2 Hz between H-6 and H-8) and the splitting pattern of signals were definitive in deciding the assignments of the chloroquinoline protons.

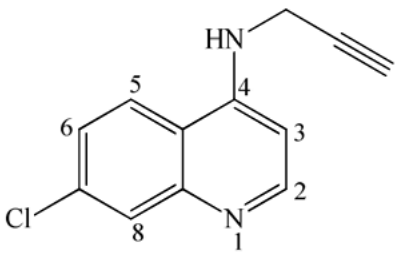

Figure 3.2.3 Structural elucidation of 7-chloro-*N*-(prop-2-yn-1-yl)quinolin-4-amine (***1***).

The most important signals were those of the newly installed propargylic amine group in addition to the expected aromatic signals for the chloroquine ring. Although amine protons are generally not considered suitable for diagnostic purposes due to lack of consistency in their shifts, a broad triplet at 7.8 ppm was assigned to the N–H proton at the γ-position with a J = 5.7 Hz corresponding to the allylic proton coupling. Moreover, a double of a doublet at 4.1 ppm was assigned to the allylic protons which were further coupled to the acetylenic proton triplet at 3.2 ppm with a J = 2.4 Hz. These signals were indicative of the successful substitution of the propargyl amine on the chloroquinoline ring system. ^{13}C NMR spectroscopy was also used to substantiate the structural elucidation of ***1*** and the three additional carbon signals were observed: namely, the high-field shifted carbon signals at 74 ppm and 81 ppm in comparison to the aromatic carbons (100 – 152 ppm) were characteristic of the *sp* hybridised acetylene carbons of a terminal alkyne and the additional carbon signal at 32 ppm provided the evidence of an aliphatic CH_2 carbon with an incremental downfield shift due to a proximal nitrogen atom.

In addition to NMR spectroscopy experiments, the positive electron spray ionisation mode in high resolution mass spectrometry (ESI^+ HRMS) was carried out to determine the isotopic mass and perhaps elemental composition of compound ***1***. The protonated molecular ions ($[M + H]^+$; *m/z*) was the dominant species and the peak with the highest isotopic abundance was customarily assigned 100%. The determined experimental monoisotopic mass of ***1*** $[M + H]^+$ = 217.0529 and was found to be in good agreement with the theoretical 217.0533 and within -1.84 ppm accuracy. In addition to the molecular ion peak, a peak at *m/z* 219.0503 with approximate abundance of 27% was considered to be due to the isotopic ^{37}Cl which has about 24% relative abundance, thus confirming the atomic composition of ***1***. Additional small clustered peaks around the base peak were ascribed to the compositional isotopic masses too.

The IR spectroscopic skeletal vibrations (υ/cm^{-1}) were further used to confirm the important functional groups: 3391 (NH stretch) was assigned to the aliphatic secondary amine; 3205 (C≡CH) acetylenic proton stretch, 3094 (Ar CH) aromatic protons stretch in the ring, 2963 (CH_2) aliphatic methylene asymmetric stretch; 2019 (C≡C) was a very broad band of acetylene; and a very weak peak at 1567 frequency further confirmed the (C=C) aromaticity in reference to Ar CH aromatic protons observed at 3094.

3.3 Synthesis of lateral chain aliphatic azides

As aforementioned, the azide building blocks were the next requirements for the CuAAC reactions with compound ***1***. It was, therefore, necessary to synthesise aliphatic azide spacers which would later be functionalized with selected amines. This section describes the synthesis that was followed to obtain azides of ethyl and propyl linear chains. Several detailed models of the structure function relationships of CQ have established the importance of carbon chain length variation in restoring the antimalarial efficacy of 4-aminoquinolines.[37-38,118] The azides of ethyl and propyl carbon chain length were therefore synthesized in two steps from ethane-1,2-diol and propane-1,3-diol starting materials, respectively, using a modified literature procedure.[119] The diols were first converted into their corresponding *bis*-mesylates using mesyl chloride under basic conditions in THF as a solvent to afford compounds ***2a*** and ***2a′*** in good yields, 94% and 99%, respectively.

The ^{1}H NMR spectra for the compounds were in agreement with the data reported in the literature.[119-120] The chemical structures of ***2a*** – ***2a′*** were also supported by the IR spectrometry (υ/cm^{-1}). The intensely sharp peaks at 1176 (S=O) and 1048 – 1045(O–S) distinctively confirmed the presence of the newly introduced, substituted sulfonate groups. The medium intensity peaks at 2963 – 2933 (CH_2) and 2884 – 2789 (CH_2) were assigned to the methylene asymmetric and symmetric stretches while the peaks at 1359 – 1352 (CH bend) were attributed to CH bend vibrations, respectively, confirming the presence of aliphatic carbon chain. In addition to the above mentioned peaks, a medium band at 748 (CH rocking), which can only appear in longer and linear aliphatic chains, was observed in the case of ***2a′*** to strengthen that ***2a′*** was of a longer propyl length (see **figure 3.3.1**).

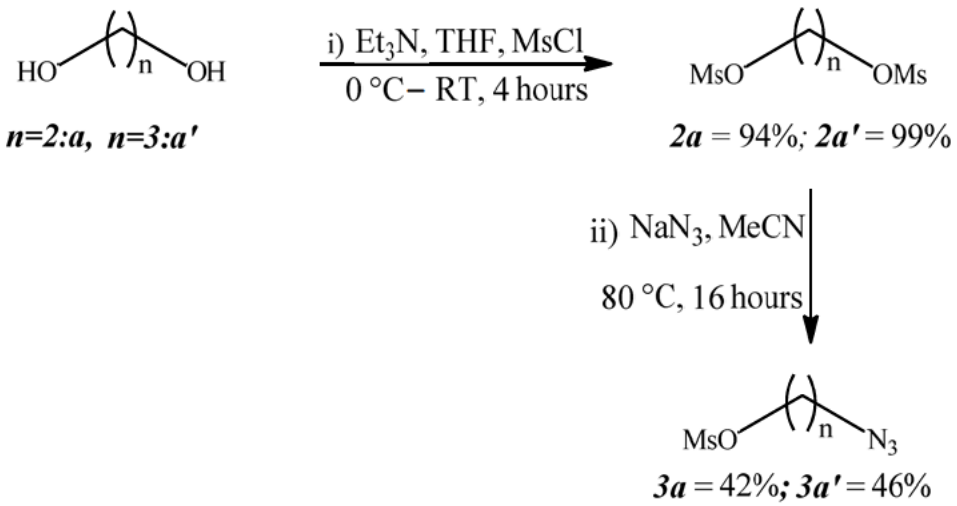

Figure 3.3.1 Synthesis of the azidomesylate intermediate precursors

These intermediates containing the mesylate leaving groups were then treated with sodium azide in acetonitrile solvent with the intention to displace one of the mesylate groups and therefore obtained compounds ***3a*** and ***3a'***. The synthesis of the azidomesylates ***3a*** and ***3a'*** proceeded smoothly via a nucleophilic substitution (S_N2) in both steps, and moderate yields of 42 – 46% were obtained. It is obvious that the azide nucleophile has the potential to displace both mesylate groups in ***2a*** and ***2a'*** and *bis*-azidation was the cause of the overall decrease of yields. Azide disubstitution was confirmed on TLC by Staudinger reduction and ninhydrin staining that revealed formation of two major products in the reaction mixture.[121] Again, the ^{1}H NMR spectra of ***3a*** and ***3a'*** resembled the literature data.[119,122] The IR spectra of the relevant compounds established the azide substitution with an intensely sharp peak at a frequency of 2093 cm^{-1}, which was otherwise not observed in the bis-mesylate intermediates. This was a conclusive confirmation of the presence of the azide functional group.

3.4 Functionalization of the aliphatic azides with amine groups

In continuation with the azides synthesis, the selected amine functional groups that are essential for optimising the biological activity were added to the aliphatic azide chains of ***3a*** and ***3a'***. The aminoalkyl azides were thus prepared next via displacement of the unreacted mesylate group with a number of secondary amines. A series of aminoalkyl azides were therefore synthesized as illustrated in **figure 3.4.1**.

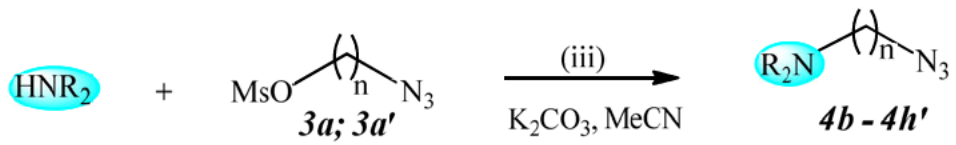

Figure 3.4.1 A general template for the synthesis of aminoalkyl azides.

The S_N2 *N*-alkylation reactions were performed under mildly basic conditions by heating starting material at reflux in MeCN for 16 hours to obtain compounds ***4b, 4b'*** and ***4d' – 4h'*** as the sole products in low to good yields of 34 – 73% (refer to **table 3.4.1** for a summary of the secondary amine utilised and for all yields obtained).

Table 3.4.1 The synthesis of aminoalkyl azides and the product yields

Entry	Amine	Product	Yield (%) n = 2	Yield (%) n = 3
4b* and *4b'	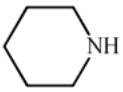	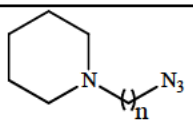	**72**	**70**
4c* and *4c'	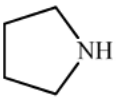	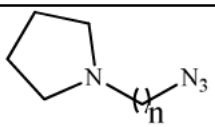	**64**	**73**
4d* and *4d'	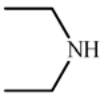	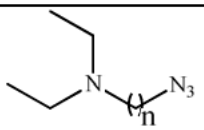	**48**	**36**
4e* and *4e'	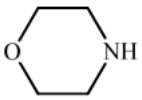	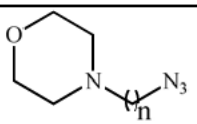	**69**	**68**
4f* and *4f'	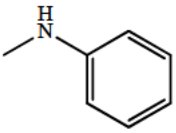	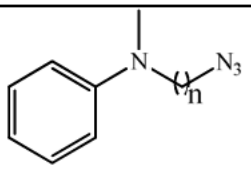	**34**	**37**
4g* and *4g'	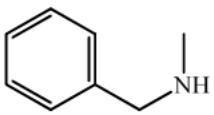	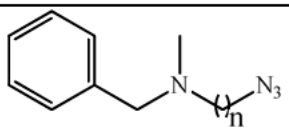	**41**	**47**
4h* and *4h'	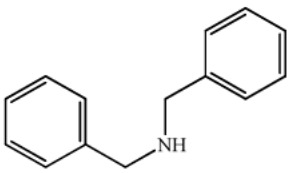	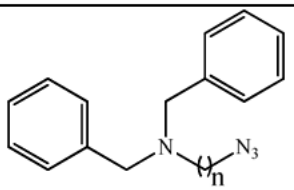	**61**	**56**
***4i*†**	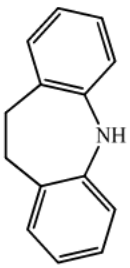	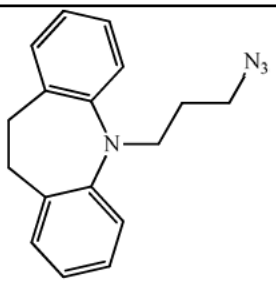	—	**61**

†Synthesized using a different route illustrated later in **figure 3.4.2**

In cases where lower yields were obtained, for instance with ***4d*** and ***4d′***, it was observed that the azides were semi-volatile and that most of the product was being lost *in vacuo* during solvent removal. The rest of samples were therefore dried by passive evaporation in a vacuumed desiccator after short treatment with once off vacuum to remove most of the solvent entrapped in the sample. The majority of synthesized aminoalkyl azides, reported in **table 3.4.1**, are not reported in the literature and as such ^{1}H NMR, ^{13}C NMR, ESI^{+} HRMS and IR spectroscopic methods were used to confirm the structures of these compounds. Depending on whether the amine functional group was aliphatic or aromatic, the characteristic signals were verified by the appropriate spectroscopic methods; however, constantly common was the important azide peak at frequency 2093 – 2136 cm^{-1} in the IR spectra.

The ^{1}H NMR spectra of compounds ***4b – 4i*** varied from one compound to the other, but the aliphatic azide chain signals remained almost unchanged (see **figure 3.4.1**). The protons in the α-position with respect to the azide at 3.3 – 3.8 ppm were equally split into a triplet signal by the neighbouring protons with a *J*-value of 6.3 – 7.9 Hz which denoted the free rotating aliphatic carbon chains. In the case of the propyl chain, an additional quintet at 1.7 – 1.8 ppm with a similar coupling constant, was observed, in the absence of other overlapping protons signals.

The efforts to achieve substitution with a pyrrolidine group (refer to **table 3.4.1**, entries ***4c*** and ***4c′***) using the described conditions (MeCN, K_2CO_3, Δ)[119] proved to be futile presumably as a result of assumed decomposition. During the reaction progress, an instant change of colour to a brown solution was considered to indicate the unidentified side reactions, in this particular case. An alternative method was therefore employed[123] and the reagents were thus homogenised at 0 °C first followed by overnight heating at reflux to afford compounds ***4c*** and ***4c′*** in good yields (64 – 73%). Furthermore, the *N*-alkylation of aromatic amines was promoted with potassium iodide (KI) in the light of their poor basicity, low nucleophilicity and problems associated with steric effects (see **table 3.4.1,** entries ***4f*** – ***4c′***). Traditionally, KI is known to promote substitutions via the Finkelstein reaction[124] in which a less labile halide or halide equivalent sulfonate is substituted by a better leaving iodine which is subsequently displaced by the amine.

The direct alkylation of the azidomesylates ***3a*** and ***3a'*** (see **table 3.4.1**, entry ***4i***) with a sterically hindered 10,11-dihydro-5*H*-dibenzo[*b*,*f*]azepine was also unsuccessful under the usual conditions described earlier. There are few similar reactions reported in the literature using the same nucleophilic amine and low yields are often obtained due to the poor basicity of this amine nucleophile.[51] It should be noted that in the literature, similar reactions have been investigated by means of metal-mediated cross-coupling or palladium allylation after which several steps, including hydroboration and the Appel reaction, were followed to produce several potential antimalarial agents with a linear chain (see **figure 2.3.1** described earlier in the dissertation).[125] In our work, we decided to investigate the two reaction routes shown in **figure 3.4.2**. The nucleophilic amine was thus deprotonated under strong basic conditions to carry out the substitution reaction with a suitable leaving group. It should also be noted that route **B** was utilised, after numerous failures when route **A** was pursued.

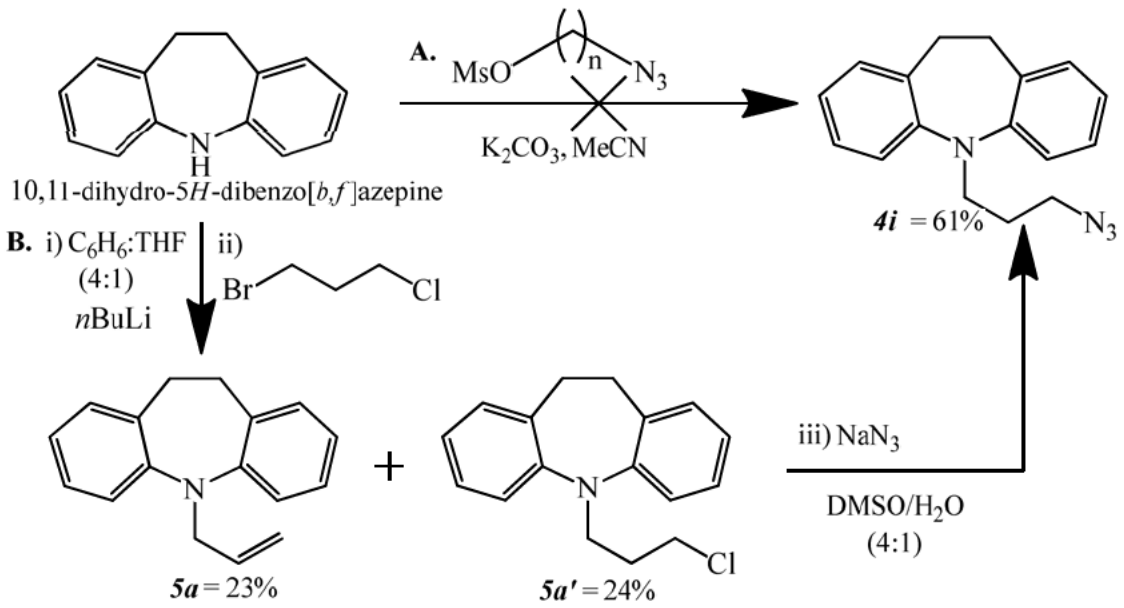

Figure 3.4.2 Synthesis of 5-(3-azidopropyl)-10,11-dihydro-5*H*-dibenzo[*b*,*f*]azepine.

Of importance is that, strong bases are generally good nucleophiles and *vice versa*; thus β-elimination is also a common competing side-reaction under strongly basic conditions. Therefore, the *N*-alkylation of azepine in **figure 3.4.2** was investigated on the azidomesylates (***3a*** and ***3a'***), as well as 1-bromo-3-chloropropane under mild and strong basic conditions and the results are presented in **table 3.4.2**. Under mildly basic conditions, substitution reactions of nucleophilic

amines are known to be promoted by heating but such efforts were inefficient in our hands (refer to **table 3.4.2**, entries **1** – **3**). Moreover, mesylate esters are good electrophiles for substitution reactions but can also undergo efficient elimination when reacted under strong base conditions. With this information at hand, it was realised that elimination reaction was the major side-reaction taking place (see **table 3.4.2**, entries **3** – **4**) and that the sulfonate leaving group also favoured elimination over substitution under these conditions.

At this point, the sulfonate leaving group was swapped for a halide and 1-bromo-3-chloropropane was used as an alkylating agent. 10,11-Dihydro-5*H*-dibenzo[*b*,*f*]azepine was thus deprotonated using *n*BuLi in THF solvent (refer to **figure 3.4.2**); however, alkylations under these conditions gave the unwanted *N*-allyl product (refer to **table 3.4.2**,entry **5**), obviously due to a subsequent E2 elimination. Reaction rate studies of similar reactions by Collum and co-workers described the formation of various diphenyl lithium aggregates to be the primary determinants of *N*-alkylation in the THF solvent.[126] In neat THF solvent, the alkylation rates exhibited fractional dependence on the amide, first order on the alkyl halide and a seventh order dependence on THF.[126-127] The alkylation success thus changes with the degree of amide solvation and aggregation states, and these factors thus influence the ratios of *N*-alkylation versus E2 elimination.

Table 3.4.2 *N*-alkylation of 10,11-dihydro-5*H*-dibenzo[*b*,*f*]azepine

Leaving group	**Solvents (Base)**	**Temp °C**	**Product (5a:5a′)**
1. -OMs	MeCN (K_2CO_3)	80 – 110	Not observed
2. -OMs	Toluene (*t*BuOK)	80 – 140	Not observed
3. -OMs	DMF (NaH)	RT – 140	Not observed
4. -OMs	DMF (NaH, *n*BuLi)	0 – RT	Insignificant product
5. -X	THF (*n*BuLi)	0 – RT	43%, ***5a***
6. -X	THF: C_6H_6 (1:1; *n*BuLi)	RT – 50	Insignificant prod.(***5a′***)
7. -X	THF:C_6H_6 (1:1; *n*BuLi)	0 – RT	44%, ***5a***/***5a′*** ~(5:1)
8. -X	THF:C_6H_6 (1:4; *n*BuLi)	0 – RT	47%, ***5a***/***5a′*** ~(1:1)

Under this paradigm, S_N2/E2 selectivity would then show propensity to favour S_N2 at low THF concentrations. However, in an attempt to perform the reaction using Collum's conditions at 50°C, an insignificantly low amount of *N*-alkyl product was formed (see **table 3.4.2**, entry **6**). The satisfactory S_N2 product ***5a′*** was however isolated from an approximated 1:1 product ratio, when employing 20% THF in benzene solvent, and when the reaction was carried out at 0 °C – RT (refer to **table 3.4.2**, entry **7**). From the chemistry point of view, the *N*-allyl product, ***5a***, could be converted into a desired terminally substituted azide via the known anti-Markovnikov hydroazidation in the presence of catecholborane,[128] but in our case the direct halide substitution of ***5a′*** with NaN_3 to produce ***4i*** (61% yield) was followed. The structural analysis of ***4i*** was carried out using the same spectroscopic methods described earlier in this section.

The identification of isolated compounds ***5a*** and ***5a′*** was established clearly by means of ^{1}H NMR and ^{13}C NMR spectroscopy. The structure of ***5a*** was distinct since it had a unique ABX allylic splitting pattern at 5.1 – 5.8 ppm together with a diagnostic vinylic proton coupling system ($^2J_{H,H}$ = 5.7 Hz, $^3J_{H,H\ cis}$ = 10.3 Hz, and $^3J_{H,H\ trans}$ = 17.3 Hz) to both *cis* and *trans* protons which could be differentiated from their *J*-values. In order to ascertain whether ***5a′*** was bromo- or chloro-substituted, ^{1}H NMR spectroscopy was again crucial in differentiating the two compounds using the protons chemical shifts. The protons at the α-position to Cl resonated at a much higher frequency of 4.4 ppm in ***5a′*** compared to those of Br at 3.6 ppm. The ESI^+ HRMS spectra data also supported the ^{1}H NMR spectral evidence.

3.5 Synthesis of the 1,4-disubstituted 1,2,3-triazole-linked chloroquinoline derivatives

Having synthesized the azide building blocks and the aminoquinoline alkyne precursor ***1***, the final step in the synthesis was to perform a Cu(I)-promoted 1,3-cycloaddition reaction between these azides and the alkyne ***1***. There are many variations in the experimental approaches to the reaction as discussed under section **2.8** and many discrepancies in the literature centre on the presence or absence of a base ligand to have the resultant effect on the reactivity of Cu(I).[109,129] The CuAAC reactions in this study were thus performed between ***1*** and ***4b – 4i*** in THF solvent by means of a modified literature procedure as shown in **figure 3.5.1**.[130] The reactions were performed under anhydrous nitrogen atmosphere for 30 – 90 minutes at room temperature using CuI, to afford the triazole-linked chloroquinoline derivatives in moderate to good yields (53 – 85%) after purification by means of silica gel column chromatography.

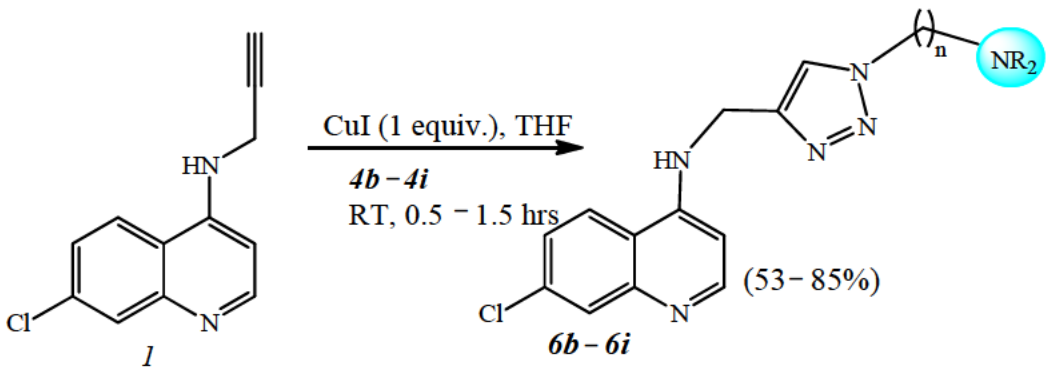

Figure 3.5.1 Synthesis of the triazole-linked chloroquinoline derivatives via CuAAC reaction.

Table 3.5.1 The product yields of the respective triazole-linked chloroquinoline derivatives

Entry	Product	Yield (%) n = 2	Yield (%) n = 3
6b* and *6b'	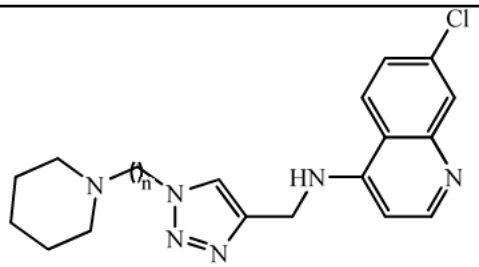	**76**	**79**
6c* and *6c'	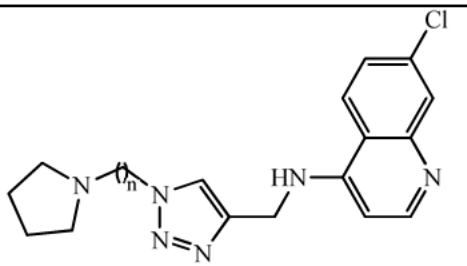	**67**	**63**
6d* and *6d'	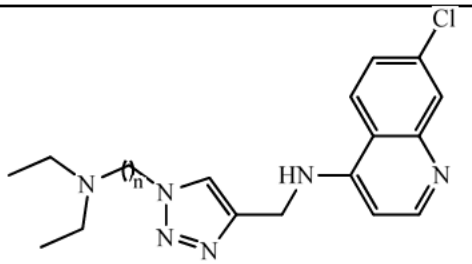	**70**	**61**
6e* and *6e'	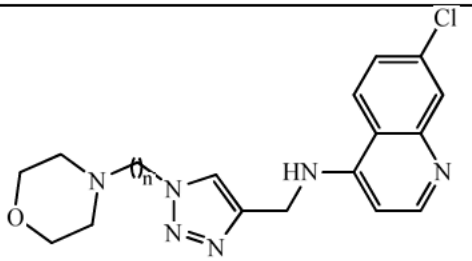	**74**	**85**
6f* and *6f'	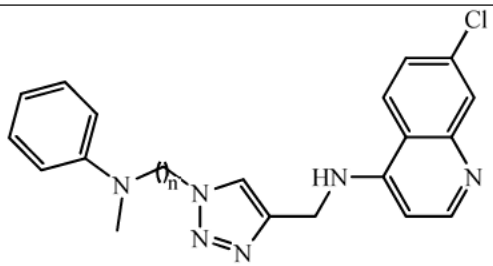	**64**	**53**

6g* and *6g'	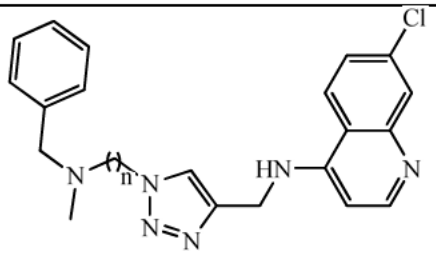	**69**	**65**
6h* and *6h'	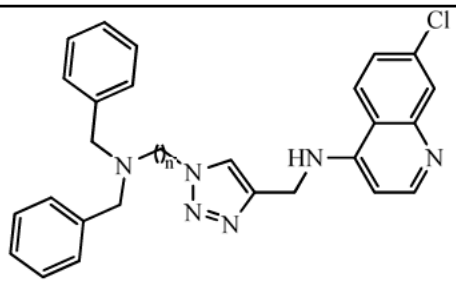	**54**	**63**
6i	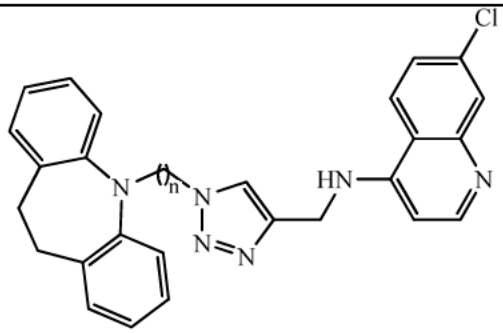	**—**	**64**

Under the above CuAAC reaction conditions utilised (refer to **figure 3.5.1**), the reactions carried out for longer than 120 minutes became thick slurries, perhaps due to coordination of the THF, the substrates or perhaps the products to free CuI forming insoluble organometallic compounds. In some cases, the products yields were lowered by the same effect as the work up procedure became difficult to perform. In addition, the presence of significant amounts of a poorly soluble by-product which could not be readily identified by ^{1}H NMR spectroscopy as a result of peak broadening in addition to poorly resolved ^{13}C NMR spectra, also complicated the experimental procedures.

A competitive oxidative Glaser coupling reaction is known to occur during CuAAC reaction, especially when direct Cu(I) salts are employed, but in our case there was no positive identification of the *bis*-acetylates of the alkyne precursor and thus the Glaser reaction was ruled out. The by-product was only occurring in prolonged reaction conditions, hence a longer (4 hour)

reaction was carried out and it was found that the intended product deteriorated until no product spot could be identified on the TLC. The 1,4-disubstituted triazole-linked chloroquinoline products (see **table 3.5.1**) were very polar, but fortunately a solvent system consisting of 10% methanol in acetone successfully developed analytical TLC for the compounds, at least two TLC runs in some cases. However, the by-product did not move from the TLC baseline with this mobile phase and increasing mobile phase polarity often resulted in poorly resolved TLC due to trailing.

3.6 Structural elucidation of the final CuAAC compounds

The structures of all the compounds obtained, ***6b*** – ***6i***, were established by ^{1}H NMR, ^{13}C NMR, ESI^{+} HRMS and IR spectroscopic methods. A representative characterisation of compound ***6f'*** is described below. In a deuterated chloroform, a similar ^{1}H NMR and ^{13}C NMR spectra pattern of the chloroquinoline ring (described under section **3.2**) was observed for all the compounds with the exception of signal migrations and swapping of the chemical environments between H-5 and H-8 (refer to **figure 3.6.1**). The order of chemical frequencies for H-5 and H-8 were swapped in the synthesized triazole derivatives as compared to the previously characterised aminoquinoline alkyne ***1***. The H-5 doublet had migrated to a lower frequency at 7.8 ppm in comparison to the initially observed 8.2 ppm in ***1***. In addition, the triazole proton H-5' appeared as a singlet in all the cases although a weak spatial coupling to the neighbouring protons was observed, as discussed later.

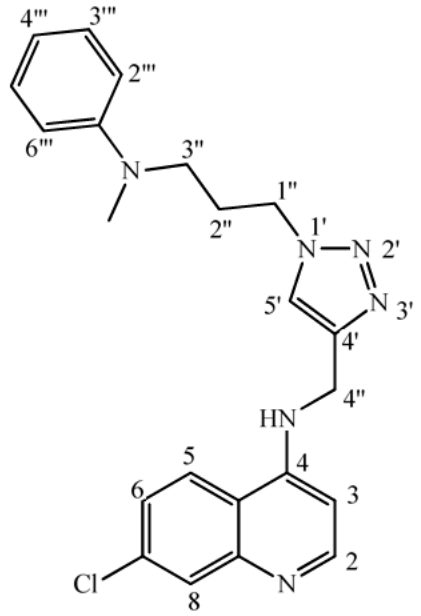

Figure 3.6.1 A representative characterisation of ***6f'*** by ^{1}H NMR and ^{13}C NMR spectroscopic methods.

With respect to compound ***6f'*** in **figure 3.6.1** above, the phenyl amine protons signals in the aromatic region were thus assigned as follows: 3 signals integrating in the ratios of 2:2:1 at 7.3 – 6.4 ppm were attributed to the aromatic protons H-2''' – H-6''' with $^{3}J_{H,H}$ *ortho* = 7.3 – 8.0 Hz where the signals multiplicity could be clearly identified as a triplet or a doublet. The broadened singlets at 6.1 ppm and 4.6 ppm were attributed to the N–H and H-4" protons, respectively. The triplets of the protons that appeared downfield were H-1" at 4.4 ppm and H-2" at 2.6 ppm compared to the chemical shifts of H-1" and H-2" (H-1" at 3.4 ppm and H-2" at 1.8 ppm) in the aliphatic azides chain, perhaps as a result of the triazole ring polarisation effects. The H-3" and N-CH_3 protons appeared at chemical shifts at 3.4 ppm and 2.9 ppm, respectively.

The ^{13}C NMR spectrum also supported the observations in the ^{1}H NMR spectrum. The disappearance of the alkyne carbon signals in the starting material, at 81 ppm and 74 ppm, with the concomitant appearance of two additional carbon signals in the aromatic region at 136 ppm and 122 ppm of the product, were conclusive that an aromatic 1,4-disubstituted triazole ring had been synthesized.

A homonuclear correlations $^{1}H–^{1}H$ COSY spectroscopy experiment was also performed on the related compound ***6c*** (refer to **figure 3.6.2**) to confirm the observed interactions between the protons (coupling constants, *J*). As mentioned earlier that there were changes in the chemical environments upon installing the triazole ring, a proper differentiation of the protons through $^{3}J_{H,H}$ was made possible by the COSY experiment. The absolute interaction between the protons ($^{3}J_{H,H}$ *ortho* coupling of H-5 and H-6, $^{3}J_{H,H}$ *meta* coupling of H-6 and H-8 and a very weak $^{3}J_{H,H}$ *para* coupling of H-5 and H-8) in the chloroquinoline ring and the vicinal protons was confirmed. In addition to the chloroquine protons, H-3 and H-5, spatial coupling with the H-4" protons was also observed. Of particular significance was that a weak cross-coupling between the triazole H-5' and both H-4" and H-1" protons hinted that a triazole ring was 1,4-regioisomer.

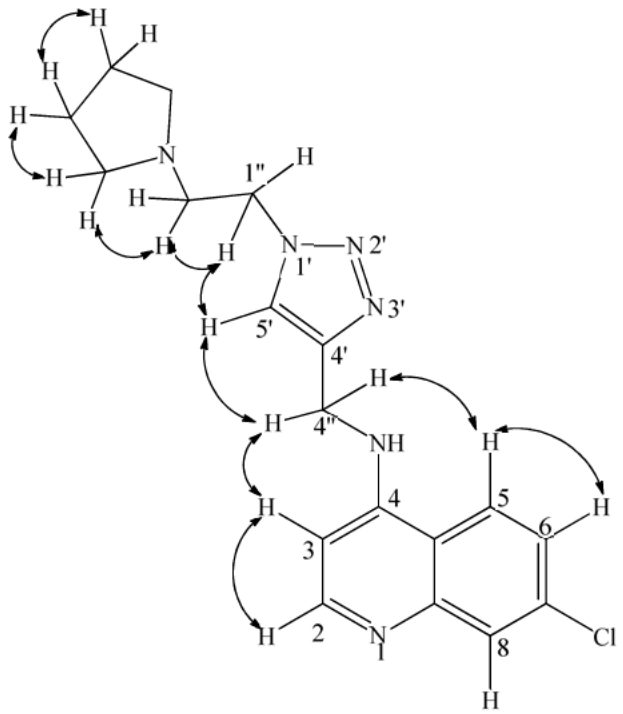

Figure 3.6.2 ^{1}H-^{1}H COSY correlations for compound ***6c***.

As previously mentioned in section **2.7**, the azides are ambivalent compounds and their reactivity is influenced by their mesomerism which can result in the formation of two possible product regioisomers. It was thus found necessary to confirm the synthesized compounds were indeed the

1,4-disubstituted triazole-linked chloroquinoline derivatives, and not the corresponding 1,5-derivatives.

To ascertain the 1,4-disubstitution and connectivity around the triazole ring, NMR spectroscopy experiments utilising gradient selected heteronuclear correlations over a single bond (gHSQCAD) and multiple bonds (gHMBC) were conducted for the compound ***6b'***. Having confirmed the proton correlations from the COSY NMR spectroscopy experiment, the gradient selected HSQCAD and HMBC spectroscopic experiments were used to trace the carbon skeleton of the identified triazole-linked chloroquinoline derivative. The HSQCAD spectra was used to selectively determine the single coherence between protons and carbons, $^{1}J_{C,H}$. From this experiment the carbon carrying the triazole proton (C-5') was clearly identified from the rest of the aromatic carbons, whose signals overlapped heavily (refer to **figure 3.6.3**). As it can be deduced from **figure 3.6.3**, it would have been very difficult to also distinguish C-5 at 121.3 ppm from the C-5' triazole carbon at 122.1 ppm. These two carbons could easily be misinterpreted when using normal APT and DEPT spectroscopic methods because of their equivalence on the ^{13}C NMR spectra. Furthermore, the regioisomeric nature of the triazole isomer could already be partly deduced at this point when taking into consideration the chemical shifts of C-5' triazole carbon at 122 ppm versus C-2 at 152 ppm of the chloroquinoline. Because these chemical shifts must be controlled by the pyrrole or the pyrimidine character of the neighbouring nitrogen atoms, it was obvious that the triazole C-5 resembled the pyrrole character which reserved for the 1,4-regiosomers that are unsubstituted at this position.

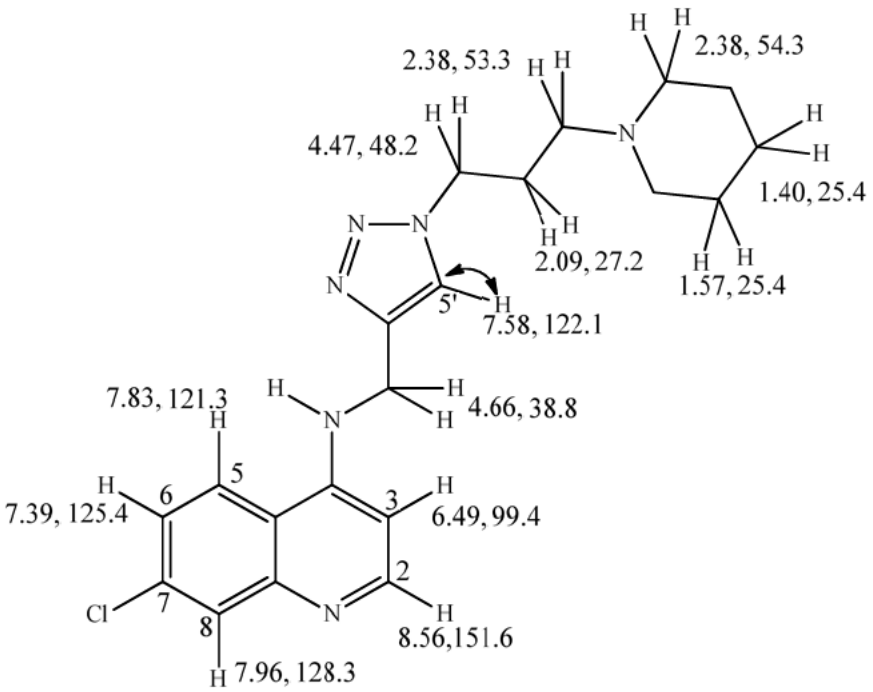

Figure 3.6.3 gHSCAD spectroscopy for $^{1}J_{C,H}$ correlations for compound ***6b'***

To justify the connectivity and nature of the triazole isomer, additional heteronuclear correlations over multiple bonds could safely be performed ($^{2}J_{C,H}$ and $^{3}J_{C,H}$) and a gHMBC spectroscopy experiment was thus conducted. Using the data from the HSQC spectra, the $^{2}J_{C,H}$ correlations of CH_2-1" and the CH-5' triazole protons were then determined (see **figure 3.6.4**). The C-1" is connected directly to a nitrogen atom of the triazole and the aliphatic chain C-2" and as a result of such connectivity the $^{2}J_{C,H}$ for CH_2-1" only displayed the correlations with the C-2". On the other hand, the $^{2}J_{C,H}$ on the triazole H-5' displayed the cross-coupling to a C-4' at 144 ppm of the triazole. Therefore, further $^{3}J_{C,H}$ investigations on the CH_2-1" proton showed additional correlations between with an aliphatic chain C-3" and C-5' of the triazole ring which were definitive in concluding the absolute structure of the triazole-linked chloroquinoline compounds ***6b*** – ***6i*** as the 1,4 derivatives.

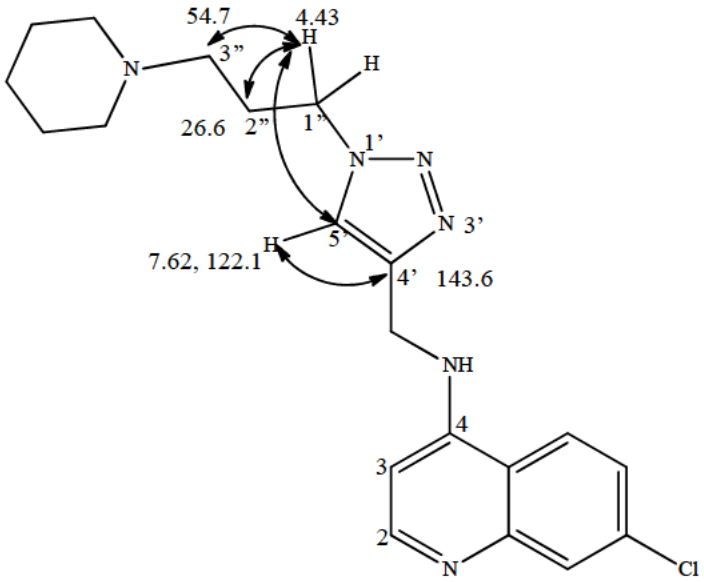

Figure 3.6.4 Multiple bond correlations (gHMBC) for ^{1}H and ^{13}C NMR spectra of compound ***6b'***.

As mentioned earlier, the ESI^{+} HRMS spectra showed the protonated molecular ions ($[M + H]^{+}$; *m/z*) as dominant species. The base peak on the *m/z* was sometimes determined to be a fragment or an adduct depending on how heavily the compound was fragmented or made into an adduct during the ionisation process. The similar signal patterns of 1 Da and dominant 2 Da were usually observed as a result of isotopic abundances, but similar cluster patterns were also observed at lower *m/z*, mainly due to a fragmentation. For instance, the mass spectra of the ***6g*** had 100% abundance molecular ion at m/z 407.1744, corresponding well to the theoretical *m/z* 407.1752. However, there was another *m/z* at 317.1293 with a similar cluster pattern as the molecular ion. The daughter peak was identified as a fragment resulting from secondary ionisation after molecular ion cleavage ion adjacent to the charged nitrogen atom as proposed in **figure 3.6.5**. These types of fragmentations, however, find a more important role when the elemental composition of compounds with unknown structure is of interest.

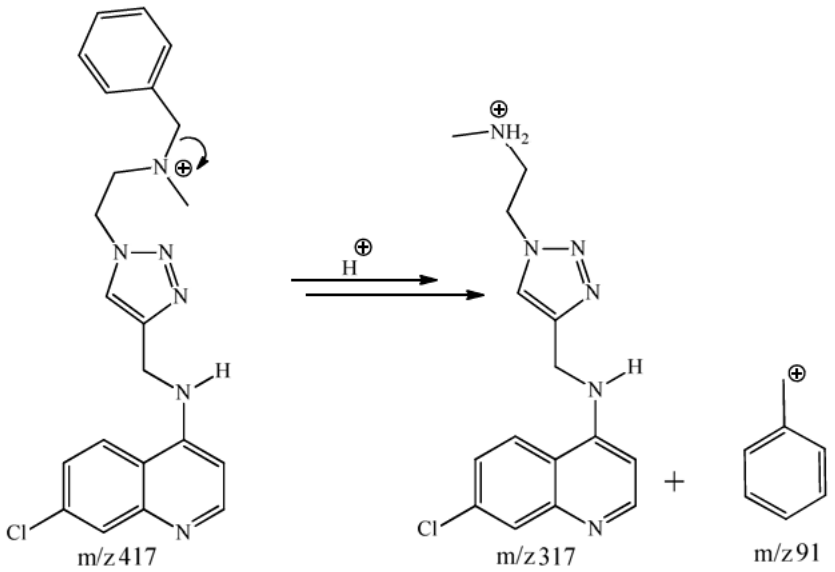

Figure 3.6.5 Bond cleavage with charge migration for ***6g*** under ESI^+ HRMS.

Finally, the use of IR spectroscopy was of limited use in the identification of the click products. For instance, in the IR spectra of the above compound, ***6g***, only a few dominant signals could be identified as peaks characteristic of functional groups found in the structure of this compound. These included the skeletal vibrations at frequencies (υ/cm^{-1}) 3493 (N–H), 2970 (CH), 1740 (C=C), 1368 (C–N) which were the typical identification peaks that have already been discussed earlier.

With the 1,4-disubstitted chloroquinoline derivatives at hand, susceptibility of human malaria strain of *P. falciparum* to these compounds was investigated *in vitro*.

3.7. Antimalarial activity

Among the purposes of this study, it was necessary to assess the ability of the synthesized compounds' antimalarial potency to inhibit *P. falciparum* strains (chemical structures of the test compounds can be reviewed on the pages 29, 43 – 44). The antimalarial potency in this context was measured from the inhibition concentration of the test compounds that produced 50% reduction in maximum growth or survival of *P. falciparum* cells in the culture media (IC_{50}). Therefore, a comparison of the *in vitro* activity of synthesized ***6b*** – ***6i*** with the reference drug CQ

and an artesunate standard was undertaken. The test compounds were evaluated on the asexual blood cycle stages, namely merozoites → trophozoites → schizonts that produce more merozoites of malaria parasitic infection.[131] At this stage, the blood cells are invaded and the symptoms of malaria infection become evident in a person suffering from malaria infection as the cycle continues. These blood schizonts can be destroyed by drugs such as CQ to terminate a continuous infection that causes red blood cell invasion by the merozoites.

The human malaria parasites rely on the anaerobic carbohydrate metabolism, i.e. glycolysis, for the supply of glucose and the pLDH enzyme which is produced during the process has been used as an index of reduction in the parasite multiplication.[132] The parasite lactate dehydrogenase (pLDH) levels[133] have been used in this study to assess *P. falciparum* strain NF54 sensitivity as a marker of antimalarial activity.

The synthesized compounds exhibited notable antiplasmodial activity with few exceptions and the data for the test compounds are illustrated in **figure 3.7.1**. Among the 15 tested compounds, 11 exhibited potent antimalarial activity below the 250 nM concentration. The highest concentration beyond which the exposed parasites had no measurable inhibition in the blank was out of measurable range and it is not shown. In addition, the inhibition activity of compound ***6h*** could not be measured under the concentration range investigated and a default IC_{50} value was extrapolated from the highest test concentration. Compound ***6e*** had a very low antiplasmodial activity but the complementary compounds ***6e'*** and ***6h'*** displayed good inhibition activities below 250 nM. The observation automatically made compounds ***6e*** and ***6h*** the qualified experimental outliers since the inhibition effect of the two compounds needed to produce 50% maximal inhibition effect was not certainly quantifiable under the concentration range investigated.

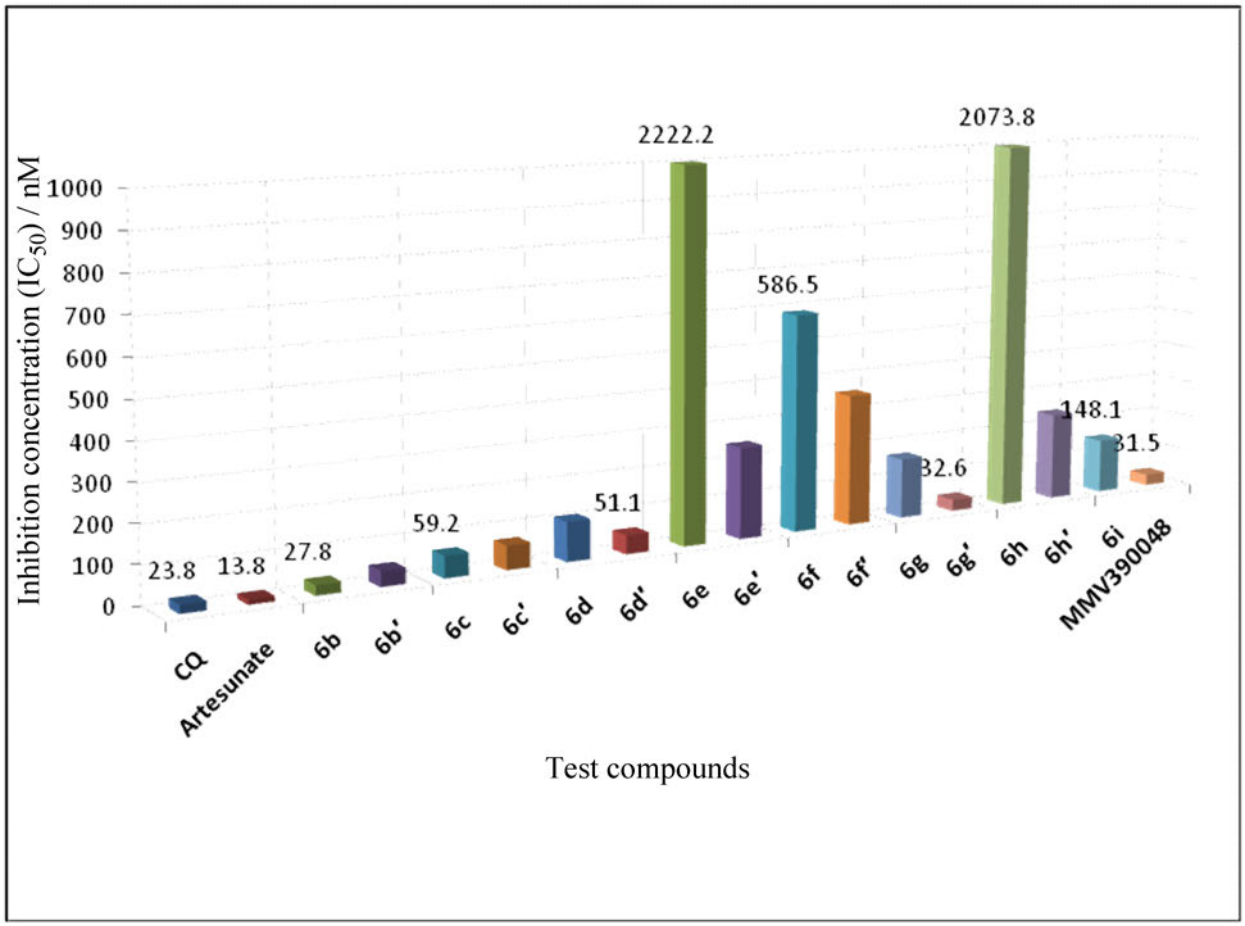

Figure 3.7.1 *In vitro* antiplasmodial activity of triazole-linked chloroquinoline derivatives ***6b*** – ***6i*** against NF54.

Compounds ***6f*** and ***6f′*** are a related pair that had lower activity status with IC_{50} values over 250 nM. These phenyl amine analogues, ***6f*** and ***6f′***, with activity in the range 247 – 587 nM were clearly distinguished from the structurally related benzyl amines, ***6g′*** and ***6g*** with activity range 32 – 163 nM. On some occasions the data for ***6b*** – ***6c′***, ***6d′*** and ***6g′*** compared closely to the standards; CQ, artesunate, and MMV 390048 (antimalarial drug in phase I clinical trials launched by the university of Cape Town), with the IC_{50} values being below 100 nM. Apart from ***6f*** and ***6f′***, the rest of aryl amine substituted compounds possessed inhibition activities below 250 nM while the aliphatic amines generally exhibited good inhibition activity below 100 nM, with the exception of the already mentioned outliers ***6e*** and ***6h***. Compounds ***6b*** and ***6b′*** were the aliphatic piperidinyl compounds with IC_{50} values in the range of 27 – 42 nM. The activity unfortunately did not reveal conclusive information on the variation of carbon chain length. The influence of chain length on

the activity varied between the individual pairs, but on average the aliphatic amine derivatives bearing an ethyl spacer were more active (***6b – 6d'***) than their counterparts with a propyl spacer. On the contrary, the activity order was reversed in the series of aryl amines, the compounds with a propyl spacer demonstrably being more active (***6f*** – ***6h'***).

Studies by Krogstad and co-workers, on the impact of the length of aliphatic chains in antimalarial activity have demonstrated that changes in the length have minimal impact on improving the activity in CQ sensitive strains of *P. falciparum*.[37,118] These observations are, however, in agreement with our results although the impact cannot be directly linked to the change in chain length as the triazole ring is also an important variable concerning the observed activities of the compounds. However it is tempting to suggest that the modifications, either chain length or incorporation of a triazole ring, perhaps constitute a primary recognition motif for the undiminished antimalarial activity of the compounds. The findings are valuable because homologation in the side chain alone alters the lipophilic character and thus is expected to affect the spatial relationship of functional groups in the molecule, and thereby influencing activity.

Other studies, from the literature, on CQ resistance reversal activity have provided substantial insights into the function of the lateral chain amine.[29] The essential features such as hydrogen bond acceptor capabilities, lipophilicity, and tertiary nitrogen atoms have been found to be optimal for activity in some CQ analogues.[52,134] Therefore the distal amine functionalities have also been associated with CQ reversal activity and on such grounds the SAR profiles of the triazole-linked CQ derivatives will have to be substantiated with the CQ resistant strains assays which are currently in progress. As aforementioned, asexual recombination of malaria parasites plays a crucial role in the development of treatment-resistive *P. falciparum* malaria. Thus the current inhibition activity results serve as a valuable prognostic indicator of the application of compounds containing a triazole linker in the restoration of antimalarial efficacy of CQ analogues.

Chapter 4

Summary, conclusion and recommendations

4.1 Summary and conclusion

The primary objectives of this work were successfully achieved. Synthesis of the chloroquinoline amino alkyne precursor ***1*** was successfully accomplished in a moderate yield of 63%. The azide building blocks were then synthesized in various yields (34 – 73%) and were obtained using different reaction routes as described in the dissertation. The triazole-linked chloroquinoline derivatives were then synthesized from chloroquinoline amino alkyne ***1*** and various aminoalkyl azides building blocks using a modular CuAAC reaction to obtain the compounds ***6b*** – ***6i*** within 30 – 90 minutes at room temperature, in moderate to good yields (53 – 85%). The characterisation and structural elucidation of the novel compounds was carried out using *inter alia* ^{1}H NMR, ^{13}C NMR, and ESI^{+} HRMS spectroscopic methods supported by the IR spectra. The antiplasmodial activity of the synthesized compounds was lastly investigated on the asexual blood stages of *P. falciparum* strain NF54. The *in vitro* biological investigations have showed the potential of a good antiplasmodial activity in some compounds which compared closely in activity to the standard antimalarial drugs.

In conclusion, a library of 15 4-aminoquinoline compounds, linked to a variety lipophilic aliphatic amino side chains by a 1,4-disubtituted 1,2,3-triazole has been created using the versatile CuAAC reaction. The compounds were synthesized in moderate to good yields and the *in vitro* antiplasmodial activity of the compounds is promising. The overall results have demonstrated that triazole-linked CQ analogues are potential inhibitors of *P. falciparum* with undiminished antimalarial activity. As there was more than one variable in the design of our compounds, including the introduction of a triazole linker as well as variation in chain lengths, the observed activity is attributable to the overall contribution of these modifications. Therefore, the results reported herein should be useful in guiding future efforts to discover CQ analogues with increased antimalarial activity. Consequently, the reported compounds are currently undergoing the *in vitro* antiplasmodial investigations.

4.2 Recommendations

Despite moderate to good synthetic results of the compounds, it has been observed that the use of excessive amounts of Cu(I) in the catalysis of amine bearing compounds can be disadvantageous even though it provides shorter reaction times and quick generation of compounds. Therefore, such syntheses should in future, be investigated using different Cu(I) sources at substoichiometric quantities. It has been shown that the triazole-linked chloroquinoline derivatives posses the antimalarial activity which justifies the compounds to be recognised as antimalarial agents.

In the recent literature, the investigations concentrating on the mode of action of CQ analogues and new targets for these compounds are evident. In terms of the latter research, these novel targets include proteases that are involved in haemoglobin degradation.[33,135] These findings necessitate further investigations as to whether there is an additional role that the triazole ring can play to potentially affect the antimalarial activity when used as a linker to various haematin complexing scaffolds. The inhibition of haemozoin formation is likely the mechanism by which the synthesized compounds exerted their antimalarial activity. However, a β-haematin inhibition assay which must reveal correlations between parasite inhibition and haemozoin formation is necessary to determine the mode of the antimalarial activity.[136] This should further serve in the SAR evaluation of the generated triazole-linked aminoquinoline derivatives in development on novel antimalarial compounds.

Chapter 5

Experimental data; chemical synthesis and *in vitro* biological investigations

5.1 General methods

Unless otherwise stated, all the reactions were carried out under inert nitrogen atmosphere in dried solvents using conventional distillation methods.

The ^{1}H, ^{13}C, COSY, gHMBC, and gHSQCAD NMR spectra were recorded on Varian Unity Inova spectrometers with ^{1}H frequency of 400MHz or 300 MHz, and ^{13}C frequency of 75 MHz or 150 MHz. All spectra were obtained on a 5mm dual broad band PFG probe with a probe temperature of 25 °C. The chemical shifts (δ) are reported in ppm relative to internal solvent peaks and the coupling constants (*J*) were measured in Hertz. The ^{1}H signals splitting pattern abbreviation were as follows: singlet (s), (doublet), triplet (t), quartet (q), quintet (p) doublet of doublet (dd), triplet of a doublet (td),multiplet (m), and a broadened signal was prefixed (br).

The fingerprint identification of specific functional groups was achieved by assigning of group frequencies (cm^{-1}) of particular peaks within the IR spectra. The IR spectra were obtained from Nexus infra-red Pc spectrometer equipped with a DTGS KBr detector and the percentage (%) transmittance was recorded against the wave length (υ/cm^{-1}) for the reported signals. The high resolution mass spectra were recorded on electrospray ionisation on positive mode (ESI^{+}) using a quadrupole MALDI-TOF LC/MS instrument.

Preparative column chromatography was carried out on a silica gel 60; 70 – 230 mesh ASTM, Fluka. Thin layer chromatography (TLC) was performed using pre-coated aluminium silica gel plates ($60F_{254}$ Merck) and the developed TLCs for the compounds were viewed after staining or under UV (254nm) light. Aliphatic mesylate intermediates were detected by means of $KMNO_4$ stain and their corresponding azides were visualized after a contrast Ruhemann's purple colour was developed with a ninhydrin stain following a TLC azide to amine reduction.[121]

Finally, the melting points were determined on a variable heat Gallenkamp melting point apparatus (temperature range 20 – 350 °C) equipped with a laboratory thermometer, and are uncorrected.

5.2. Chemical syntheses

5.2.0.1 *7-Chloro-N-(prop-2-yn-1-yl)quinolin-4-amine (**1**).*

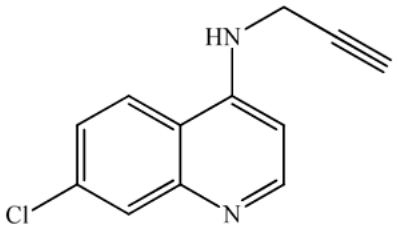

In a Schlenk reaction tube, a solution of 4,7-dichloroquinoline (500 mg, 2.52 mmol) and a catalytic amount of anhydrous *p*TSA (43 mg, 0.25 mmol, 10 mol %) in 1,4-dioxane (0.5 mL) was stirred at 50 °C for 30 minutes. To the solution, propargyl amine (0.35 mL, 5.1 mmol) was added and the Schlenk tube was sealed with a stopper; the reaction was then stirred for 24 hours at 85 °C. After cooling to a room temperature, 10% aqueous $NaHCO_3$ (20 mL) was added and the product was extracted into DCM (3 × 20 mL). The extract was dried with $MgSO_4$ and the organic solvent was evaporated under vacuum and the crude product was purified through a silica gel column (Hex/EtOAc; 6:4) to obtain compound ***1*** (344 mg, 63% yield) as an off-white to a pale yellow solid (mp: 186 – 190 °C).

IR υ_{max} 3461 (NH), 3089 (Ar CH), 2947 & 2872 (aliphatic CH), 2161 (C≡C), 1573 (C=C); ^{1}H NMR (300 MHz, DMSO) δ 8.49 (d, J = 5.4 Hz, 1H), 8.19 (d, J = 9.0 Hz, 1H), 7.83 (d, J = 2.2 Hz, 1H), 7.76 (t, J = 5.7 Hz, 1H), 7.49 (dd, J = 9.0, 2.3 Hz, 1H), 6.59 (d, J = 5.4 Hz, 1H), 4.14 (dd, J = 5.7, 2.3 Hz, 2H), 3.19 (t, J = 2.3 Hz, 1H); ^{13}C NMR (75 MHz, DMSO) δ 152.3, 149.7, 149.4, 134.0, 128.0, 125.0, 124.3, 118.0, 100.3, 80.9, 74.2, 32.0; MS (ESI$^+$) 217.0533 calculated for $C_{12}H_9ClN_2$ $[M + H]^+$, found 217.0529 (-1.84 ppm).

5.2.0.2 *Ethane-1,2-diyl dimethanesulfonate (**2a**).*

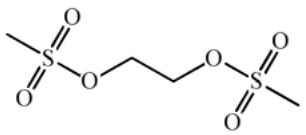

Compounds ***2a*** and ***2a'*** were prepared by the same method; a representative procedure for the synthesis ***2a***, carried out according a literature procedure,[119] using THF as a solvent is described below. In the round-bottomed flask placed in water was added a THF solvent (200 mL), ethane-

1,2-diol (4.50 mL, 0.08 mol) and Et_3N (34.0 mL, 0.24 mmol). After stirring the solution for about 5 minutes, mesyl chloride (15.0 mL, 193.9 mmol) was added in a drop-wise manner via a syringe for about 10 minutes. The reaction was stirred for 1 h at 0 °C then warmed to room temperature under continuous stirring for another 3 h. The white precipitate removed by filtration and excess THF solvent was evaporated *in vacuo* to obtain a pale yellow oil. The oil was purified on a silica gel column using 20% ethyl acetate in hexane to afford ***2a*** as colourless oil (16.5 g, 94% yield) that slowly solidified to an off-white solid after drying. The ^{1}H NMR and ^{13}C NMR spectroscopic data for ***2a*** was found to match cited literature values as shown below.[119]

IR υ_{max} 2961 – 2789 ($CH_{stretch}$), 1352 (CH_{bend}), 1173 (S=O), 1045 (S–O); ^{1}H NMR (400 MHz, $CDCl_3$) δ 4.47 (s, 4H), 3.08 (s, 6H); ^{13}C NMR (75 MHz, $CDCl_3$) δ 66.6, 36.8.

5.2.0.3 *Propane-1,3-diyl dimethanesulfonate (**2a'**).*

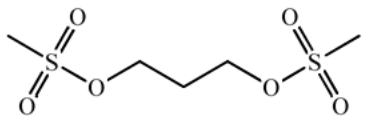

Compound ***2a'*** was obtained as a colourless oil (14.7 g, 99% yield) prepared from propane-1,3-diol and the spectroscopic data was found to be consistent with the literature.[120]

IR υ_{max} 3019 – 2944 (CH), 1359 (CH), 1176 (S=O), 1048 (S–O), 922, 743 ($CH_{rocking}$); ^{1}H NMR (300 MHz, $CDCl_3$) δ 4.33 (t, J = 7.2 Hz, 4H), 3.04 (s, 6H), 2.02 (p, J = 7.6, 4.5 Hz, 2H); ^{13}C NMR (101 MHz, $CDCl_3$) δ 66.8, 37.5, 28.9.

5.2.0.4 *2-Azidoethyl methane sulfonate (**3a**).*

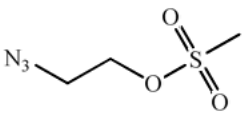

As azidation reactions of both compounds ***3a*** and ***3a'*** were similar, a representative literature procedure is described here.[119] Compound ***2a*** (10.0 g, 0.05 mol) was dissolved in MeCN (200 mL), sodium azide (3.6 g, 0.06 mol) was added and the reaction mixture was heated at 80 °C for 12 h. The white precipitated was removed by filtration, excess solvent was evaporated *in vacuo* and the crude product was purified on a silica gel column using 30% ethyl acetate in hexane as

eluant to give ***3a*** (3.18 g, 42% yield) as a colourless oil. The NMR spectroscopic data, referred below, resembled the cited literature.[119]

IR υ_{max} 2963 – 2784 (CH), 2136 (N≡N), 1347 (C–N), 1163 (S=O), 917 (S–O); ^{1}H NMR (300 MHz, $CDCl_3$) δ 4.28 (t, *J* = 7.7 Hz, 2H), 3.53 (t, *J* = 6.5 Hz, 2H), 3.02 (s, 1H); ^{13}C NMR (101 MHz, $CDCl_3$) δ 66.4, 48.9, 36.8.

5.2.0.5 *3-Azidopropyl methane sulfonate (**3a'**).*

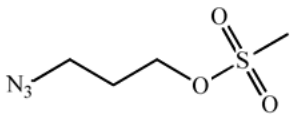

A colourless oil of ***3a'*** (5.00 g, 46% yield) was obtained from ***2a'*** at 14 g scale. The ^{1}H NMR spectroscopic data was analogous to the literature data.[122]

IR υ_{max} 3029 – 2938 (CH), 2136 (N≡N), 1347 (C–N), 1163 (S=O), 967 (S–O), 915, 780;^{1}H NMR (300 MHz, $CDCl_3$) δ 4.34 (t, *J* = 6.0 Hz, 2H), 3.50 (t, *J* = 6.5 Hz, 2H), 3.05 (s, 3H), 2.02 (p, *J* = 6.4 Hz, 2H); ^{13}C NMR (75MHz, $CDCl_3$) δ 66.5, 47.4, 37.4, 28.7.

5.2.0.6 *1-(2-Azidoethyl)piperidine (**4b**).*

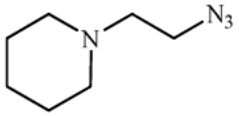

Compounds ***4b – 4e'*** were synthesized using a similar method, with the exception of ***4c*** and ***4c'***, obtained from literature[119] and a representative procedure for compound ***4b*** is described in detail below. The compounds were prepared from azido mesylates ***3a*** and ***3a'*** in excess amounts of 500 mg with minor modifications. To a stirred solution of ***3a*** (500 mg, 3.03 mmol) and K_2CO_3 (1.25 mg, 9.09 mmol) in MeCN (15 mL) was added piperidine (0.25 mL, 2.55 mmol). The resulting mixture was heated at reflux overnight, the K_2CO_3 was removed by filtration, and excess solvent was removed by evaporating *in vacuo* to obtain a crude product. A colourless oil of ***4b*** (282 mg, 72% yield) was obtained after purification by silica gel chromatography using 70% EtOAc/Hex as eluant. The ^{1}H MNR data for ***4b*** was found to be in good agreement with the data reported by Benalil *et al.*[137]

IR υ_{max} 2943 – 2810 (CH), 2096 (N≡N), 1451, 1281 (C–N), 1115; ^{1}H NMR (300 MHz, $CDCl_3$) δ 3.34 (t, *J* = 6.3 Hz, 2H), 2.55 (t, *J* = 6.3 Hz, 2H), 2.43 (br t, *J* = 6.2 Hz, 4H), 1.57 (p, *J* = 6.2 Hz, 4H), 1.43 (ddd, *J* = 9.0, 6.2, 2.2 Hz, 2H); ^{13}C NMR (75 MHz, $CDCl_3$) δ 57.8, 54.6, 48.4, 25.7, 24.3.

5.2.0.7 *1-(3-Azidopropyl)piperidine (**4b'**).*

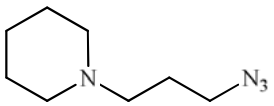

Compound ***4b'*** was obtained as a pale yellow oil (273 mg, 70% yield) using the method already described for ***4b***.The NMR data was found to match the cited literature.[138]

IR υ_{max} 2933 – 2799 (CH), 2093 (N≡N), 1445, 1278 (C–N), 1123; ^{1}H NMR (300 MHz, $CDCl_3$) δ 3.33 (t, *J* = 6.8 Hz, 2H), 2.37 (td, *J* = 7.9, 6.7 Hz, 6H), 1.79 (p, *J* = 6.9 Hz, 2H), 1.59 (td, *J* = 10.8, 5.6 Hz, 4H), 1.41 (dd, *J* = 12.2, 7.2 Hz, 2H); ^{13}C NMR (75 MHz, $CDCl_3$) δ 56.2, 54.6, 49.8, 26.4, 26.0, 24.4.

5.2.0.8 *1-(2-Azidoethyl)pyrrolidine (**4c**).*

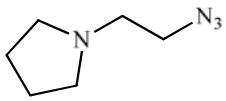

Compounds ***4c*** and ***4c'*** were synthesized by the same method the corresponding azido mesylates ***3a*** and ***4a'*** by adapting a literature method as follows:[123] to a stirred solution of methane sulfonate ***3a*** (500 mg, 3.03 mmol) in THF (15 mL) were added K_2CO_3 (1250 mg, 9.09 mmol) and pyrrolidine (0.21 mL, 2.53 mmol) at 0°C. The resulting mixture was allowed to warm to room temperature and then heated at reflux overnight. The reaction mixture was diluted with DCM (15 mL), the K_2CO_3 was removed by filtration and the excess organic solvent was evaporated to obtain a crude product that was purified by silica gel column using 50% EtOAc/Hex to afford ***4c*** as a pale yellow oil (204 mg, 64%). The NMR data for ***4c*** was consistent with the same compound reported in the literature.[139]

IR υ_{max} 2933 (CH), 2093 (N≡N), 1278 (C–N); ^{1}H NMR (300 MHz, $CDCl_3$) δ 3.38 (t, *J* = 6.4 Hz, 2H), 2.67 (t, *J* = 6.4 Hz, 2H), 2.56 – 2.52 (m, 4H), 1.79 (td, *J* = 6.4, 3.1, 4H); ^{13}C NMR (75 MHz, $CDCl_3$) δ 54.9, 54.2, 50.2, 23.5.

5.2.0.9 *1-(3-Azidopropyl)pyrrolidine (**4c′**).*

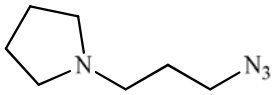

Compound ***4c′*** was prepared using the experimental procedure already described above to afford a pale yellow oil (261 mg, 73% yield).

Yield 73%, IR υ_{max} 2961 – 2789 (CH), 2093 (N≡N), 1456, 1276 (C–N), 1147; ^{1}H NMR (300 MHz, $CDCl_3$) δ 3.36 (t, *J* = 6.8 Hz, 2H), 2.57 – 2.45 (m, 6H), 1.87 – 1.72 (m, 6H); ^{13}C NMR (151 MHz, $CDCl_3$) δ 54.2, 53.3, 49.7, 28.4.4, 23.4; MS (ESI^+) 155.1297 calculated for $C_7H_{14}N_4$ $[M + H]^+$, found 155.1297 (100%, 0.00 ppm), 84.0182 (40%).

5.2.1.0 *2-Azido-N,N-diethylenamine (**4d**).*

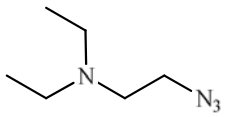

Compound ***4d*** was synthesized from ***3a*** using the same methods already described for ***4b*** to obtain a colourless oil (189 mg, 48%). The ^{1}H NMR spectra was found to be similar with one reported in the literature.[140]

IR υ_{max} 2947 – 2791 (CH), 2092 (N≡N), 1453, 1253 (C–N); ^{1}H NMR (300 MHz, $CDCl_3$) δ 3.29 (t, *J* = 6.3 Hz, 2H), 2.66 (t, *J* = 7.4 Hz, 2H), 2.57 (q, *J* = 6.1 Hz, 4H), 1.04 (t, *J* = 7.1 Hz, 6H); ^{13}C NMR (75 MHz, $CDCl_3$) δ 52.1, 49.5, 47.2, 11.8.

5.2.1.1 *3-Azido-N,N-diethylpropan-1-amine (**4d′**).*

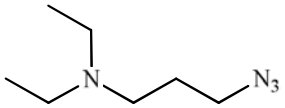

Compound ***4d′*** was prepared as in ***4d*** to afford a colourless oil (129 mg, 36% yield).

IR υ_{max} 2942 (CH), 2097 (N≡N), 1343 (C–N), 1169; ^{1}H NMR (300 MHz, $CDCl_3$) δ 3.34 (t, *J* = 6.8 Hz, 2H), 2.52 (ddd, *J* = 8.0, 7.3, 5.0 Hz, 6H), 1.73 (p, *J* = 6.8 Hz, 2H), 1.03 (t, *J* = 7.3 Hz, 6H); ^{13}C NMR (75 MHz, $CDCl_3$) δ 49.8, 46.8, 31.8, 29.3, 11.5; MS (ESI^+) 157.1454 calculated for $C_7H_{16}N_4$ $[M + H]^+$, found 157.1446 (-5.09 ppm).

5.2.1.2 *4-(2-Azidoethyl)morpholine (**4e**).*

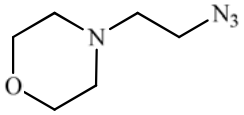

Compound ***4e*** was also prepared similarly to ***4d*** and the product was obtained as a colourless oil (271 mg, 69% yield).

IR υ_{max} 2933 – 2789 (CH), 2093(N≡N), 1276 (C–N), 1147; ^{1}H NMR (300 MHz, $CDCl_3$) δ 3.73 (t, *J* = 4.8 Hz, 4H), 3.35 (t, *J* = 6.4 Hz, 2H), 2.60 (t, *J* = 6.0 Hz, 2H), 2.51 (t, *J* = 4.8 Hz, 2H); ^{13}C NMR (75 MHz, $CDCl_3$) δ 66.9, 57.6, 53.6, 47.9.

5.2.1.3 *4-(3-Azidopropyl)morpholine (**4e′**).*

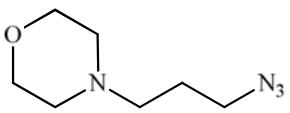

Compound ***4e′*** was prepared in a similar fashion to ***4d*** to recover a product as a colourless oil (268 mg, 68% yield).[141]

IR υ_{max} 2947 – 2810 (CH), 2096 (N≡N), 1451, 1281 (C–N), 1115, 1069 (COC); ^{1}H NMR (300 MHz, $CDCl_3$) δ 3.71 (t, *J* = 4.5 Hz, 4H), 3.35 (t, *J* = 6.7 Hz, 2H), 2.50 – 2.32 (m, 6H), 1.77 (p, *J* = 6.0 Hz, 2H); ^{13}C NMR (75 MHz, $CDCl_3$) δ 66.9, 55.6, 53.6, 47.5, 25.9.

5.2.1.4 *General procedure for alkylation of N-(benzyl or phenyl)amine (**4f – 4h'**).*

Compounds ***4f – 4h'*** were prepared from ***3a*** and ***3a'*** by as described in the following procedure.[119,142] To a solution of ***3a*** (500 mg, 3.03 mmol) and K_2CO_3 (1250 mg, 9.09 mmol) in MeCN (15 mL) were added KI (38.2 mg, 0.20 mmol) and an appropriate aryl amine (2.02 mmol). The resulting mixture was continuously stirred at 90 °C until TLC displayed complete consumption of the starting material (28 h for benzylamines and 72 h for phenylamine). The K_2CO_3 was removed by filtration, after which the solvent was evaporated *in vacuo*, the crude was rinsed with 10% $Na_2S_2O_4$ (20 mL) and then extracted into DCM (3 × 20 mL). The extract was dried with MgSO4 and the solvent was removed under vacuum to obtain a crude product that was purified on a silica gel column using hexane to afford the products described below.

5.2.1.5 *N-(2-Azidoethyl)-N-methylaniline (**4f**).*

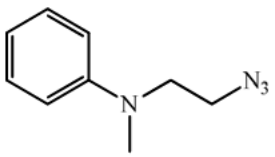

A pale yellow oil (121 mg, 34% yield).

IR υ_{max} 2947 – 2791 (aliphatic CH), 2092 (N≡N), 1741 (C=C), 1453, 1253 (C–N), 1141; ^{1}H NMR (300 MHz, $CDCl_3$) δ 7.33 – 7.23 (m, 2H), 6.81 – 6.71 (m, 3H), 3.57 (t, J = 5.7 Hz, 2H), 3.47 (t, J = 5.7 Hz, 2H), 3.03 (s, 3H); ^{13}C NMR (75 MHz, $CDCl_3$) δ 148.9, 129.3, 116.3, 111.9, 52.0, 49.8, 38.7, 29.7; MS (ESI$^+$) 177.1142 calculated for $C_9H_{12}N_4$ $[M + H]^+$, found 177.1142 (0.00 ppm).

5.2.1.6 *N-(3-Azidopropyl)-N-methylaniline (**4f'**).*

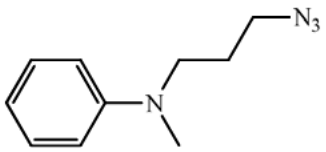

A pale yellow oil (131 mg, 37% yield).

IR υ_{max} 3140 – 3056 (Ar CH), 2945 – 2875 (aliphatic CH), 2092 (N≡N), 1588 (C=C), 1492, 1243 (C–N); ^{1}H NMR (300 MHz, $CDCl_3$) δ 7.32 – 7.21 (m, 2H), 6.79 – 6.71 (m, 3H), 3.45 (t, J = 6.5 Hz, 2H), 3.40 (t, J = 6.5 Hz, 2H), 2.97 (s, 3H), 1.89 (p, J = 6.6 Hz, 2H); ^{13}C NMR (75 MHz, $CDCl_3$) δ 149.3, 129.3, 116.5, 112.2, 49.7, 49.8, 49.0, 38.8, 26.3; MS (ESI^+) 191.1294 calculated for $C_{10}H_{14}N_4$ $[M + H]^+$, found 191.1294 (-1.57 ppm).

5.2.1.7 *2-Azido-N-benzyl-N-methylethanamine (**4g**).*

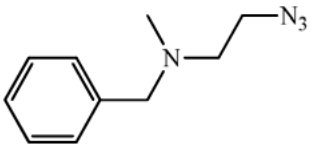

A colourless oil (157 mg, 41% yield).

IR υ_{max} 2941 – 2791 (aliphatic CH), 2092 (N≡N), 1588 (C=C), 1453, 1253 (C–N), 735; ^{1}H NMR (300 MHz, $CDCl_3$) δ 7.41 – 7.23 (m, 5H), 3.59 (s, 2H), 3.36 (t, J = 6.1 Hz, 2H), 2.67 (t, J = 6.1 Hz, 2H), 2.29 (s, 3H); ^{13}C NMR (151 MHz, $CDCl_3$) δ 138.7, 128.8, 128.3, 127.1, 62.5, 56.2, 48.9, 42.2; MS (ESI^+) 191.1297 calculated for $C_{10}H_{14}N_4$ $[M + H]^+$, found 191.1300 (1.57 ppm).

5.2.1.8 *3-Azido-N-benzyl-N-methylpropan-1-amine (**4g'**).*

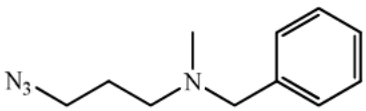

A colourless oil (178 mg, 47% yield).

IR υ_{max} 3096 – 3059 (Ar CH), 2937 – 2873 (aliphatic CH), 2090 (N≡N), 1598 and 1503 (C=C), 1366, 1258 (C–N); ^{1}H NMR (300 MHz, $CDCl_3$) δ 7.38 – 7.22 (m, 5H), 3.51 (s, 2H), 3.37 (t, J = 6.9 Hz, 2H), 2.48 (t, J = 6.9 Hz, 2H), 2.21 (s, 3H), 1.80 (p, J = 6.9 Hz, 2H); ^{13}C NMR (151 MHz, $CDCl_3$) δ 139.0, 128.9, 128.2, 126.9, 62.4, 54.2, 49.5, 42.0, 25.5; MS (ESI^+) 205.1454 calculated for $C_{11}H_{16}N_4$ $[M + H]^+$, found 205.1457 (1.46 ppm).

5.2.1.9 *2-Azido-N,N-dibenzylethanamine (**4h**).*

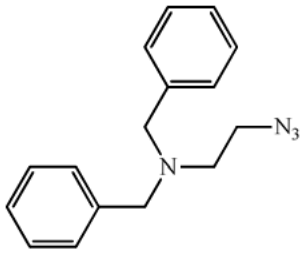

A colourless oil (327 mg, 61% yield) that slowly solidified into an off-white solid at room temperature.

IR υ_{max} 3021 (Ar CH), 2947 – 2796 (aliphatic CH), 2089 (N≡N), 1493 (C=C), 1449, 1294 (C–N); ^{1}H NMR (300 MHz, $CDCl_3$) δ 7.47 – 7.25 (m, 10H), 3.67 (s, 4H), 3.28 (t, J = 6.1 Hz, 2H), 2.74 (t, J = 6.1 Hz, 2H); ^{13}C NMR (75 MHz, $CDCl_3$) δ 139.02, 128.8, 128.4, 127.1, 58.9, 53.0, 49.3; MS (ESI$^+$) 267.1610 calculated for $C_{16}H_{18}N_4$ $[M + H]^+$, found 267.1610 (0.00 ppm).

5.2.2.0 *3-Azido-N,N-dibenzylpropan-1-amine (**4h'**).*

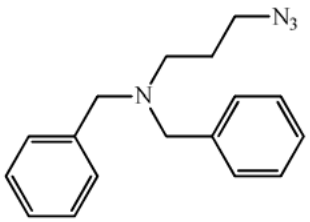

A pale yellow oil (296 mg, 57% yield).

IR υ_{max} 3021 (Ar CH), 2947 – 2796 (aliphatic CH), 2093 (N≡N), 1490 (C=C), 1449, 1294 (C–N); ^{1}H NMR (400 MHz, $CDCl_3$) δ 7.37 – 7.22 (m, 10H), 3.56 (s, 4H), 3.29 (t, J = 7.0 Hz, 2H), 2.51 (t, J = 6.8 Hz, 2H), 1.75 (p, J = 6.9 Hz, 2H); ^{13}C NMR (75 MHz, $CDCl_3$) δ 138.6, 128.9, 128.3, 127.1, 62.6, 56.2, 48.9, 42.2; MS (ESI$^+$) 281.1767 calculated for $C_{17}H_{20}N_4$ $[M + H]^+$, found 281.1775 (2.85 ppm).

5.2.2.1 *Synthesis of 5-(3-Chloropropyl)-10,11-dihydro-5H-dibenzo[b,f]azepine (**5a'**).*

Compound ***5a'*** was synthesized by adapting a procedure from the literature methods as described.[126-127] In a Schlenk reaction tube, 10,11-dihydro-5*H*-dibenzo[*b*,*f*]azepine (252 mg, 1.29 mmol) was dissolved in C_6H_6-THF (1:4, 10 mL) to which was added *n*BuLi (0.76 mL, 1.20 mmol) in a drop-wise fashion under a constant stirring for 30 minutes at 0 °C. The reaction was allowed to warm to room temperature after which 1-bromo-3-chloropropane (0.160 mL, 55 mmol) was added and stirring was continued for 4 hours. The resultant light brown solution was concentrated *in vacuo* and the crude product was purified on a silica gel column using hexane eluant to isolate a mixture of ***5a*** and ***5a'*** with the amounts described below.

*5-allyl-10,11-dihydro-5H-dibenzo[b,f]azepine (**5a**).*

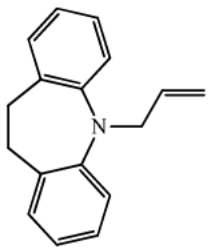

A colourless oil (70 mg, 23 % yield).

IR υ_{max} 3058 – 3022 (Ar CH), 2917 – 2842 (aliphatic CH), 1588 and 1485 (C=C), 1448, 1333 and 1227 (C–N), 1112, 742; ^{1}H NMR (300 MHz, $CDCl_3$) δ 7.21 – 7.03 (m, 6H), 7.00 – 6.89 (m, 2H), 5.82 (ddt, *J* = 17.3, 10.3, 5.7 Hz, 1H), 5.28 (dq, *J* = 17.3, 1.6 Hz, 1H), 5.12 (dq, *J* = 10.3, 1.5 Hz, 1H), 4.43 (dt, *J* = 5.7, 1.6 Hz, 2H), 3.20 (s, 4H); ^{13}C NMR (75 MHz, $CDCl_3$) δ 148.0, 135.6, 134.1, 129.7, 126.2, 122.4, 120.4, 117.1, 54.4, 32.4.

*5-(3-chloropropyl)-10,11-dihydro-5H-dibenzo[b,f]azepine (**5a'**).*

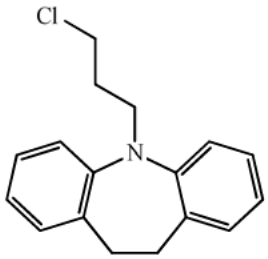

A pale yellow solid (84 mg, 24 % yield).

Melting point: 43 – 45 °C; IR υ_{max} 3056 (Ar CH), 2953 (aliphatic CH), 1587 (C=C), 1492, 1364, 1265 and 1244 (C–N), 747, 693 (C–Cl) ; ^{1}H NMR (300 MHz, $CDCl_3$) δ 7.25 – 7.05 (m, 6H), 7.01 – 6.94 (m, 2H), 3.94 (t, J = 6.5 Hz, 2H), 3.60 (t, J = 6.5 Hz, 2H), 3.20 (s, 4H), 2.08 (p, J = 6.4 Hz, 2H); ^{13}C NMR (75 MHz, $CDCl_3$) δ 147.0, 133.3, 128.9, 125.4, 121.7, 118.8, 46.5, 41.9, 31.1, 29.6; MS (ESI^+) 272.1207 calculated for $C_{17}H_{18}ClN$ $[M + H]^+$, found 272.1215 (-2.94 ppm).

5.2.2.2 *5-(3-Azidopropyl)-10,11-dihydro-5H-dibenzo[b,f]azepine (**4i**).*

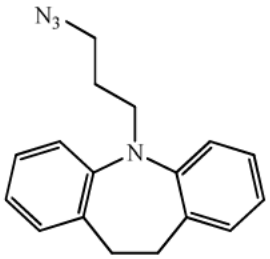

Compound ***5a'*** (70 mg, 0.26 mmol) was dissolved in C_6H_6 (2.5 mL) and to this was transferred NaN_3 (25 mg, 0.39 mmol) in DMSO (2.5 mL). The reaction was then stirred at 100 °C until TLC showed a complete consumption of the starting material (48 h). The reaction mixture was then diluted with distilled water (15 mL) and the product was extracted into DCM (3 × 15 mL). The extract was dried with $MgSO_4$ and the organic solvent was evaporated *in vacuo* and ***4i*** (61%, 44 mg) was obtained as a pale yellow oil after silica gel column purification using hexane as eluant.

IR υ_{max} 3057 (Ar CH); 2921 – 2843 (aliphatic CH), 2091 (N≡N), 1592 (C=C), 1485, 1229 (C–N), 1112; ^{1}H NMR (300 MHz, $CDCl_3$) δ 7.23 – 7.06 (m, 6H), 7.02 – 6.92 (m, 2H), 3.86 (t, J = 6.7 Hz, 2H), 3.36 (t, J = 6.7 Hz, 2H), 3.19 (s, 4H), 1.89 (p, J = 6.6 Hz, 2H); ^{13}C NMR (75 MHz, $CDCl_3$) δ

148.0, 134.3, 130.0, 126.5, 122.8, 119.8, 49.6, 47.5, 32.2, 27.2; MS (ESI^+) 279.1610 calculated for $C_{17}H_{18}N_4$ $[M + H]^+$, found 279.1619 (3.22 ppm).

5.2.2.3 *General procedure for CuAAC reactions of chloroquine derivatives (**6b** – **6i**).*

Coupling reactions were carried out using a literature procedure[130] with minor modifications. In a 2.5 mL round-bottomed flask, ***1*** (20 mg, 0.09 mmol) and CuI (17 mg, 0.09 mmol) were dissolved in anhydrous THF (0.5 mL). To this was added appropriate alkyl azide (0.08 mmol) and the reaction was then stirred for 30 – 90 minutes at room temperature, until the starting material was consumed. The reaction mixture was diluted with DCM (2 mL), the CuI was removed by filtration, and the crude product was purified on a silica gel column under gradient elution with 50% EtOAc:Hex to 10% MeOH:Me_2CO as eluant. The product quantities, as well as the nature and description that were obtained are given below.

5.2.2.4 *7-Chloro-N-((1-(2-(piperidin-1-yl)ethyl)-1H-1,2,3-triazol-4-yl)methyl)quinolin-4-amine (**6b**).*

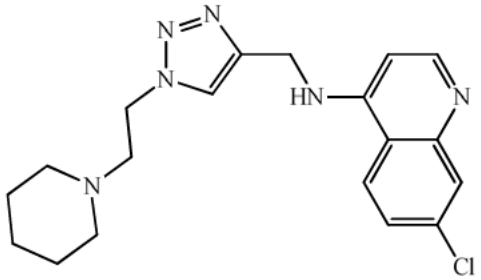

A light yellow solid (22 mg, 76% yield, mp: 132 – 134 °C).

IR υ_{max} 3336 (NH), 3145 (Ar CH), 2925 – 2854 (aliphatic CH), 1576 (C=C), 1451, 1370 (C–N); ^1H NMR (400 MHz, $CDCl_3$) δ 8.53 (d, J = 5.2 Hz, 1H), 7.96 (d, J = 2.1 Hz, 1H), 7.77 (s, 1H), 7.74 (d, J = 9.0 Hz, 1H), 7.38 (dd, J = 6.8, 2.0 Hz, 1H), 6.52 (d, J = 5.4 Hz, 1H), 5.95 (br s, 1H), 4.63 (d, J = 4.1 Hz, 2H), 4.45 (t, J = 6.2 Hz, 2H), 2.75 (t, J = 6.2 Hz, 2H), 2.48 – 2.36 (m, 4H), 1.51 (td, J = 9.7, 4.3 Hz, 4H), 1.46 – 1.38 (m, 2H); ^{13}C NMR (75 MHz, $CDCl_3$) δ 150.3, 148.4, 147.7, 143.0, 134.2, 127.4, 124.6, 121.2, 120.4, 116.2, 98.4, 54.0, 53.3, 47.3, 38.0, 26.1, 24.6; MS (ESI^+) 371.1752 calculated for $C_{19}H_{23}ClN_6$ $[M + H]^+$, found 371.1751 (-0.27 ppm).

5.2.2.5 *7-Chloro-N-((1-(3-(piperidin-1-yl)propyl)-1H-1,2,3-triazol-4-yl)methyl)quinolin-4-amine* ***(6b')***.

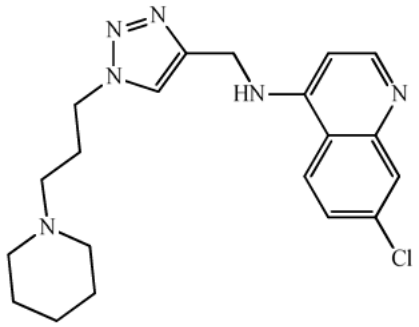

A light yellow solid (23 mg, 79% yield, mp: 133 – 135).

IR υ_{max} 3489 – 3390 (NH), 3145 (Ar CH), 2922 – 2854 (aliphatic CH), 1461 (C=C), 1260 (C–N), 1022 ;^{1}H NMR (300 MHz, $CDCl_3$) δ 8.53 (d, *J* = 5.4 Hz, 1H), 7.94 (d, *J* = 2.1 Hz, 1H), 7.78 (d, *J* = 9.0 Hz, 1H), 7.57 (s, 1H), 7.33 (dd, *J* = 8.9, 2.1 Hz, 1H), 6.48 (d, *J* = 5.4 Hz, 1H), 6.08 (br s, 1H), 4.64 (d, *J* = 3.6 Hz, 2H), 4.42 (t, *J* = 6.9 Hz, 2H), 2.35 – 2.14 (m, 6H), 2.06 (p, *J* = 6.6 Hz, 2H), 1.58 – 1.47 (m, 4H), 1.41 (br d, *J* = 5.1 Hz, 2H overlapping); ^{13}C NMR (101 MHz, $CDCl_3$) δ 152.1, 149.6, 149.1, 144.0, 135.3, 128.7, 125.7, 122.4, 121.6, 117.5, 99.6, 55.3, 54.6, 48.6, 39.1, 27.6, 26.2, 24.5; MS (ESI^+) 385.1876 calculated for $C_{20}H_{25}ClN_6$ $[M + H]^+$, found 385.1895 (-4.9 ppm).

5.2.2.6 *7-Chloro-N-((1-(2-(pyrrolidin-1-yl)ethyl)-1H-1,2,3-triazol-4-yl)methyl)quinolin-4-amine* ***(6c)***.

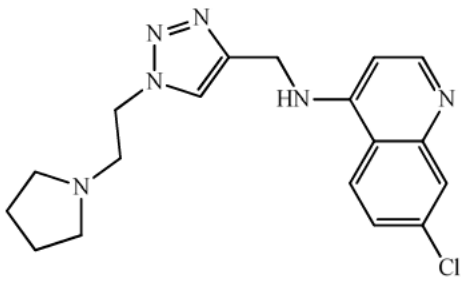

A light yellow solid (18 mg, 67% yield, mp: 117 – 119 °C).

IR υ_{max} 3452 (NH), 2925 – 2854 (aliphatic CH), 1576 (C=C), 1461, 1370 (C–N); ^{1}H NMR (300 MHz, $CDCl_3$) δ 8.52 (d, *J* = 5.4 Hz, 1H), 7.95 (d, *J* = 2.1 Hz, 1H), 7.81 (d, *J* = 9.0 Hz, 1H), 7.75 (s, 1H), 7.35 (dd, *J* = 8.9, 2.1 Hz, 1H), 6.54 (d, *J* = 5.4 Hz, 1H), 6.17 (br s, 1H), 4.65 (s, 2H), 4.50

(t, J = 6.4 Hz, 2H), 2.98 (t, J = 6.4 Hz, 2H), 2.60 – 2.51 (m, 4H), 1.78 (td, J = 6.4, 3.1 Hz, 4H); ^{13}C NMR (101 MHz, $CDCl_3$) δ 151.4, 149.3, 148.2, 143.5, 135.4, 128.0, 125.8, 122.5, 121.7, 117.1, 99.5, 55.7, 54.1, 49.7, 39.0, 23.6; MS (ESI^+) 357.1595 calculated for $C_{18}H_{21}ClN_6$ $[M + H]^+$, found 357.1581 (-1.40 ppm).

5.2.2.7 *7-Chloro-N-((1-(3-(pyrrolidin-1-yl)propyl)-1H-1,2,3-triazol-4-yl)methyl)quinolin-4-amine* ***(6c')***.

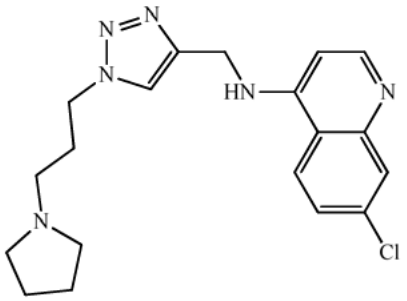

A light yellow solid (18 mg, 63% yield, mp: 115 – 117 °C).

IR υ_{max} 3390 (NH), 2925 – 2854 (aliphatic CH), 1576 (C=C), 1451, 1370 (C–N); ^{1}H NMR (300 MHz, $CDCl_3$) δ 8.54 (s, 1H), 7.97 (s, 1H), 7.80 (d, J = 9.0 Hz, 1H), 7.60 (s, 1H), 7.37 (dd, J = 8.9, 1.6 Hz, 1H), 6.51 (d, J = 5.2 Hz, 1H), 6.02 (br s, 1H), 4.65 (br s, 2H), 4.44 (t, J = 6.4 Hz, 2H), 2.98 (t, J = 6.4 Hz, 2H), 2.62 – 2.53 (m, 4H), 1.83 – 1.76 (m, 4H); ^{13}C NMR (75 MHz, $CDCl_3$) δ 150.4, 148.3, 147.9, 142.8, 134.1, 127.6, 124.6, 121.0, 120.3, 116.2, 98.5, 52.9, 51.4, 47.4, 38.0, 28.7, 22.4; MS (ESI^+) 371.1752 calculated for $C_{19}H_{23}ClN_6$ $[M + H]^+$, found 371.1751 (-0.27 ppm).

5.2.2.8 *7-Chloro-N-((1-(2-(diethylamino)ethyl)-1H-1,2,3-triazol-4-yl)methyl)quinolin-4-amine* ***(6d)***.

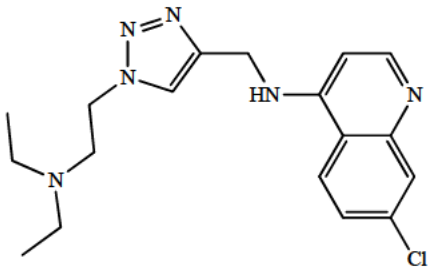

A light yellow solid (19 mg, 70% yield, mp: 83 – 85 °C).

IR υ_{max} 3493 (NH), 3054 (Ar CH), 2976 (aliphatic CH), 1581 (C=C bend), 1495, 1365, 1265 (C–N), 747; ^{1}H NMR (300 MHz, $CDCl_3$) δ 8.52 (br s, 1H), 7.94 (s, 1H), 7.75 (d, J = 8.9 Hz, 1H), 7.70 (s, 1H), 7.34 (d, J = 9.0 Hz, 1H), 6.50 (d, J = 5.2 Hz, 1H), 5.95 (br s, 1H), 4.63 (s, 2H), 4.39 (t, J = 6.2 Hz, 2H), 2.85 (t, J = 6.1 Hz, 2H), 2.52 (q, J = 6.9Hz, 4H), 0.92 (t, J = 7.1 Hz, 6H); ^{13}C NMR (75 MHz, $CDCl_3$) δ 151.7, 149.4, 148.8, 143.2, 135.4, 128.4, 125.7, 122.6, 121.3, 117.3, 99.5, 52.9, 49.2, 47.3, 39.0, 11.8; MS (ESI^+) 359.1752 calculated for $C_{18}H_{23}ClN_6$ $[M + H]^+$, found 359.1758 (-1.67 ppm).

5.2.2.9 *7-Chloro-N-((1-(3-(diethylamino)propyl)-1H-1,2,3-triazol-4-yl)methyl)quinolin-4-amine* ***(6d')***.

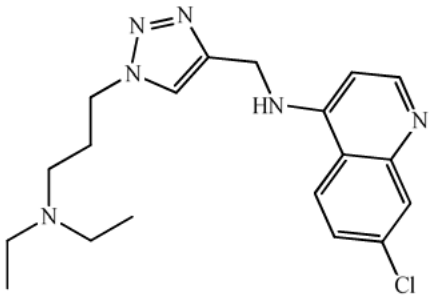

A light yellow solid (17 mg, 61% yield, mp: 82 – 84 °C).

IR υ_{max} 3493 (NH), 3080 (Ar CH 2970), 2922 – 2852 (aliphatic CH), 1513 (C=C bend), 1336, 1216 (C–N), 856, 748; ^{1}H NMR (300 MHz, $CDCl_3$) δ 8.55 (d, J = 5.4 Hz, 1H), 7.98 (d, J = 2.1 Hz, 1H), 7.79 (d, J = 9.0 Hz, 1H), 7.61 (s, 1H), 7.39 (dd, J = 8.9, 2.2 Hz, 1H), 6.52 (d, J = 5.4 Hz,

1H), 5.92 (br s, 1H), 4.66 (br s, 2H), 4.45 (t, J = 6.9 Hz, 2H), 2.55 (q, J = 7.2 Hz, 4H), 2.47 (t, J = 6.9 Hz, 2H), 2.11 (p, J = 6.8 Hz, 2H), 1.00 (t, J = 7.2 Hz, 6H); ^{13}C NMR (101 MHz, $CDCl_3$) δ 152.1, 149.7, 149.5, 144.2, 135.6, 129.1, 126.2, 122.6, 121.8, 117.8, 100.2, 50.2, 49.4, 47.7, 40.1, 28.9, 12.5. MS (ESI^+) 373.1908 calculated for $C_{19}H_{25}ClN_6$ $[M + H]^+$, found 373.1904 (1.07 ppm).

5.2.3.0 *7-Chloro-N-((1-(2-morpholinoethyl)-1H-1,2,3-triazol-4-yl)methyl)quinolin-4-amine* ***(6e)***.

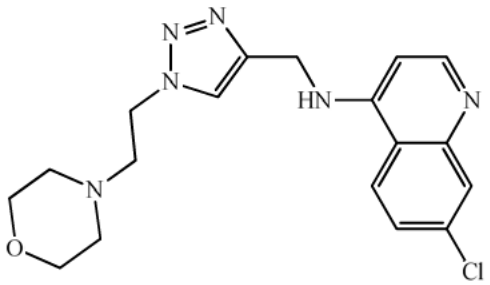

A light yellow solid (21 mg, 74% yield, mp: 180 – 182 °C).

IR υ_{max} 3485 (NH), 2921 – 2849 (aliphatic CH), 1581 (C=C), 1460, 1374, 1260 (C–N), 795; ^{1}H NMR (300 MHz, $CDCl_3$) δ 8.53 (s, 1H), 7.95 (d, J = 2.0 Hz, 1H), 7.78 (d, J = 9.0 Hz, 1H), 7.71 (s, 1H), 7.32 (dd, J = 8.9, 2.0 Hz, 1H), 6.51 (d, J = 5.3 Hz, 1H), 6.15 (br s, 1H), 4.63 (d, J = 3.6 Hz, 2H), 4.46 (t, J = 6.9 Hz, 2H), 3.66 (br t, J = 4.8 Hz, 4H), 2.81 (br t, J = 4.6 Hz, 4H), 2.47 (t, J = 6.8 Hz, 2H); ^{13}C NMR (75 MHz, $CDCl_3$) δ 150.4, 148.5, 147.8, 142.9, 134.2, 127.2, 124.6, 121.5, 120.5, 116.3, 98.8, 65.9, 53.8, 52.5, 47.2, 37.9; MS (ESI^+) 373.1544 calculated for $C_{18}H_{21}ClN_6O$ $[M + H]^+$, found 373.1537 (-1.88 ppm).

5.2.3.1 *7-Chloro-N-((1-(3-morpholinopropyl)-1H-1,2,3-triazol-4-yl)methyl)quinolin-4-amine (**6e'**).*

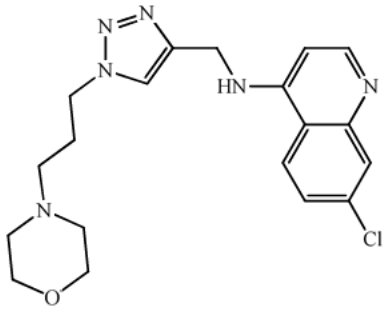

A light yellow solid (25 mg, 85% yield, mp: 153 – 155 °C).

IR υ_{max} 3452 – 3317 (NH), 3032 (Ar CH), 2932 – 2794 (aliphatic CH), 1576 (C=C), 1450, 1366; ^{1}H NMR (300 MHz, $CDCl_3$) δ 8.53 (s, 1H), 7.97 (d, *J* = 2.0 Hz, 1H), 7.77 (d, *J* = 9.0 Hz, 1H), 7.55 (s, 1H), 7.37 (dd, *J* = 8.9, 2.0 Hz, 1H), 6.51 (d, *J* = 5.3 Hz, 1H), 5.97 (br s, 1H), 4.66 (d, *J* = 3.6 Hz, 2H), 4.45 (t, *J* = 6.9 Hz, 2H), 3.66 (br t, *J* = 4.8 Hz, 4H), 2.37 (br t, *J* = 4.6 Hz, 4H), 2.32 (t, *J* = 6.8 Hz, 2H overlapping), 2.08 (p, *J* = 6.9 Hz, 2H); ^{13}C NMR (75 MHz, $CDCl_3$) δ 150.4, 148.5, 147.8, 142.9, 134.2, 127.2, 124.6, 121.5, 120.5, 116.3, 98.8, 65.9, 53.8, 52.5, 47.2, 37.9, 25.9; MS (ESI$^+$) 387.1701 calculated for $C_{19}H_{23}ClN_6O$ $[M + H]^+$, found 387.1707 (1.55 ppm).

5.2.3.2 *7-Chloro-N-((1-(2-(methyl(phenyl)amino)ethyl)-1H-1,2,3-triazol-4-yl)methyl)quinolin-4-amine (**6f**).*

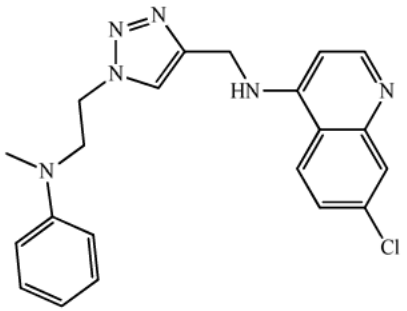

An off-white solid (19 mg, 64% yield, mp: 167 – 169 °C).

IR υ_{max} 3493 (NH), 2970 – 2759 (aliphatic CH), 1740 (C=C), 1368 and 1217 (C–N); ^{1}H NMR (300 MHz, $CDCl_3$) δ 8.54 (d, *J* = 5.3 Hz, 1H), 7.97 (d, *J* = 2.1 Hz, 1H), 7.78 (d, *J* = 8.9 Hz, 1H), 7.62 (s, 1H), 7.36 (dd, *J* = 8.7, 2.2 Hz, 1H), 7.26 – 7.12 (m, 5H), 6.53 (d, *J* = 5.3 Hz, 1H), 6.01 (s,

1H), 4.65 (d, J = 1.6 Hz, 2H), 4.45 (t, J = 6.1 Hz, 2H), 3.54 (s, 2H), 2.78 (t, J = 6.1 Hz, 2H), 2.29 (s, 3H); ^{13}C NMR (75 MHz, $CDCl_3$) δ 151.5, 149.5, 148.5, 144.1, 135.1, 129.4 , 128.8, 125.6, 122.8, 121.1, 117.6, 112.3, 99.5, 53.1, 48.0, 38.9, 38.6; MS (ESI^+) 407.1752 calculated for $C_{21}H_{21}ClN_6$ $[M + H]^+$, found 407.1744 (-1.96 ppm).

5.2.3.3 *7-Chloro-N-((1-(3-(methyl(phenyl)amino)propyl)-1H-1,2,3-triazol-4-yl)methyl)quinolin-4-amine (**6f'**).*

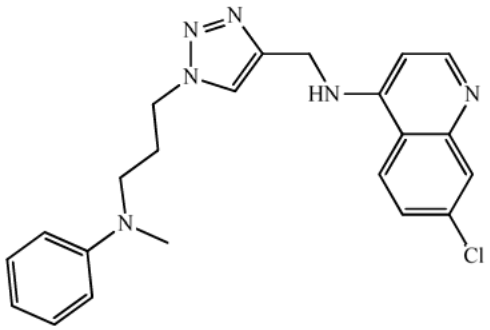

An off-white solid (17 mg, 53% yield, mp: 163 – 165 °C).

IR υ_{max} 3452 – 3317 (NH), 2932 – 2847 (aliphatic CH), 1576 (C=C), 1450, 1366, 1323, 1220 (C–N), 1138, 738; ^{1}H NMR (400 MHz, $CDCl_3$) δ 8.50 (d, J = 5.4 Hz, 1H), 7.94 (d, J = 2.1 Hz, 1H), 7.77 (d, J = 9.0 Hz, 1H), 7.47 (s, 1H), 7.33 (dd, J = 9.0, 2.1 Hz 1H), 7.19 (td, J = 8.4, 1.2 Hz, 2H), 6.71 (t, J = 7.3 Hz, 1H), 6.65 (d, J = 8.0 Hz, 2H), 6.49 (d, J = 5.4 Hz, 1H), 6.09 (br s, 1H) 4.63 (s, 2H), 4.38 (t, J = 7.0 Hz, 2H), 3.37 (t, J = 6.9 Hz, 2H), 2.89 (s, 3H), 2.21 (p, J = 7.0 Hz, 2H); ^{13}C NMR (101 MHz, $CDCl_3$) δ 152.1, 150.3, 149.8, 149.2, 144.7, 136.0, 130.0, 128.9, 126.4, 122.5, 122.2, 117.8, 113.4, 100.2, 50.2, 49.0, 39.7, 39.3, 30.4; MS (ESI^+) 407.1752 calculated for $C_{22}H_{23}ClN_6$ $[M + H]^+$, found 407.1743 (-2.21 ppm).

5.2.3.4 *7-Chloro-N-((1-(2-(benzyl(methyl)amino)ethyl)-1H-1,2,3-triazol-4-yl)methyl) quinolin-4-amine (**6g**).*

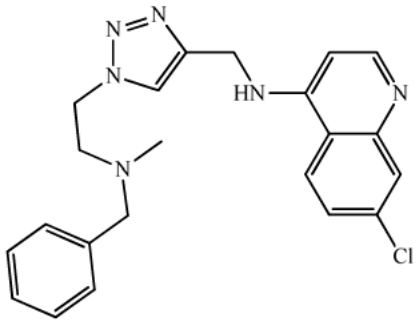

A light yellow solid (22 mg, 69% yield, mp: 133 – 135 °C).

IR υ_{max} 3444 – 3317 (NH), 3144 (Ar CH), 2932 – 2847 (aliphatic CH), 1579 (C=C), 1448, 1367, 1220 (C–N), 736; ^{1}H NMR (300 MHz, $CDCl_3$) δ 8.54 (s, 1H), 7.97 (s, 1H), 7.78 (d, J = 8.9 Hz, 1H), 7.62 (s, 1H), 7.36 (d, J = 7.6 Hz, 1H), 7.26 – 7.12 (m, 5H), 6.53 (d, J = 5.2 Hz, 1H), 6.01 (s, 1H), 4.65 (d, J = 2.8 Hz, 2H), 4.45 (t, J = 6.1 Hz, 2H), 3.54 (s, 2H), 2.87 (t, J = 6.1 Hz, 2H), 2.29 (s, 3H); ^{13}C NMR (75 MHz, $CDCl_3$) δ 151.5, 149.5, 148.6, 143.6, 138.2, 135.23, 129.0, 128.8, 128.3, 127.3, 125.9, 122.3, 121.4, 117.2, 99.4, 62.4, 56.4, 48.4, 42.23, 39.02; MS (ESI^+) 407.1752 calculated for $C_{22}H_{23}ClN_6$ $[M + H]^+$, found 407.1744 (100%, -1.96 ppm), 317.1293 (30%).

5.2.3.5 *7-Chloro-N-((1-(3-(benzyl(methyl)amino)propyl)-1H-1,2,3-triazol-4-yl)methyl)quinolin-4-amine (**6g'**).*

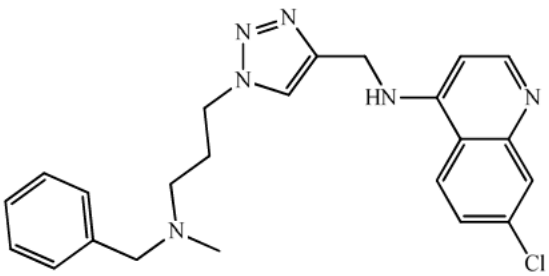

An off-white solid (21 mg, 65% yield, mp: 131 – 133 °C).

IR υ_{max} 3444 – 3317 (NH), 2932 (aliphatic CH), 1579 (C=C), 1448, 1367, 1220 (C–N), 1137, 736; ^{1}H NMR (300 MHz, $CDCl_3$) δ 8.56 (s, 1H), 7.98 (s, 1H), 7.77 (d, J = 7.7 Hz, 1H), 7.42 – 7.18 (m, 7H), 6.50 (s, 1H), 5.95 (s, 1H), 4.58 (s, 2H), 4.43 (t, J = 6.8 Hz, 2H), 3.46 (s, 2H), 2.35 (t, J = 6.4 Hz, 2H), 2.22 (s, 3H), 2.07 (p, J = 6.5 Hz, 2H). ^{13}C NMR (75 MHz, $CDCl_3$) δ 151.5, 149.5, 148.6,

143.6, 138.2, 135.2, 129.1, 128.8, 128.3, 127.3, 125.7, 122.3, 121.4, 117.2, 99.4, 62.4, 56.4, 48.4, 42.2, 39.0, 29.7; MS (ESI+) 421.1908 calculated for $C_{23}H_{25}ClN_6$ $[M + H]^+$; found 421.1905 (-0.71 ppm).

5.2.3.6 *7-Chloro-N-((1-(2-(dibenzylamino)ethyl)-1H-1,2,3-triazol-4-yl)methyl)quinolin-4-amine* ***(6h)***.

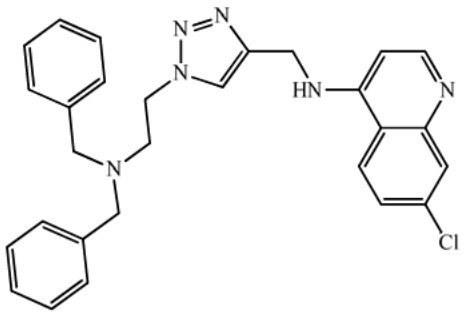

A yellow solid (20 mg, 54% yield, mp: 115 – 118 °C).

IR υ_{max} 3493 (NH), 3004 (Ar CH), 2970 (aliphatic CH); 1740 (C=C), 1368, 1217 (C–N), 1054; ^{1}H NMR (300 MHz, $CDCl_3$) δ 8.43 (s, 1H), 7.94 (s, 1H), 7.88 (d, J = 9.0 Hz, 1H), 7.41 – 7.17 (m, 11H), 6.89 (s, 1H), 6.50 (br s, 1H), 4.54 (s, 2H), 4.34 (t, J = 6.1 Hz, 2H), 3.58 (s, 6H), 2.46 (t, J = 6.3 Hz, 2H); ^{13}C NMR (75 MHz, $CDCl_3$) δ 151.3, 150.1, 149.2, 143.8, 139.8, 136.1, 129.8, 129.1, 128.8, 127.8, 126.4, 122.8, 122.1, 117.8, 99.4, 59.5, 50.4, 48.7, 39.5; MS (ESI^+) 483.2065 calc for $C_{28}H_{27}ClN_6$ $[M + H]^+$, found 483.2063 (-0.41 ppm)

5.2.3.7 *7-Chloro-N-((1-(3-(dibenzylamino)propyl)-1H-1,2,3-triazol-4-yl)methyl)quinolin-4-amine* ***(6h')***.

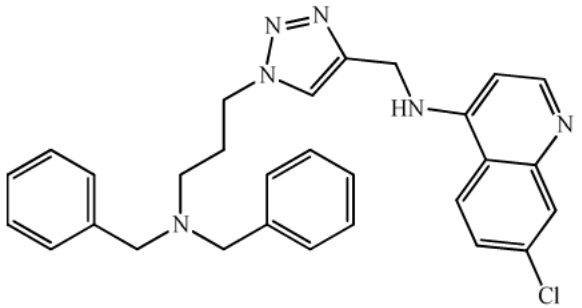

A yellow solid (24 mg, 64% yield, mp: 114 – 115 °C).

IR υ_{max} 3484 (NH), 3206 (Ar CH), 2994 – 2931 (aliphatic CH), 1580 and 1543 (C=C), 1431, 1365, 775; ^{1}H NMR (300 MHz, $CDCl_3$) δ 8.55 (d, J = 4.8 Hz, 1H), 7.98 (d, J = 1.8 Hz, 1H), 7.76 (d, J = 9.0 Hz, 1H), 7.39 – 7.22 (m, 11H), 6.79 (s, 1H), 6.47 (d, J = 5.4 Hz, 1H), 5.96 (br s, 1H), 4.49 (d, J = 2.3 Hz, 2H), 4.35 (t, J = 6.8 Hz, 2H), 3.56 (s, 4H), 2.46 (t, J = 6.2 Hz, 2H), 2.05 (p, J = 6.3 Hz, 2H); ^{13}C NMR (75 MHz, $CDCl_3$) δ 151.9, 150.3, 149.2, 143.9, 140.1, 136.1, 129.8, 129.1, 128.8, 127.9, 126.4, 122.8, 122.2, 117.9, 100.0, 59.5, 50.4, 48.7, 39.5, 28.8; MS (ESI^+) 497.2221 calculated for $C_{29}H_{29}ClN_6$ $[M + H]^+$, found 497.2214 (37%, -1.41 ppm), 407.1749 (40%), 249.1146 (100%).

5.2.3.8 *7-Chloro-N-((1-(2-(10,11-dihydro-5H-dibenzo[b,f]azepin-5-yl)ethyl)-1H-1,2,3-triazol-4-yl)methyl)quinolin-4-amine* ***(6i)***.

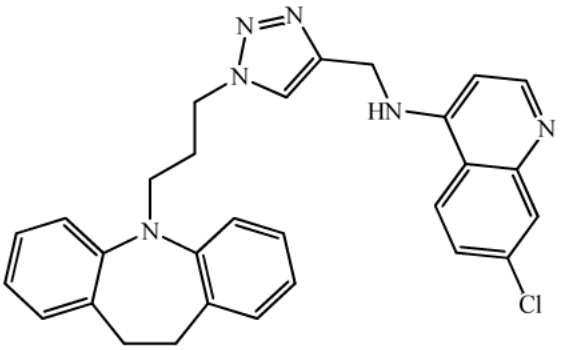

A light brown solid (24 mg, 64% yield, mp: 67 – 69 °C).

IR υ_{max} 3484 – 3371 (NH), 3147 (Ar CH), 2927 and 2851 (aliphatic CH), 1576 and 1544 (C=C), 1258 (C –N), 1058, 767; ^{1}H NMR (300 MHz, $CDCl_3$) δ 8.50 (d, J = 5.4 Hz, 1H), 7.97 (d, J = 2.1

Hz, 1H), 7.74 (d, *J* = 9.0 Hz, 1H), 7.38 (d, *J* = 2.1 Hz, 1H overlapping), 7.35 (d, *J* = 2.0 Hz, 1H overlapping), 7.16 – 6.90 (m, 8H), 6.44 (d, *J* = 5.5 Hz, 1H), 4.57 (d, *J* = 3.1 Hz, 2H), 4.41 (t, *J* = 6.9 Hz, 2H), 3.77 (t, *J* = 6.4 Hz, 2H), 3.18 (s, 4H), 2.20 (p, *J* = 5.7 Hz, 2H); ^{13}C NMR (75 MHz, $CDCl_3$) δ 151.1, 150.6, 147.6, 143.8, 135.4, 134.1, 130.1, 129.5, 128.0, 126.6, 125.7, 123.1, 121.9, 121.4, 119.7, 117.0, 99.3, 48.1, 46.9, 38.9, 32.1, 28.3; MS (ESI^+) 495.2065 calculated for $C_{29}H_{27}ClN_6$ $[M + H]^+$, found 495.2067 (0.40 ppm).

5.3 *In vitro* antimalarial activity investigations.

The biological analysis of the test compounds was performed by the Professor Peter Smith in Division of Pharmacology, University of Cape Town. Reported, herein, was the only received data by the time of writing a thesis and additional data is expected once the ongoing tests have been finalised.

5.3.1 *Quantitative assessment of antiplasmodial activity*.

The antiplasmodial activity of ***6b – 6i*** were carried out on asexual erythrocyte stages of a continuously maintained culture of NF54, a CQ-sensitive strain of *P. falciparum*, by a modified literature method of parasite lactate dehydrogenase assay (pLDH).[131,133] Briefly, the compounds were prepared to a 20 mg/mL stock solution or a suspension in DMSO and sonicated to enhance the solubility. Serial dilutions of stock solutions were carried out in triplicate in a 96-well plate using a multichannel pipette and the compounds were tested on a concentration range of 1000 µg/mL and 0.2 ng/mL. CQ was used as a reference compound while DMSO solvent was a blank. Additional positive controls such artesunate standard antimalarial drug and MMV390048 currently in the clinical trials were included with triazole-linked chloroquinoline derivatives test compounds. The 50% inhibition concentration value of parasite growth (IC_{50}) for each compound was deduced from a non-linear full-dose response curve performed by Graph Pad Prism v.4.0 software. Data were collected using a microplate reader and analyzed as described above The IC_{50} activity values are shown in **table 5.3.0.1**.

Table 5.3.1 Antiplasmodial activity of triazole-linked chloroquinoline derivatives against CQ-sensitive NF 54

Compound	Chemical Structure	IC_{50} (nM) NF54
CQ♠	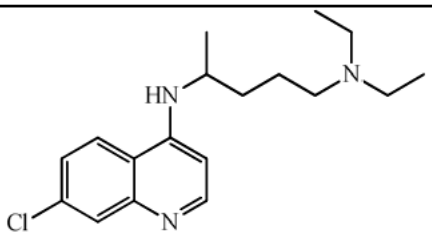	**23.8**
artesunate	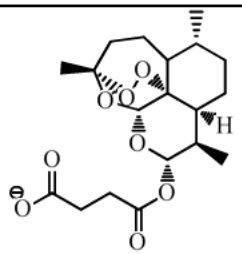	**13.8**
6b	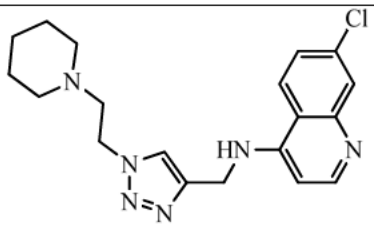	**27.8**
6b'	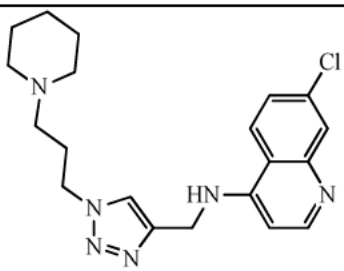	**42.2**
6c	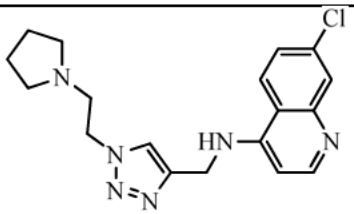	**59.2**
6c'	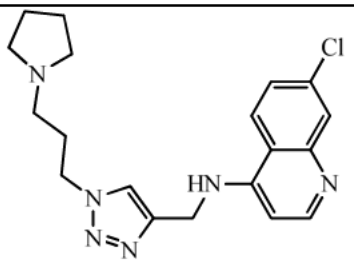	**65.1**

6d	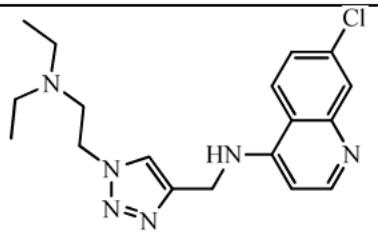	**106.4**
6d'	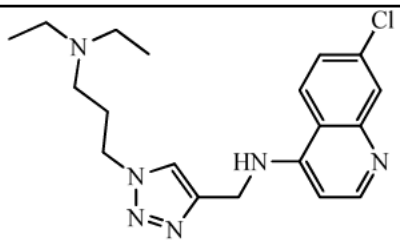	**51.1**
6e	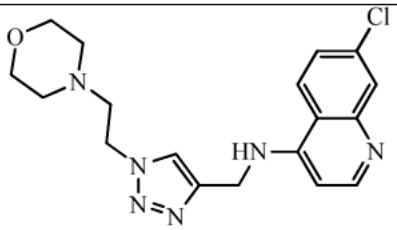	**>1000**
6e'	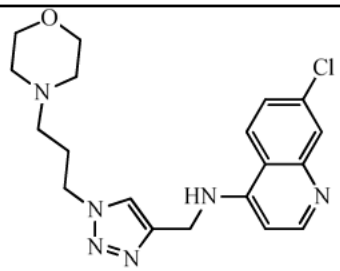	**247.0**
6f	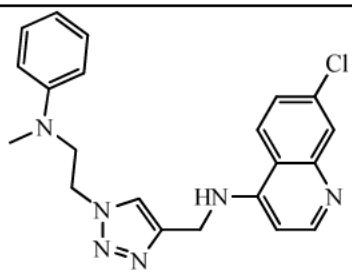	**586.5**
6f'	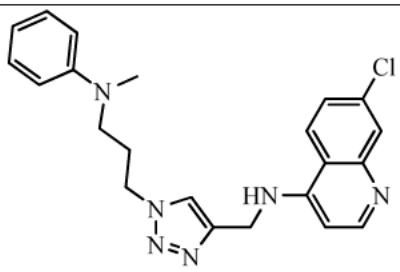	**354.5**

6g	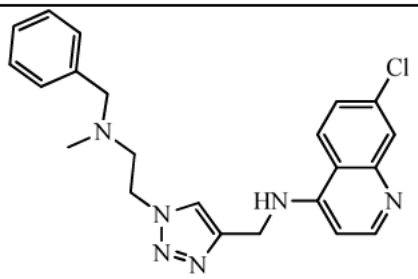	**163.7**
6g'	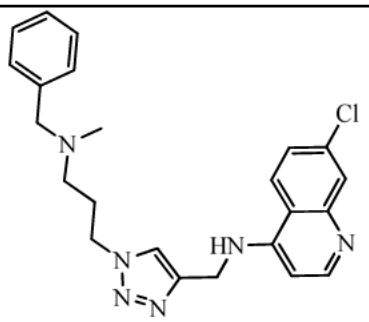	**32.6**
6h	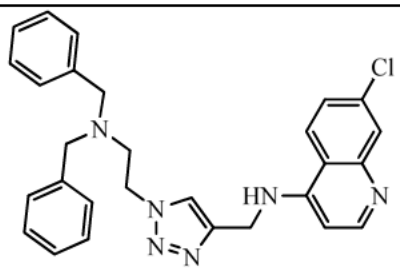	**>1000**
6h'	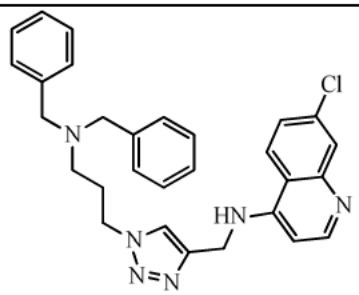	**237.8**
6i	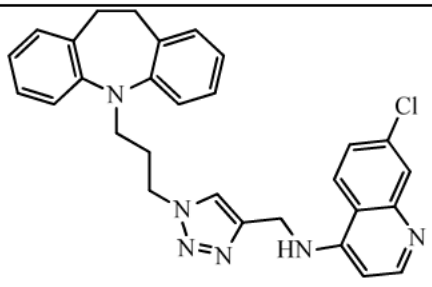	**148.1**

MMV390048♠	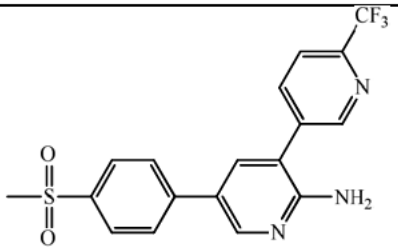	**31.5**

♠ Standard antimalarial drugs

References

(1) Cox, F. *Parasit. Vectors* **2010**, *3*, 5.

(2) Hay, S. I.; Guerra, C. A.; Gething, P. W.; Patil, A. P.; Tatem, A. J.; Noor, A. M.; Kabaria, C. W.; Manh, B. H.; Elyazar, I. R. F.; Brooker, S.; Smith, D. L.; Moyeed, R. A.; Snow, R. W. *Plos Med.* **2009**, *6*, e1000048.

(3) Ross, R. In *Exile*; Murray, J., Ed. London, 1931, p 77.

(4) WHO In *World Malaria Report 2011*. 2011.

(5) Ta, T. T.; Salas, A.; Ali-Tammam, M.; Martinez, C. M.; Lanza, M.; Arroyo, E.; Rubio, J. M. *Malaria J.* **2010**, *9*, 219.

(6) Kantele, A.; Jokiranta, S. *Duodecim* **2010**, *126*, 427.

(7) Frevert, U. *Trends Parasitol.* **2004**, *20*, 417.

(8) Schlitzer, M. *ChemMedChem* **2007**, *2*, 944.

(9) Roepe, D. P. *Biochem.* **2011**, *50*, 163.

(10) Walliker, D. In *Molecular Epidemiology of Infectious Diseases*; Thompson, R. C. A., Ed.; Arnold: London, 2000, p 93.

(11) Babiker, H. A.; Hastings, I. M.; Swedberg, G. *Expert Rev. Anti. Infect. Ther.* **2009**, *7*, 581.

(12) Sharma, M.; Chauhan, K.; Chauhan, S. S.; Kumar, A.; Singh, S. V.; Saxena, J. K.; Agarwal, P.; Srivastava, K.; Raja Kumar, S.; Puri, S. K.; Shah, P.; Siddiqi, M. I.; Chauhan, P. M. S. *Med. Chem.Commun.* **2012**, *3*, 71.

(13) Muregi, F. W.; Kirira, P. G.; Ishih, A. *Curr. Med. Chem.* **2011**, *18*, 113.

(14) Meunier, B. *Acc. Chem. Res.* **2008**, *41*, 69.

(15) Turner, R. B.; Woodward, R. B. In *The Alkaloids*; Manske, R. H. F., Ed.; Academic Press: New York, 1953; Vol. III, p 181.

(16) Greenwood, D. *J. Antimicrob. Chemother.* **1995**, *36*, 857.

(17) Foley, M.; Tilley, L. *Pharmacol. Ther.* **1998**, *79*, 55.

(18) Coatney, G. R. *Am. J. Trop. Med. Hyg.* **1963**, *12*, 121.

(19) Gardner, M. J.; Hall, N.; Fung, E.; White, O.; Berriman, M.; Hyman, R. W.; Carlton, J. M.; Pain, A.; Nelson, K. E.; Bowman, S.; Paulsen, I. T.; James, K.; Eisen, J. A.; Rutherford, K.; Salzberg, S. L.; Craig, A.; Kyes, S.; Chan, M.; Nene, V.; Shallom, S. J.; Suh, B.; Peterson, J.; Angiuoli, S.; Pertea, M.; Allen, J.; Selengut, J.; Haft, D.; Mather, M. W.; Vaidya, A. B.; Martin, D. M. A.; Fairlamb, A. H.; Fraunholz, M. J.; Roos, D. S.; Ralph, S. A.; McFadden, G. I.; Cummings, L. M.; Subramanian, G. M.;

Mungall, C.; Venter, J. C.; Carucci, D. J.; Hoffman, S. L.; Newbold, C.; Davis, R. W.; Fraser, C. M.; Barrell, B. *Nature* **2002**, *419*, 498.

(20) Stocks, P. A.; Raynes, K. J.; Bray, P. G.; Park, B. K.; O'Neill, P. M.; Ward, S. A. *J. Med. Chem.* **2002**, *45*, 4975.

(21) Ryall, J. C. *Parasitol. Today* **1987**, *3*, 256.

(22) Madrid, P. B.; Wilson, N. T.; DeRisi, J. L.; Guy, R. K. *J. Comb. Chem.* **2004**, *6*, 437.

(23) Kelly, J. X.; Smilkstein, M. J.; Brun, R.; Wittlin, S.; Cooper, R. A.; Lane, K. D.; Janowsky, A.; Johnson, R. A.; Dodean, R. A.; Winter, R.; Hinrichs, D. J.; Riscoe, M. K. *Nature* **2009**, *459*, 270.

(24) Kaschula, C. H.; Egan, T. J.; Hunter, R.; Basilico, N.; Parapini, S.; Taramelli, D.; Pasini, E.; Monti, D. *J. Med. Chem.* **2002**, *45*, 3531.

(25) Egan, T. J. *Targets* **2003**, *3*, 115

(26) Payne, D. D. *Parasitol. Today* **1988**, *4*, 112.

(27) Kouznetsov, V. V.; Gómez-Barrio, A. *Eur. J. Med. Chem.* **2009**, *44*, 3091.

(28) Macreadi, I.; Ginsburg, H.; Sirawaraporn, W.; Tilley, L. *Parasitol. Today* **2000**, *16*, 438

(29) Lakshmanan, V.; Bray, P. G.; Verdier-Pinard, D.; Johnson, D. J.; Horrocks, P.; Muhle, R. A.; Alakpa, G. E.; Hughes, R. H.; Ward, S. A.; Krogstad, D. J.; Sidhu, A. B.; Fidock, D. A. *EMBO J.* **2005**, *24*, 2294.

(30) Fidock, D. A.; Nomura, T.; Talley, A. K.; Cooper, R. A.; Dzekunov, S. M.; Ferdig, M. T.; Ursos, L. M.; Sidhu, A. B.; Naude, B.; Deitsch, K. W.; Su, X. Z.; Wootton, J. C. *Mol. Cell* **2000**, *6*, 861.

(31) Hyde, J. E. *FEBS J.* **2007**, *274*, 4688.

(32) Martin, R. E.; Marchetti, R. V.; Cowan, A. I.; Howitt, S. M.; Broer, S.; Kirk, K. *Science* **2009**, *325*, 1680.

(33) Fidock, D. A.; Eastman, R. T.; Ward, S. A.; Meshnick, S. R. *Trends Parasitol.* **2008**, *24*, 537.

(34) Sidhu, A. B. S.; Verdier-Pinard, D.; Fidock, D. A. *Science* **2002**, *298*, 210.

(35) Johnson, D. J.; Fidock, D. A.; Mungthin, M.; Lakshmanan, V.; Sidhu, A. B.; Bray, P. G.; Ward, S. A. *Mol. Cell* **2004**, *15*, 867.

(36) Egan, T. J.; Hunter, R.; Kaschula, C. H.; Marques, H. M.; Misplon, A.; Walden, J. *J. Med. Chem.* **2000**, *43*, 283.

(37) De, D.; Krogstad, F. M.; Byers, L. D.; Krogstad, D. J. *J. Med. Chem.* **1998**, *41*, 4918.

(38) Ridley, R. G.; Hofheinz, W.; Matile, H.; Jaquet, C.; Dorn, A.; Masciadri, R.; Jolidon, S.; Richter, W. F.; Guenzi, A.; Girometta, M. A.; Urwyler, H.; Huber, W.; Thaithong, S.; Peters, W. *Antimicrob. Agents Chemother.* **1996**, *40*, 1846.

(39) Krogstad, D.; ClinicalTrials.gov: Bamako, 18 July 2012; Vol. 2012.

(40) Fu, S.; Bjorkman, A.; Wahlin, B.; Ofori-Adjei, D.; Ericsson, O.; Sjoqvist, F. *Br. J. Clin. Pharmacol.* **1986**, *22*, 93.

(41) Mzayek, F.; Deng, H.; Mather, F. J.; Wasilevich, E. C.; Liu, H.; Hadi, C. M.; Chansolme, D. H.; Murphy, H. A.; Melek, B. H.; Tenaglia, A. N.; Mushatt, D. M.; Dreisbach, A. W.; Lertora, J. J.; Krogstad, D. J. *PLoS Clin. Trials* **2007**, *2*, e6.

(42) Raynes, K. J.; Stocks, P. A.; O'Neill, P. M.; Park, B. K.; Ward, S. A. *J. Med. Chem.* **1999**, *42*, 2747.

(43) Bray, P. G.; Hawley, S. R.; Ward, S. A. *Mol. Pharmacol.* **1996**, *50*, 1551.

(44) Peters, W. *Chemotherapy and drug resistance in malaria, 2nd Edn*; Academic Press: London, 1987.

(45) Clarke, J. B.; Neftel, K.; Kitteringham, N. R.; Park, B. K. *Int. Arch. Allergy Appl. Immunol.* **1991**, *95*, 369.

(46) Kumar, A.; Srivastava, K.; Kumar, S. R.; Puri, S. K.; Chauhan, P. M. *Bioorg. Med. Chem. Lett.* **2010**, *20*, 7059

(47) Kumar, A.; Srivastava, K.; Kumar, S. R.; Siddiqi, M. I.; Puri, S. K.; Sexana, J. K.; Chauhan, P. M. S. *Eur. J. Med. Chem.* **2011**, *46*, 676

(48) Zishiri, V. K.; Mukesh, C. J.; Hunter, R.; Chibale, K.; Smith, P. J.; Summers, R. L.; Martin, R. E.; Egan, T. J. *J. Med. Chem.* **2011**, *54*, 6956.

(49) Zishiri, V. K.; Hunter, R.; Smith, P. J.; Taylor, D.; Summers, R.; Kirk, K.; Martin, R. E.; Egan, T. J. *Eur. J. Med. Chem.* **2011**, *46*, 1729.

(50) Martin, S. K.; Oduola, A. M.; Milhous, W. K. *Science* **1987**, *235*, 899.

(51) Guan, J.; Kyle, D. E.; Gerena, L.; Zhang, Q.; Milhous, W. K.; Lin, A. J. *J. Med. Chem.* **2002**, *45*, 2741.

(52) Bhattacharjee, A. K.; Kyle, D. E.; Vennerstrom, J. L.; Milhous, W. K. *J. Chem. Inf. Comput. Sci.* **2002**, *42*, 1212.

(53) Hofheinz, W.; Merkli, B. In *Antimalarial Drugs*; Peters, W., Richards, W. H. G., Eds.; Springler Verlag: Berlin, 1984; Vol. II.

(54) Wallace, D. J. *Lupus* **1996**, *5*, S59.

(55) Suh, K. N.; Kain, K. C.; Keystone, J. S. *Can. Med. Assoc. J.* **2004**, *170*, 1693.

(56) Baird, J. K. *N. Engl. J. Med.* **2005**, *352*, 1565.

(57) Pasvol, G. *Infect. Dis. Clin. North Am.* **2005**, *19*, 211.

(58) Rieckmann, K.; Suebsaeng, L.; Rooney, W. *Am. J. Trop. Med. Hyg.* **1987**, *37*, 211

(59) Peters, W.; Robinson, B. L. *Ann. Trop. Med. Parasitol.* **1984**, *78*, 459

(60) Kremsner, P. G.; Krishna, S. *Lancet* **2004**, *364*, 10.

(61) Price, R. N.; Nosten, F.; Luxemburger, C.; van Vugt, M.; Phaipun, L.; Chongsuphajaisiddhi, T.; White, N. J. *Trans. R. Soc. Trop. Med. Hyg.* **1997**, *91*, 574.

(62) WHO *Guidelines for the Treatment of Malaria*; World Health Organization: Switzerland, 2010.

(63) White, N. *Philos. Trans. R. Soc. Lond., B, Biol. Sci.* **1999**, *354*, 739.

(64) White, N. J.; Olliaro, P. L. *Parasitol. Today* **1996**, *12*, 399.

(65) Eisenstein, M. *Nature* **2012**, *484*, S16.

(66) O'Brien, C.; Henrich, P. P.; Passi, N.; Fidock, D. A. *Curr. Opin. Infect. Dis.* **2011**, *24*, 570.

(67) Wang, Z.; Parker, D.; Meng, H.; Wu, L.; Li, J.; Zhao, Z.; Zhang, R.; Fan, Q.; Wang, H.; Cui, L.; Yang, Z. *Plos Med.* **2012**, *7*, e30927.

(68) Michael, A. *Prak. Chem.* **1893**, *48*, 94.

(69) Bourne, Y.; Kolb, H. C.; Radic, Z.; Sharpless, K. B.; Taylor, P.; Marchot, P. *Proc. Nat. Acad. Sci. USA.* **2004**, *101*, 1449.

(70) Zhou, C. H.; Wang, Y. *Curr. Med. Chem.* **2012**, *19*, 239.

(71) Singhai, N.; Sharma, P. K.; Dudhe, R.; Kumar, N. *J. Chem. Pharm. Res.* **2011**, *3*, 126.

(72) Guantai, E. M.; Ncokazi, K.; Egan, T. J.; Gut, J.; Rosenthal, P. J.; Smith, P. J.; Chibale, K. *Bioorg. Med. Chem.* **2010**, *18*, 8243.

(73) Bakunov, S. A.; Bakunova, S. M.; Wenzler, T.; Ghebru, M.; Werbovetz, K. A.; Brun, R.; Tidwell, R. R. *J. Med. Chem.* **2010**, *53*, 254.

(74) Vatmurge, N. S.; Hazra, B. G.; Pore, V. S.; Shirazi, F.; Chavan, P. S.; Deshpande, M. V. *Bioorg. Med. Chem. Lett.* **2008**, *18*, 2043.

(75) Soltis, M. J.; Yeh, H. J.; Cole, K. A.; Whittaker, N.; Wersto, R. P.; Kohn, E. C. *Drug Metab. Dispos.* **1996**, *24*, 799.

(76) Costa, M. S.; Boechat, N.; Rangel, E. A.; da Silva Fde, C.; de Souza, A. M.; Rodrigues, C. R.; Castro, H. C.; Junior, I. N.; Lourenco, M. C.; Wardell, S. M.; Ferreira, V. F. *Bioorg. Med. Chem.* **2006**, *14*, 8644.

(77) Whiting, M.; Tripp, J. C.; Lin, Y. C.; Lindstrom, W.; Olson, A. J.; Elder, J. H.; Sharpless, K. B.; Fokin, V. V. *J. Med. Chem.* **2006**, *49*, 7697.

(78) Agalave, S. G.; Maujan, S. R.; Pore, V. S. *Chem. Asian J.* **2011**, *6*, 2696.

(79) Chen, X.; Ji, Z. L.; Chen, Y. Z. *Nucleic Acids Res.* **2002**, *30*, 412.

(80) Wishart, D. S.; Knox, C.; Guo, A. C.; Cheng, D.; Shrivastava, S.; Tzur, D.; Gautam, B.; Hassanali, M. *Nucleic Acids Res.* **2008**, *36*, D901.

(81) Urbina, J. A.; Payares, G.; Sanoja, C.; Molina, J.; Lira, R.; Brener, Z.; Romanha, A. J. *Int. J. Antimicrob. Agents* **2003**, *21*, 39.

(82) Kappagoda, S.; Singh, U.; Blackburn, B. G. *Mayo Clin. Proc.* **2011**, *86*, 561.

(83) Vlahakis, J. Z.; Lazar, C.; Crandall, I. E.; Szarek, W. A. *Bioorg. Med. Chem.* **2010**, *18*, 6184.

(84) Alam, M. S.; Kajiki, R.; Hanatani, H.; Kong, X.; Ozoe, F.; Matsui, Y.; Matsumura, F.; Ozoe, Y. *J. Agric. Food Chem.* **2006**, *54*, 1361.

(85) Hou, J.; Liu, X.; Shen, J.; Zhao, G.; Wang, P. G. *Expert Opin. Drug Discov.* **2012**, *7*, 489.

(86) Brik, A.; Alexandratos, J.; Lin, Y. C.; Elder, J. H.; Olson, A. J.; Wlodawer, A.; Goodsell, D. S.; Wong, C. H. *ChemBioChem* **2005**, *6*, 1167.

(87) Morphy, R.; Rankovic, Z. *J. Med. Chem.* **2005**, *48*, 6523.

(88) Gordon, E. M.; Barrett, R. W.; Dower, W. J.; Fodor, S. P. A.; Gallop, M. A. *J. Med. Chem.* **1994**, *37*, 1385.

(89) Mishra, N.; Arora, P.; Kumar, B.; Mishra, L. C.; Bhattacharya, A.; Awasthi, S. K.; Bhasin, V. K. *Eur. J. Med. Chem.* **2008**, *43*, 1530.

(90) Kolb, H. C.; Finn, M. G.; Sharpless, K. B. *Angew. Chem. Int. Ed.* **2001**, *40*, 2004.

(91) Walsh, J. C.; Kolb, H. C. *Chimia (Aarau)* **2010**, *64*, 29.

(92) Huisgen, R. In *1,3-Dipolar Cycloaddition Chemistry*; Padwa, A., Ed.; Wiley-Interscience: New York, 1984; Vol. 1, p 176.

(93) Huisgen, R. *Proc. Chem. Soc.* **1961**, *4*, 357.

(94) Dimroth, O.; Fester, G. *Ber. Dtsch. Chem. Ges.* **1910**, *43*, 2219.

(95) Huisgen, R. *Angew. Chem. Int. Ed.* **1963**, *2*, 633.

(96) Kolb, H. C.; Sharpless, K. B. *Drug Discov. Today* **2003**, *8*, 1120.

(97) Wu, P.; Fokin, V., V *Aldrichim. Acta* **2007**, *40*, 7.

(98) Zhang, L.; Chen, X.; Xue, P.; Sun, H. Y.; Williams, I. D.; Sharpless, K. B.; Fokin, V. V.; Jia, G. *J. Am. Chem. Soc.* **2005**, *127*, 15998.

(99) Pauling, L.; Brockway, L. O. *J. Am. Chem. Soc.* **1937**, *59*, 13.

(100) Huisgen, R. *Angew. Chem. Int. Ed.* **1963**, *2*, 565.

(101) Kinugasa, M.; Hashimoto, S. *J. Chem, Soc., Chem. Commun.* **1972**, 466.

(102) Tornøe, C. W.; Christensen, C.; Meldal, M. *J. Org. Chem.* **2002**, *67*, 3057.

(103) Hou, D.; Kuan, T.; Li, Y.; Lee, R.; Huang, K. *Tetrahedron* **2010**, *66*, 9415.

(104) Demko, Z. P.; Sharpless, K. B. *Angew. Chem. Int. Ed.* **2002**, *41*, 2110.

(105) Golas, P. L.; Matyjaszewski, K. *Chem. Soc. Rev.* **2010**, *39*, 1338.

(106) Rostovtsev, V. V.; Green, L. G.; Fokin, V. V.; Sharpless, K. B. *Angew. Chem. Int. Ed.* **2002**, *41*, 2596.

(107) Himo, F.; Lovell, T.; Hilgraf, R.; Rostovtsev, V. V.; Noodleman, L.; Sharpless, K. B.; Fokin, V. V. *J. Am. Chem. Soc.* **2004**, *127*, 210.

(108) Schilling, C.; Jung, N.; Bräse, S. In *Organic Azides*; Bräse, S., Bernnet, K., Eds.; John Wiley & Sons, Ltd: 2010, p 269.

(109) Meldal, M.; Tornoe, C. W. *Chem. Rev.* **2008**, *108*, 2952.

(110) Rodionov, V. O.; Presolski, S. I.; Diaz, D. D.; Fokin, V. V.; Finn, M. G. *J. Am. Chem. Soc.* **2007**, *129*, 12705.

(111) Hein, J. E.; Fokin, V. V. *Chem. Soc. Rev.* **2010**, *39*, 1302.

(112) Joule, J. A.; Mills, K. *Heterocyclic Chemistry*; 5th ed.; John Wiley & Sons: West Sussex, UK, 2010.

(113) de Souza, M. V. N.; Pais, K. C.; Kaiser, C. R.; Peralta, M. A.; Ferreira, M. D.; Lourenco, M. C. S. *Bioorg. Med. Chem.* **2009**, *17*, 1474.

(114) Biot, C.; Glorian, G.; Maciejewski, L. A.; Brocard, J. S.; Domarle, O.; Blampain, G.; Millet, P.; Georges, A. J.; Abessolo, H.; Dive, D.; Lebibi, J. *J. Med. Chem.* **1997**, *40*, 3715.

(115) Chiyanzu, I.; Clarkson, C.; Smith, P. J.; Lehman, J.; Gut, J.; Rosenthal, P. J.; Chibale, K. *Bioorg. Med. Chem.* **2005**, *13*, 3249.

(116) Musonda, C. C.; Gut, J.; Rosenthal, P. J.; Yardley, V.; de Souza, R. C. C.; Chibale, K. *Bioorg. Med. Chem.* **2006**, *14*, 5605

(117) Pawar, V. G.; Sos, M. L.; Rode, H. B.; Rabiller, M.; Heynck, S.; van Otterlo, W. A. L.; Thomas, R. K.; Rauh, D. *J. Med. Chem.* **2010**, *53*, 2892.

(118) De, D.; Krogstad, F. M.; Cogswell, F. B.; Krogstad, D. J. *Am. J. Trop. Med. Hyg.* **1996**, *55*, 579.

(119) Tahtaoui, C.; Parrot, I.; Klotz, P.; Guillier, F.; Galzi, J. L.; Hibert, M.; Ilien, B. *J. Med. Chem.* **2004**, *47*, 4300.

(120) Gu, X. H.; Zong, R.; Kula, N. S.; Baldessarini, R. J.; Neumeyer, J. L. *Bioorg. Med. Chem. Lett.* **2001**, *11*, 3049.

(121) Cegielska, B.; Kacprzak, K. M. *Chem. Anal.* **2009**, *54*.

(122) Conrad, P. C.; Kwiatkowski, P. L.; Fuchs, P. L. *J. Org. Chem.* **1987**, *52*, 586.

(123) Nagase, T.; Mizutani, T.; Ishikawa, S.; Sekino, E.; Sasaki, T.; Fujimura, T.; Ito, S.; Mitobe, Y.; Miyamoto, Y.; Yoshimoto, R.; Tanaka, T.; Ishihara, A.; Takenaga, N.; Tokita, S.; Fukami, T.; Sato, N. *J. Med. Chem.* **2008**, *51*, 4780.

(124) Finkelstein, H. *Ber. Dtsch. Chem. Ges.* **1910**, *43*, 1528.

(125) Dollinger, S.; Lo¨ber, S.; Klingenstein, R.; Korth, C.; Gmeiner, P. *J. Med. Chem.* **2006**, *49*, 6561

(126) DePue, J. S.; Collum, D. B. *J. Am. Chem. Soc.* **1988**, *110*, 5518.

(127) DePue, J. S.; Collum, D. B. *J. Am. Chem. Soc.* **1988**, *110*, 5224.

(128) Kapat, A.; Konig, A.; Montermini, F.; Renaud, P. *J. Am. Chem. Soc.* **2011**, *133*, 13890.

(129) Reddy, K. R.; Rajgopal, K.; Kantam, M. L. *Synlett* **2006**, *124*, 957.

(130) Stefani, H. A.; Canduzini, H. A.; Manarin, F. *Tetrahedron Lett.* **2011**, *52*, 6086

(131) Trager, W.; Jensen, J. B. *Science* **1976**, *193*, 673.

(132) Noedl, H.; Wongscrichanalai, C.; Wernsdorfer, W. H. *Trends Parasitol.* **2003**, *19*, 175.

(133) Makler, M. T.; Ries, J. M.; Williams, J. A.; Bancroft, J. E.; Piper, R. C.; Gibbins, B. L.; Hinrichs, D. J. *Am. J. Trop. Med. Hyg.* **1993**, *48*, 739.

(134) Alibert, S.; Santelli-Rouvier, C.; Pradiness, B.; Houdin, C.; Parzy, D.; Karolak-Wojciechowska, J.; Barbe, J. *J. Med. Chem.* **2002**, *45*, 3195.

(135) Jana, S.; Paliwal, J. *Int. J. Antimicrob. Agents* **2007**, *30*, 4

(136) Combrinck, J. M.; Mabotha, T. E.; Ncokazi, K. K.; Ambele, M. A.; Taylor, D.; Smith, P. J.; Hoppe, H. C.; Egan, T. J. *ACS Chem. Biol.* **2012**, *8*, 133.

(137) Benalil, A.; Carboni, B.; Vaultier, M. *Tetrahedron* **1991**, *47*, 8177.

(138) Sander, K.; Kottke, T.; Hoffend, C.; Walter, M.; Weizel, L.; Camelin, J. C.; Ligneau, X.; Schneider, E. H.; Seifert, R.; Schwartz, J. C.; Stark, H. *Org. Lett.* **2010**, *12*, 2578.

(139) Dash, J.; Waller, Z. A. E.; Pantoş, G. D.; Balasubramanian, S. *Chem. Euro. J.* **2011**, *17*, 4571.

(140) Jung, S.; Song, H.; Lee, Y.; Jeong, H.; Lee, H. *Macromol.* **2011**, *44*, 1628.

(141) Wijtmans, M.; de Graaf, C.; de Kloe, G.; Istyastono, E. P.; Smit, J.; Lim, H.; Boonnak, R.; Nijmeijer, S.; Smits, R. A.; Jongejan, A.; Zuiderveld, O.; de Esch, I. J. P.; Leurs, R. *J. Med. Chem.* **2011**, *54*, 1693.

(142) Romera, J. L.; Cid, J. M.; Trabanco, A. A. *Tetrahedron Lett.* **2004**, *45*, 4.

Supporting information

^{1}H NMR spectra

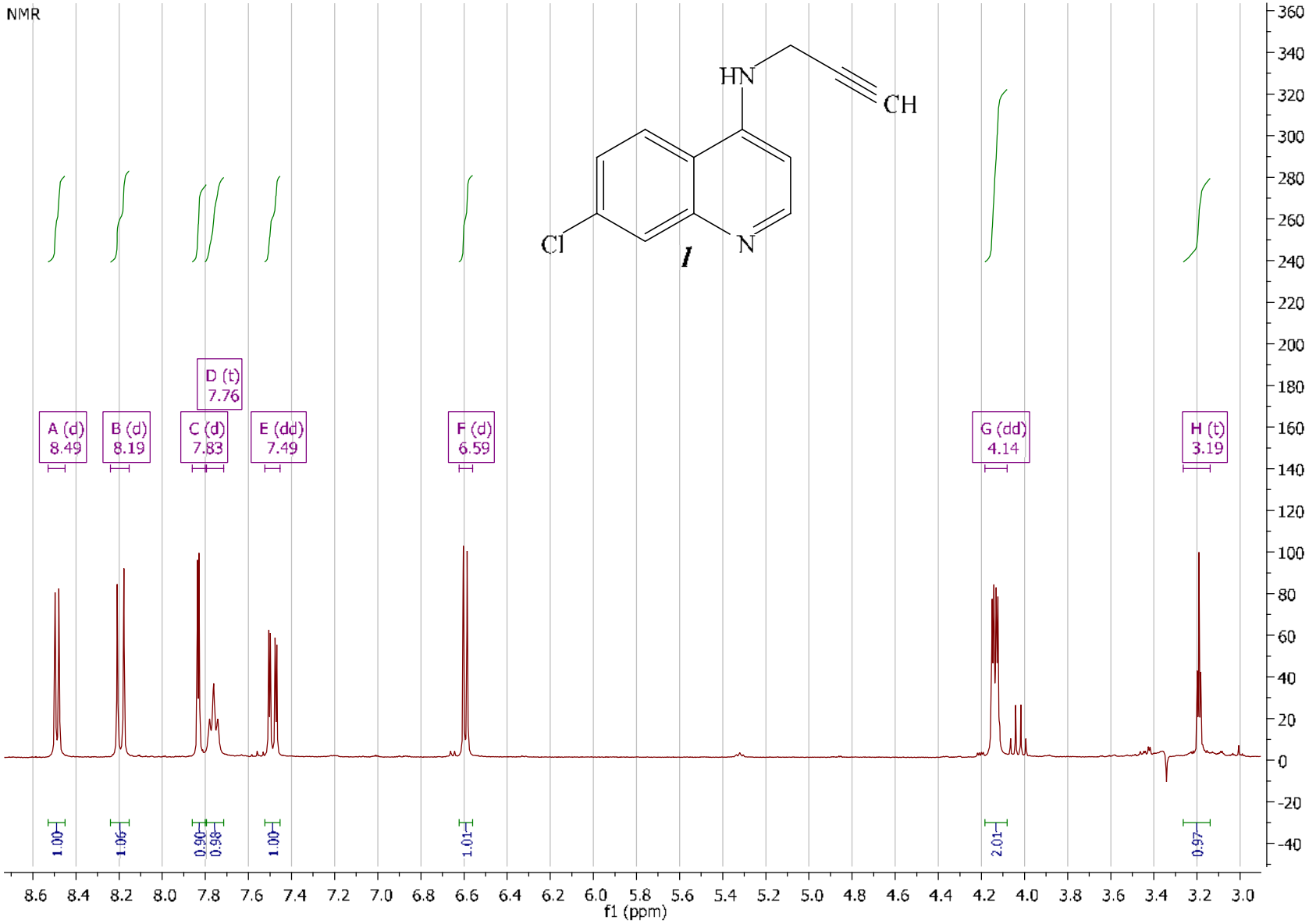
NMR
HN
CH
Cl
N
1
A (d)
8.49
B (d)
8.19
D (t)
7.76
C (d)
7.83
E (dd)
7.49
F (d)
6.59
G (dd)
4.14
H (t)
3.19
1.00
1.06
0.90
0.98
1.00
1.01
2.01
0.97
f1 (ppm)

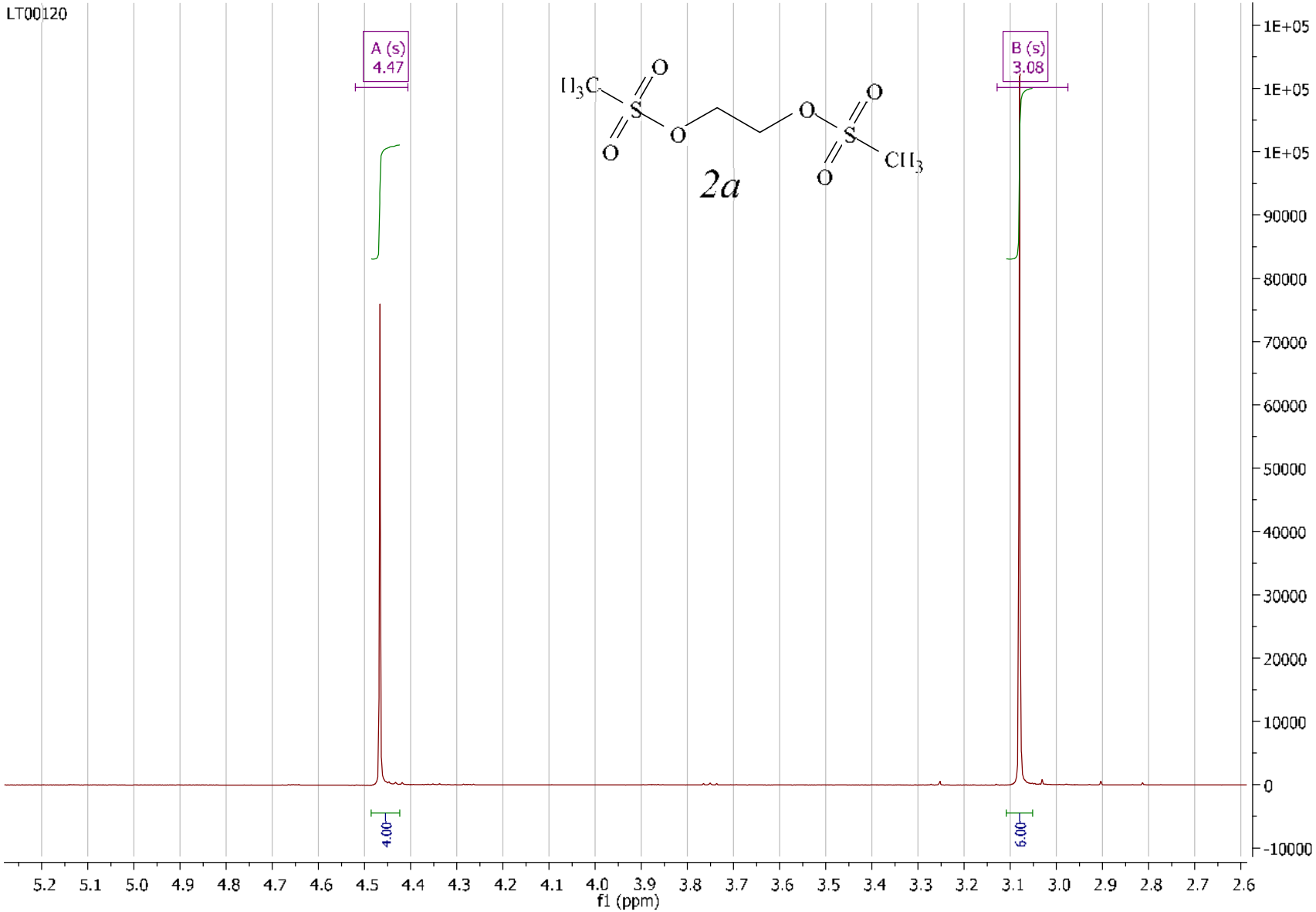
LT00120
A (s)
4.47
B (s)
3.08
2a
4.00
6.00
f1 (ppm)

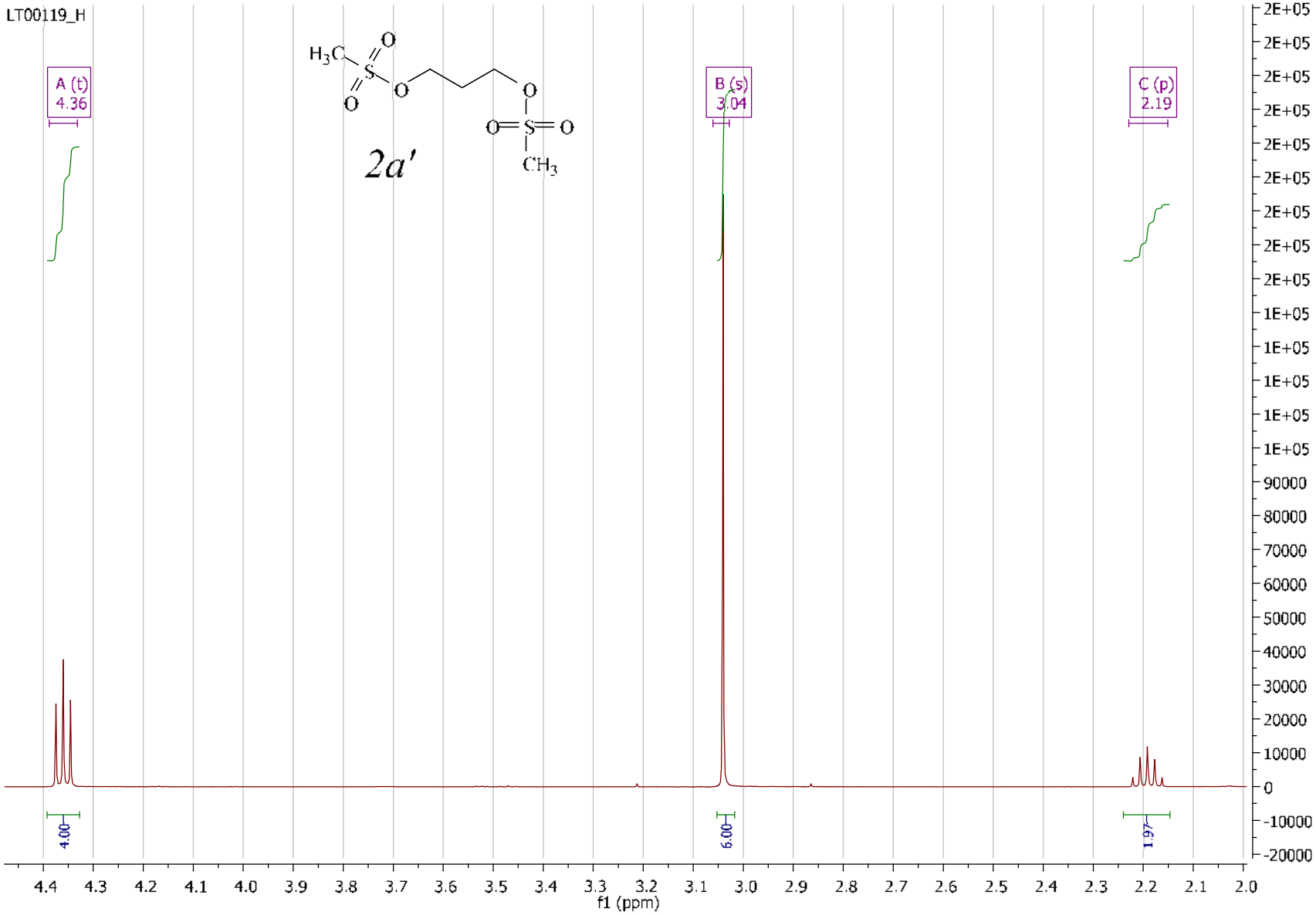
LT00119_H
A (t)
4.36
B (s)
3.04
C (p)
2.19
2a′
4.00
6.00
1.97
f1 (ppm)

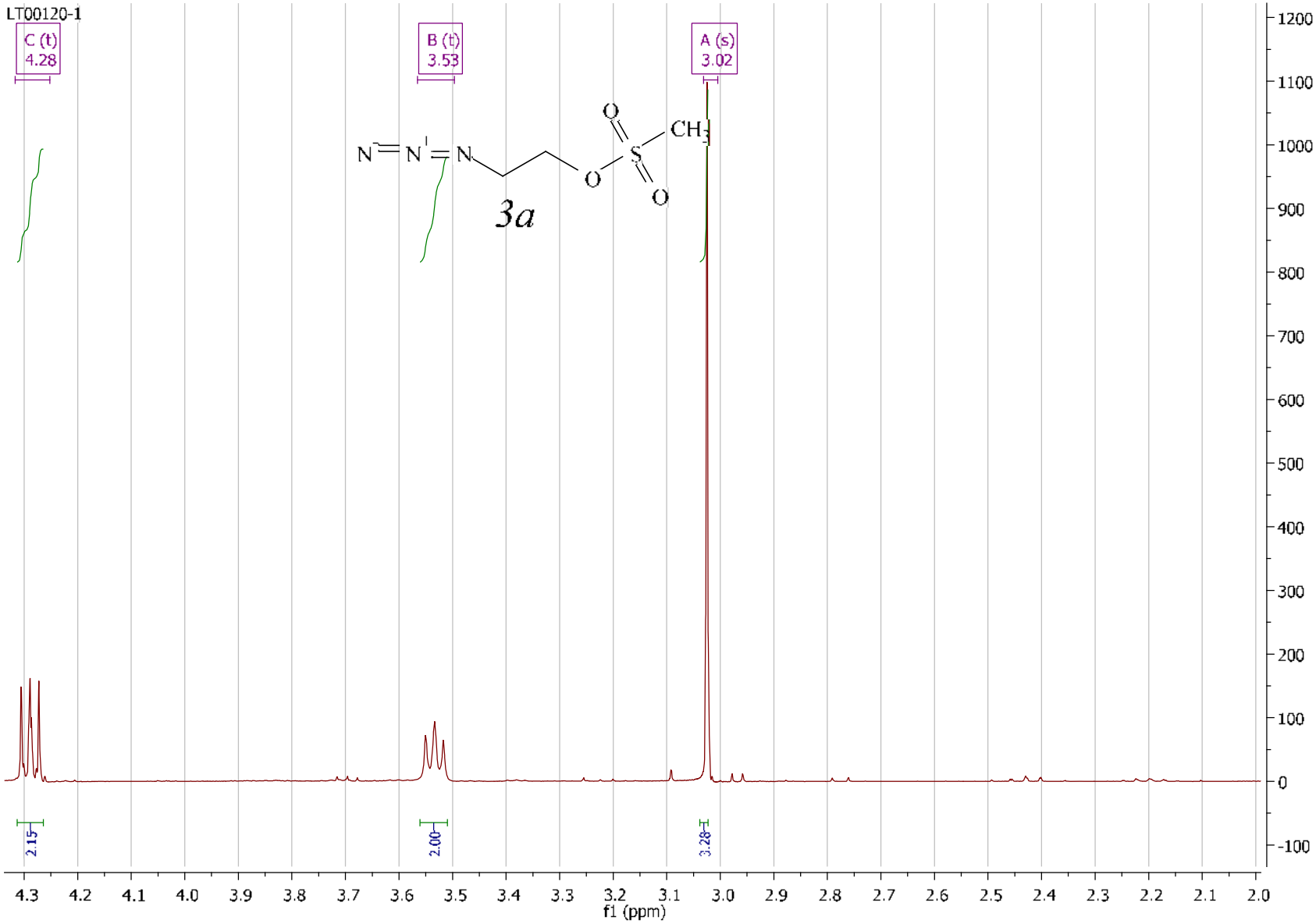
LT00120-1
C (t)
4.28
B (t)
3.53
A (s)
3.02
3a
2.15
2.00
3.28
f1 (ppm)

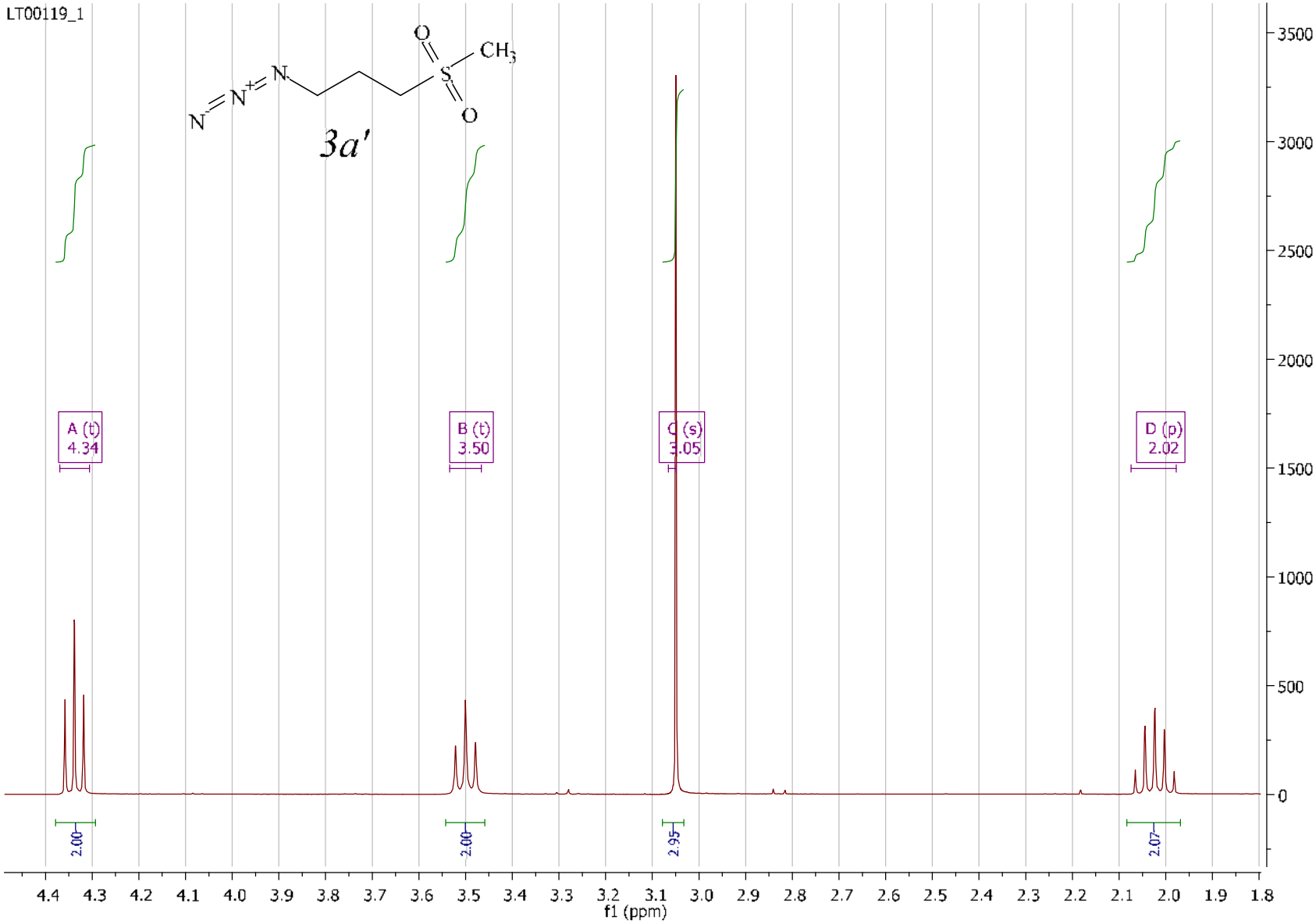
LT00119_1
3a'
A (t)
4.34
B (t)
3.50
C (s)
3.05
D (p)
2.02
2.00
2.00
2.95
2.07
f1 (ppm)

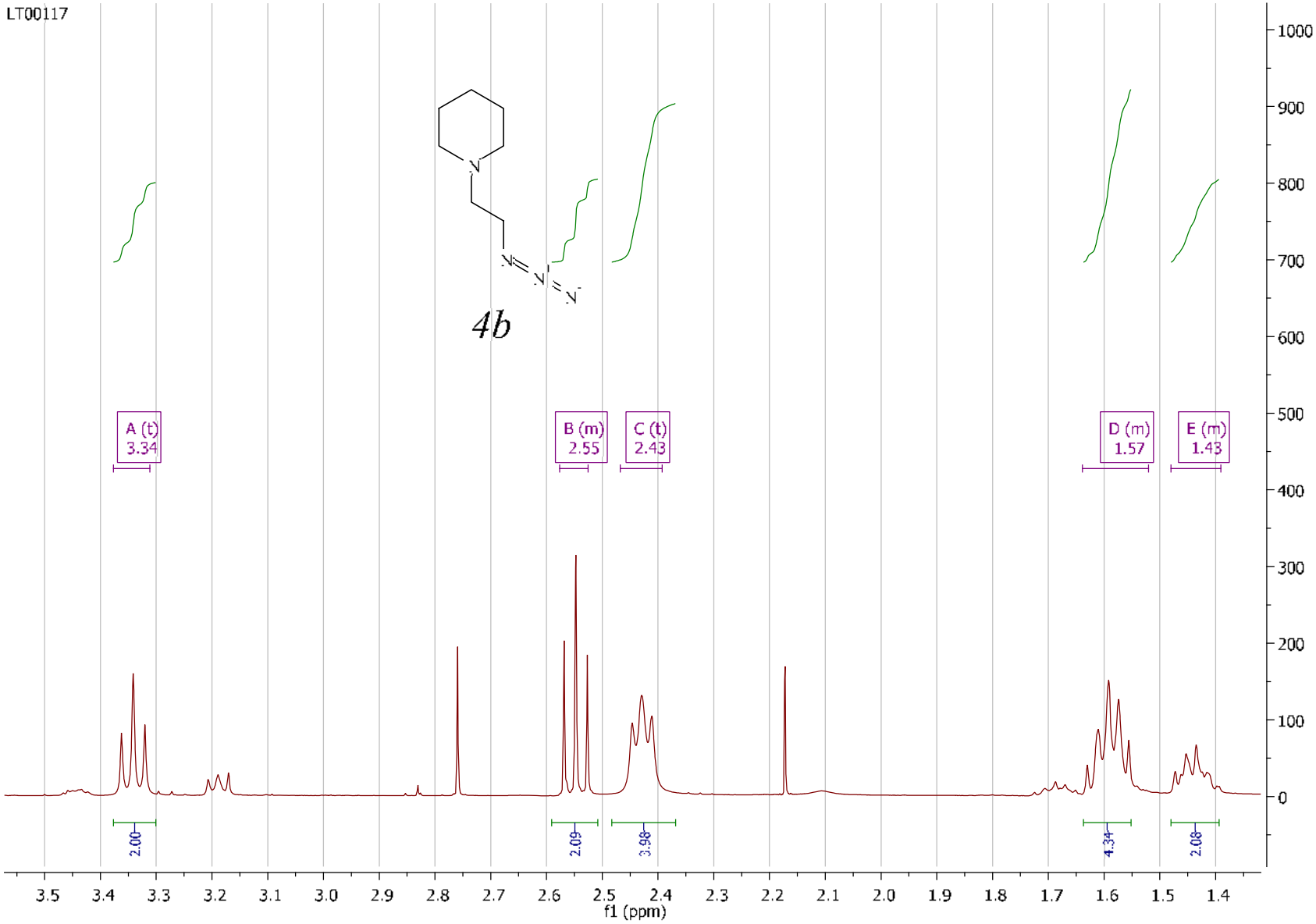
LT00117
4b
A (t)
3.34
B (m)
2.55
C (t)
2.43
D (m)
1.57
E (m)
1.43
2.00
2.09
3.98
4.34
2.08
f1 (ppm)

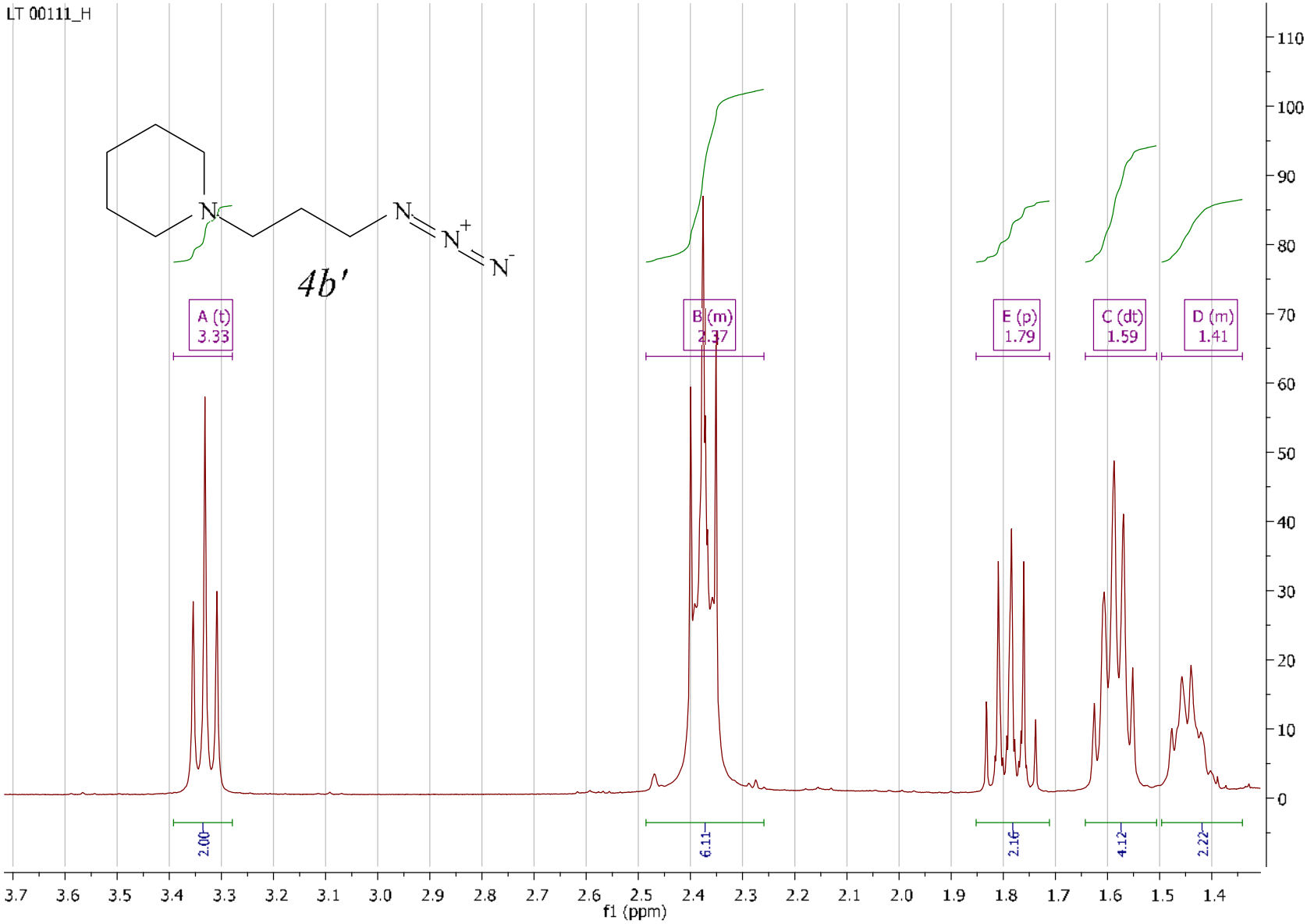
LT 00111_H
4b'
A (t)
3.33
B (m)
2.37
E (p)
1.79
C (dt)
1.59
D (m)
1.41
2.00
6.11
2.16
4.12
2.22
f1 (ppm)

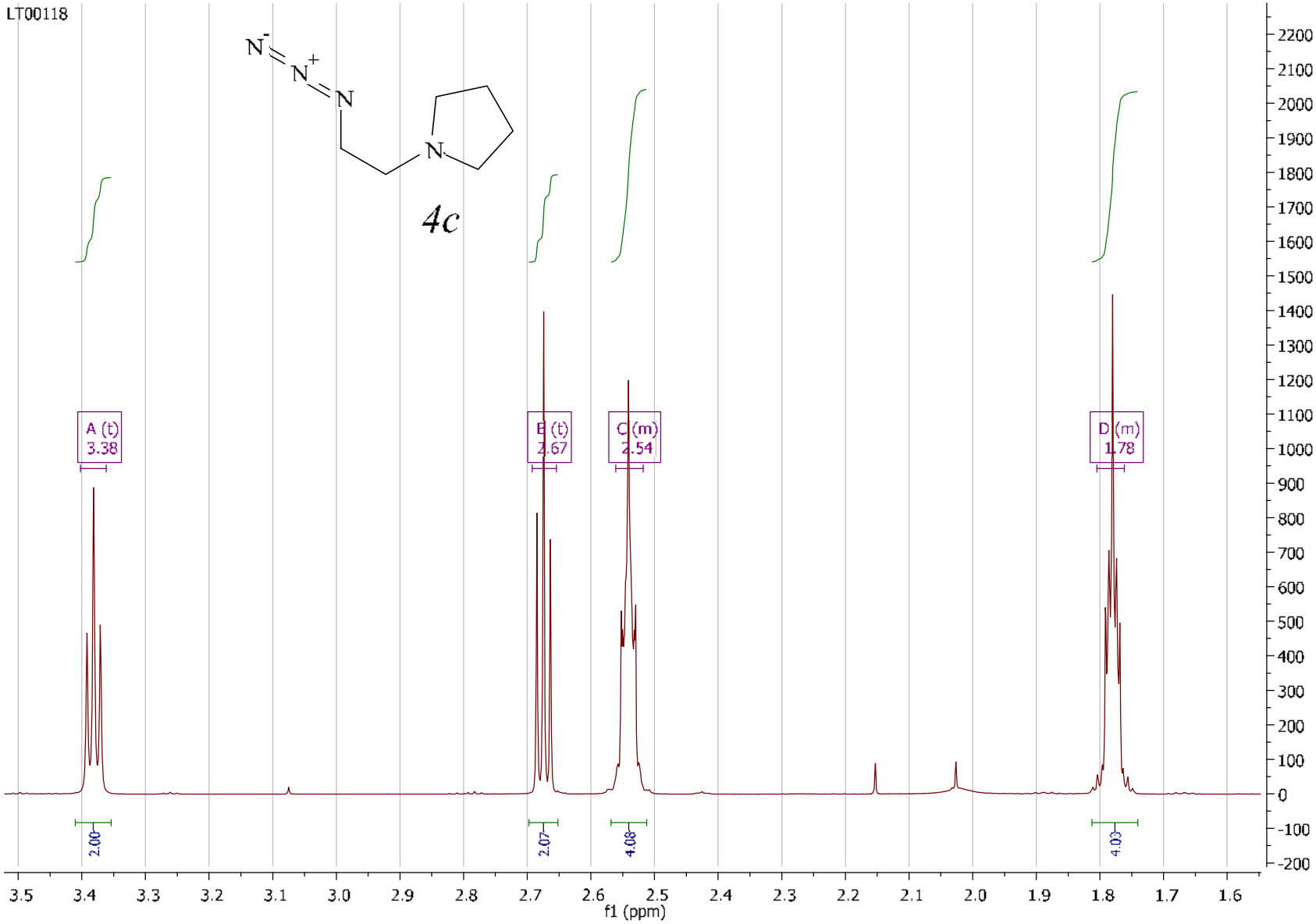
LT00118
4c
A (t)
3.38
B (t)
2.67
C (m)
2.54
D (m)
1.78
2.00
2.07
4.08
4.03
f1 (ppm)

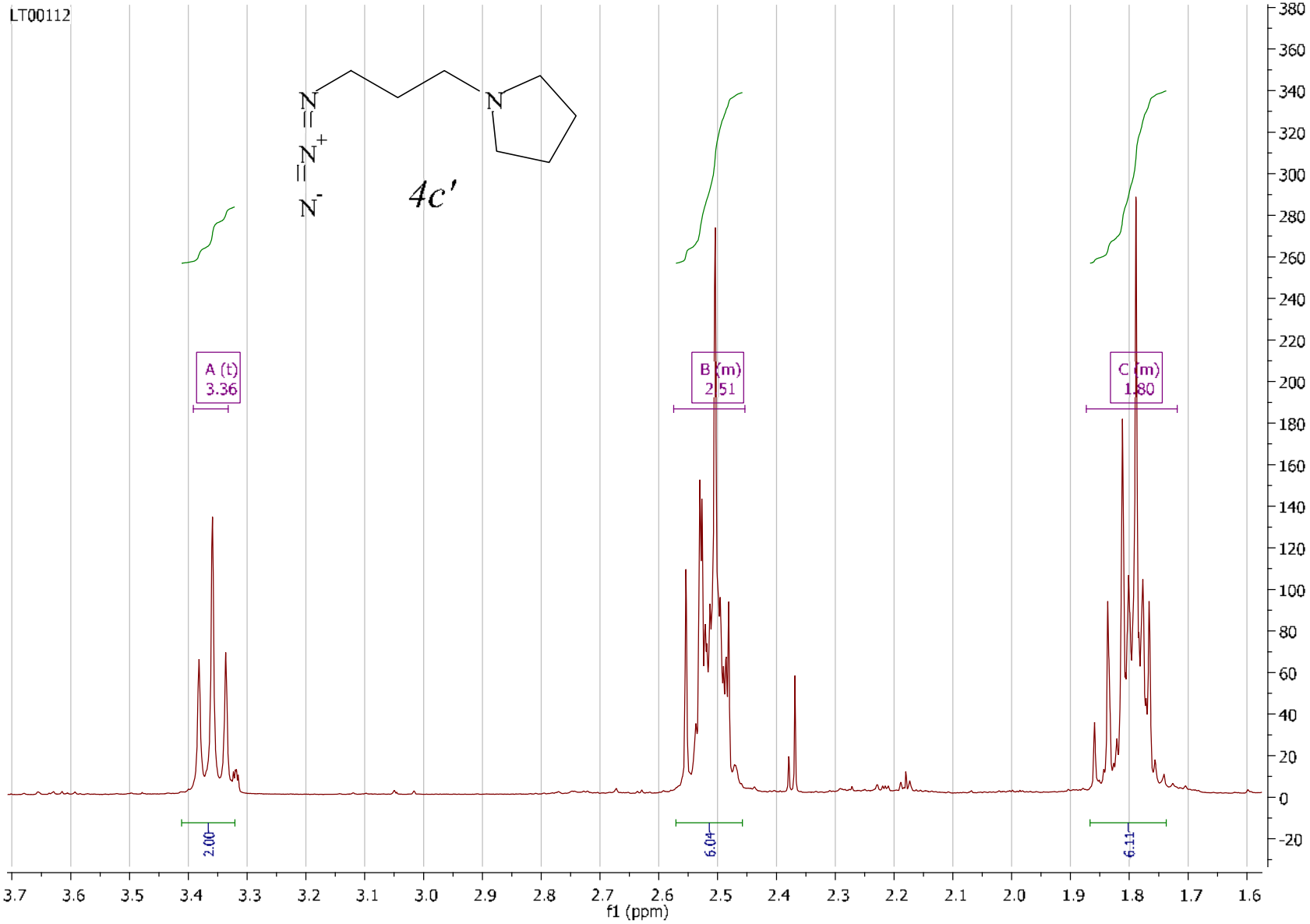
LT00112
4c'
A (t)
3.36
B (m)
2.51
C (m)
1.80
2.00
6.04
6.11
f1 (ppm)

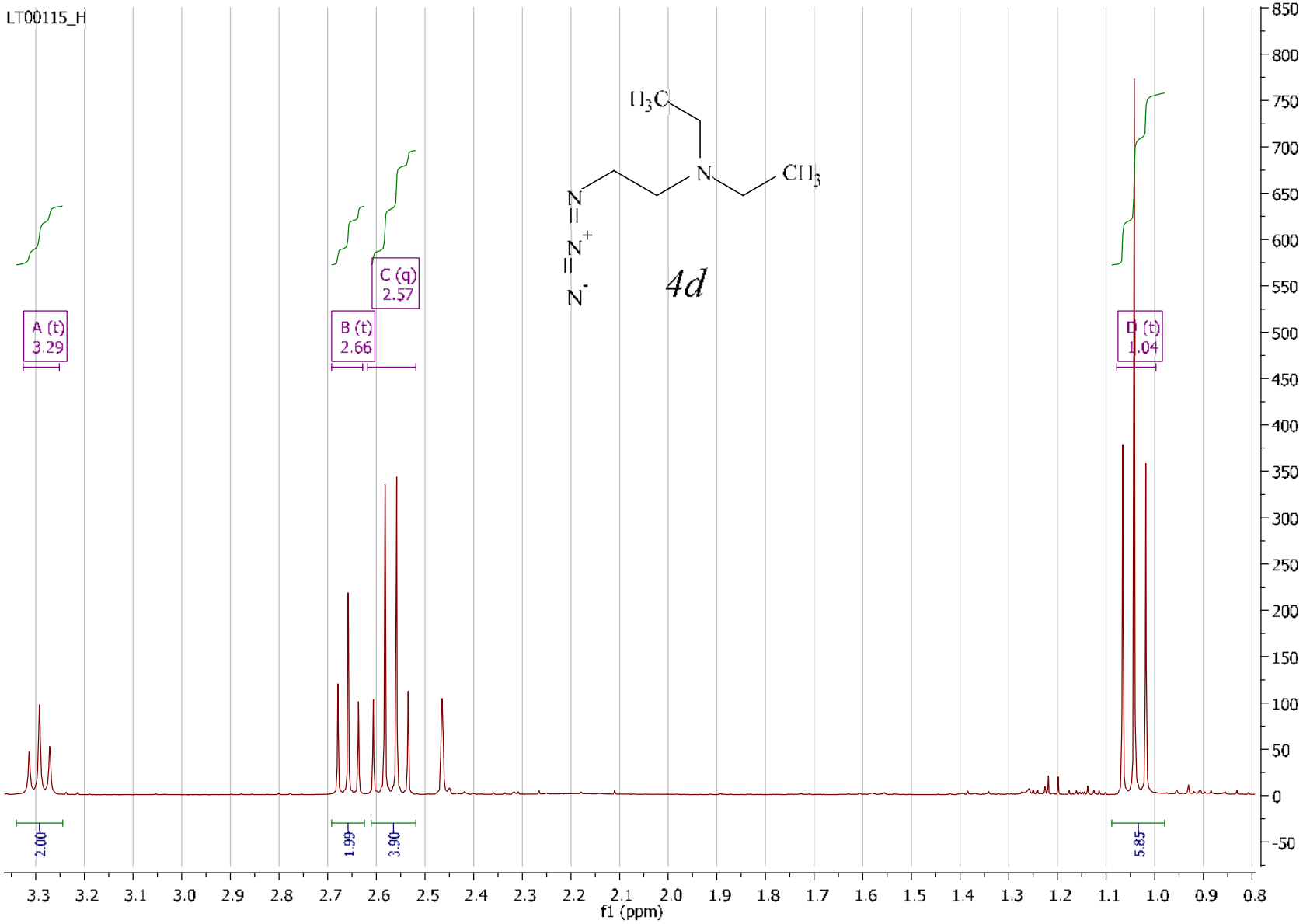
LT00115_H
A (t)
3.29
B (t)
2.66
C (q)
2.57
D (t)
1.04
4d
2.00
1.99
3.90
5.85
f1 (ppm)

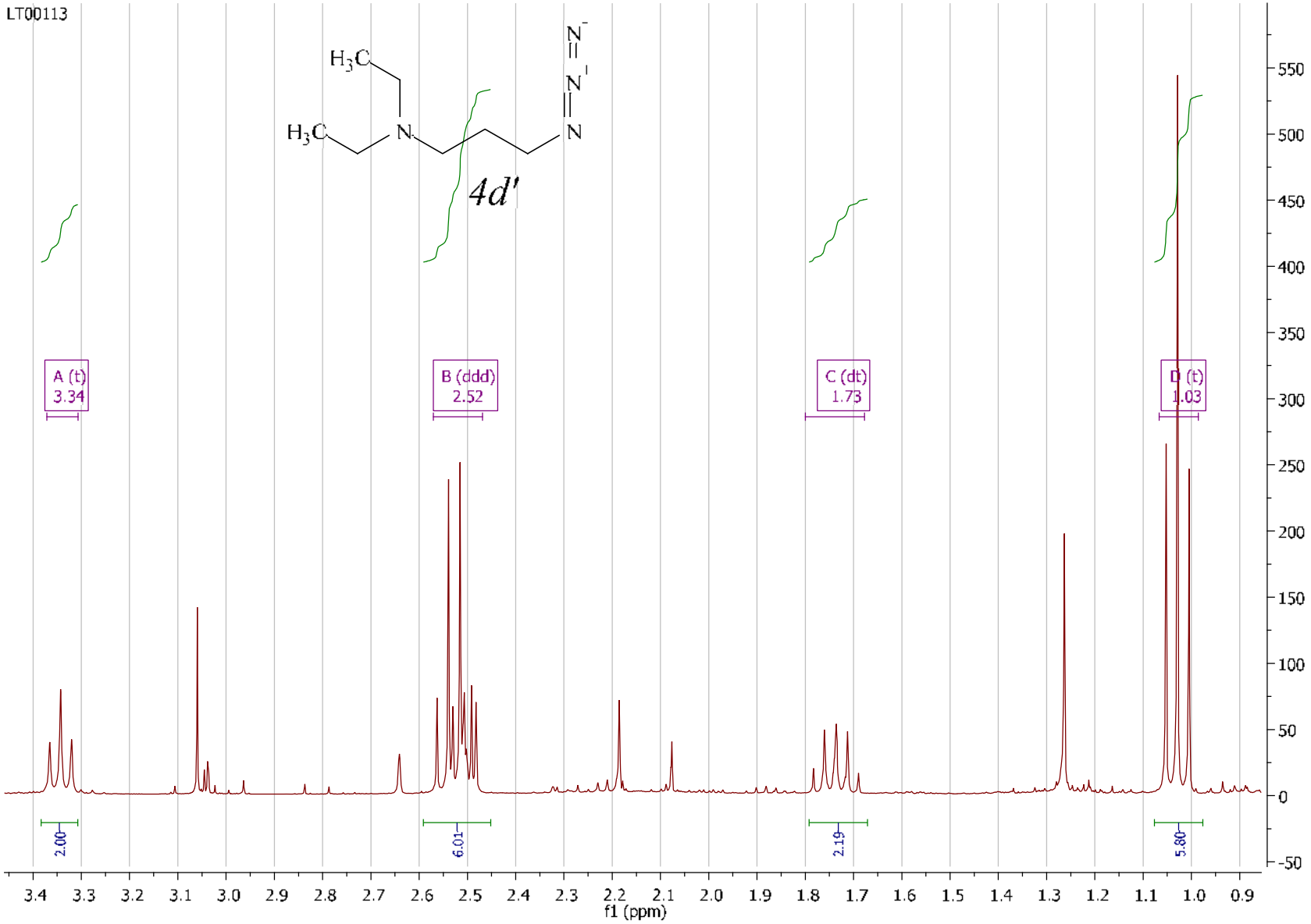
LT00113
4d'
A (t)
3.34
B (ddd)
2.52
C (dt)
1.73
D (t)
1.03
2.00
6.01
2.19
5.80
f1 (ppm)

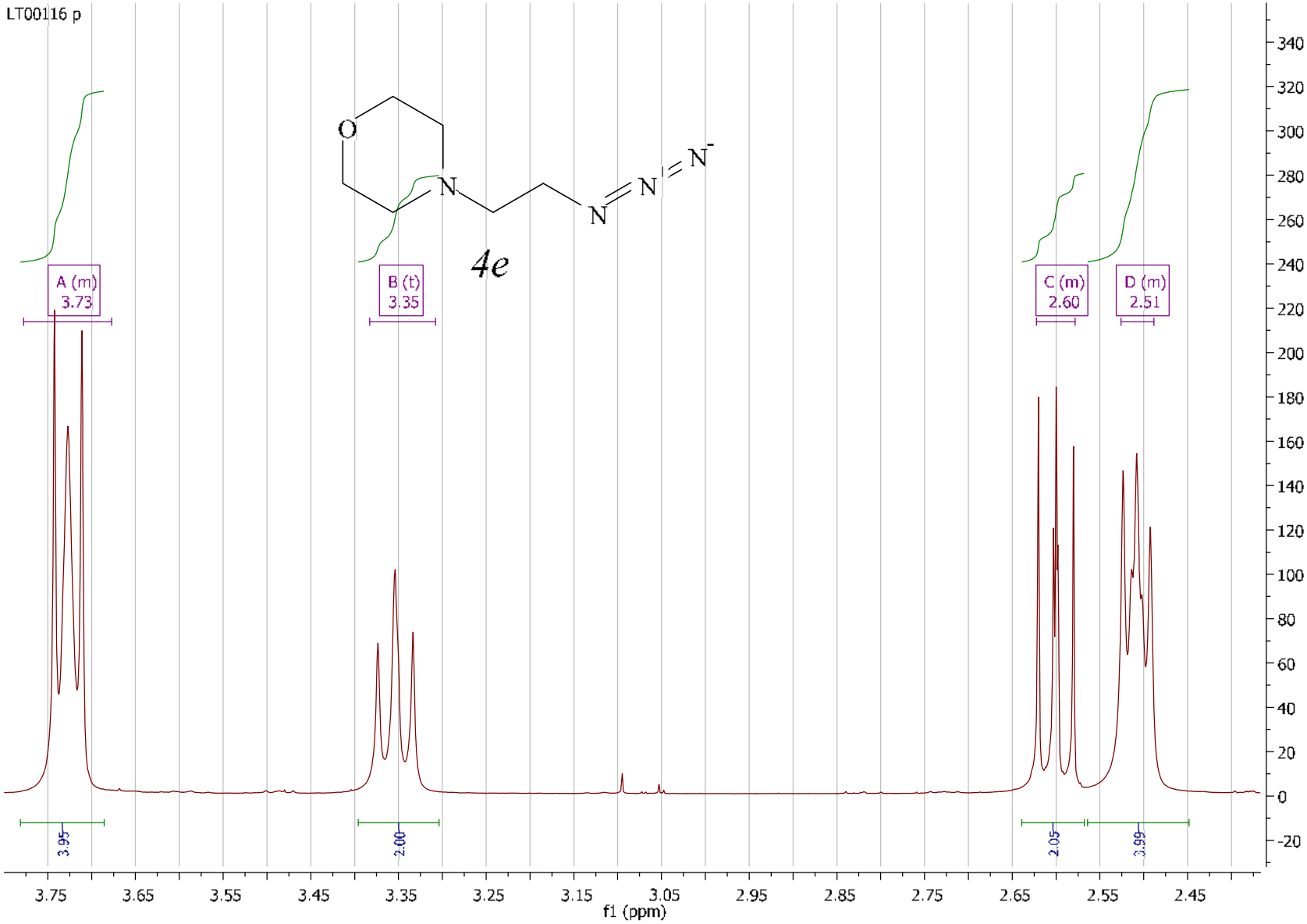
LT00116 p
O
N
N
N
N
4e
A (m)
3.73
B (t)
3.35
C (m)
2.60
D (m)
2.51
3.95
2.00
2.05
3.99
f1 (ppm)

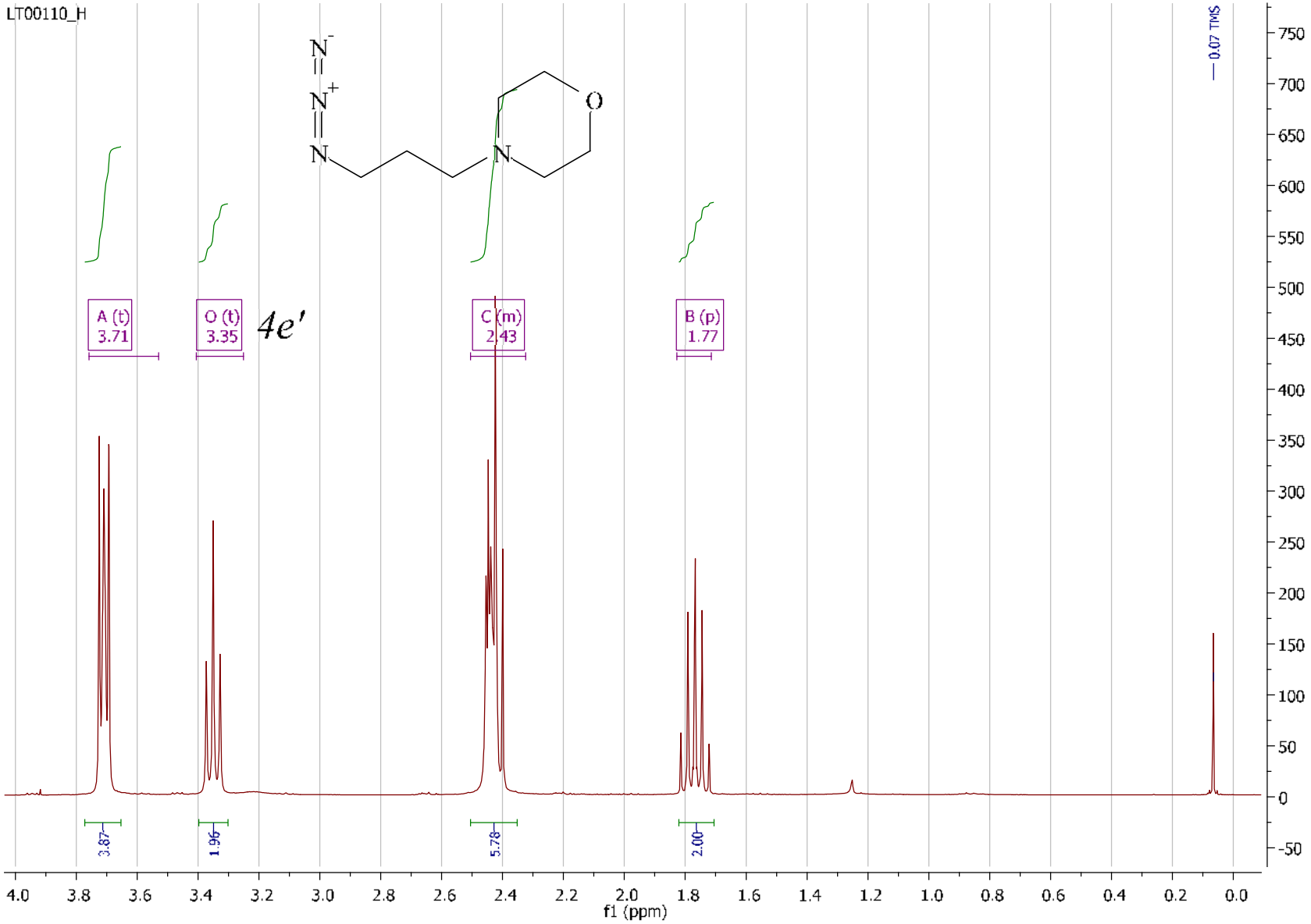
LT00110_H
A (t)
3.71
O (t)
3.35
4e'
C (m)
2.43
B (p)
1.77
0.07 TMS
3.87
1.96
5.78
2.00
f1 (ppm)

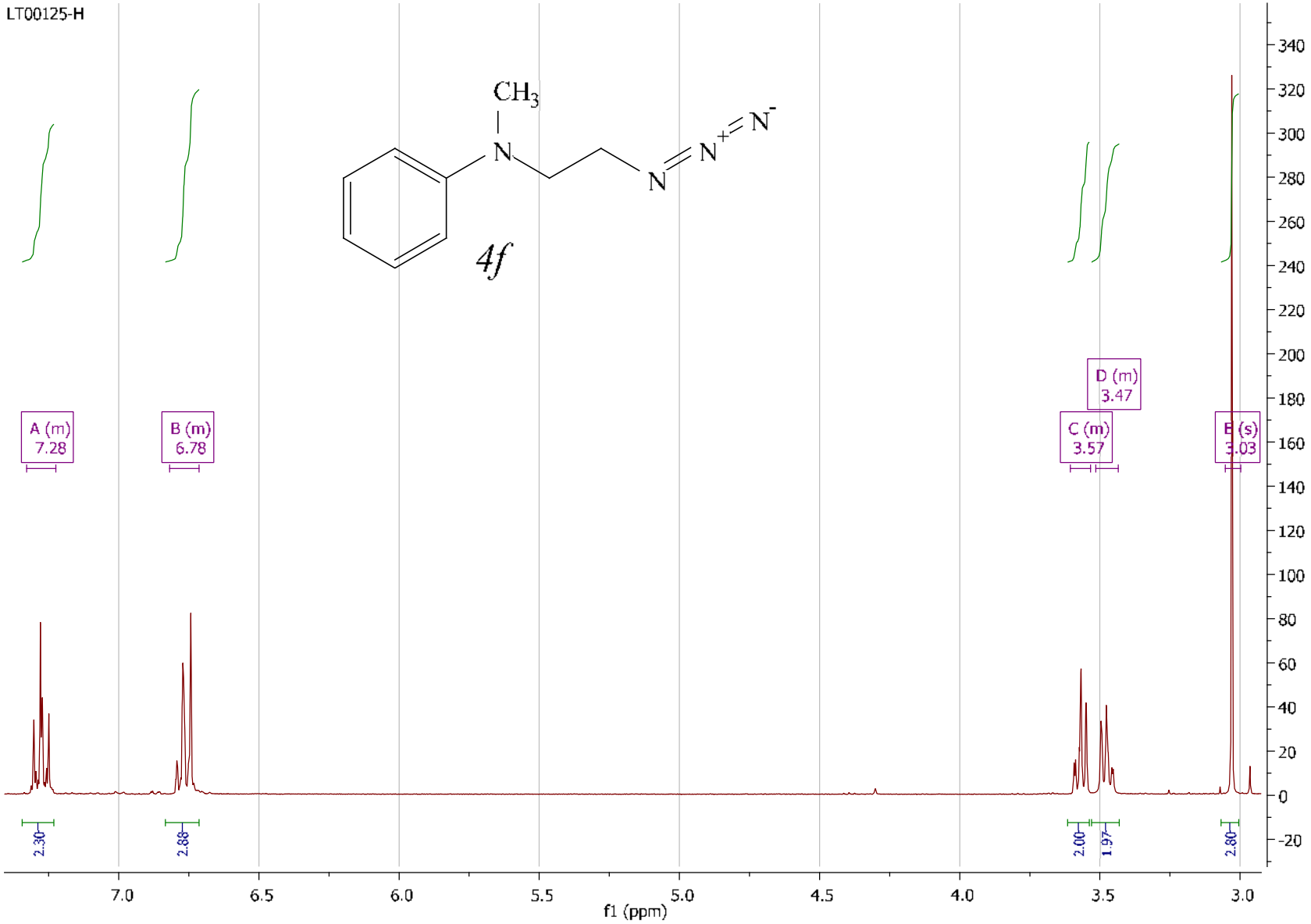
LT00125-H
CH3
N
N
N+
N-
4f
A (m)
7.28
B (m)
6.78
D (m)
3.47
C (m)
3.57
E (s)
3.03
2.30
2.88
2.00
1.97
2.80
7.0
6.5
6.0
5.5
5.0
4.5
4.0
3.5
3.0
f1 (ppm)
340
320
300
280
260
240
220
200
180
160
140
120
100
80
60
40
20
0
-20

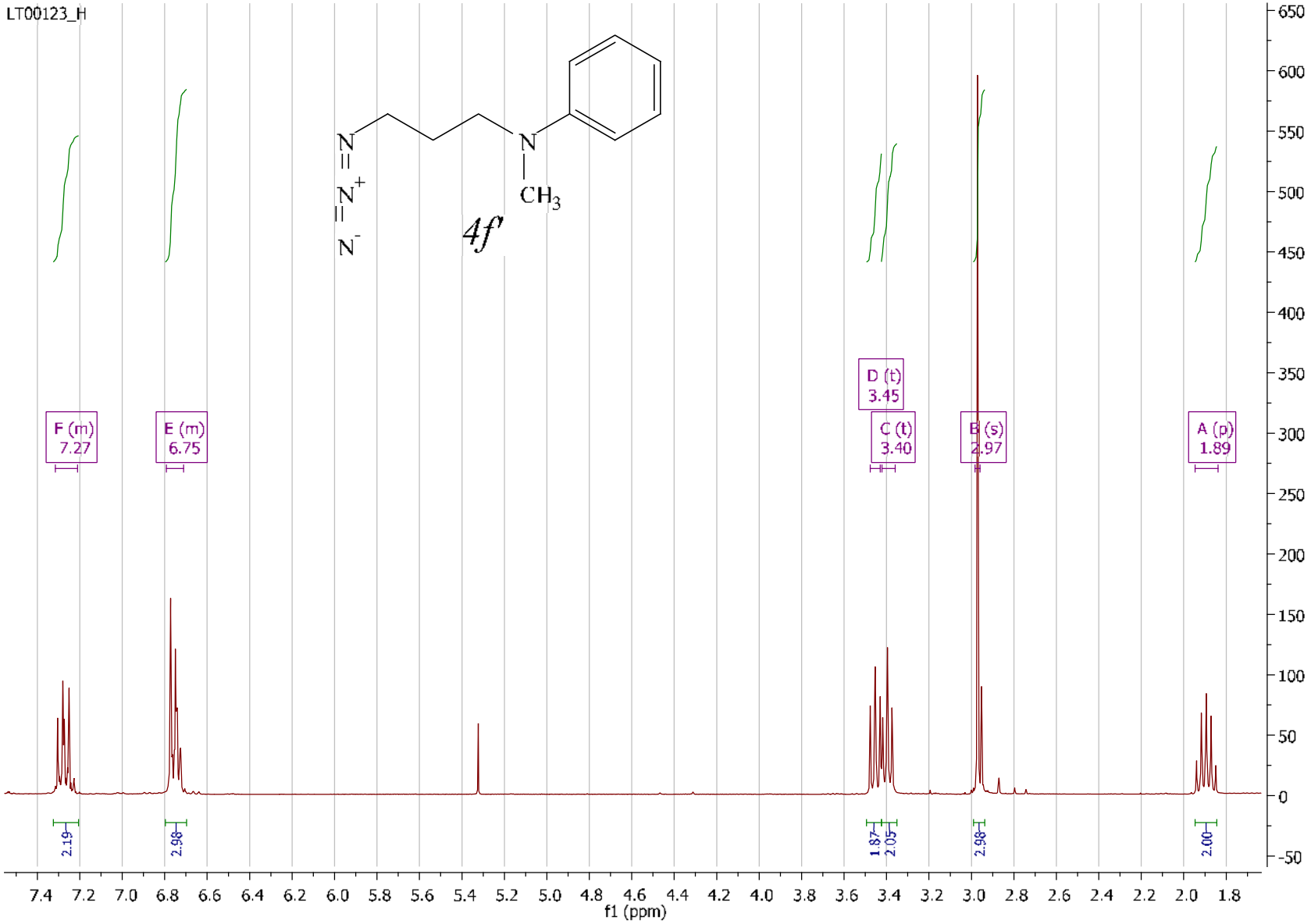
LT00123_H
4f
F (m)
7.27
E (m)
6.75
D (t)
3.45
C (t)
3.40
B (s)
2.97
A (p)
1.89
2.19
2.98
1.87
2.05
2.98
2.00
f1 (ppm)

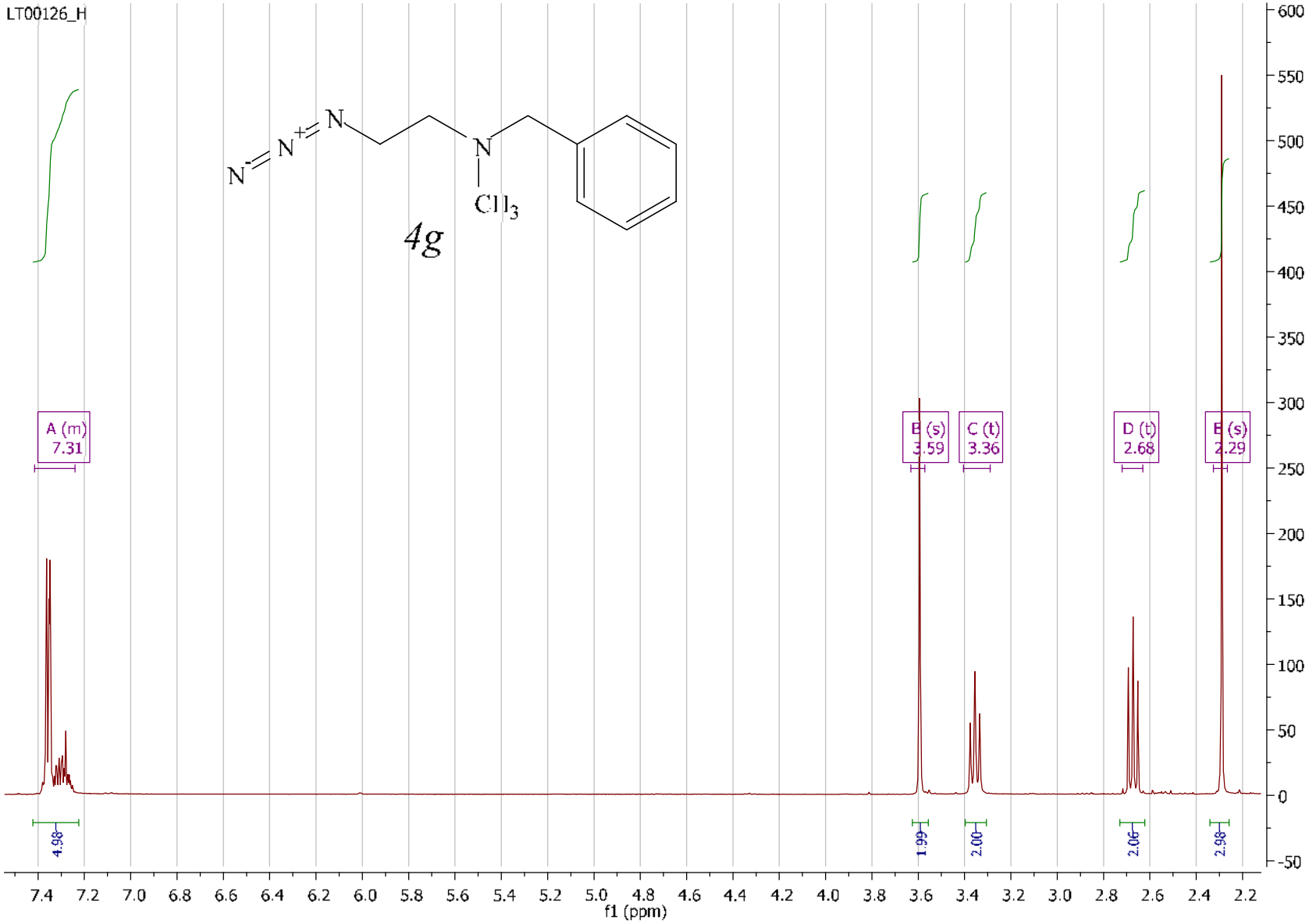
LT00126_H
4g
A (m)
7.31
B (s)
3.59
C (t)
3.36
D (t)
2.68
E (s)
2.29
4.98
1.99
2.00
2.06
2.98
f1 (ppm)

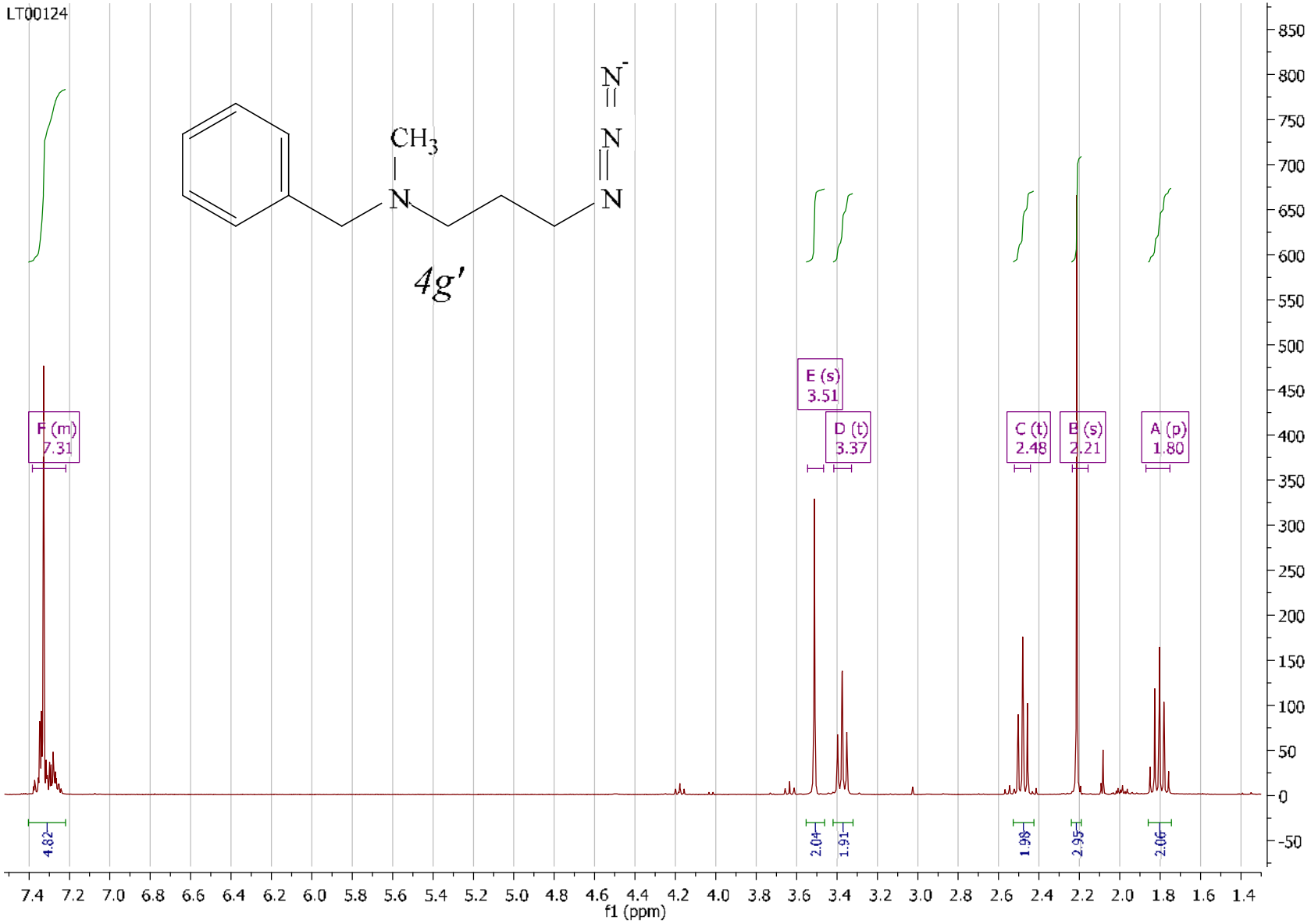
LT00124
CH3
N
N
N
N
4g'
F (m)
7.31
E (s)
3.51
D (t)
3.37
C (t)
2.48
B (s)
2.21
A (p)
1.80
4.82
2.04
1.91
1.98
2.95
2.06
f1 (ppm)

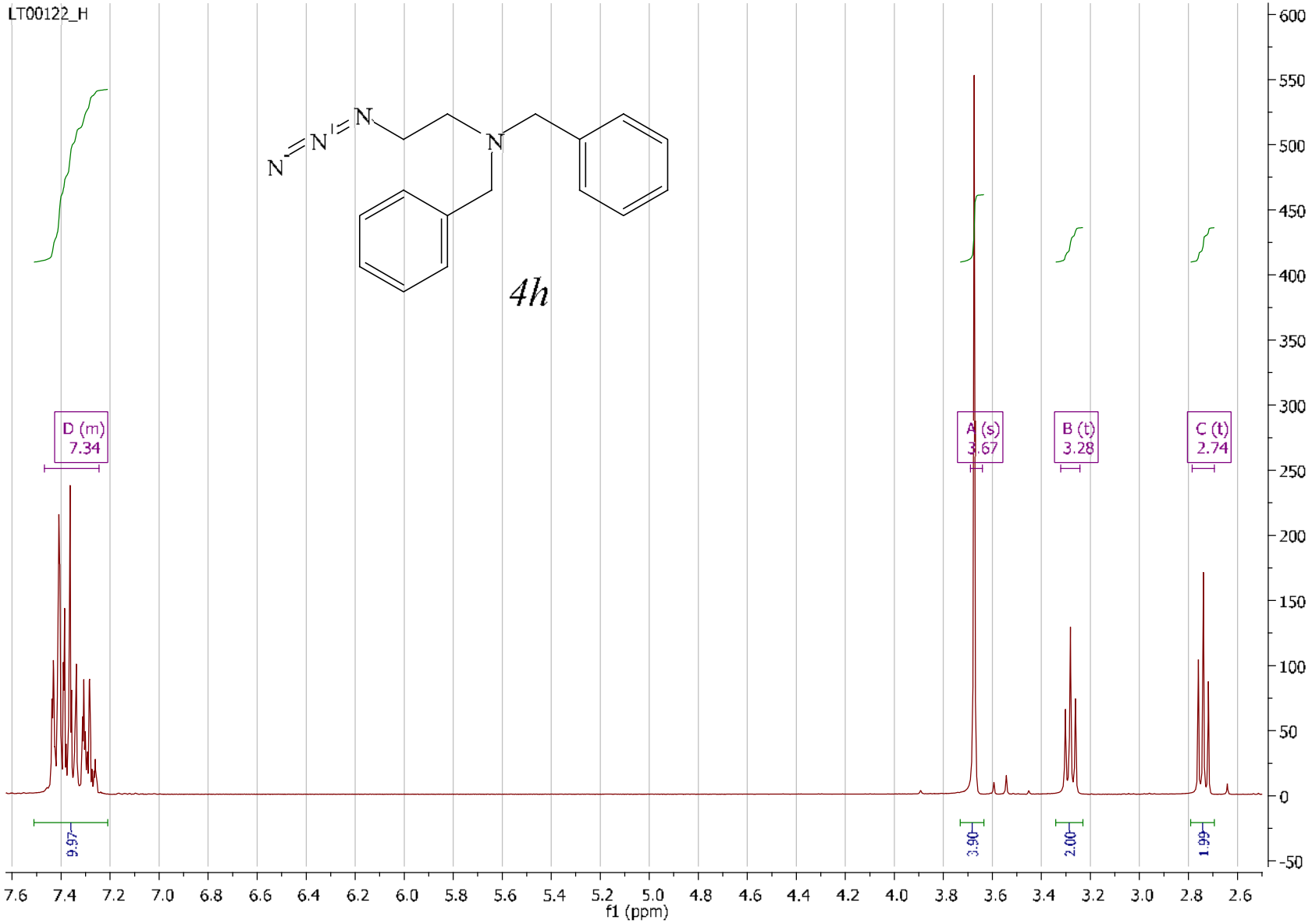
LT00122_H
4h
D (m)
7.34
A (s)
3.67
B (t)
3.28
C (t)
2.74
9.97
3.90
2.00
1.99
f1 (ppm)

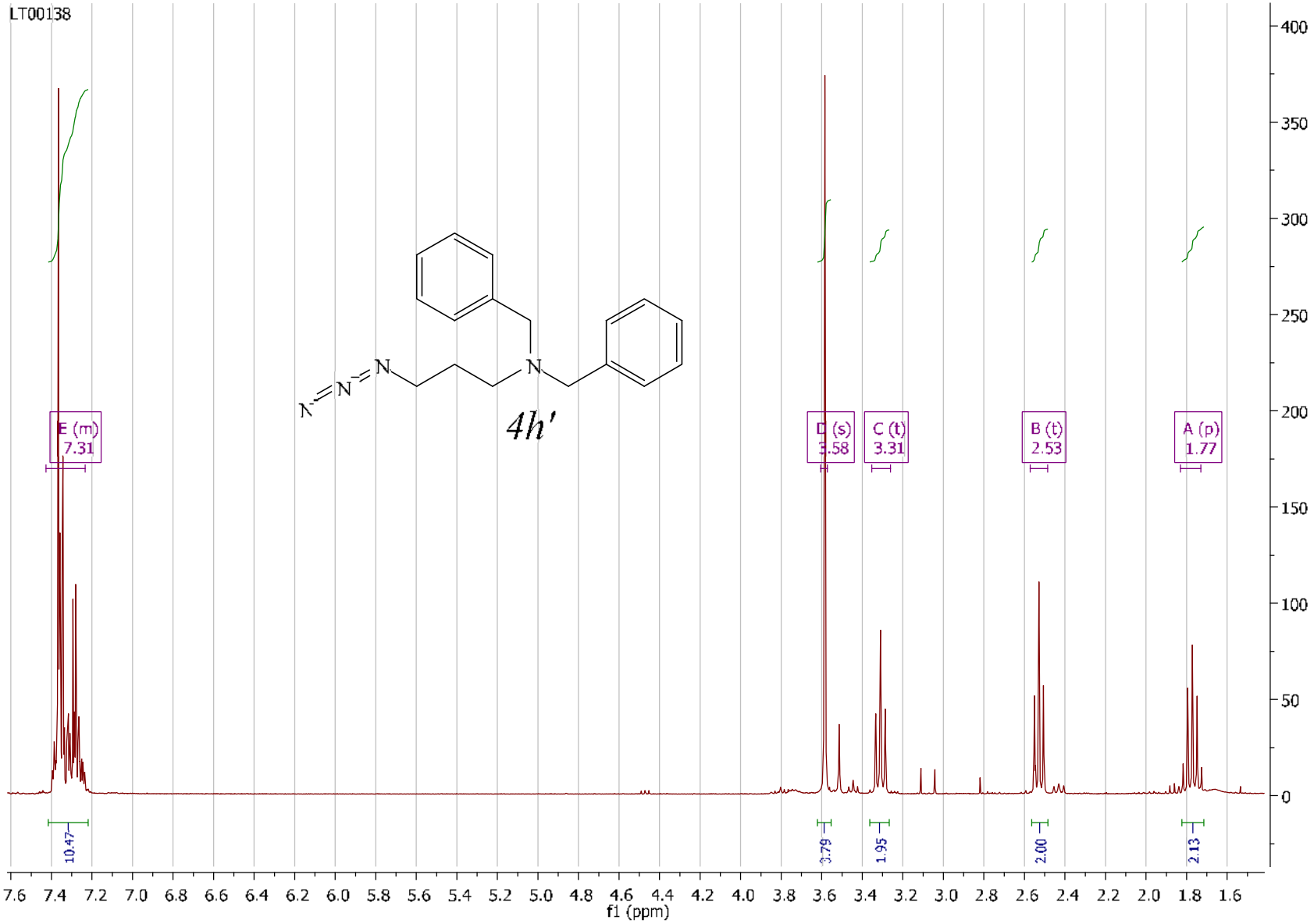
LT00138
4h'
E (m)
7.31
D (s)
3.58
C (t)
3.31
B (t)
2.53
A (p)
1.77
10.47
3.79
1.95
2.00
2.13
f1 (ppm)

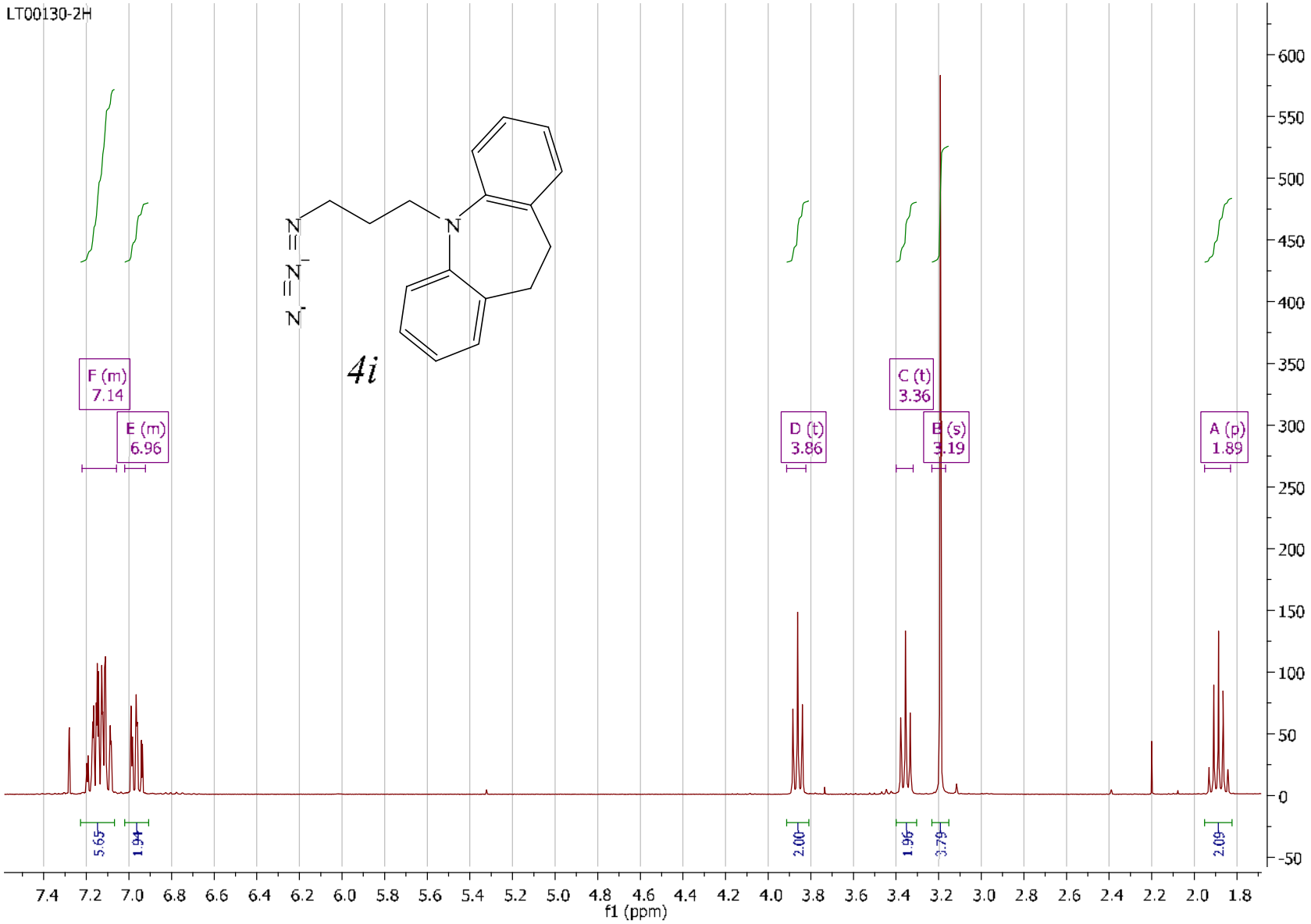
LT00130-2H
4i
F (m)
7.14
E (m)
6.96
D (t)
3.86
C (t)
3.36
B (s)
3.19
A (p)
1.89
5.65
1.94
2.00
1.96
3.79
2.09
f1 (ppm)

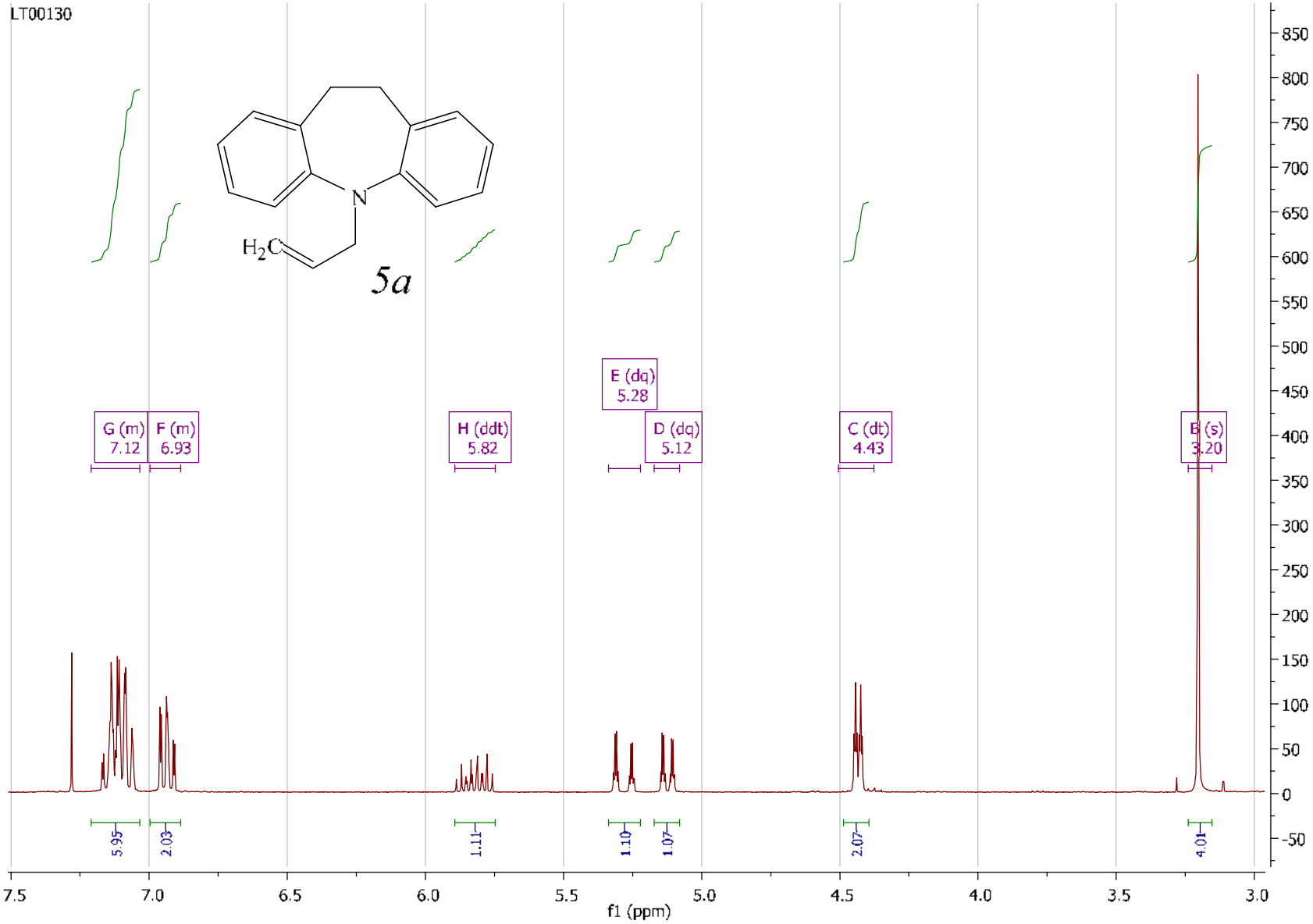
LT00130
N
H2C
5a
G (m)
7.12
F (m)
6.93
H (ddt)
5.82
E (dq)
5.28
D (dq)
5.12
C (dt)
4.43
B (s)
3.20
5.95
2.03
1.11
1.10
1.07
2.07
4.01
7.5
7.0
6.5
6.0
5.5
5.0
4.5
4.0
3.5
3.0
f1 (ppm)
850
800
750
700
650
600
550
500
450
400
350
300
250
200
150
100
50
0
-50

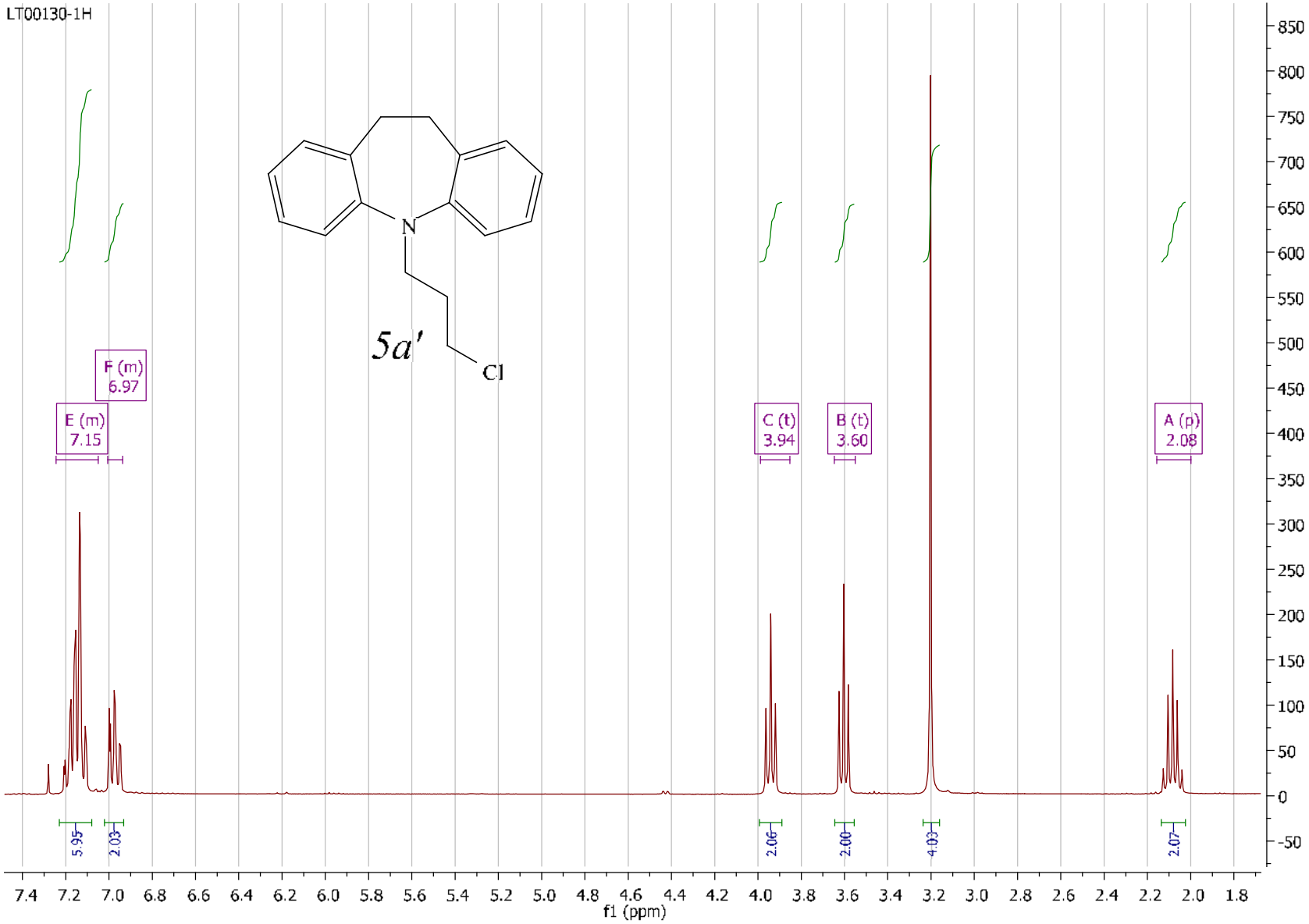
LT00130-1H
N
Cl
5a'
F (m)
6.97
E (m)
7.15
C (t)
3.94
B (t)
3.60
A (p)
2.08
5.95
2.03
2.06
2.00
4.03
2.07
f1 (ppm)

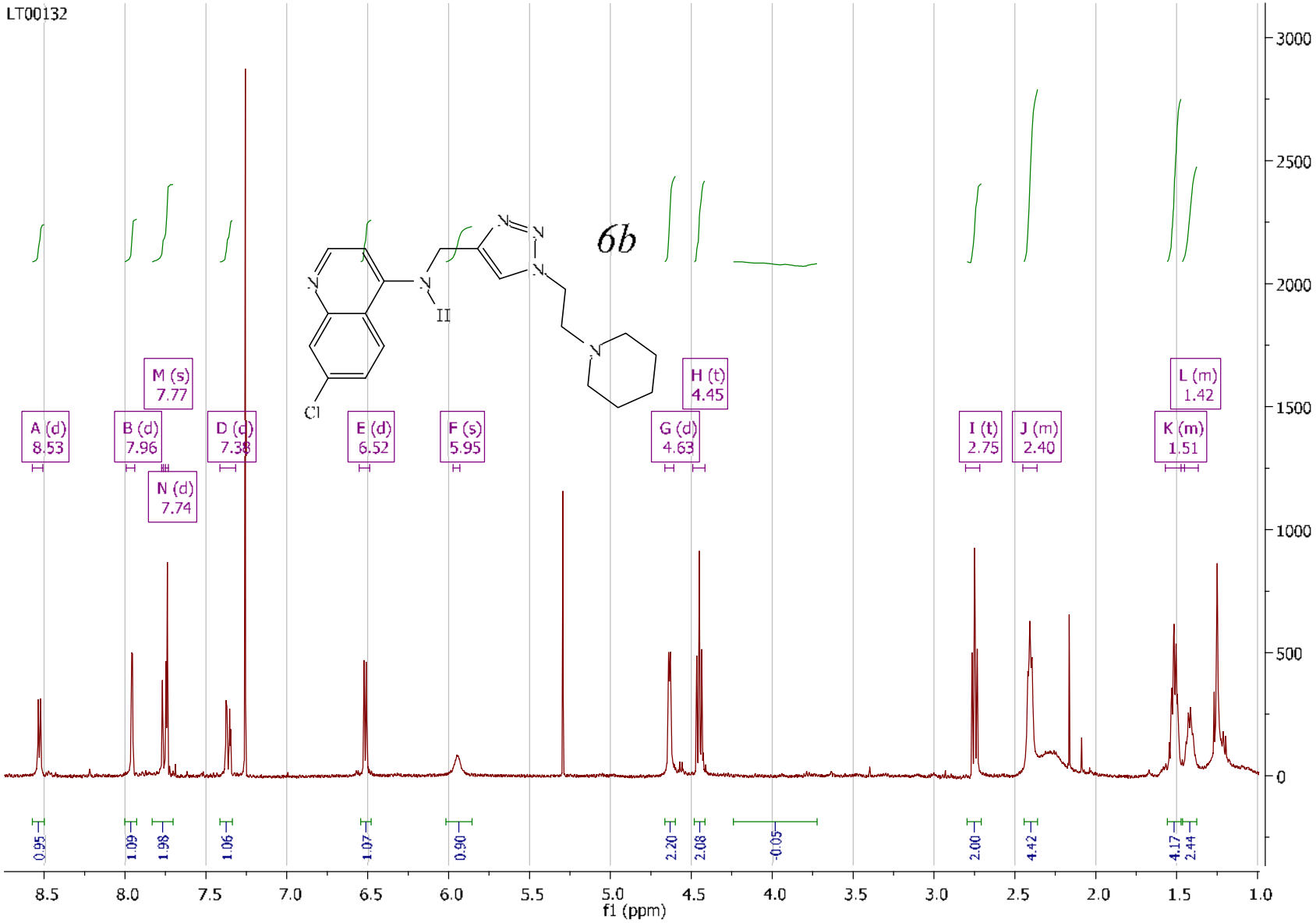
LT00132
6b
A (d) 8.53
B (d) 7.96
M (s) 7.77
N (d) 7.74
D (d) 7.38
E (d) 6.52
F (s) 5.95
G (d) 4.63
H (t) 4.45
I (t) 2.75
J (m) 2.40
K (m) 1.51
L (m) 1.42
Cl
0.95
1.09
1.98
1.06
1.07
0.90
2.20
2.08
0.05
2.00
4.42
4.17
2.44
f1 (ppm)

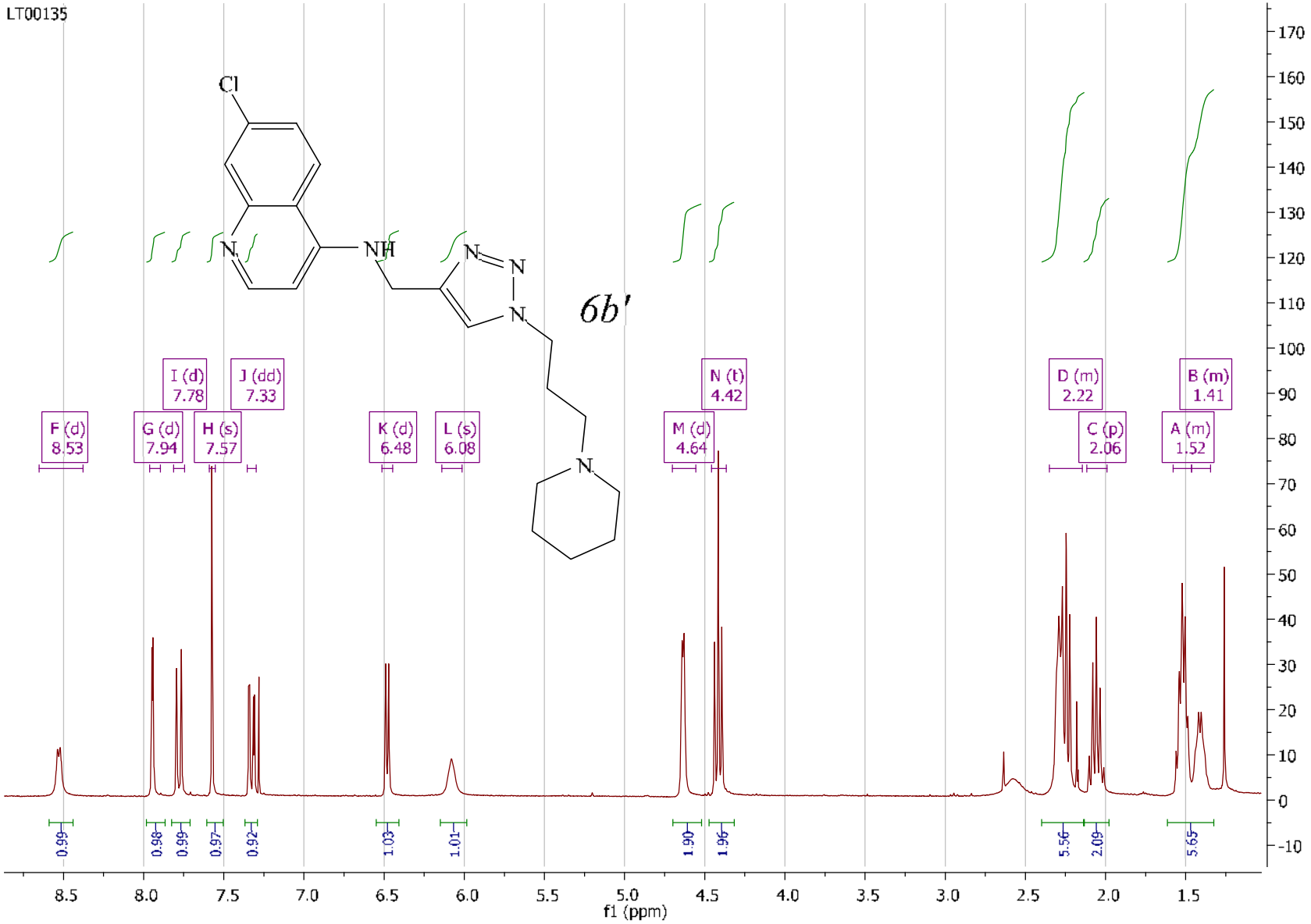
LT00135
Cl
NH
N
N
N
N
6b'
F (d) 8.53
G (d) 7.94
I (d) 7.78
H (s) 7.57
J (dd) 7.33
K (d) 6.48
L (s) 6.08
M (d) 4.64
N (t) 4.42
D (m) 2.22
C (p) 2.06
A (m) 1.52
B (m) 1.41
0.99
0.98
0.99
0.97
0.92
1.03
1.01
1.90
1.96
5.56
2.09
5.65
f1 (ppm)

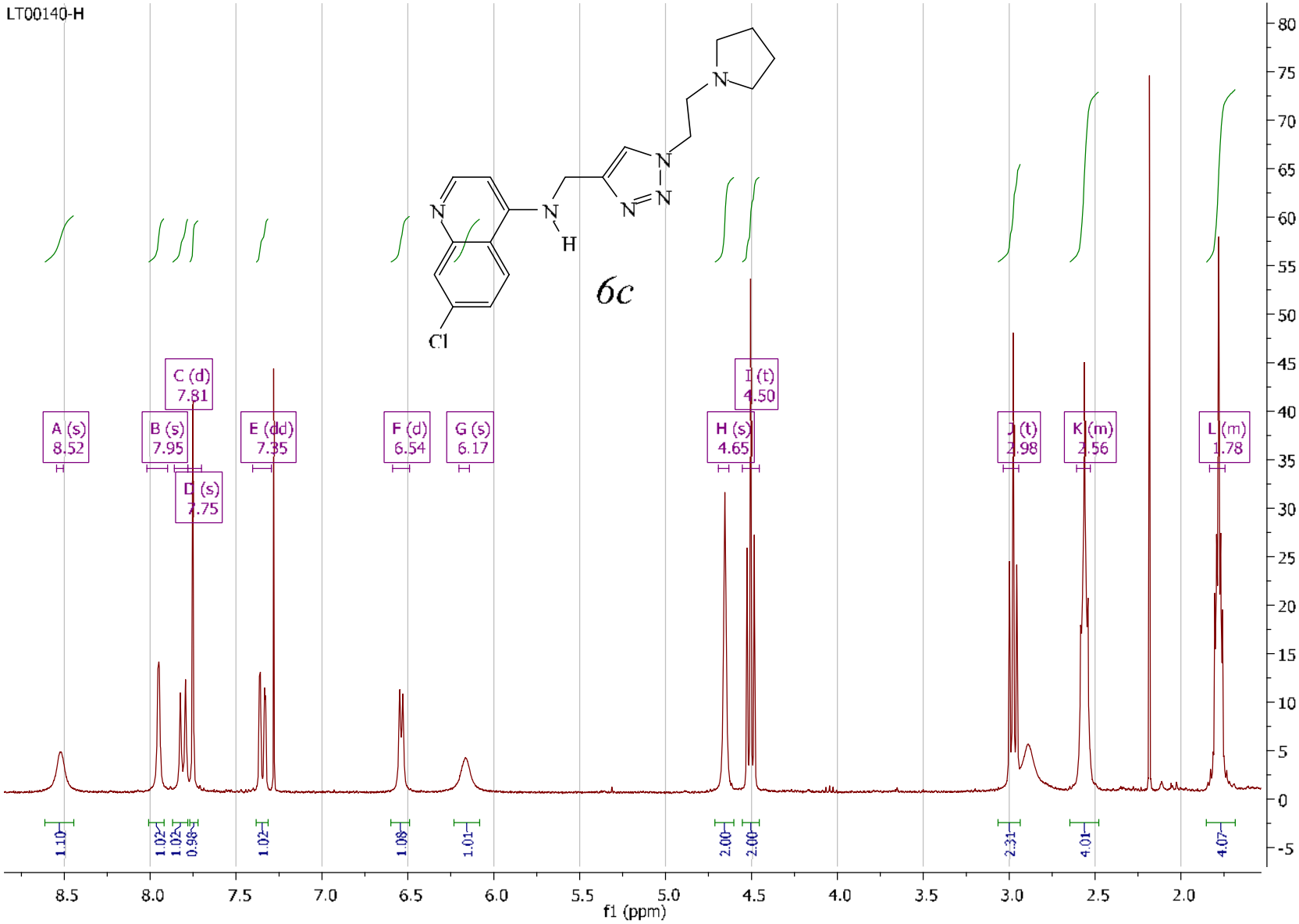
LT00140-H
6c
A (s) 8.52
B (s) 7.95
C (d) 7.81
D (s) 7.75
E (dd) 7.35
F (d) 6.54
G (s) 6.17
H (s) 4.65
I (t) 4.50
J (t) 2.98
K (m) 2.56
L (m) 1.78
1.10
1.02
1.02
0.98
1.02
1.08
1.01
2.00
2.00
2.31
4.01
4.07
f1 (ppm)

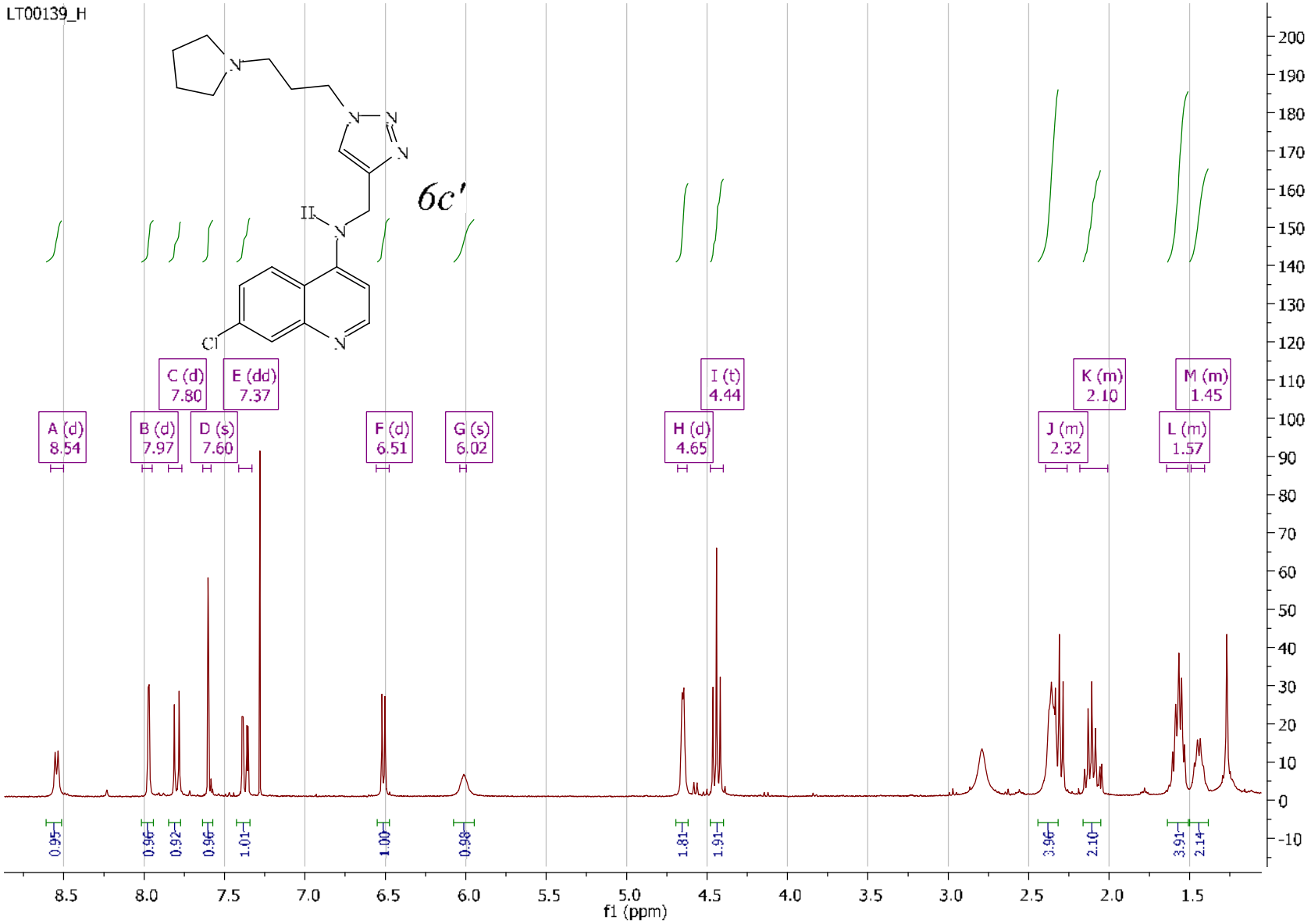
LT00139_H
6c'
A (d) 8.54
B (d) 7.97
C (d) 7.80
D (s) 7.60
E (dd) 7.37
F (d) 6.51
G (s) 6.02
H (d) 4.65
I (t) 4.44
J (m) 2.32
K (m) 2.10
L (m) 1.57
M (m) 1.45
0.95
0.96
0.92
0.96
1.01
1.00
0.98
1.81
1.91
3.96
2.10
3.91
2.14
f1 (ppm)

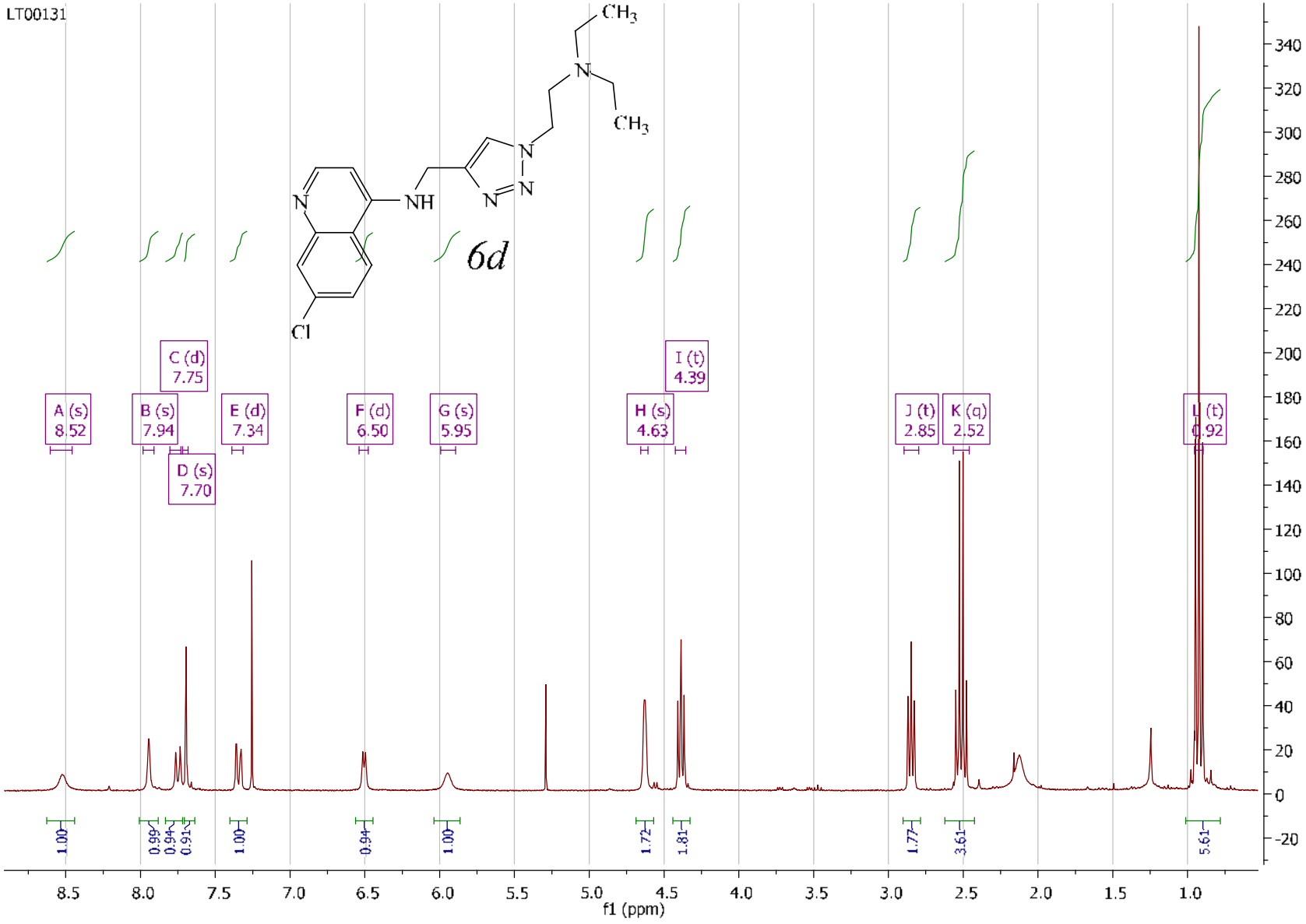
LT00131
6d
A (s) 8.52
B (s) 7.94
C (d) 7.75
D (s) 7.70
E (d) 7.34
F (d) 6.50
G (s) 5.95
H (s) 4.63
I (t) 4.39
J (t) 2.85
K (q) 2.52
L (t) 0.92
f1 (ppm)

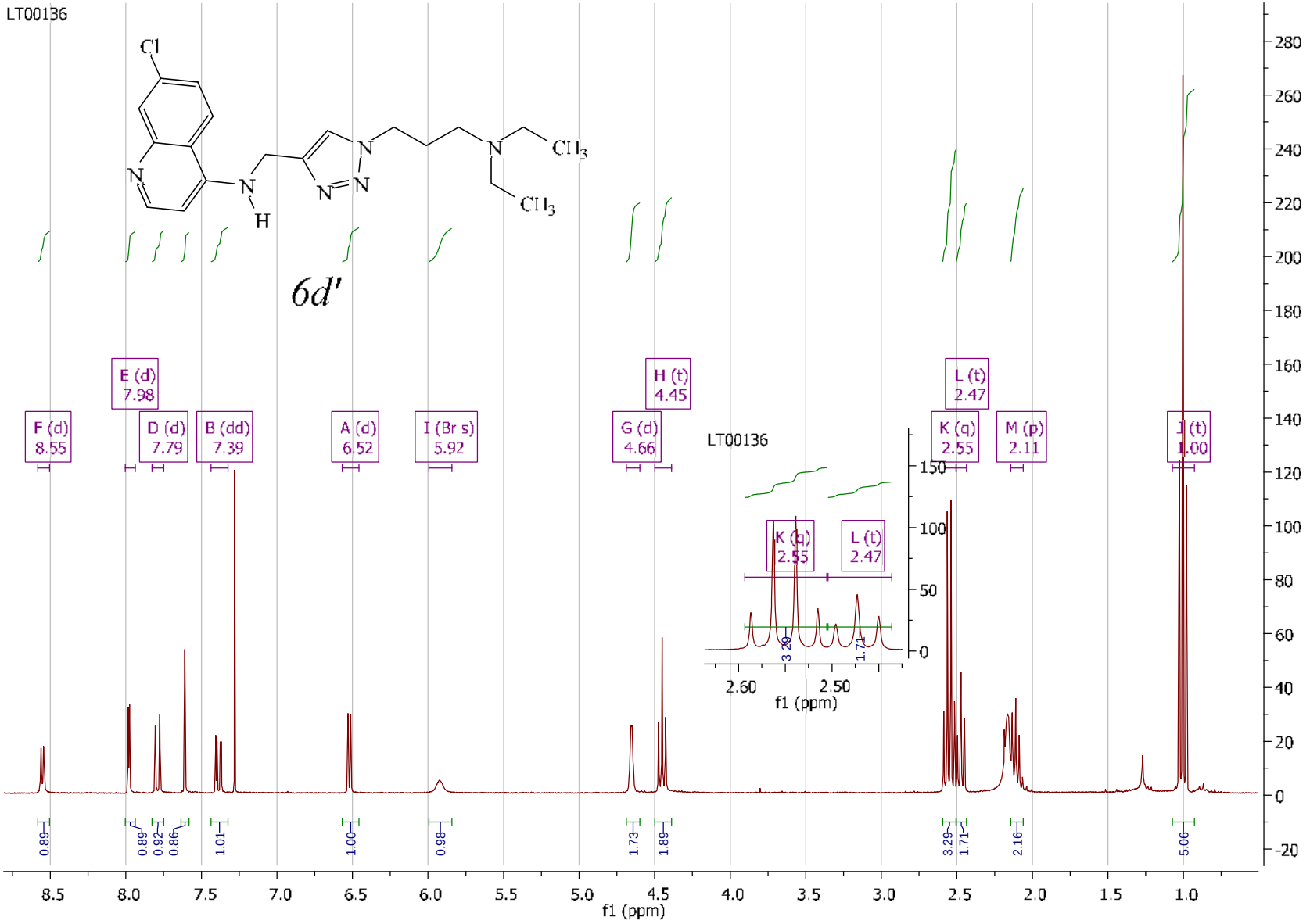
LT00136
6d'
F (d) 8.55
E (d) 7.98
D (d) 7.79
B (dd) 7.39
A (d) 6.52
I (Br s) 5.92
G (d) 4.66
H (t) 4.45
K (q) 2.55
L (t) 2.47
M (p) 2.11
J (t) 1.00
f1 (ppm)

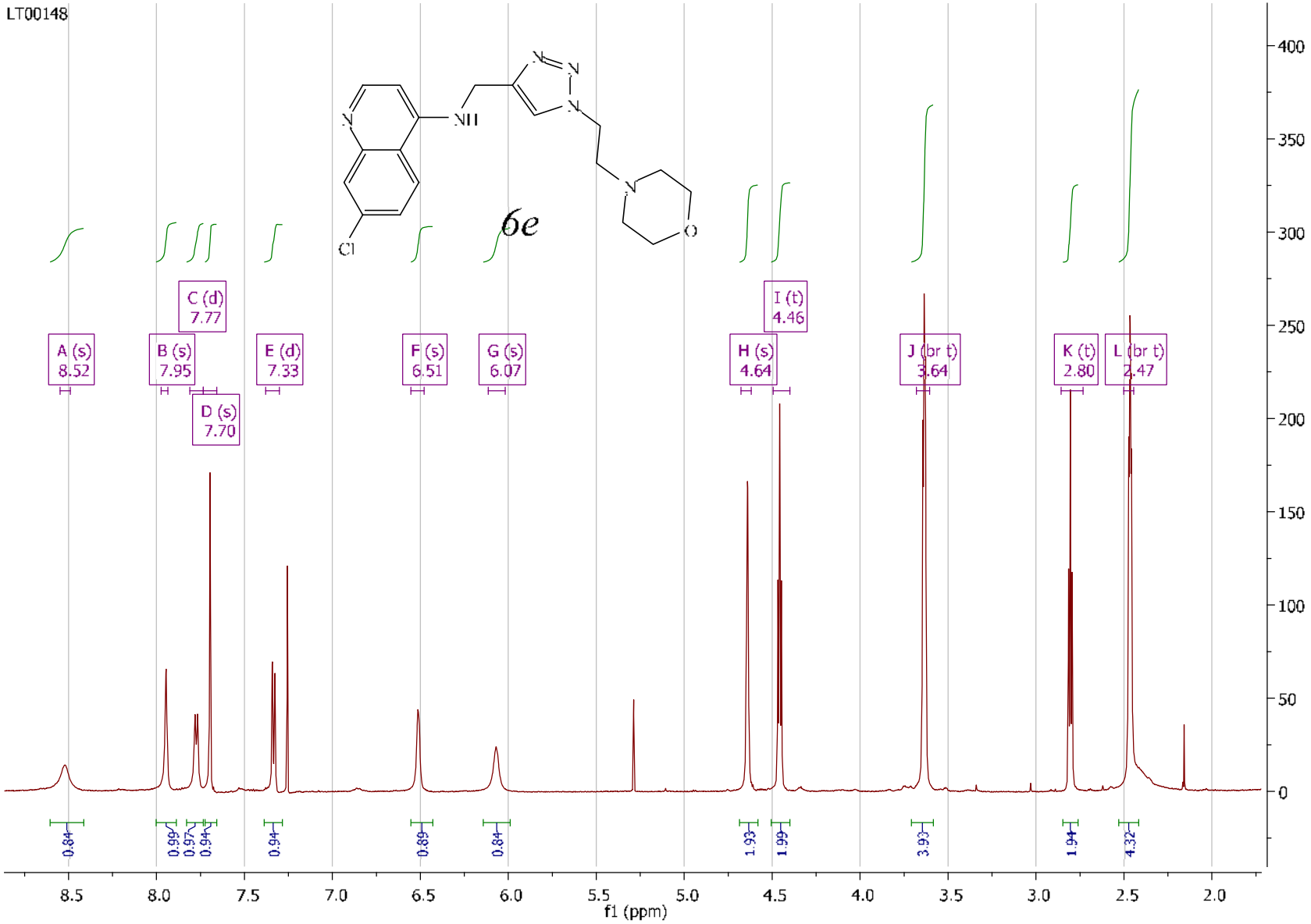
LT00148
6e
A (s) 8.52
B (s) 7.95
C (d) 7.77
D (s) 7.70
E (d) 7.33
F (s) 6.51
G (s) 6.07
H (s) 4.64
I (t) 4.46
J (br t) 3.64
K (t) 2.80
L (br t) 2.47
0.84
0.99
0.97
0.94
0.94
0.89
0.84
1.93
1.99
3.93
1.94
4.32
f1 (ppm)

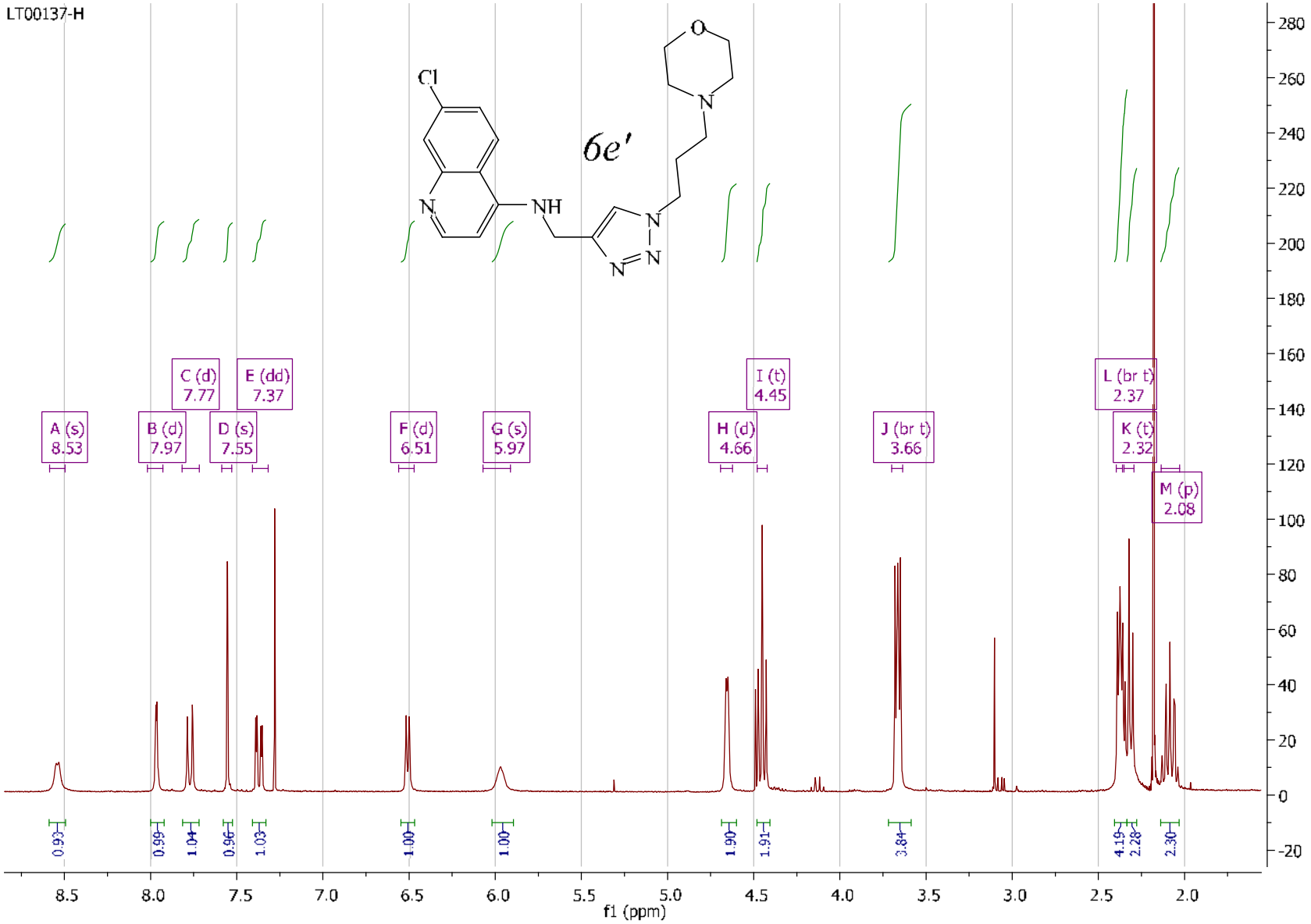
LT00137-H
6e'
A (s) 8.53
B (d) 7.97
C (d) 7.77
D (s) 7.55
E (dd) 7.37
F (d) 6.51
G (s) 5.97
H (d) 4.66
I (t) 4.45
J (br t) 3.66
K (t) 2.32
L (br t) 2.37
M (p) 2.08
f1 (ppm)

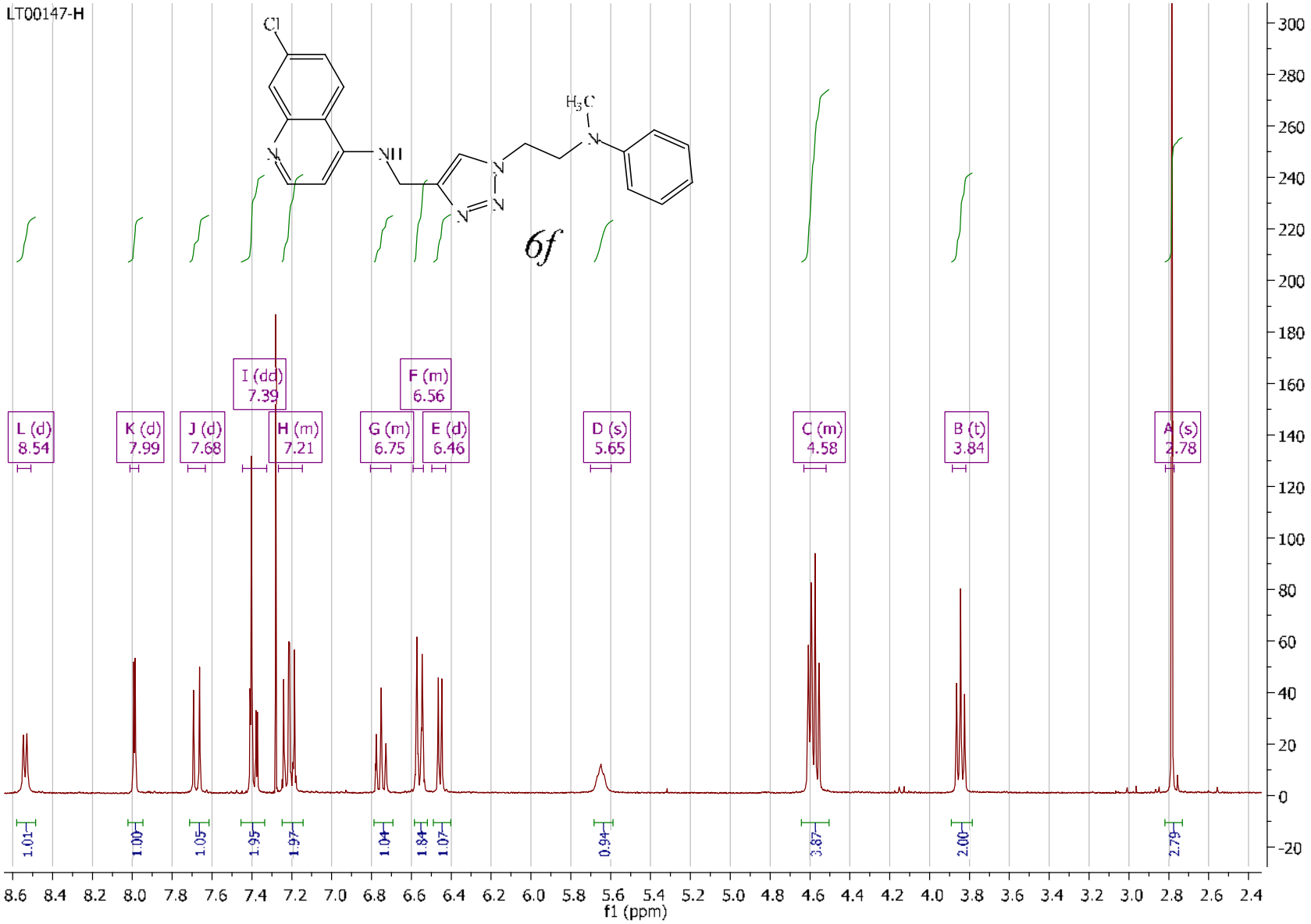
LT00147-H
Cl
NH
H_3C
N
N
N
N
6f
L (d) 8.54
K (d) 7.99
J (d) 7.68
I (dd) 7.39
H (m) 7.21
G (m) 6.75
F (m) 6.56
E (d) 6.46
D (s) 5.65
C (m) 4.58
B (t) 3.84
A (s) 2.78
1.01
1.00
1.05
1.95
1.97
1.04
1.84
1.07
0.94
3.87
2.00
2.79
f1 (ppm)

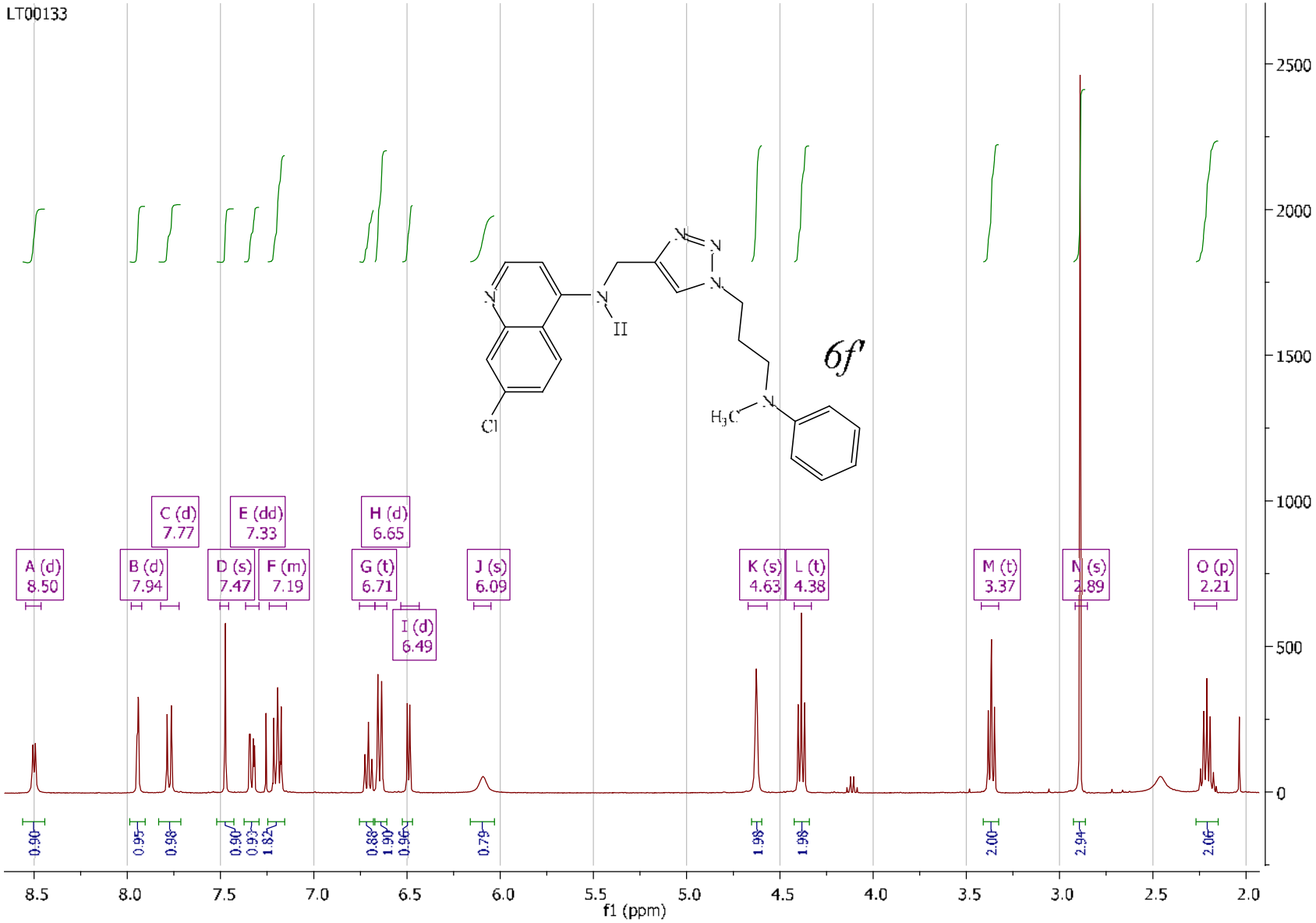
LT00133
6f
A (d) 8.50
B (d) 7.94
C (d) 7.77
D (s) 7.47
E (dd) 7.33
F (m) 7.19
G (t) 6.71
H (d) 6.65
I (d) 6.49
J (s) 6.09
K (s) 4.63
L (t) 4.38
M (t) 3.37
N (s) 2.89
O (p) 2.21
0.90
0.95
0.98
0.90
0.93
1.82
0.88
1.90
0.96
0.79
1.98
1.98
2.00
2.94
2.06
8.5
8.0
7.5
7.0
6.5
6.0
5.5
5.0
4.5
4.0
3.5
3.0
2.5
2.0
f1 (ppm)
2500
2000
1500
1000
500
0

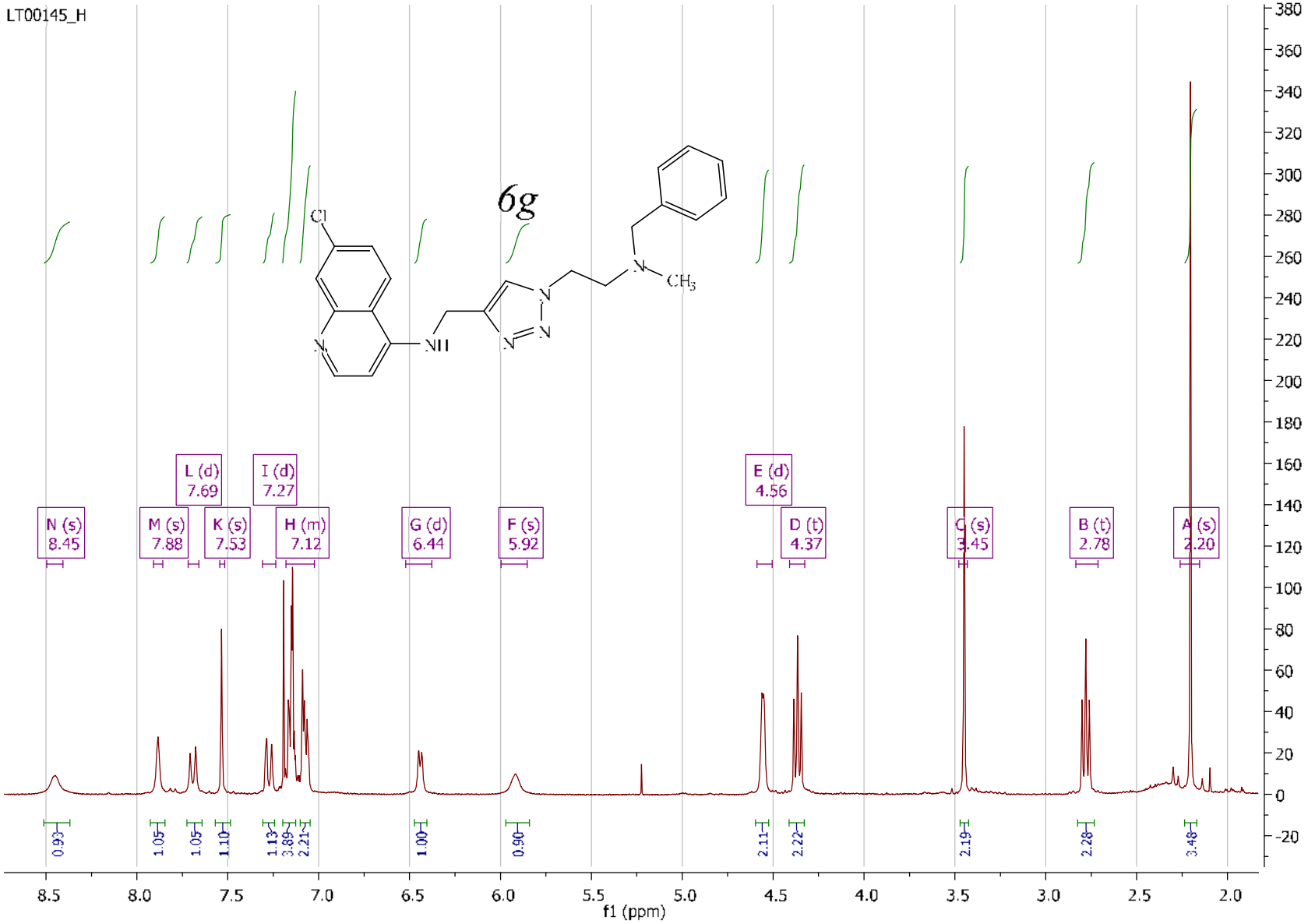
LT00145_H
6g
Cl
NH
N
CH3
N (s) 8.45
M (s) 7.88
L (d) 7.69
K (s) 7.53
I (d) 7.27
H (m) 7.12
G (d) 6.44
F (s) 5.92
E (d) 4.56
D (t) 4.37
C (s) 3.45
B (t) 2.78
A (s) 2.20
0.93
1.05
1.05
1.10
1.13
3.89
2.21
1.00
0.90
2.11
2.22
2.19
2.28
3.48
f1 (ppm)

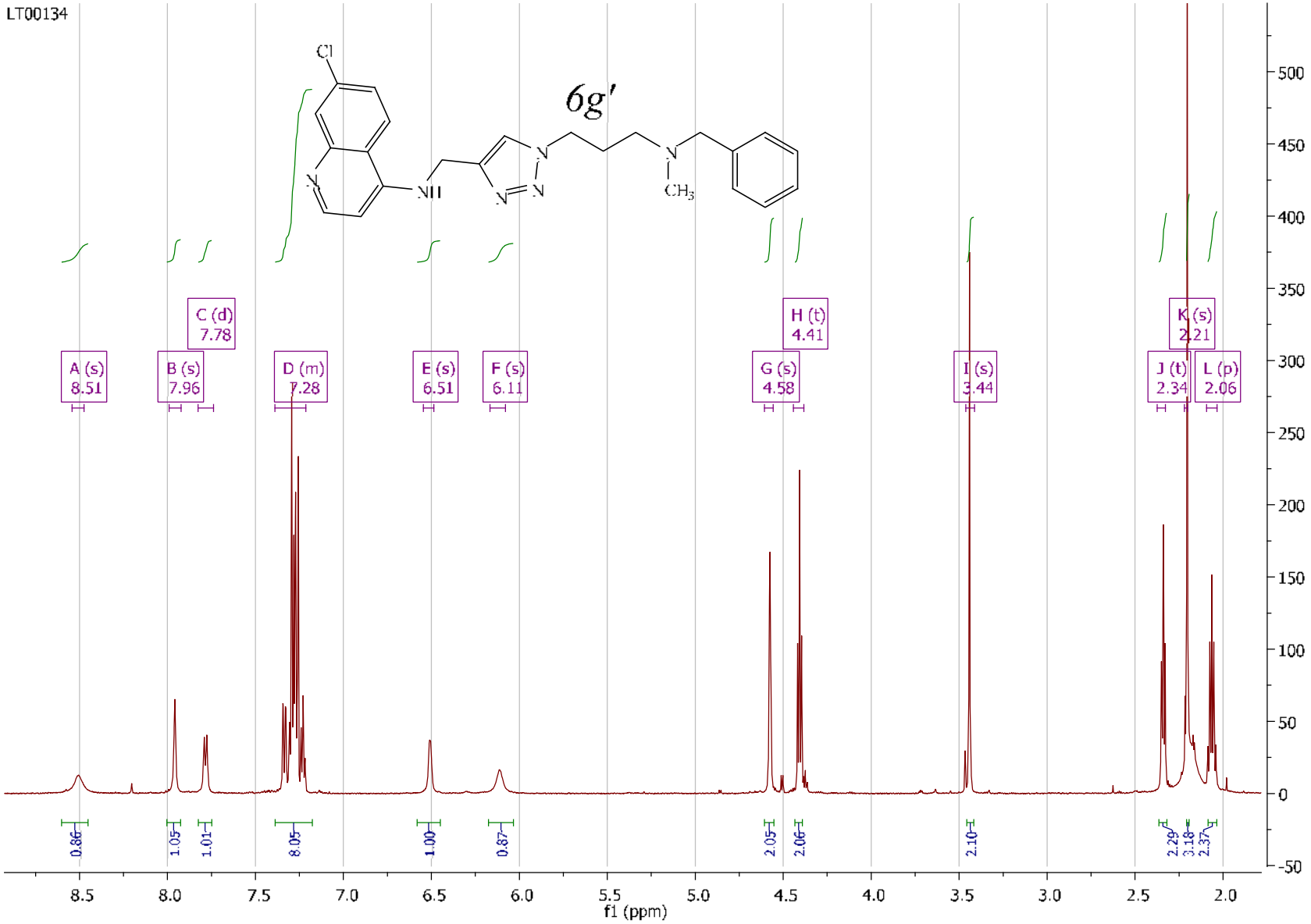
LT00134
6g'
Cl
NH
N
N
N
N
CH3
A (s) 8.51
B (s) 7.96
C (d) 7.78
D (m) 7.28
E (s) 6.51
F (s) 6.11
G (s) 4.58
H (t) 4.41
I (s) 3.44
J (t) 2.34
K (s) 2.21
L (p) 2.06
0.86
1.05
1.01
8.05
1.00
0.87
2.05
2.06
2.10
2.29
3.18
2.37
f1 (ppm)

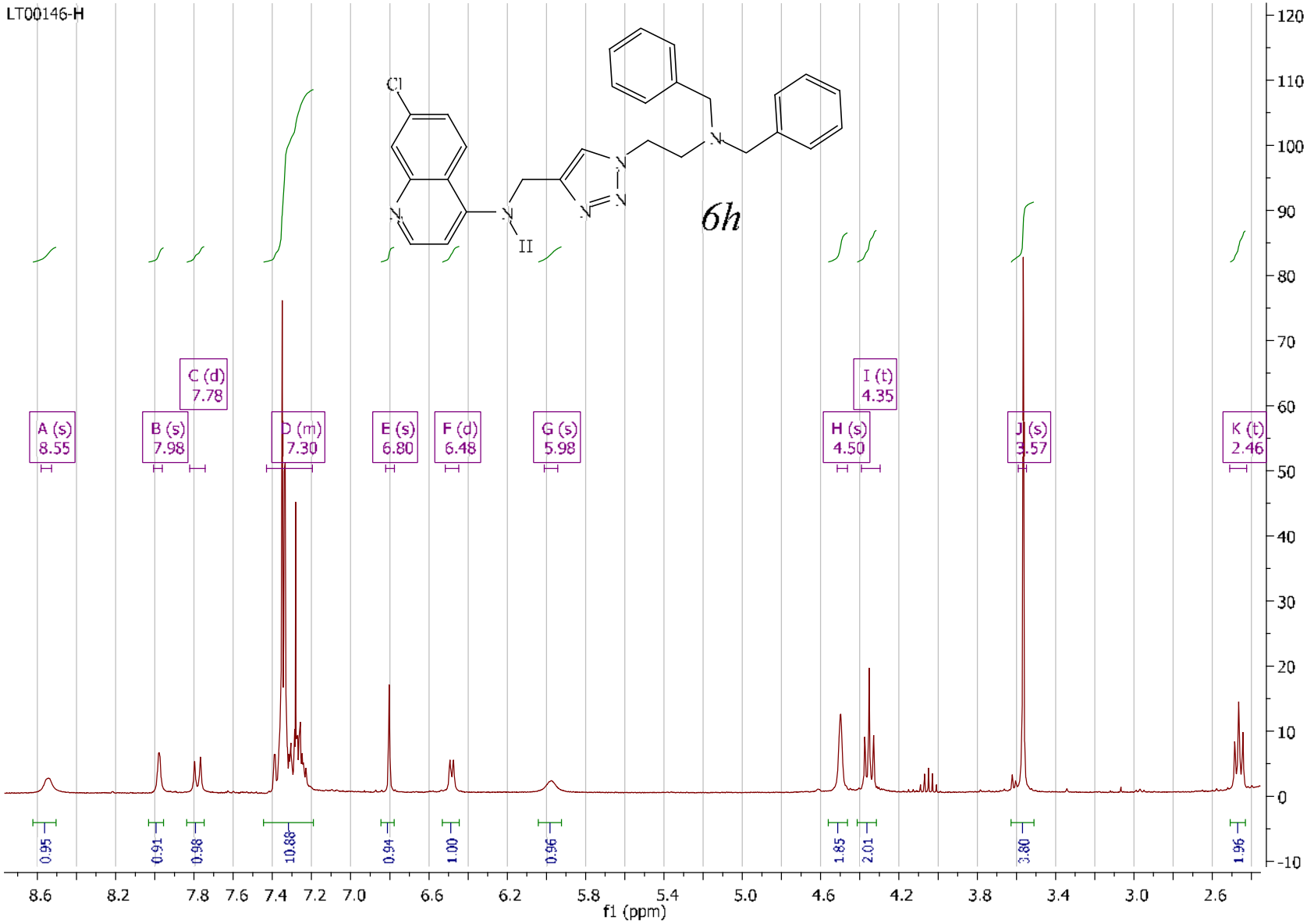
LT00146-H
Cl
6h
A (s) 8.55
B (s) 7.98
C (d) 7.78
D (m) 7.30
E (s) 6.80
F (d) 6.48
G (s) 5.98
H (s) 4.50
I (t) 4.35
J (s) 3.57
K (t) 2.46
0.95
0.91
0.98
10.88
0.94
1.00
0.96
1.85
2.01
3.80
1.96
f1 (ppm)

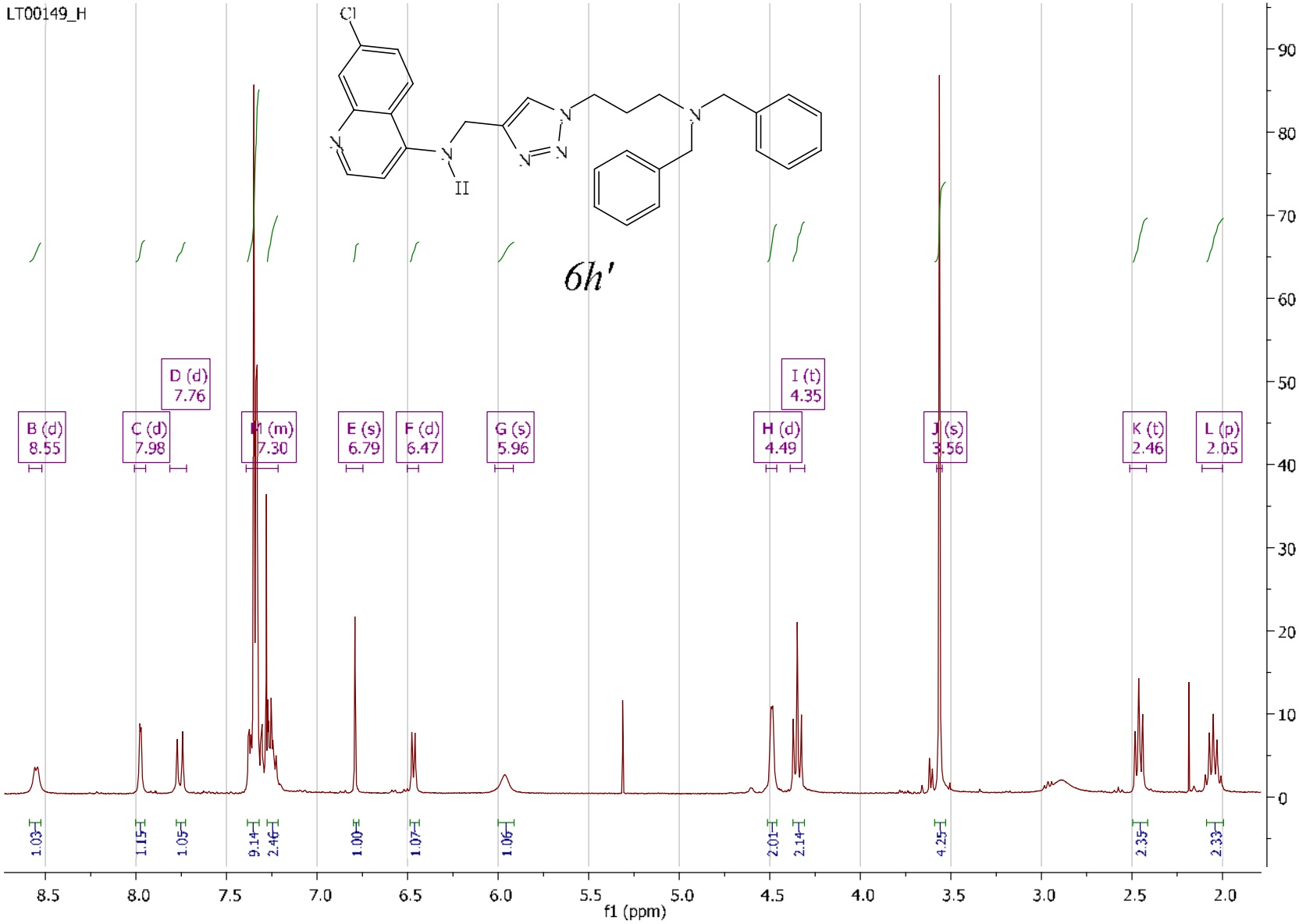
LT00149_H
Cl
N
N
N
N
N
N
II
6h'
B (d) 8.55
C (d) 7.98
D (d) 7.76
M (m) 7.30
E (s) 6.79
F (d) 6.47
G (s) 5.96
H (d) 4.49
I (t) 4.35
J (s) 3.56
K (t) 2.46
L (p) 2.05
1.03
1.15
1.05
9.14
2.46
1.00
1.07
1.06
2.01
2.14
4.25
2.35
2.33
8.5
8.0
7.5
7.0
6.5
6.0
5.5
5.0
4.5
4.0
3.5
3.0
2.5
2.0
f1 (ppm)
90
80
70
60
50
40
30
20
10
0

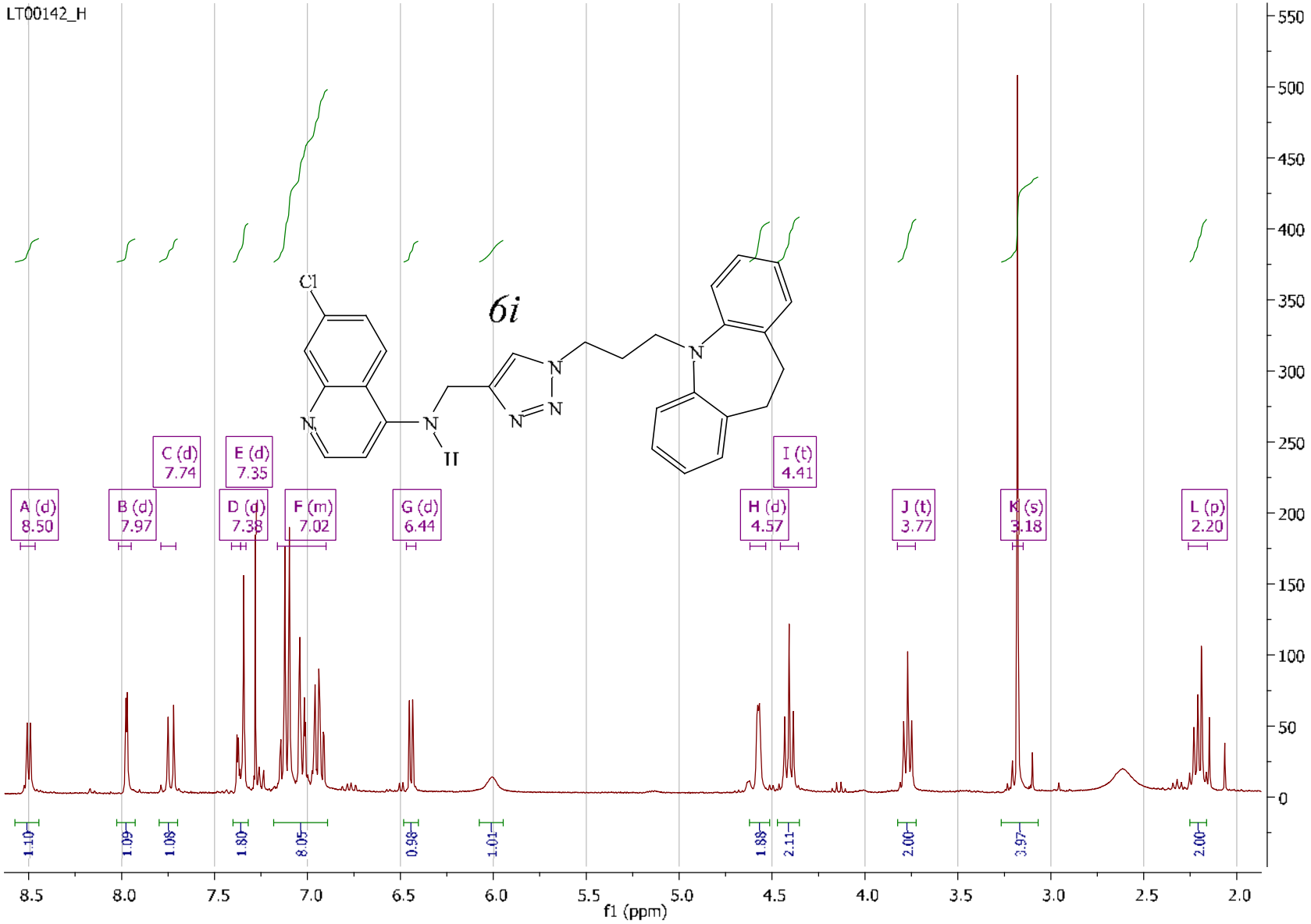
LT00142_H
6i
Cl
N
N
N
N
N
N
H
A (d) 8.50
B (d) 7.97
C (d) 7.74
D (d) 7.38
E (d) 7.35
F (m) 7.02
G (d) 6.44
H (d) 4.57
I (t) 4.41
J (t) 3.77
K (s) 3.18
L (p) 2.20
1.10
1.09
1.08
1.80
8.05
0.98
1.01
1.88
2.11
2.00
3.97
2.00
f1 (ppm)

^{13}C NMR spectra

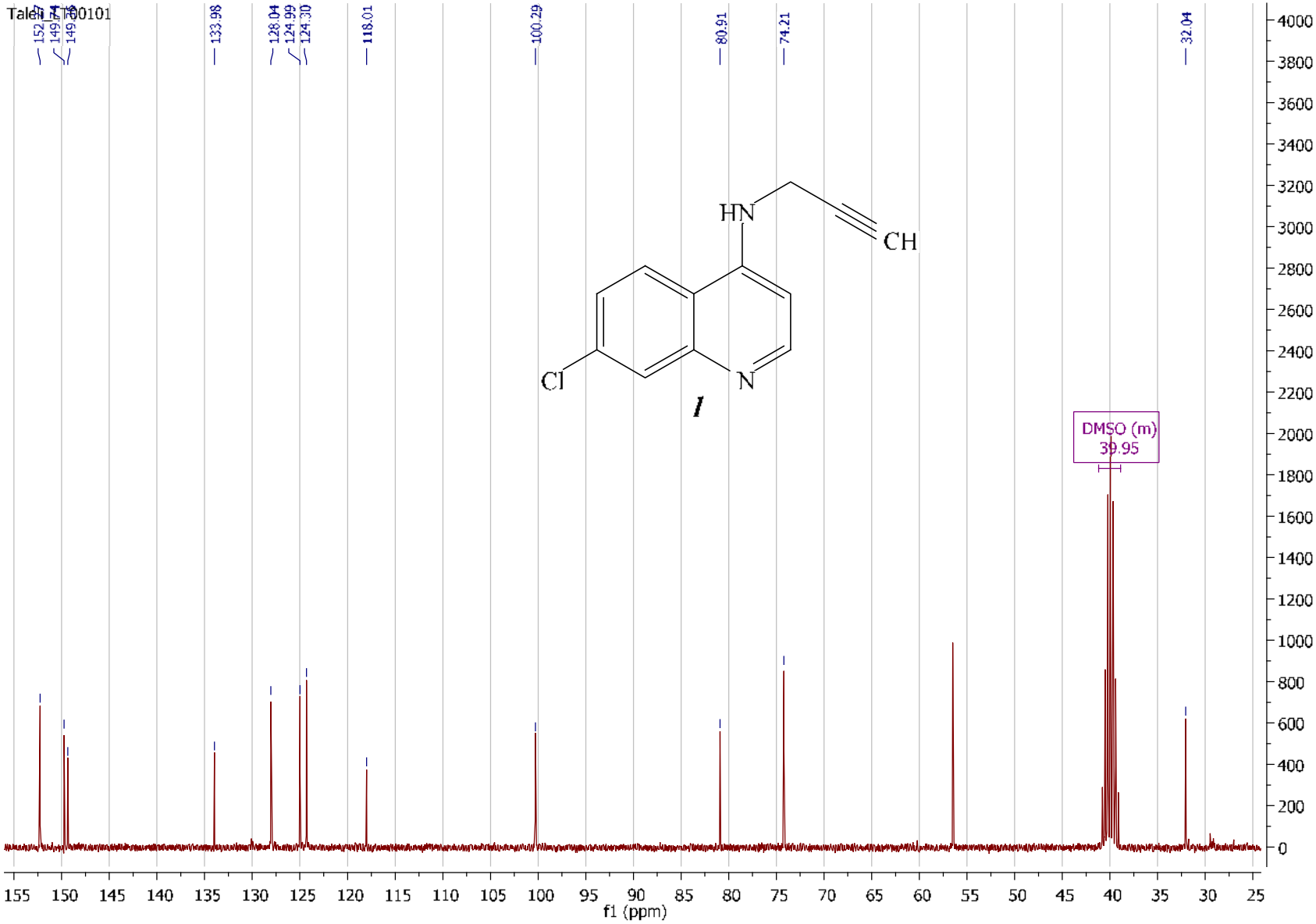
Talen_1_100101
152.74
149.74
149.30
133.98
128.04
124.99
124.30
118.01
100.29
80.91
74.21
32.04
HN
CH
Cl
N
1
DMSO (m)
39.95
f1 (ppm)

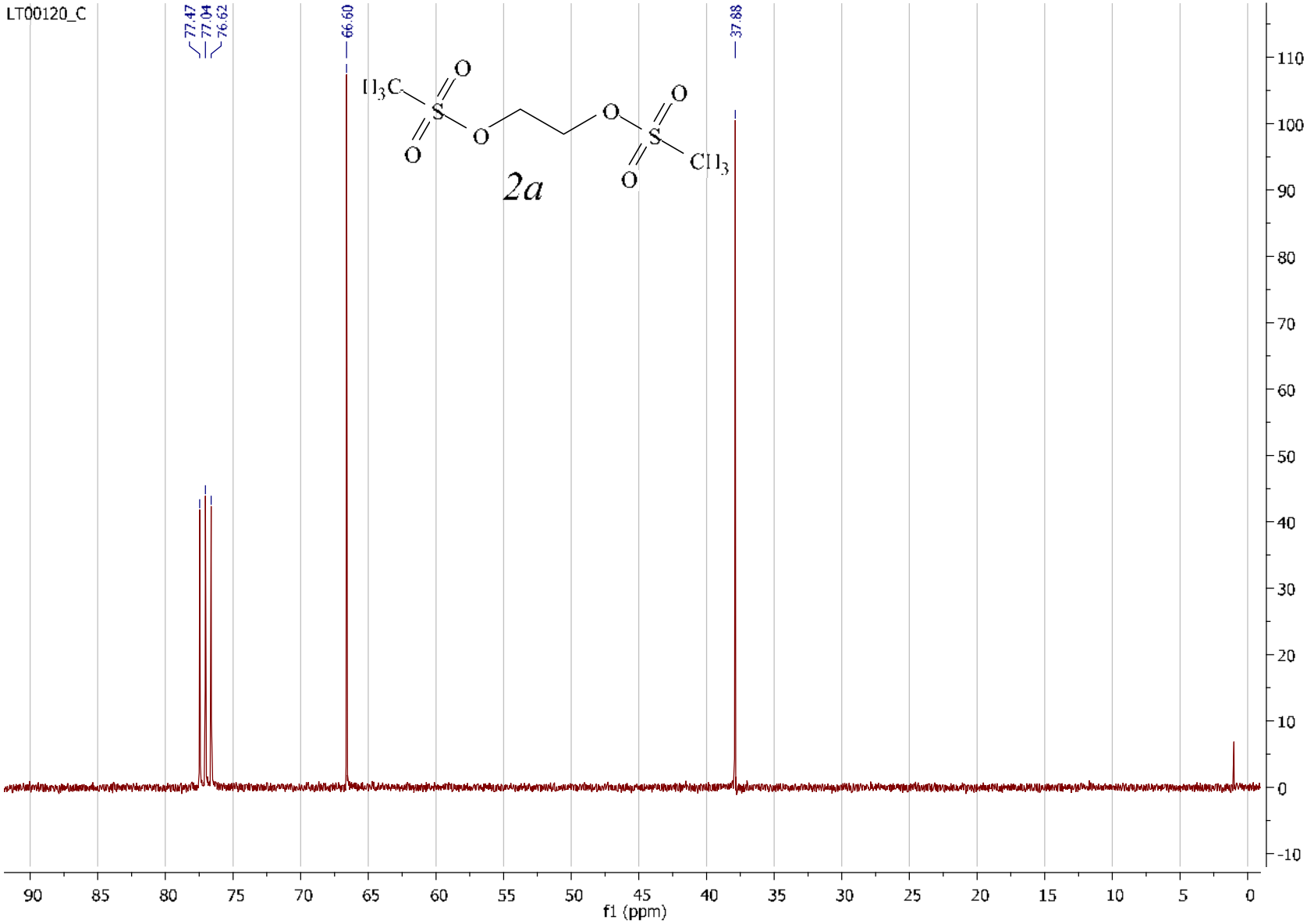
LT00120_C
77.47
77.04
76.62
66.60
37.88
2a
f1 (ppm)

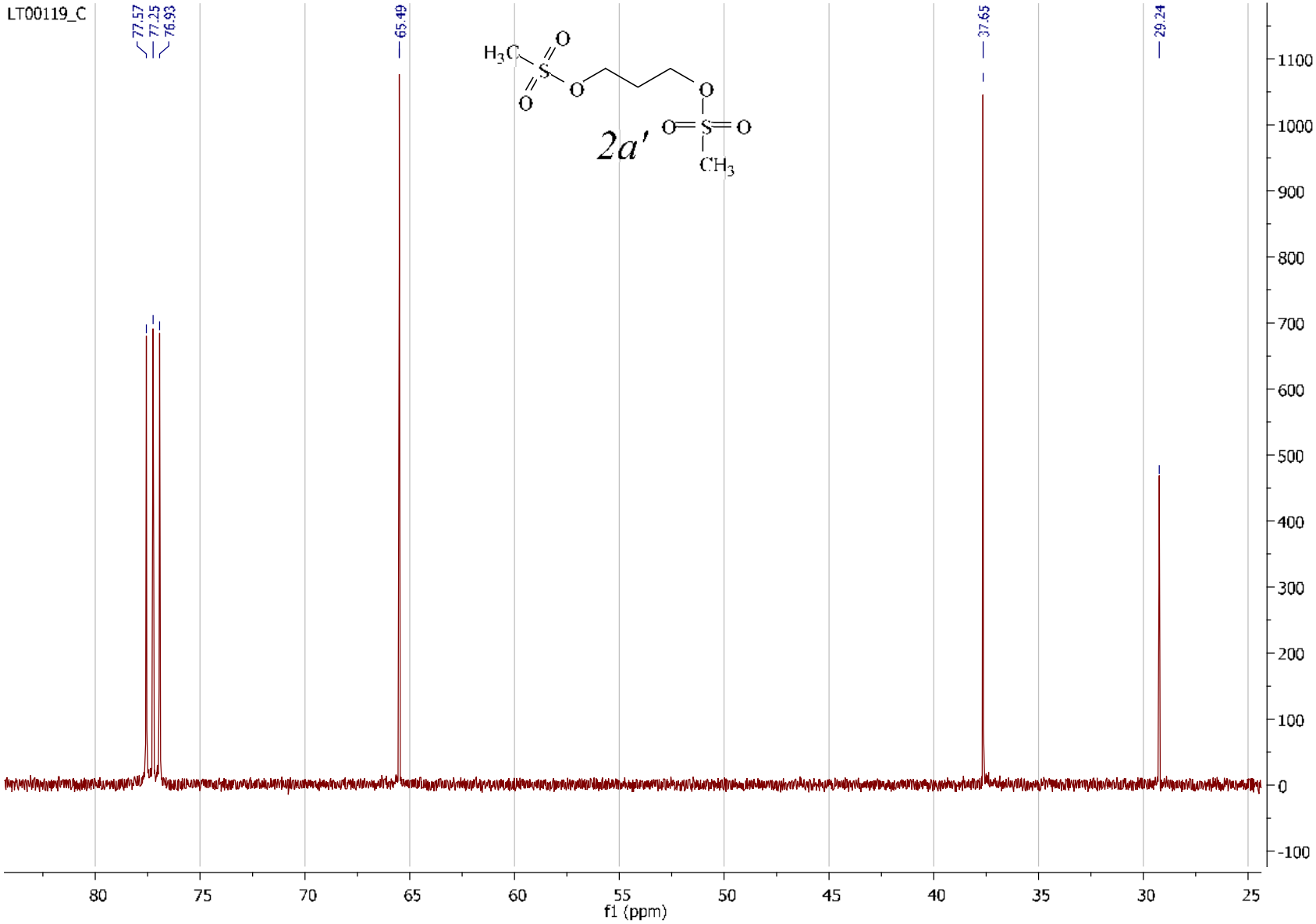
LT00119_C
77.57
77.25
76.93
65.49
37.65
29.24
2a'
f1 (ppm)

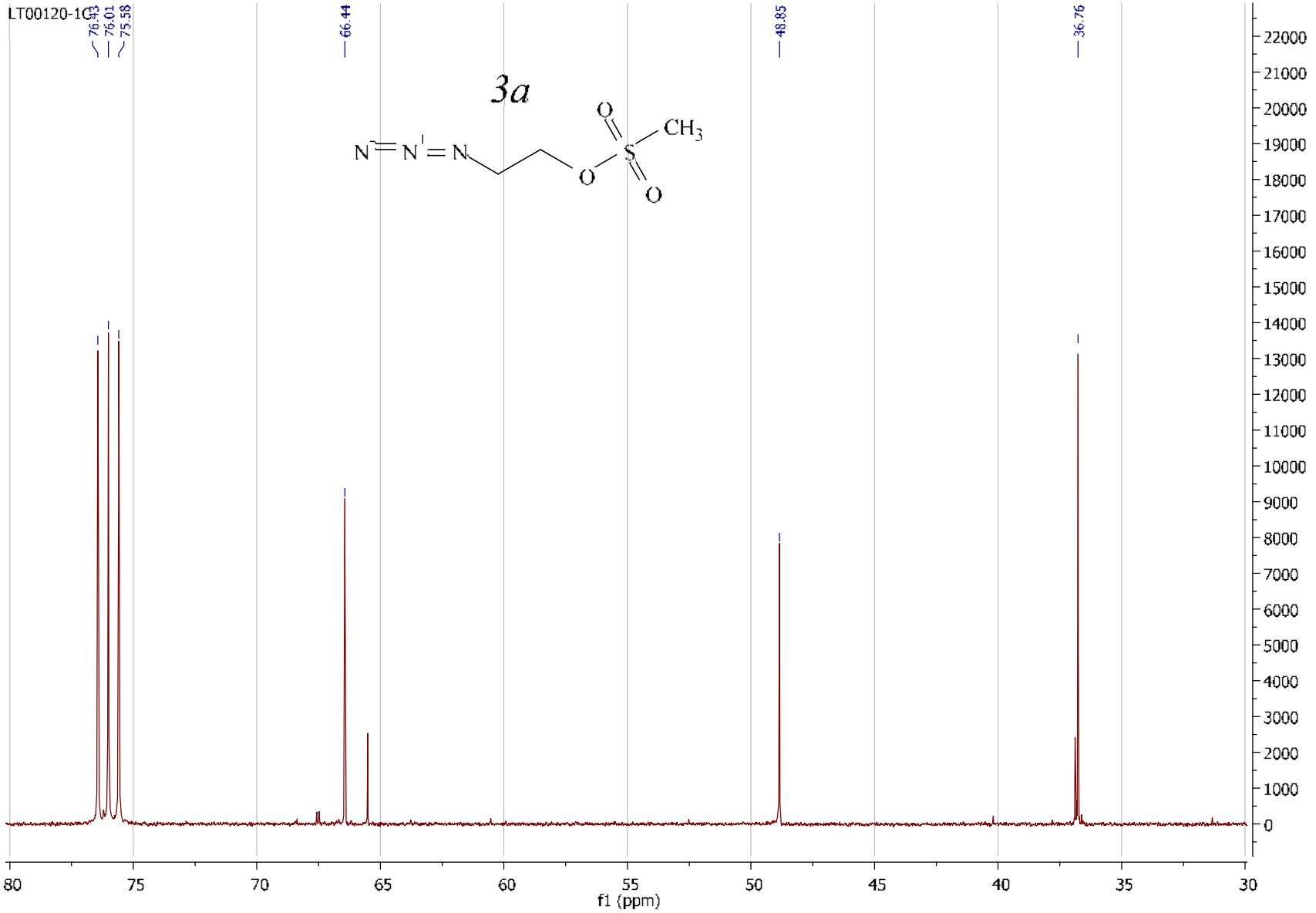
LT00120-1C3
76.43
76.01
75.58
66.44
48.85
36.76
3a
N
N
N
O
O
S
O
CH3
22000
21000
20000
19000
18000
17000
16000
15000
14000
13000
12000
11000
10000
9000
8000
7000
6000
5000
4000
3000
2000
1000
0
80
75
70
65
60
55
50
45
40
35
30
f1 (ppm)

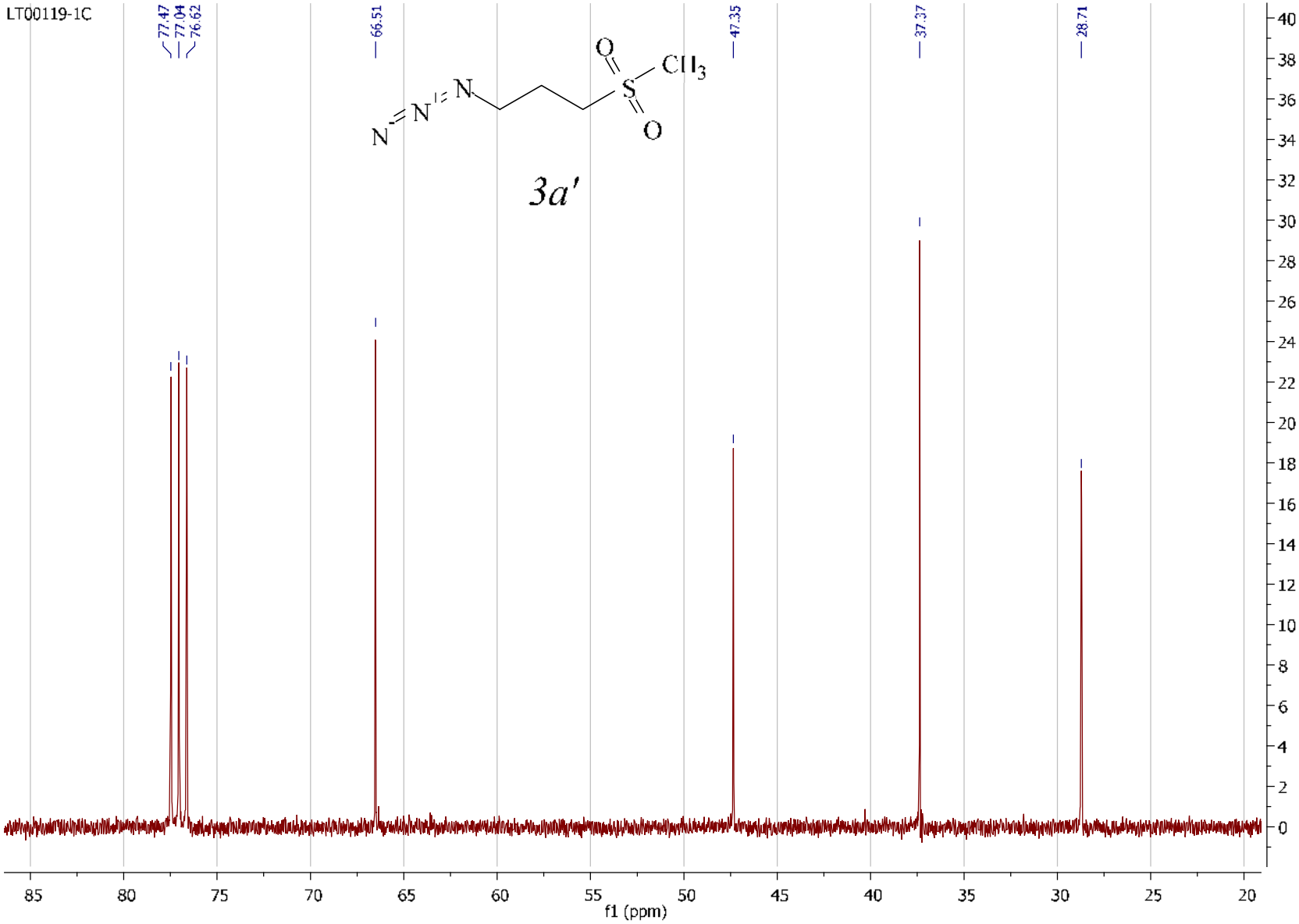
LT00119-1C
77.47
77.04
76.62
66.51
47.35
37.37
28.71
3a′
f1 (ppm)

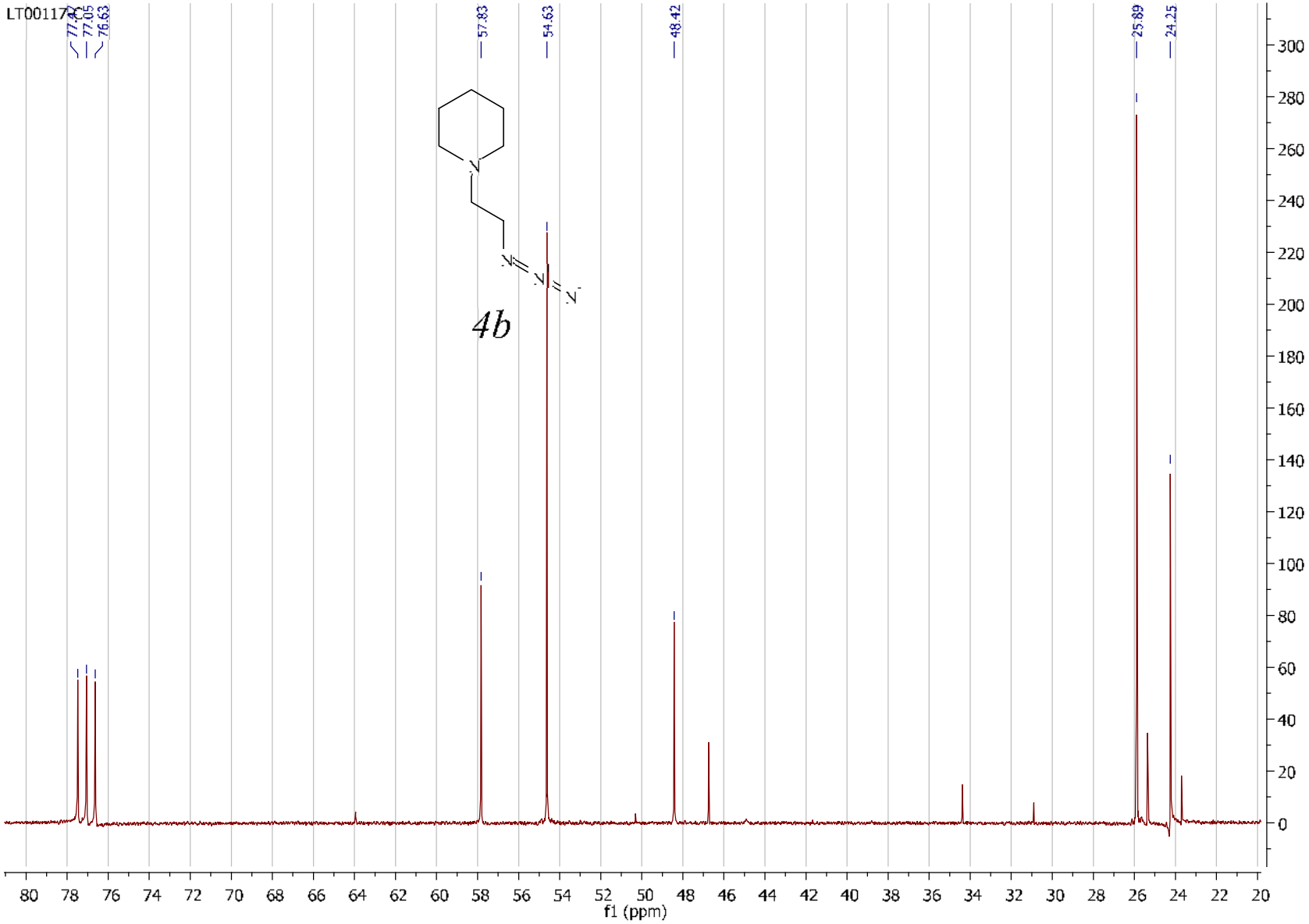
LT0011742
77.42
77.05
76.63
57.83
54.63
48.42
25.89
24.25
4b
f1 (ppm)

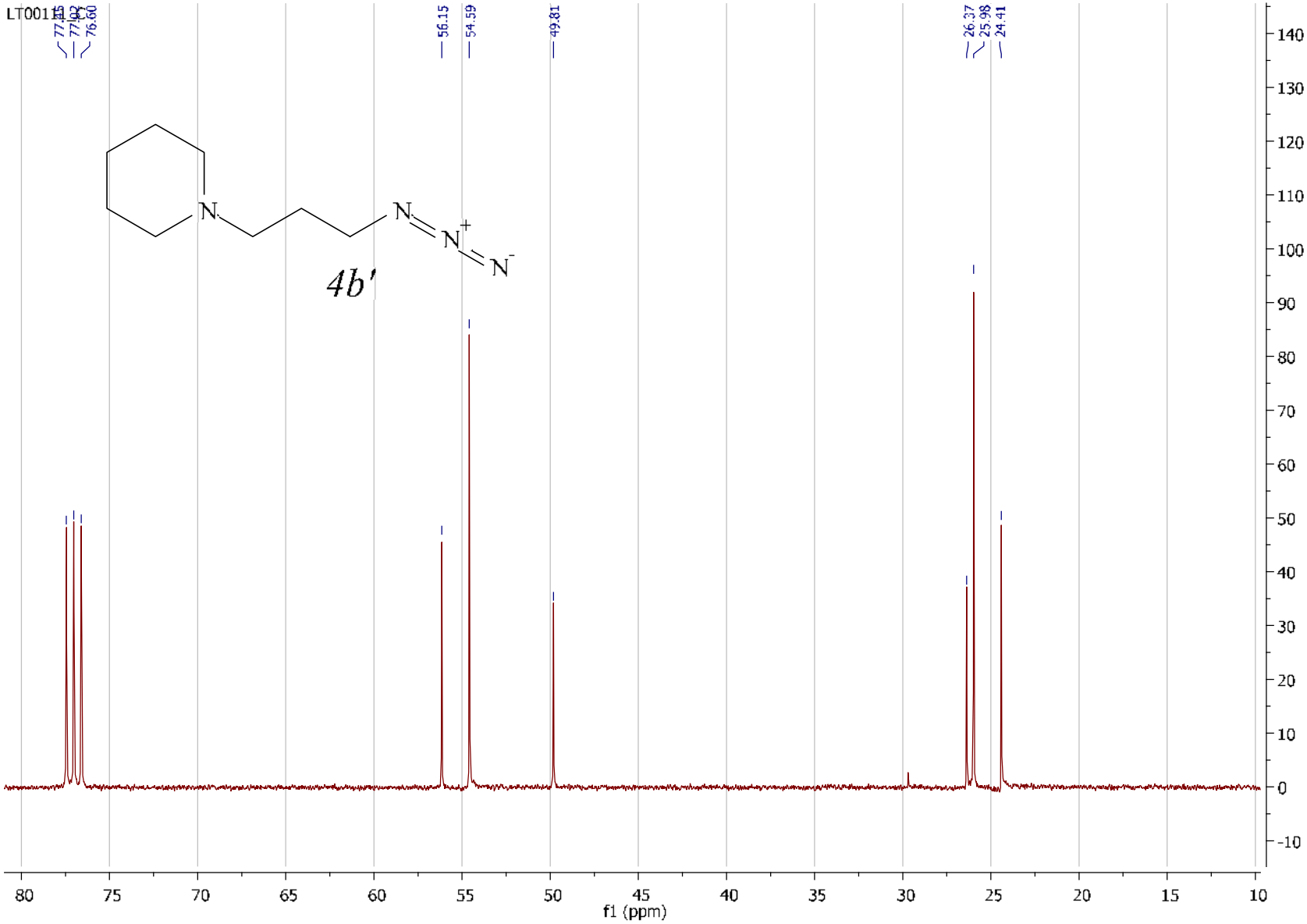
LT00115
77.15
77.02
76.60
56.15
54.59
49.81
26.37
25.98
24.41
4b'
f1 (ppm)

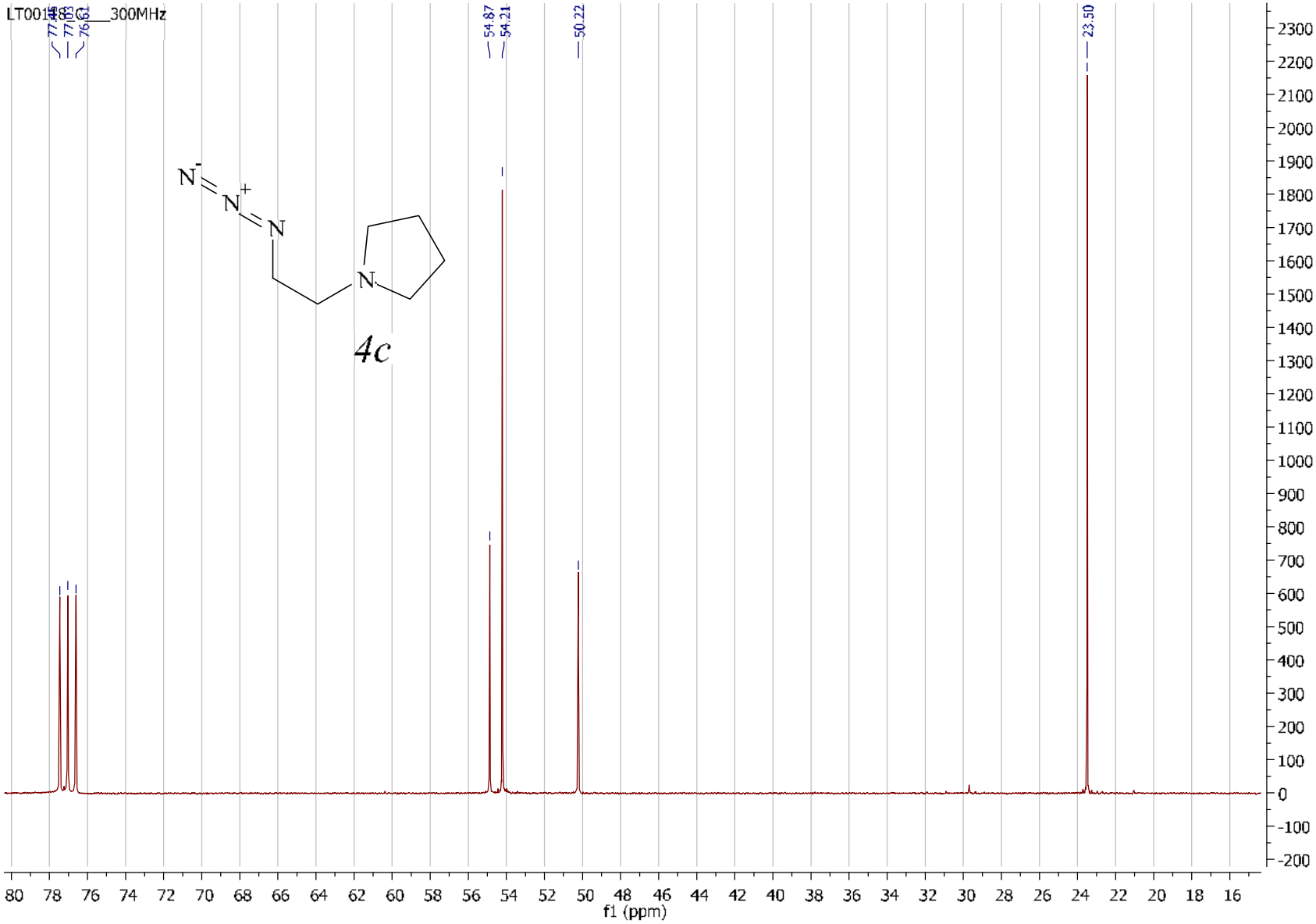
LT00148C 300MHz
77.48
77.22
76.61
54.87
54.21
50.22
23.50
4c
f1 (ppm)

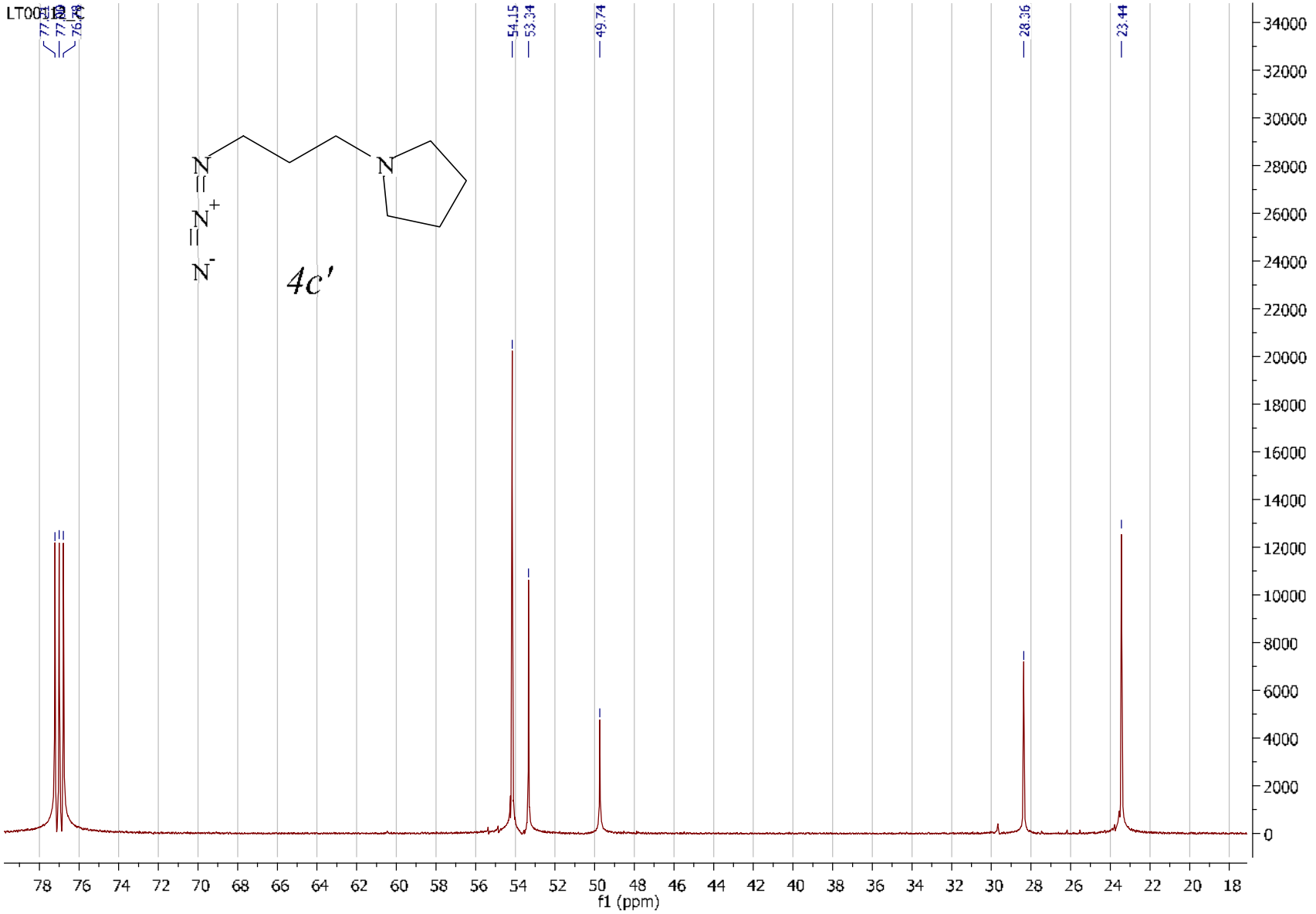
77.12
77.54
76.78
54.15
53.34
49.74
28.36
23.44
4c′
f1 (ppm)

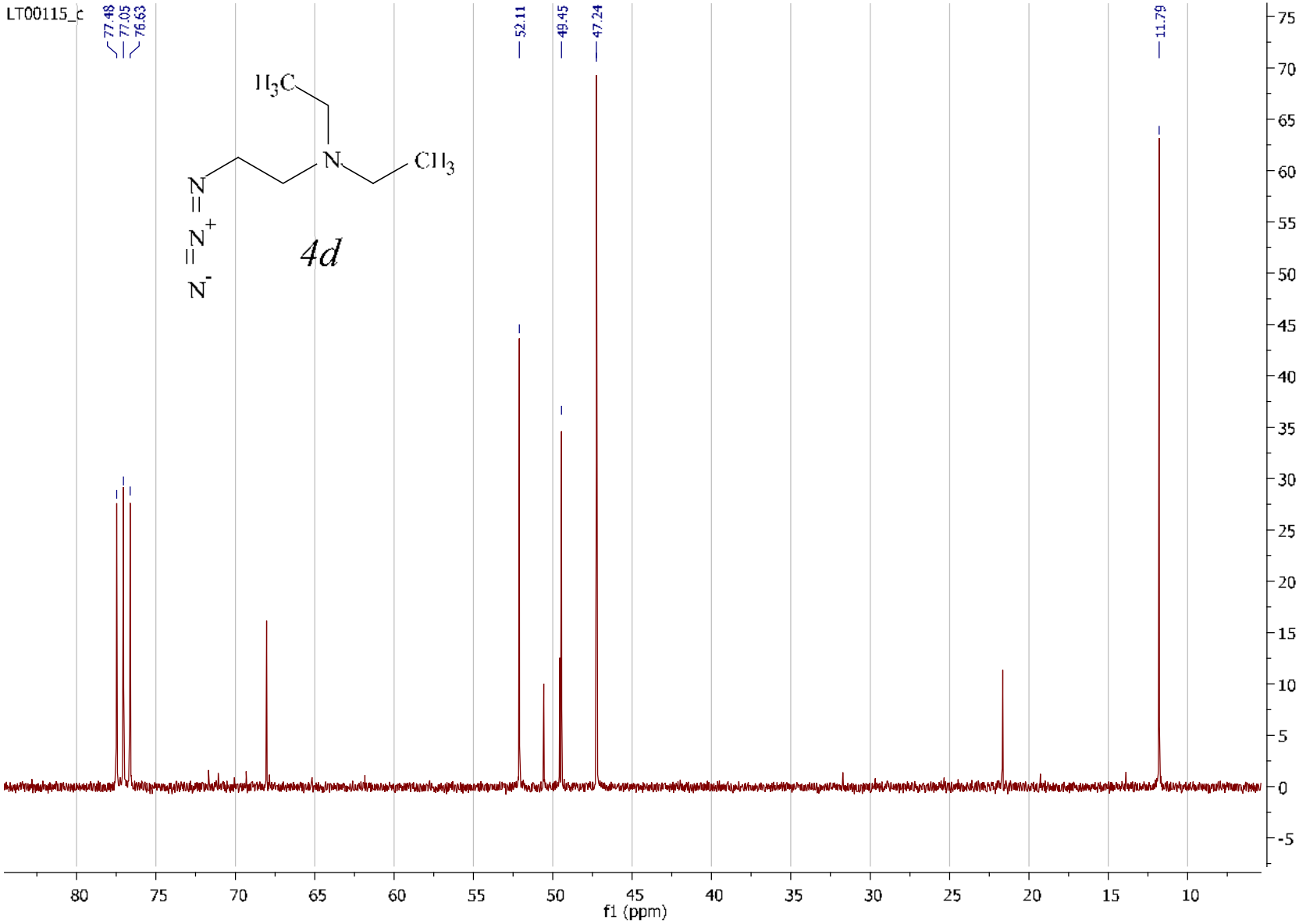
LT00115_c
77.48
77.05
76.63
52.11
49.45
47.24
11.79
4d
f1 (ppm)

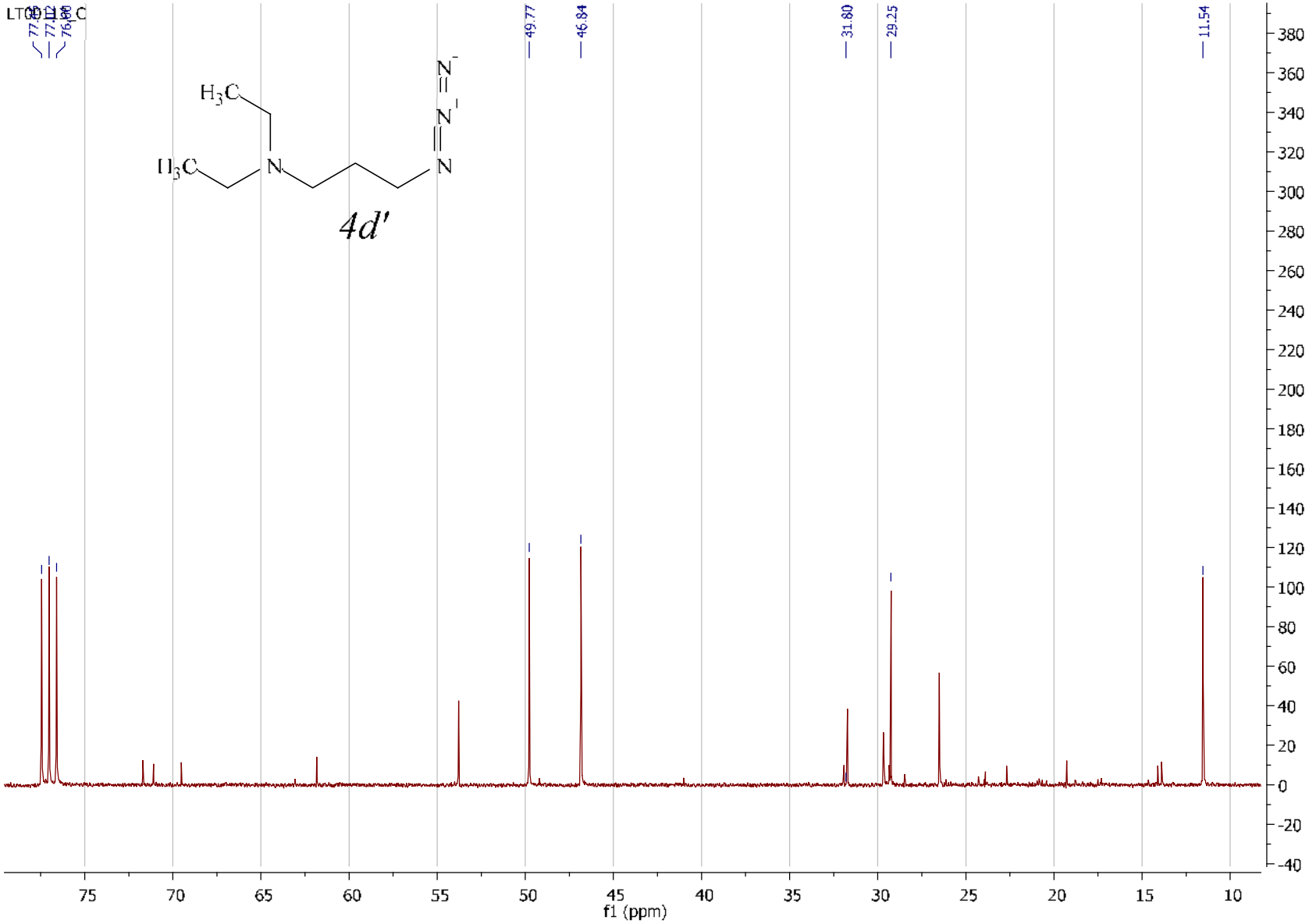
77.00
77.21
77.42
76.58
49.77
46.84
31.80
29.25
11.54
H_3C
H_3C
N
N
N
N
4d'
f1 (ppm)

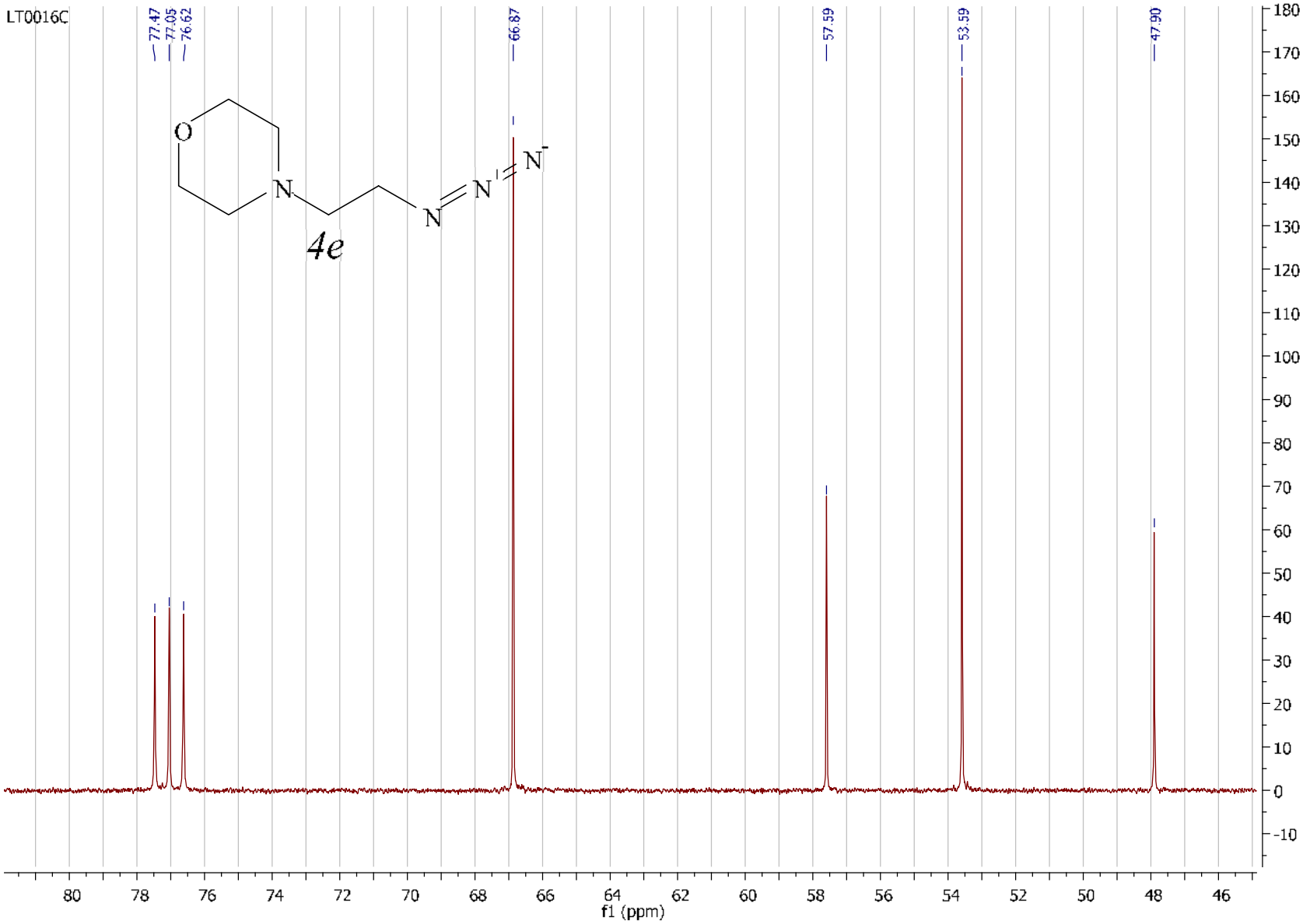
LT0016C
77.47
77.05
76.62
66.87
57.59
53.59
47.90
O
N
N
N
N
4e
f1 (ppm)

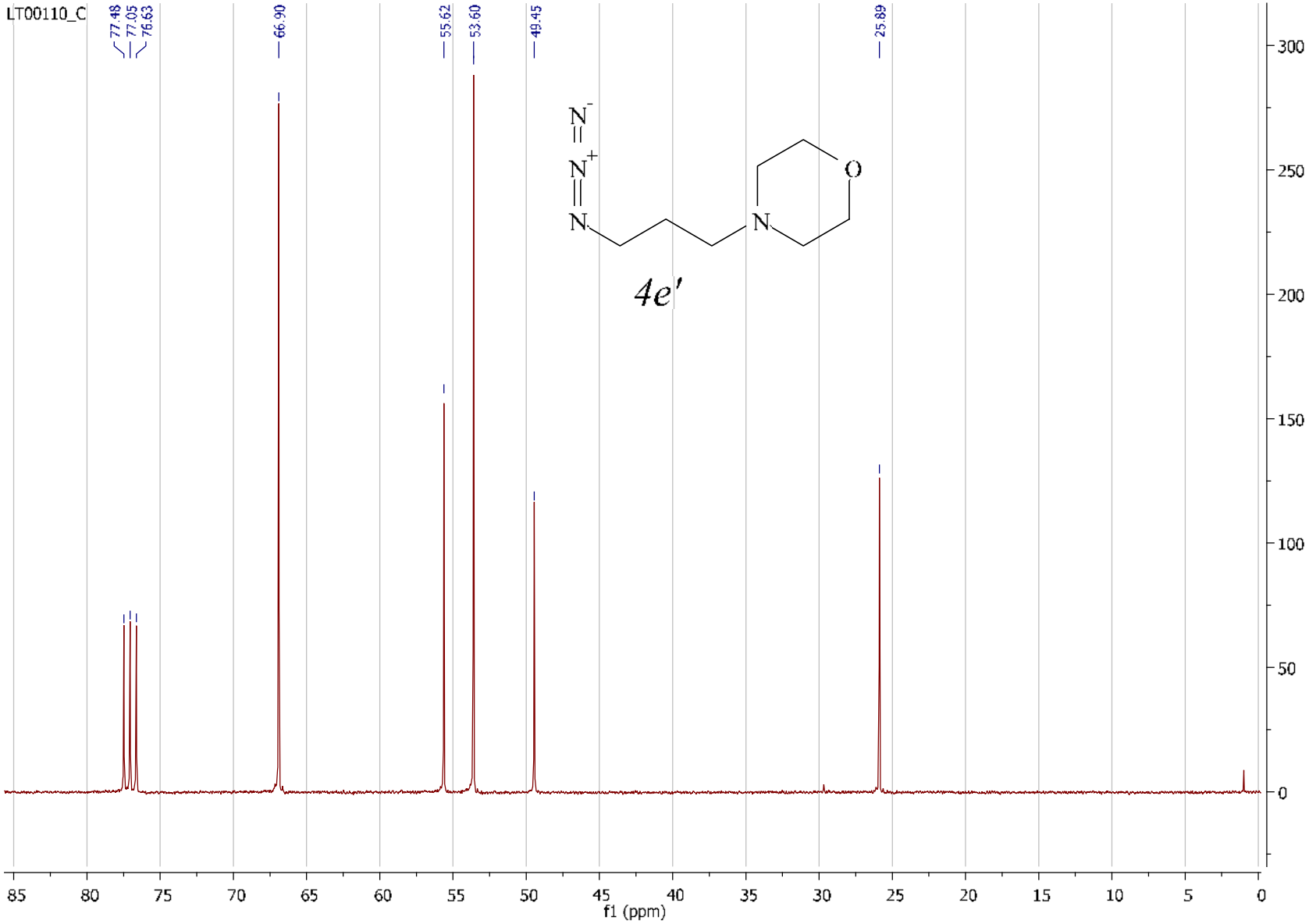
LT00110_C
77.48
77.05
76.63
66.90
55.62
53.60
49.45
25.89
4e'
f1 (ppm)

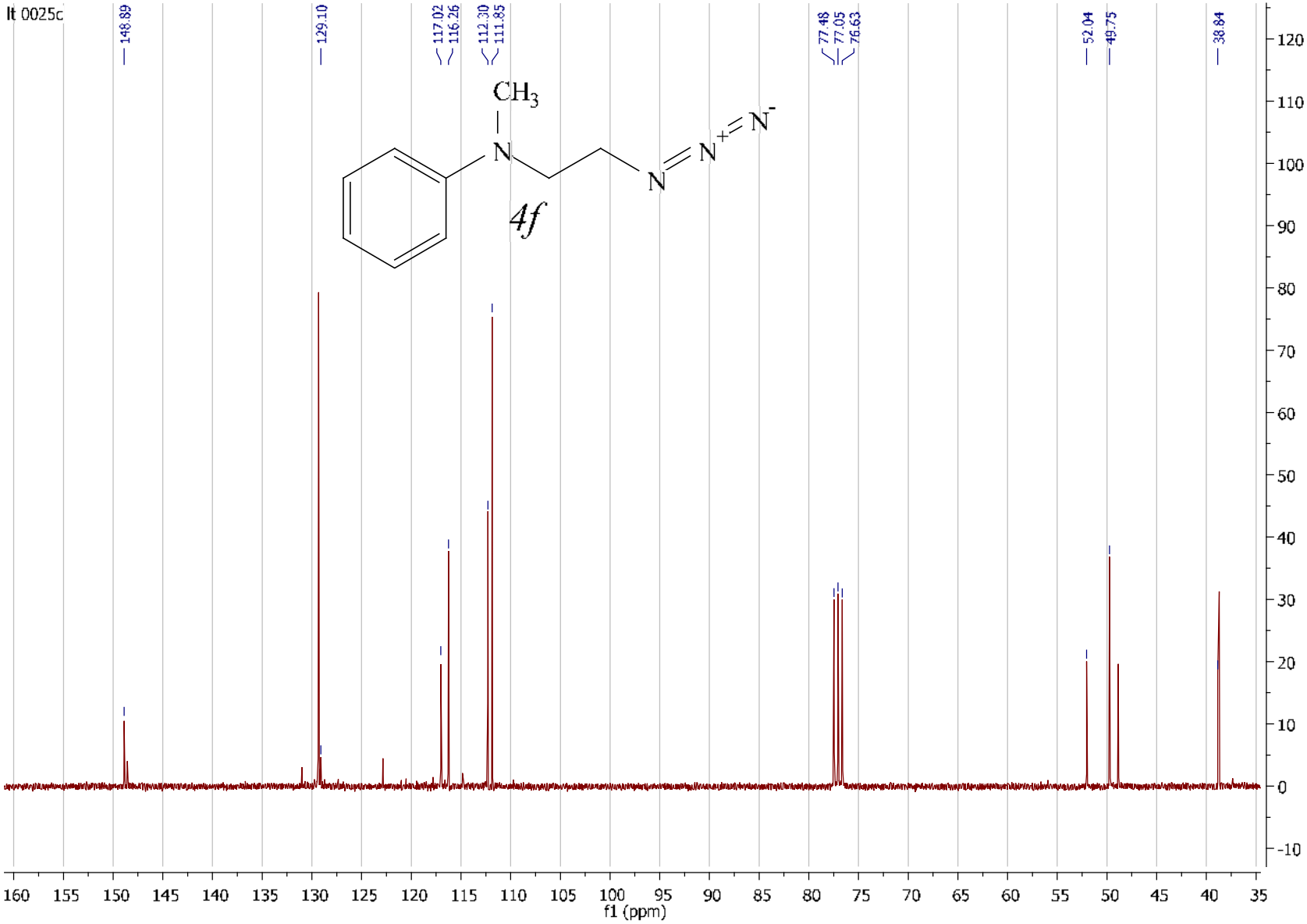
lt 0025c
148.89
129.10
117.02
116.26
112.30
111.85
77.48
77.05
76.63
52.04
49.75
38.84
CH3
N
N
N+
N-
4f
f1 (ppm)

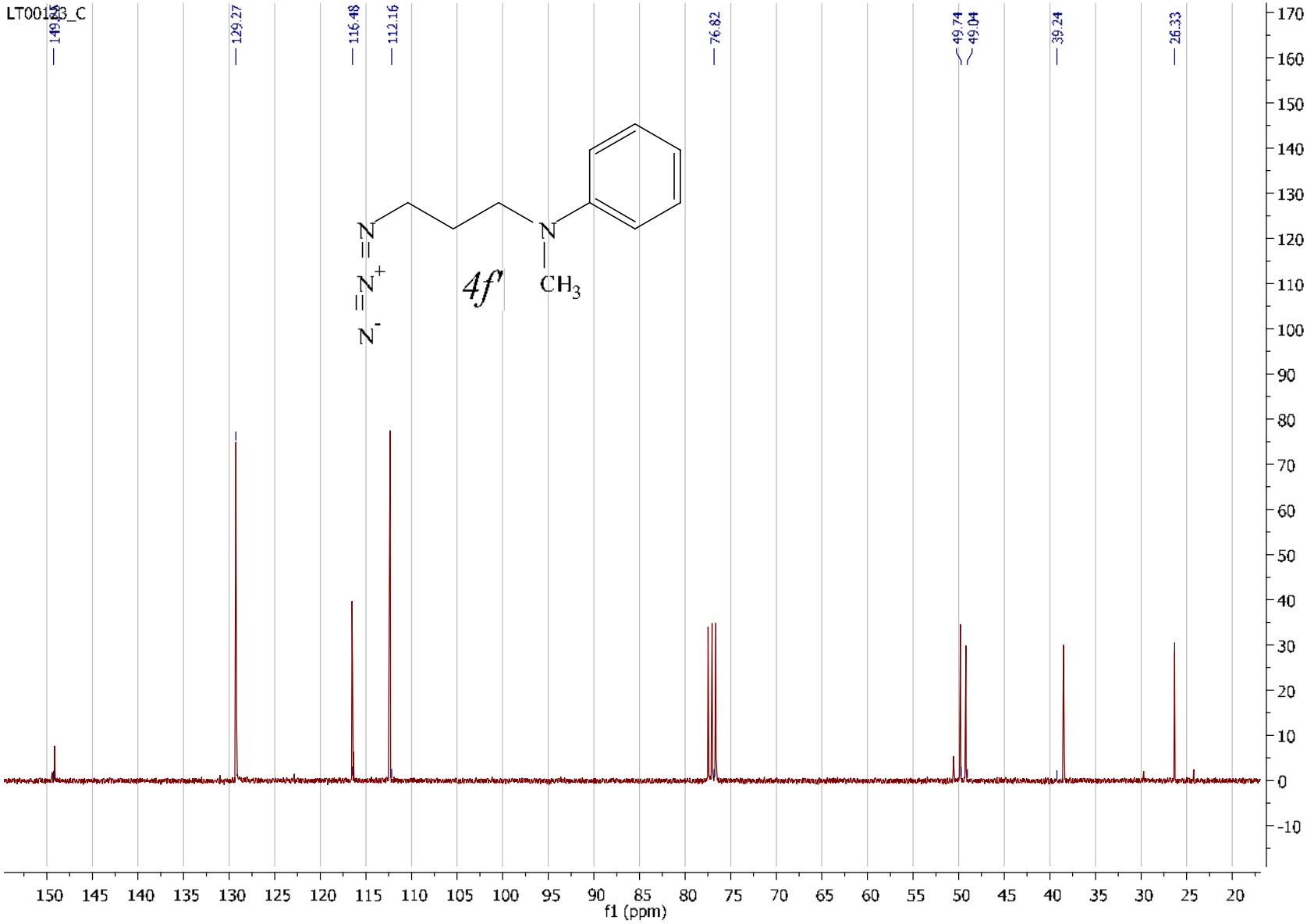
LT00123_C
149.43
129.27
116.48
112.16
76.82
49.74
49.04
39.24
26.33
4f
CH3
f1 (ppm)

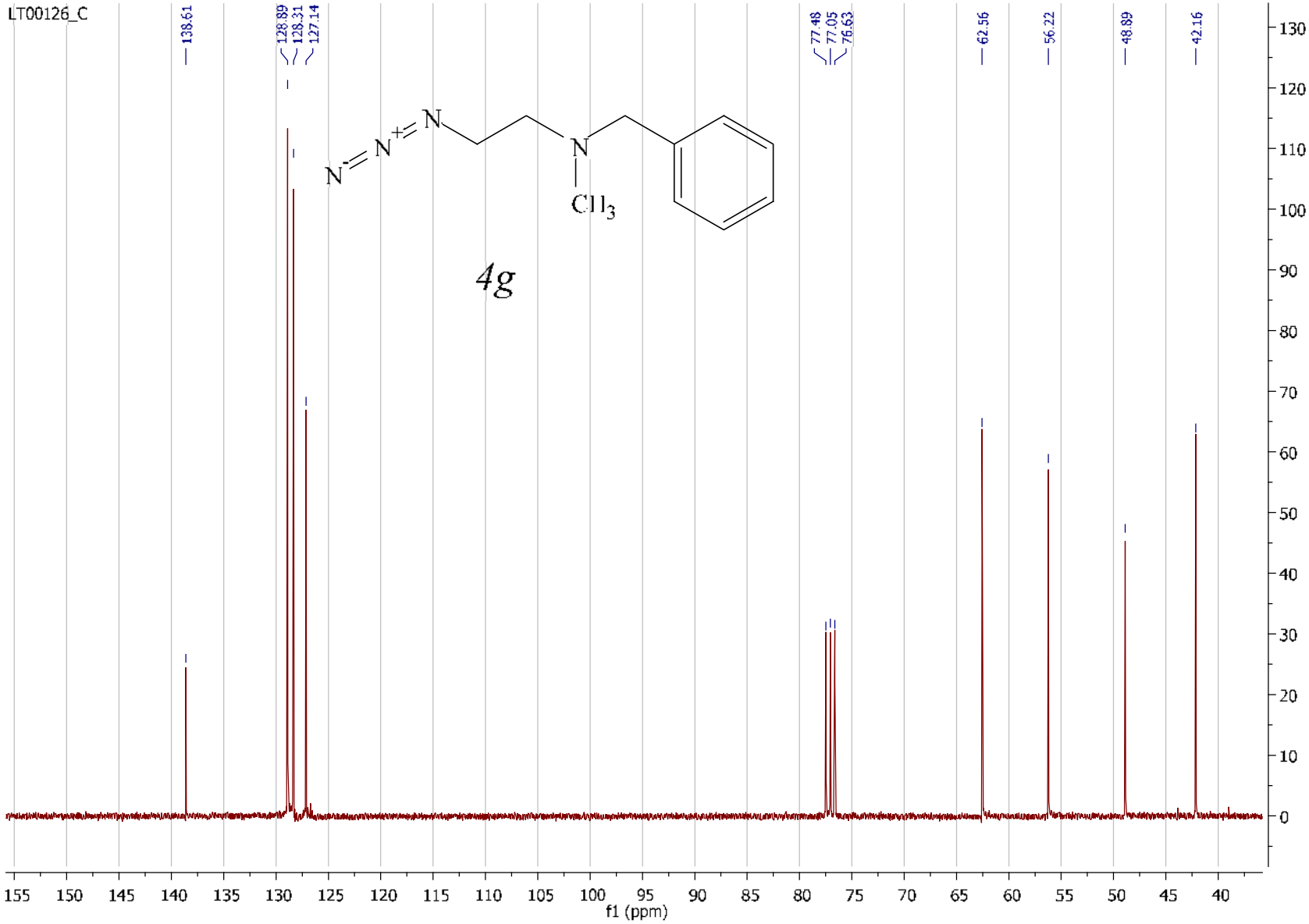
LT00126_C
138.61
128.89
128.31
127.14
77.48
77.05
76.63
62.56
56.22
48.89
42.16
4g
f1 (ppm)

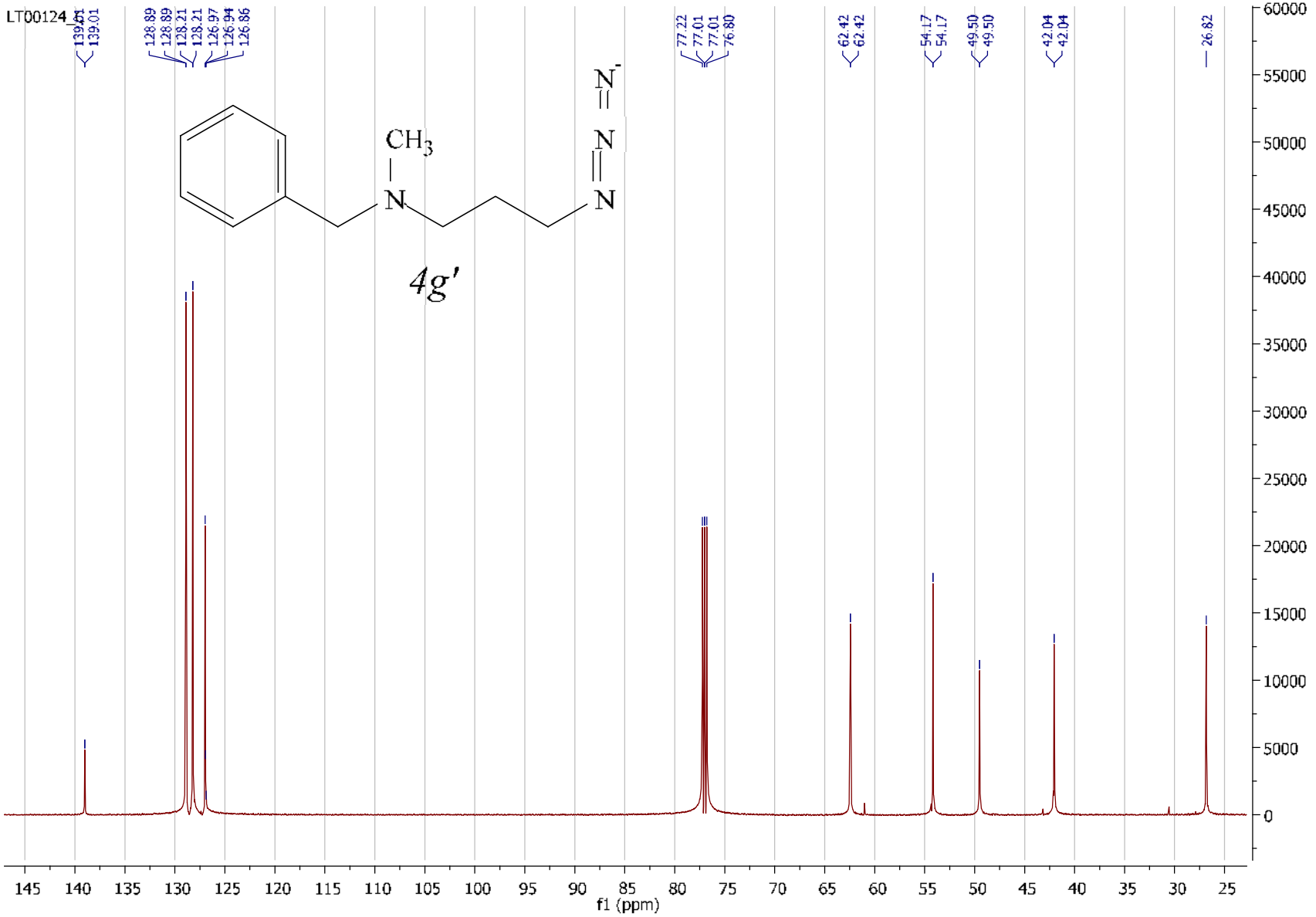
LT00124_01
139.01
128.89
128.89
128.21
128.21
126.97
126.94
126.86
77.22
77.01
77.01
76.80
62.42
62.42
54.17
54.17
49.50
49.50
42.04
42.04
26.82
CH3
N
N
N
N
4g'
f1 (ppm)

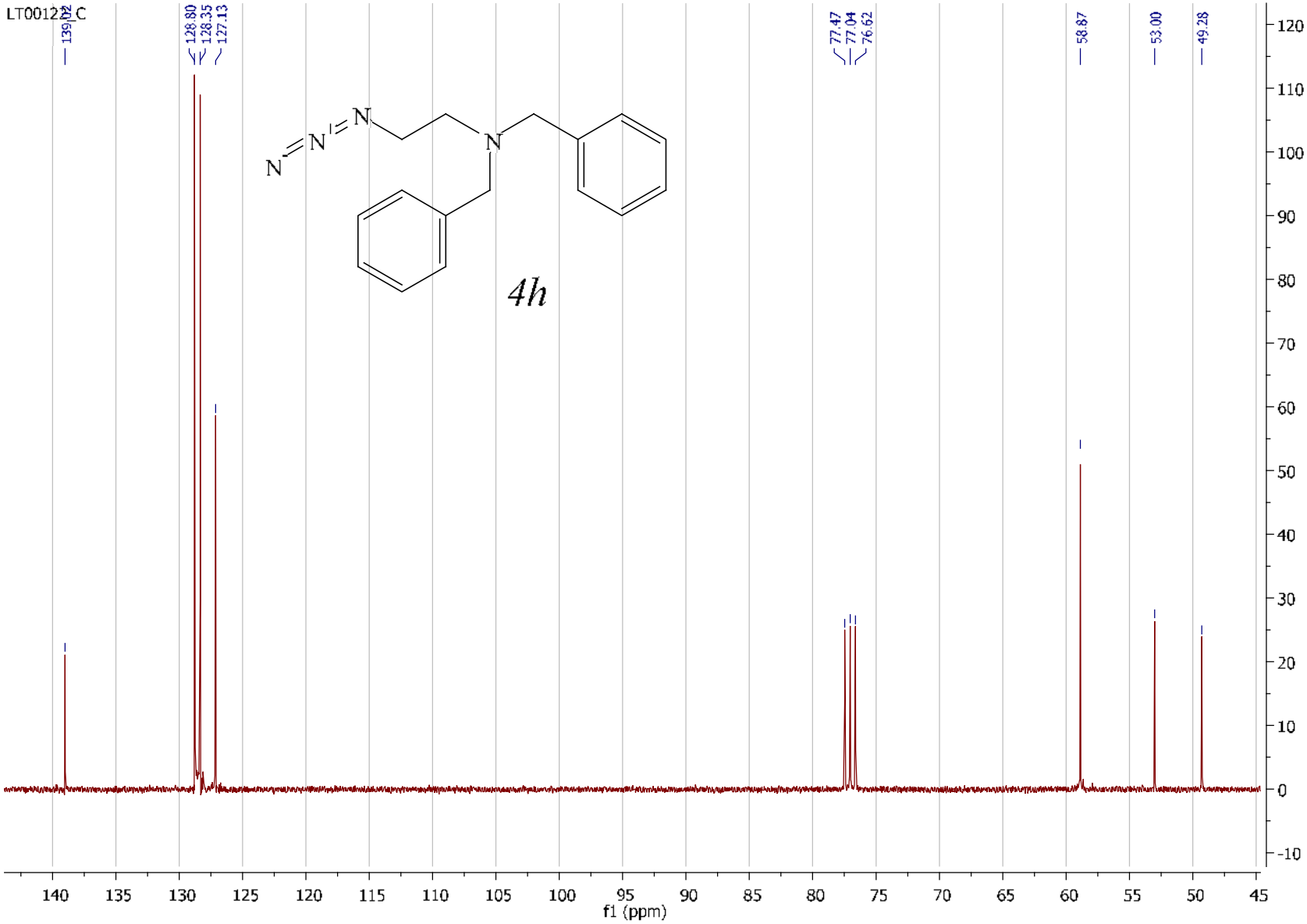
LT00122_C
139.02
128.80
128.35
127.13
77.47
77.04
76.62
58.87
53.00
49.28
4h
f1 (ppm)

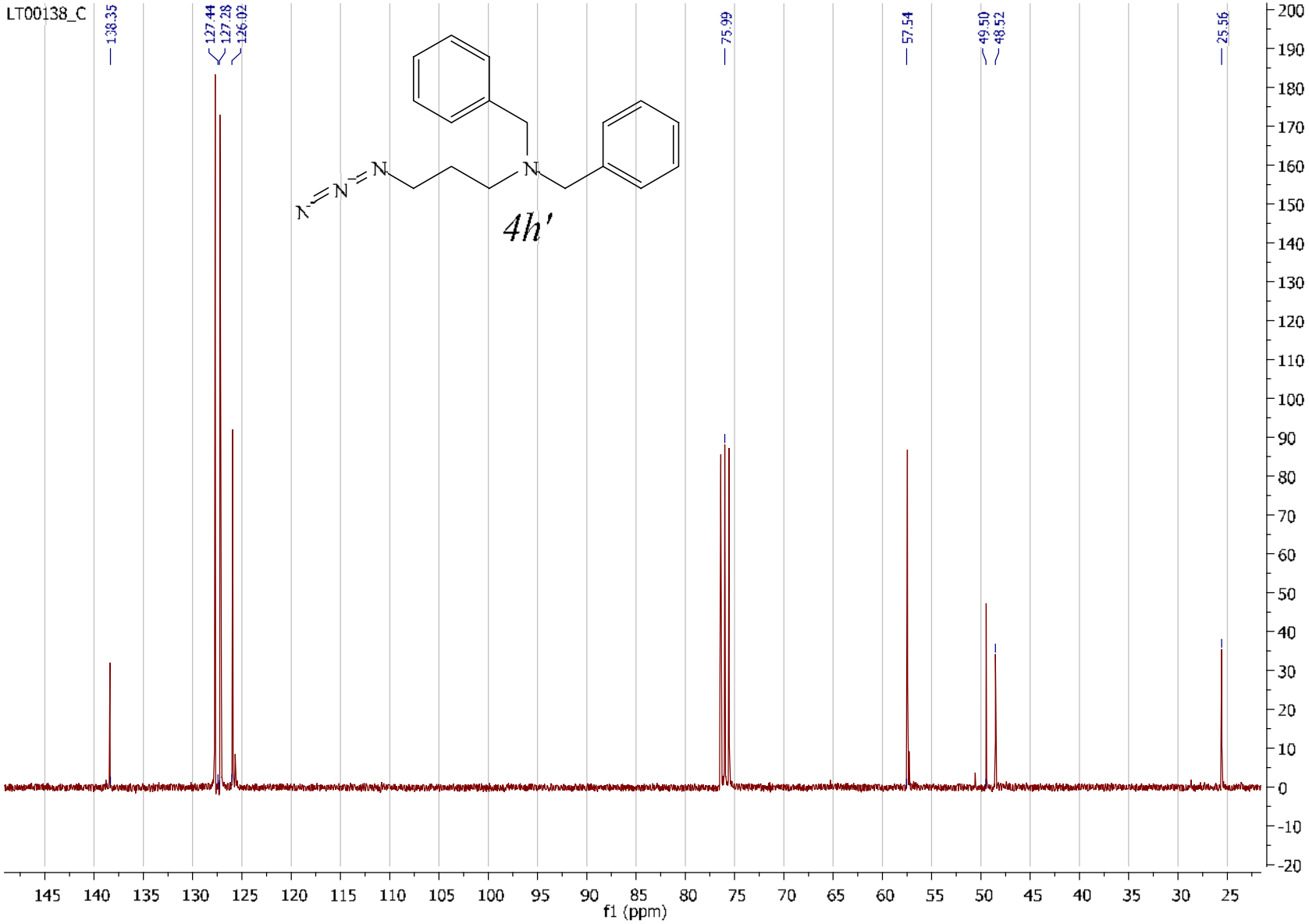
LT00138_C
138.35
127.44
127.28
126.02
75.99
57.54
49.50
48.52
25.56
4h'
f1 (ppm)

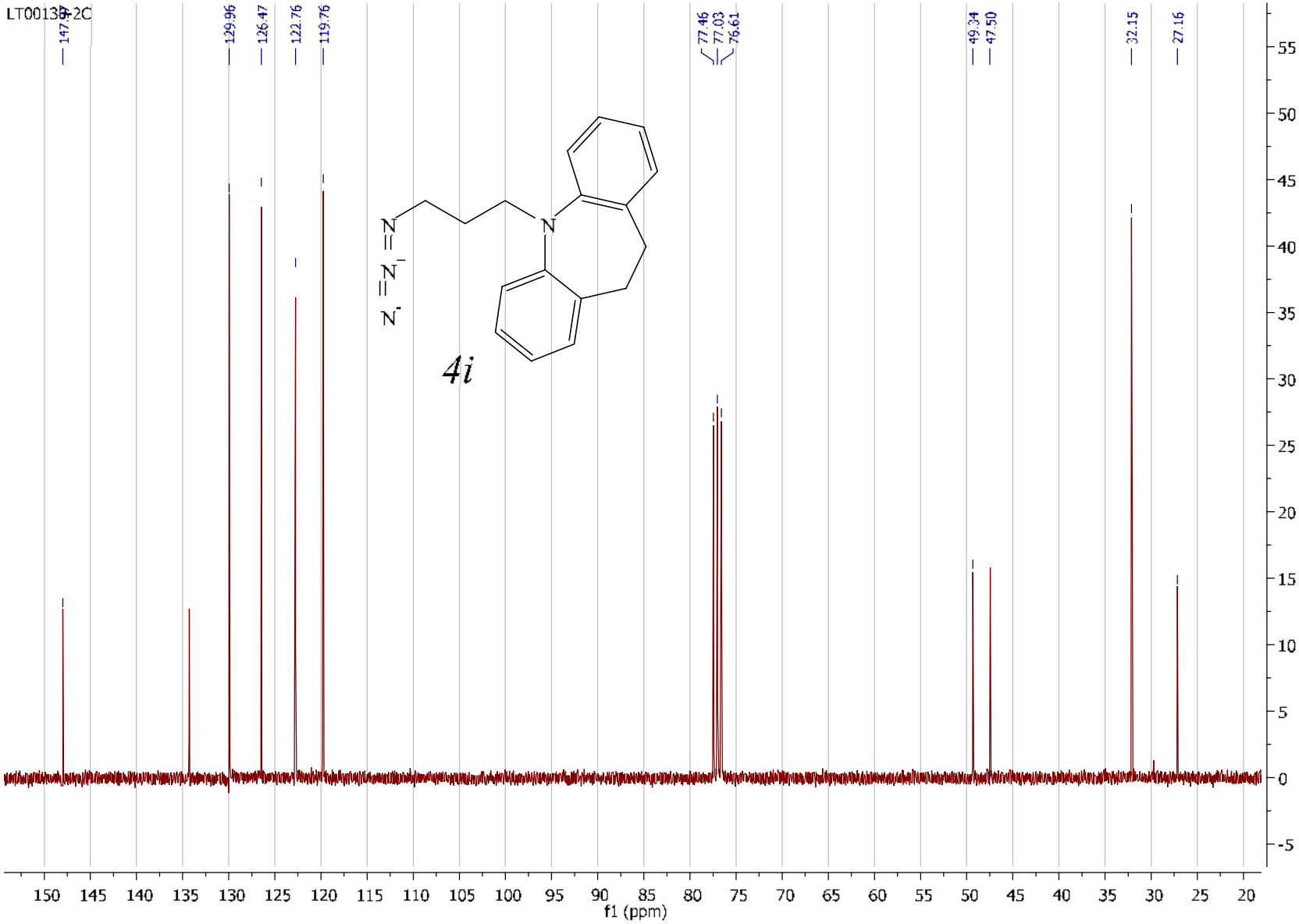
LT00139-2C
147.94
129.96
126.47
122.76
119.76
77.46
77.03
76.61
49.34
47.50
32.15
27.16
4i
f1 (ppm)

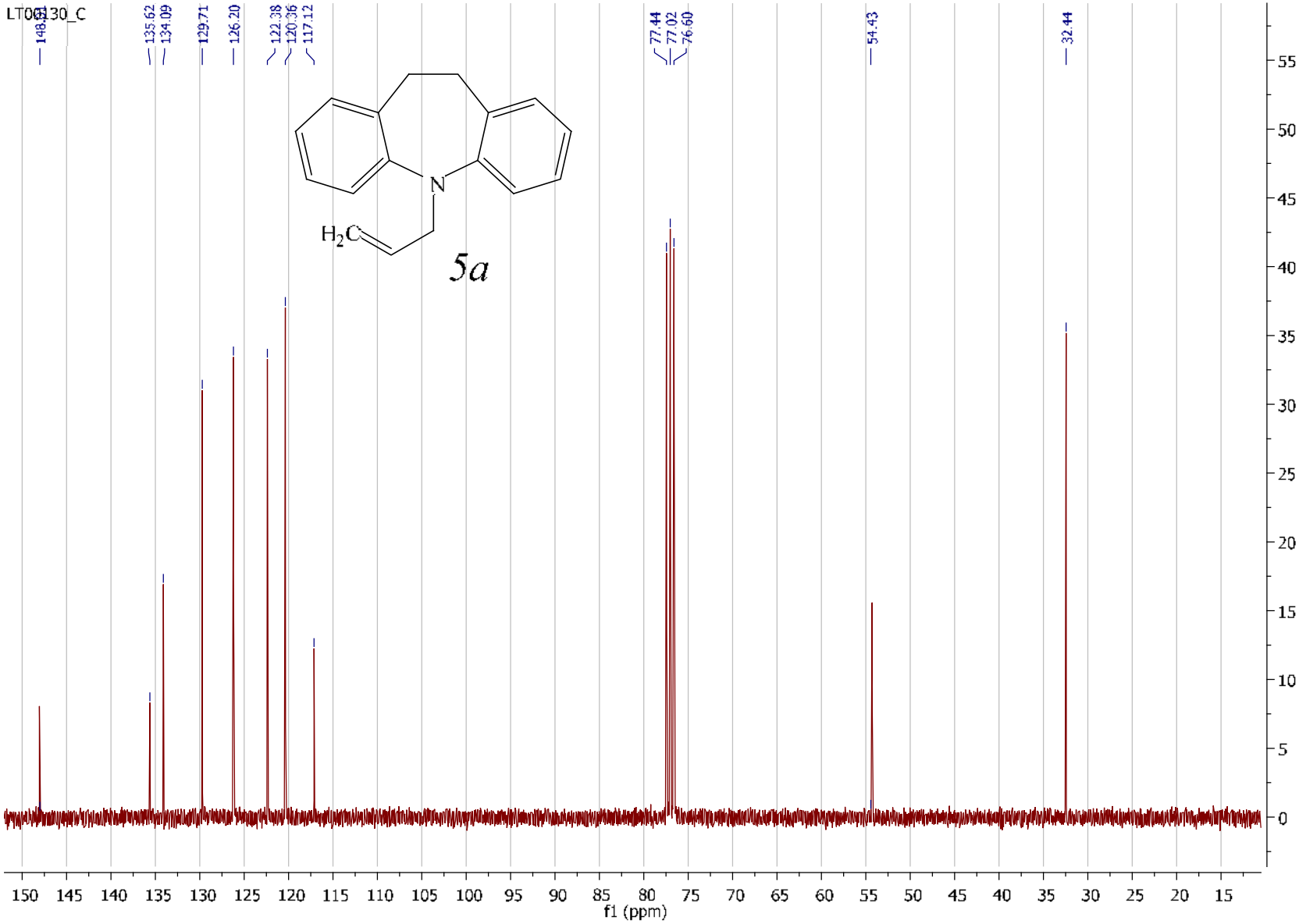
LT0630_C
148.51
135.62
134.09
129.71
126.20
122.38
120.36
117.12
77.44
77.02
76.60
54.43
32.44
N
H2C
5a
f1 (ppm)

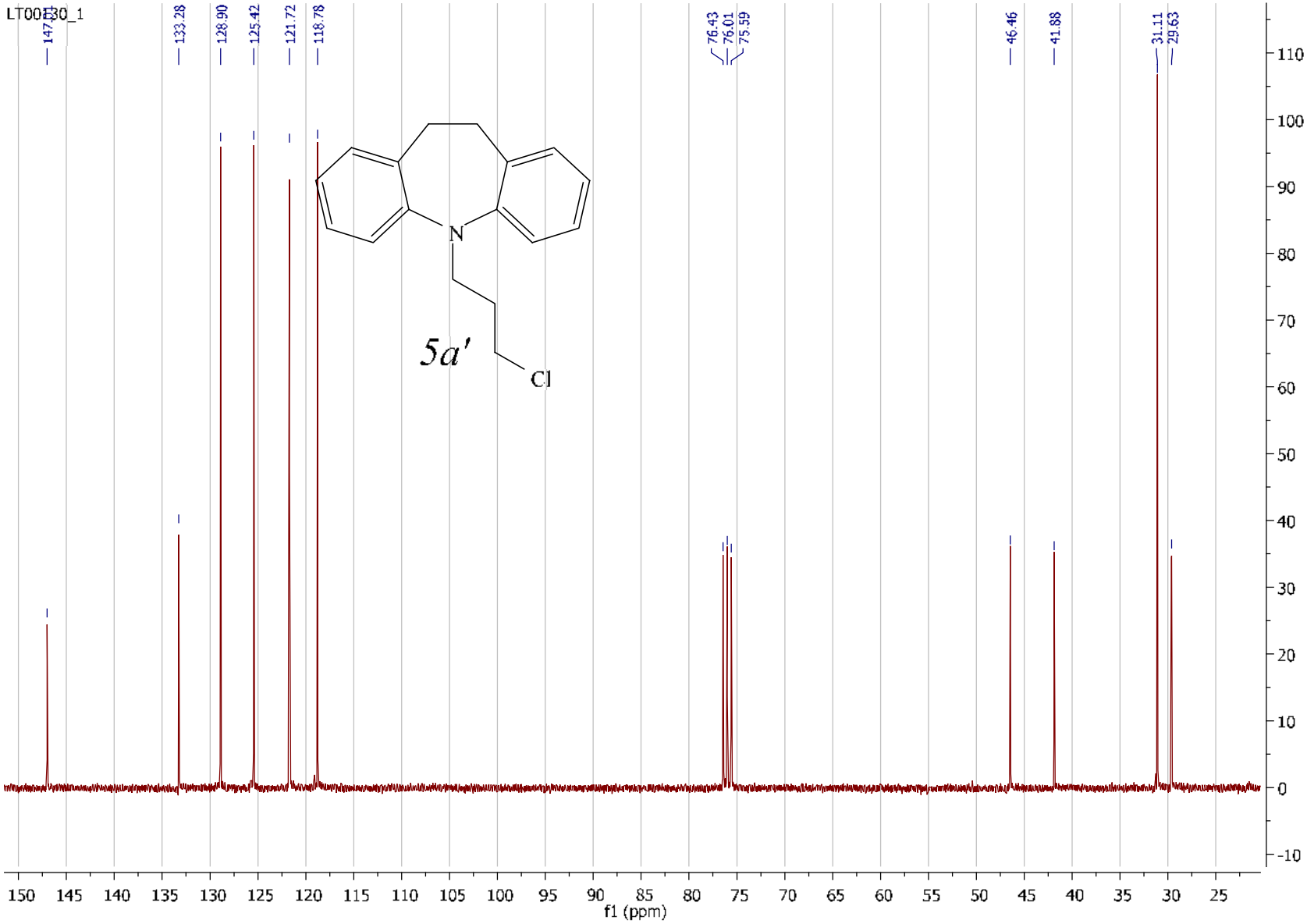
LT00130_1
147.50
133.28
128.90
125.42
121.72
118.78
76.43
76.01
75.59
46.46
41.88
31.11
29.63
N
Cl
5a′
f1 (ppm)

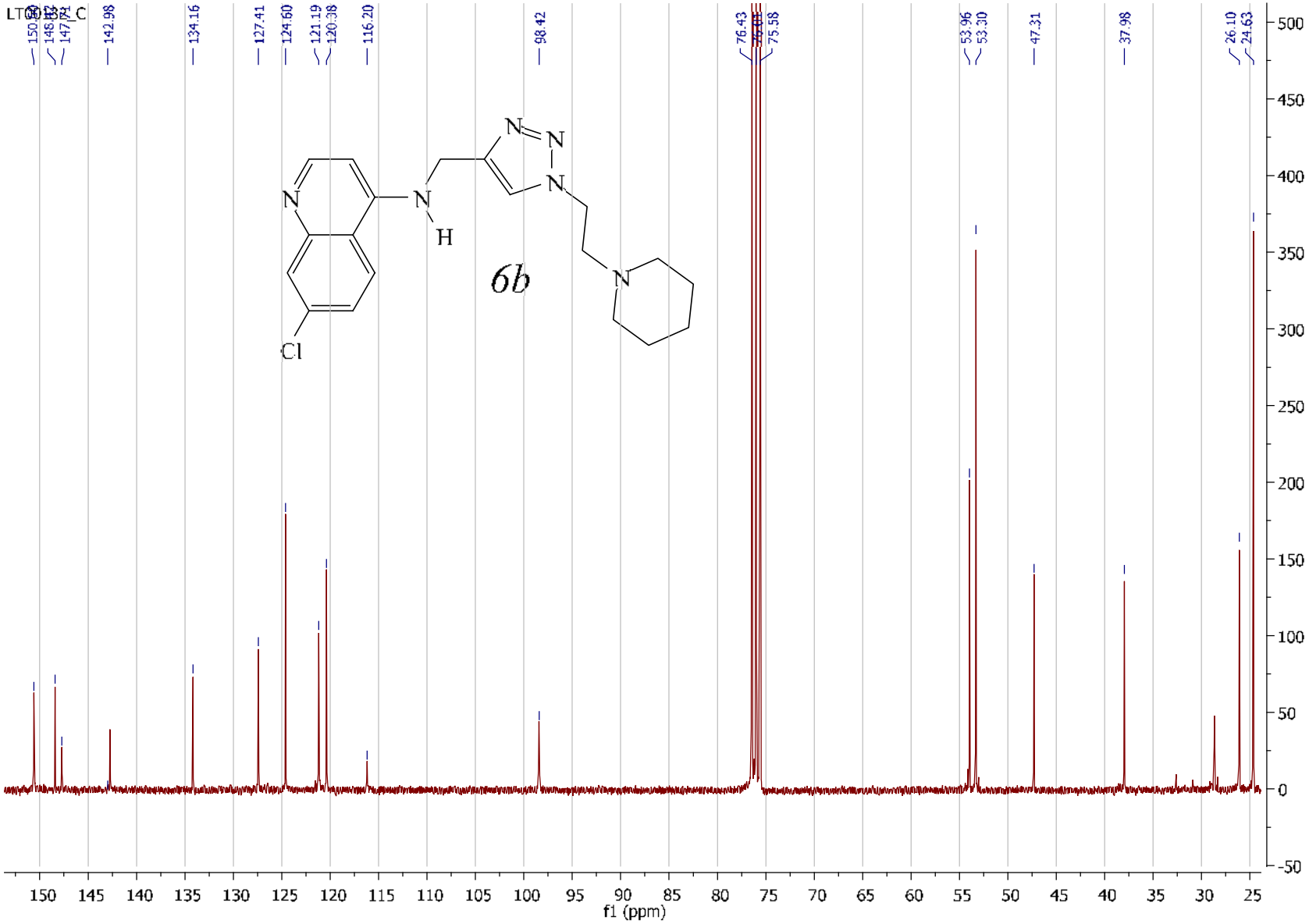
150.61
146.83
147.71
142.98
134.16
127.41
124.60
121.19
120.38
116.20
98.42
76.43
75.58
53.96
53.30
47.31
37.98
26.10
24.63
N
N
N
N
H
N
Cl
6b
f1 (ppm)

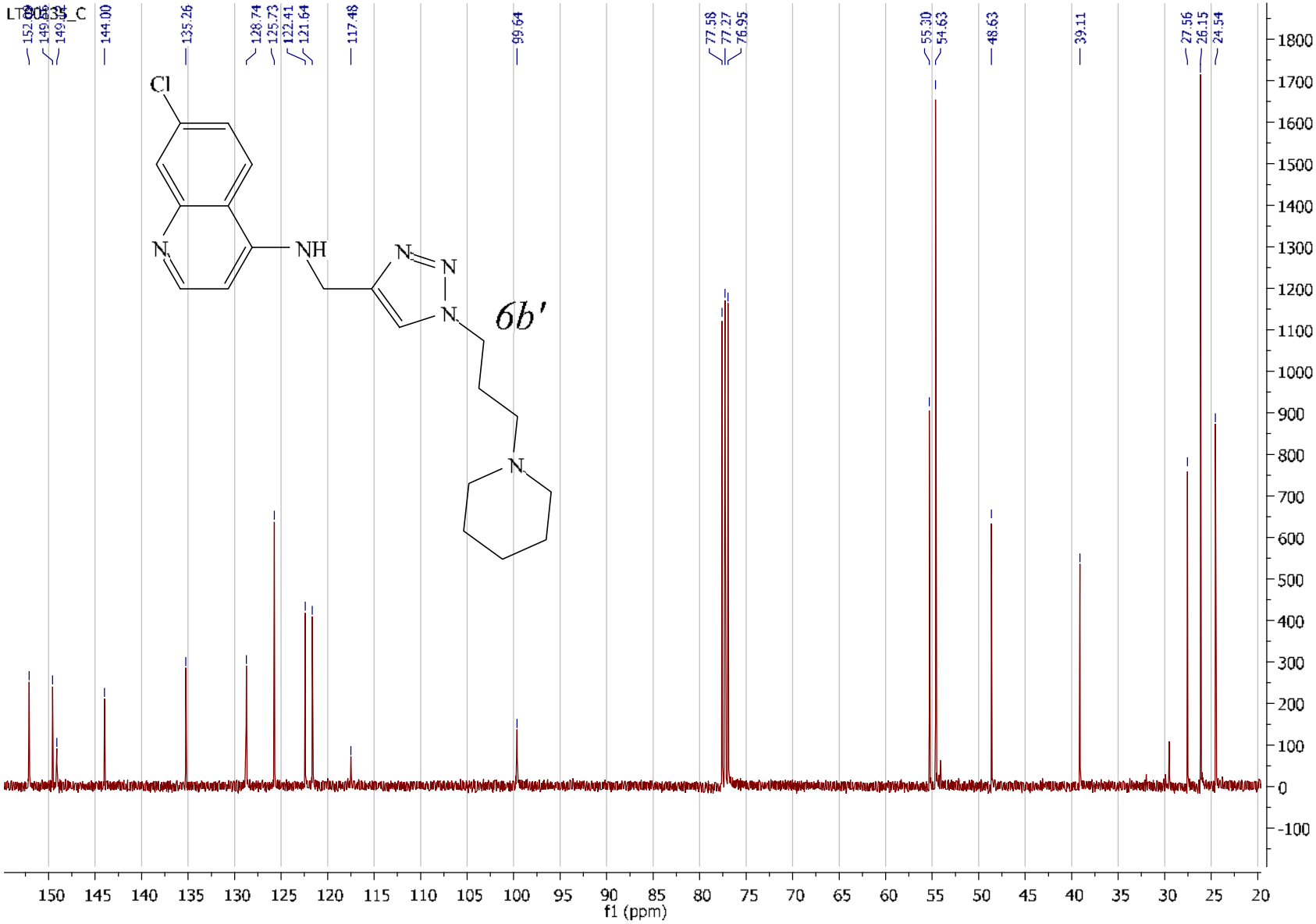
LT-80-35_C
152.83
149.63
149.31
144.00
135.26
128.74
125.73
122.41
121.64
117.48
99.64
77.58
77.27
76.95
55.30
54.63
48.63
39.11
27.56
26.15
24.54
Cl
N
NH
N
N
N
N
6b'
f1 (ppm)

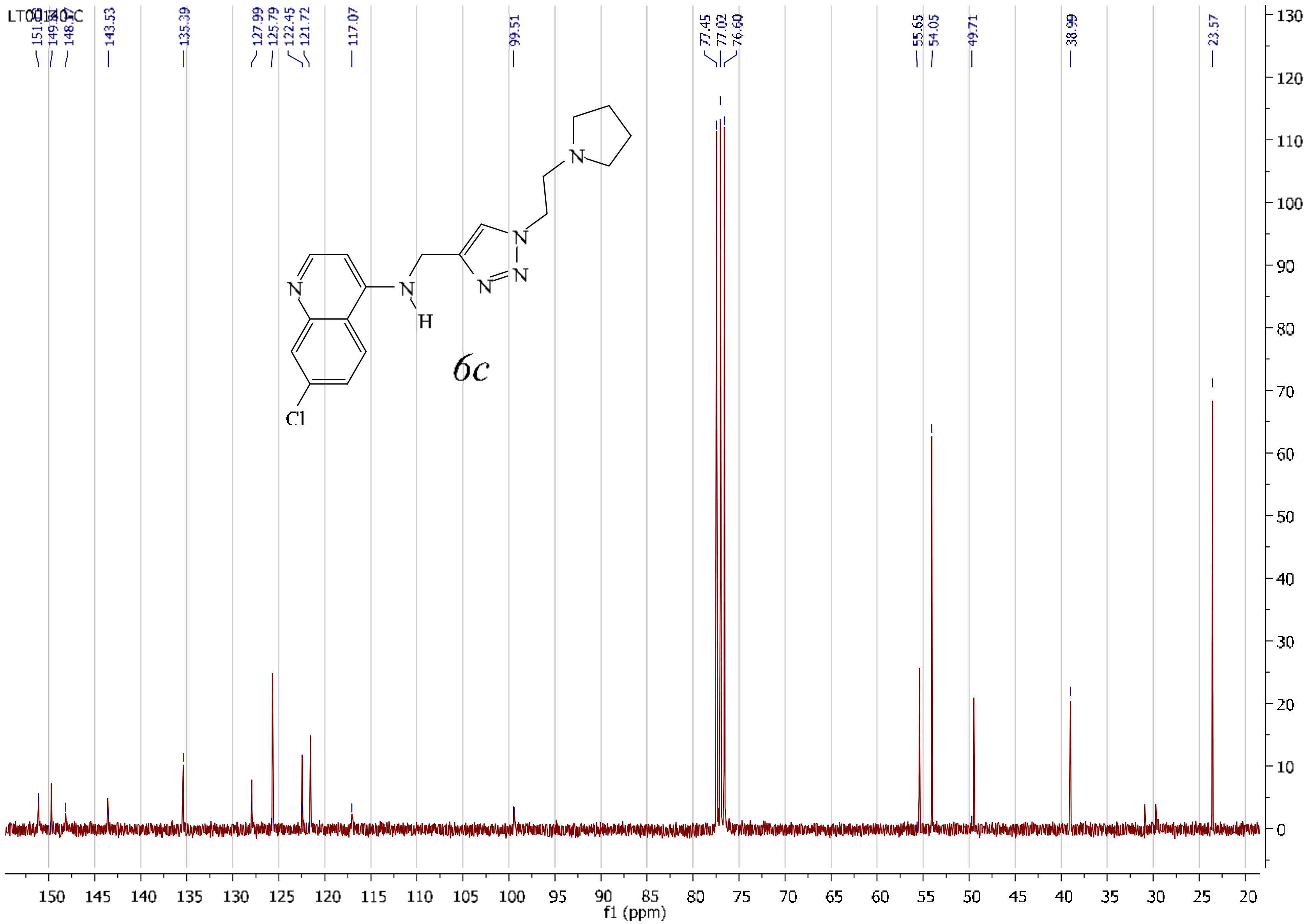
143.53
135.39
127.99
125.79
122.45
121.72
117.07
99.51
77.45
77.02
76.60
55.65
54.05
49.71
38.99
23.57
6c
f1 (ppm)

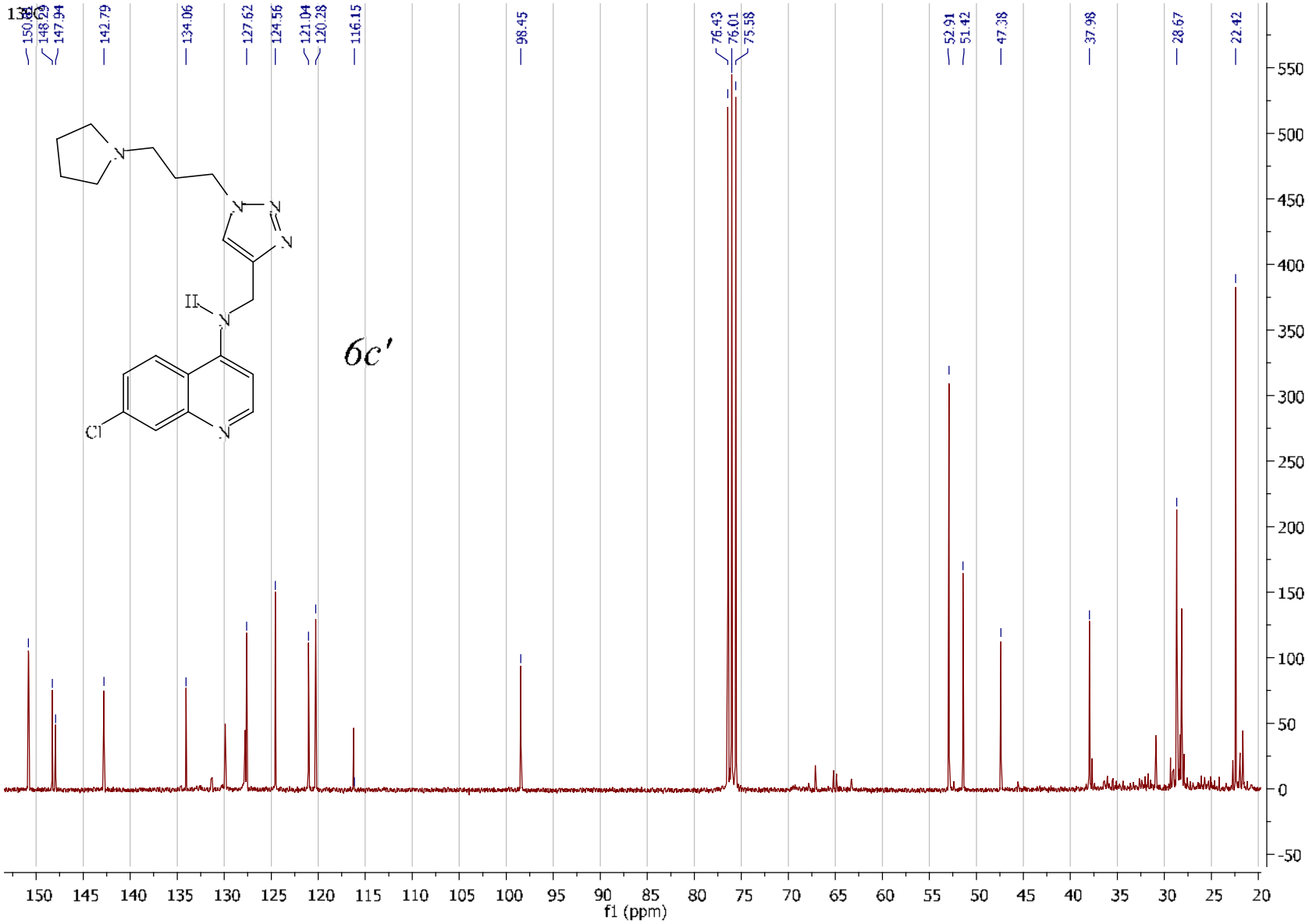
150.63
148.29
147.94
142.79
134.06
127.62
124.56
121.04
120.28
116.15
98.45
76.43
76.01
75.58
52.91
51.42
47.38
37.98
28.67
22.42
6c'
Cl
f1 (ppm)

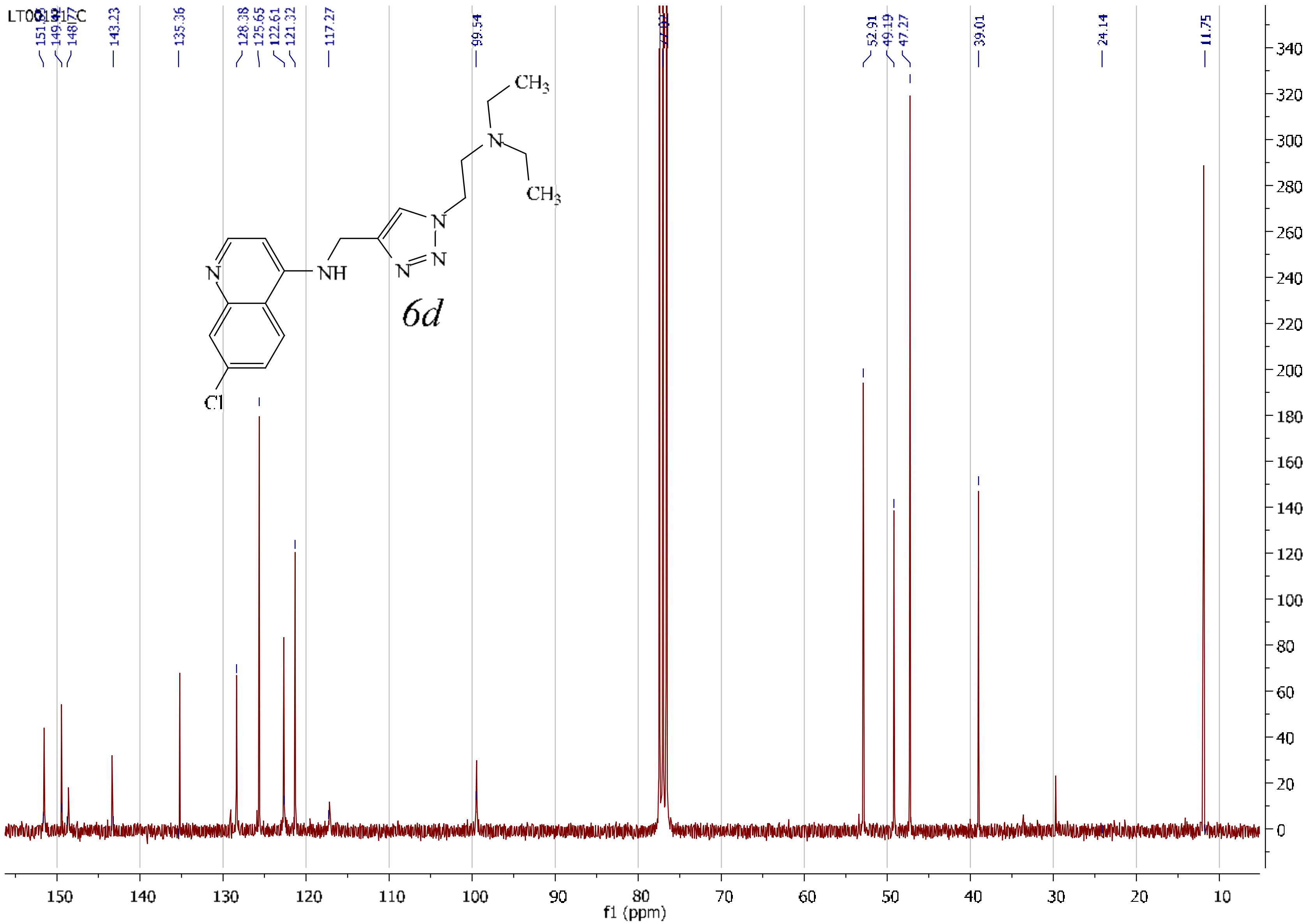
LT00131-C
151.3
149.42
148.77
143.23
135.36
128.38
125.65
122.61
121.32
117.27
99.54
77.02
52.91
49.19
47.27
39.01
24.14
11.75
6d
f1 (ppm)

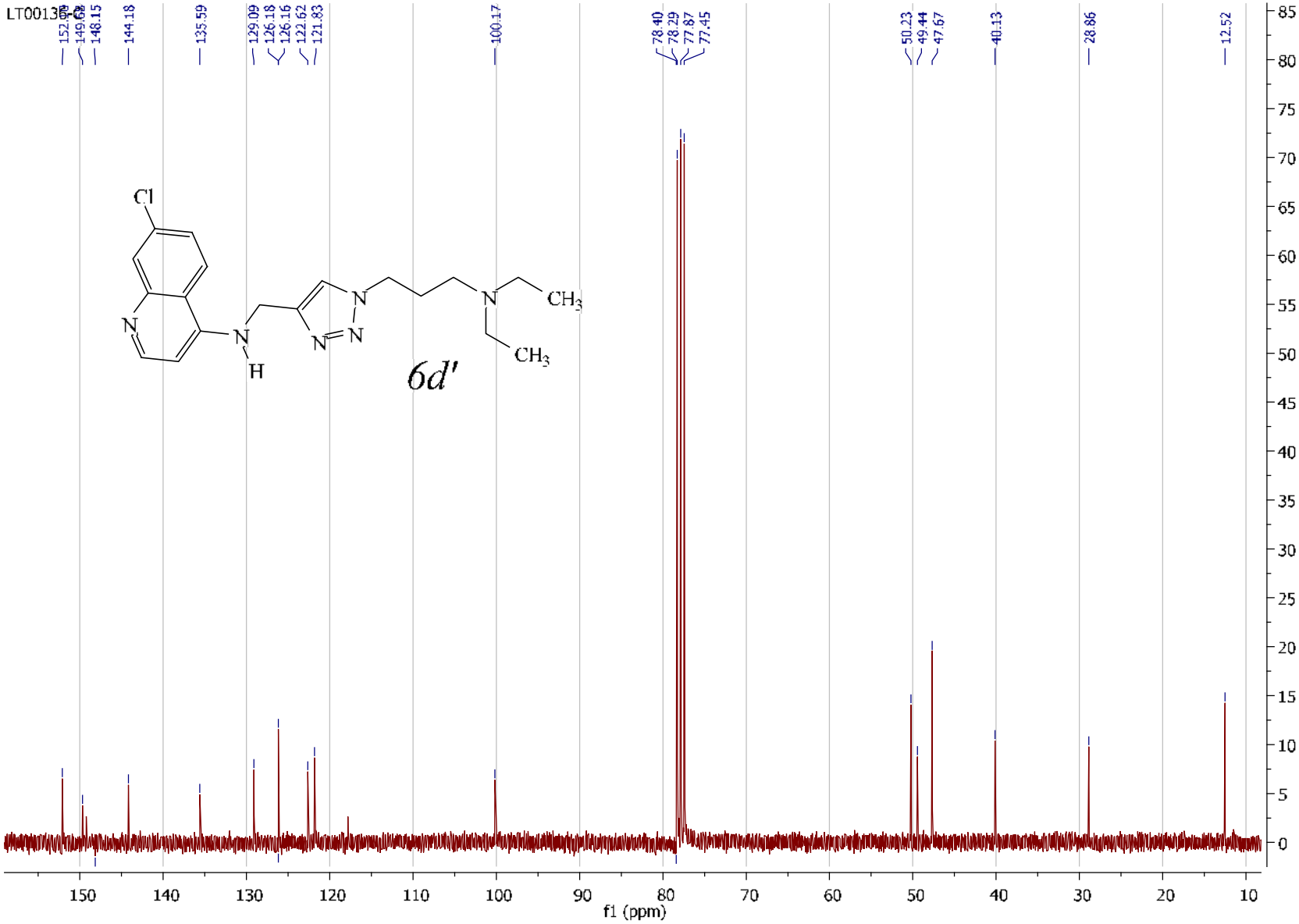
LT00136
152.66
149.63
148.15
144.18
135.59
129.09
126.18
126.16
122.62
121.83
100.17
78.40
78.29
77.87
77.45
50.23
49.44
47.67
40.13
28.86
12.52
Cl
N
N
H
N
N
N
N
CH3
CH3
6d'
f1 (ppm)

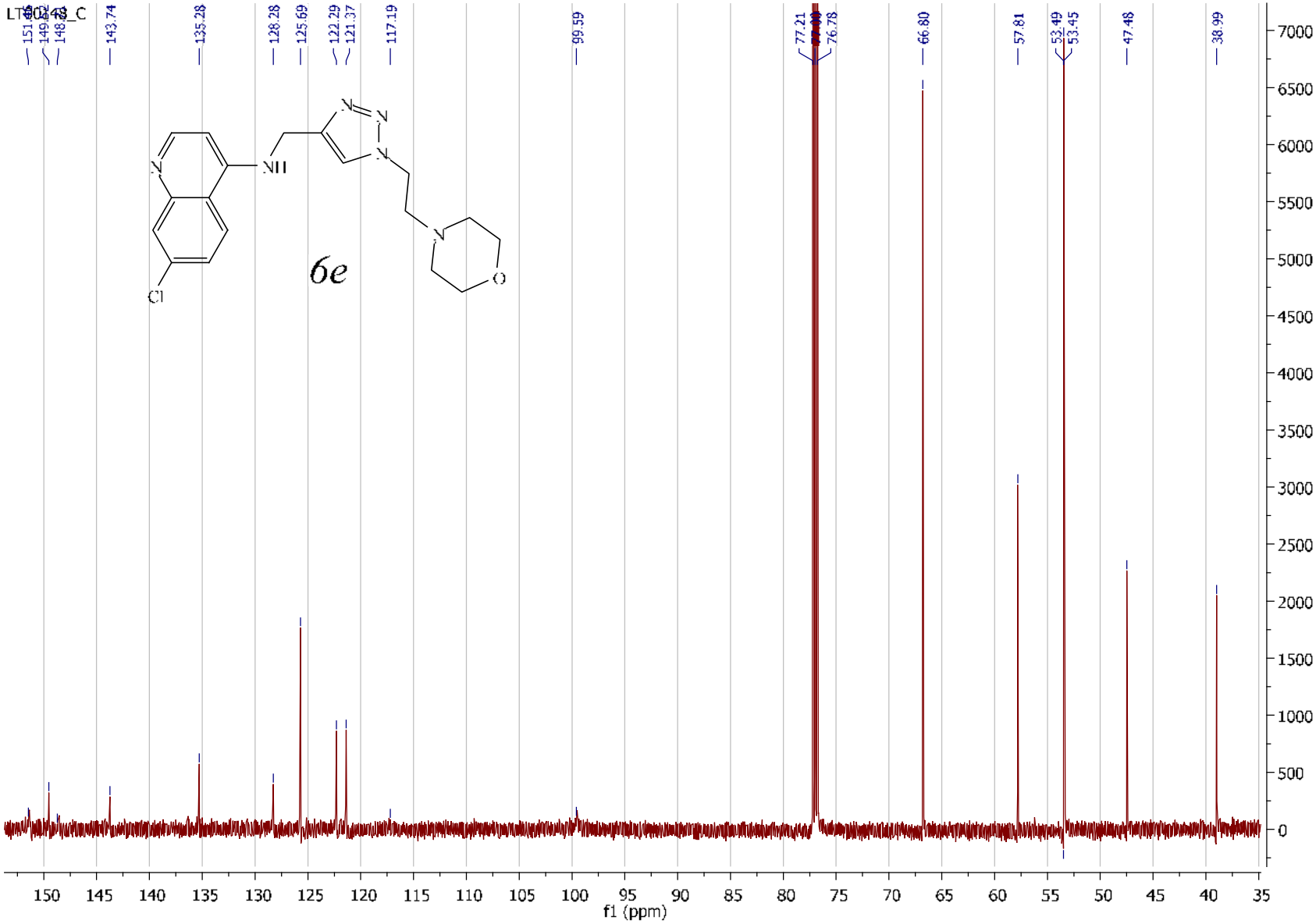
151.60
149.92
148.78
143.74
135.28
128.28
125.69
122.29
121.37
117.19
99.59
77.21
76.78
66.80
57.81
53.49
53.45
47.48
38.99
NH
Cl
O
6e
f1 (ppm)

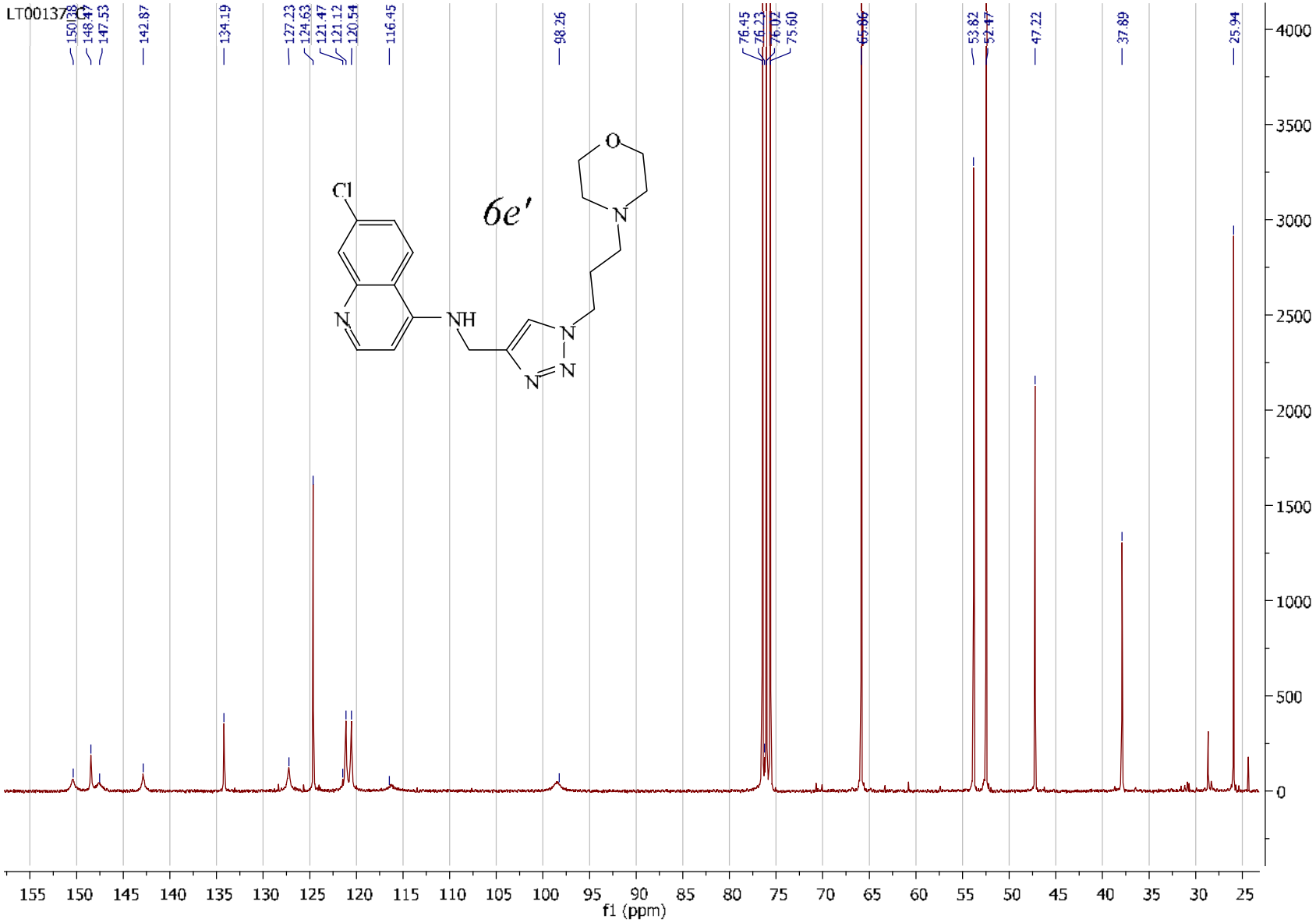
LT0013730
150.29
148.47
147.53
142.87
134.19
127.23
124.63
121.47
121.12
120.54
116.45
98.26
76.45
76.23
76.02
75.60
65.06
53.82
52.47
47.22
37.89
25.94
6e'
Cl
N
NH
N
N
N
N
O
N
f1 (ppm)

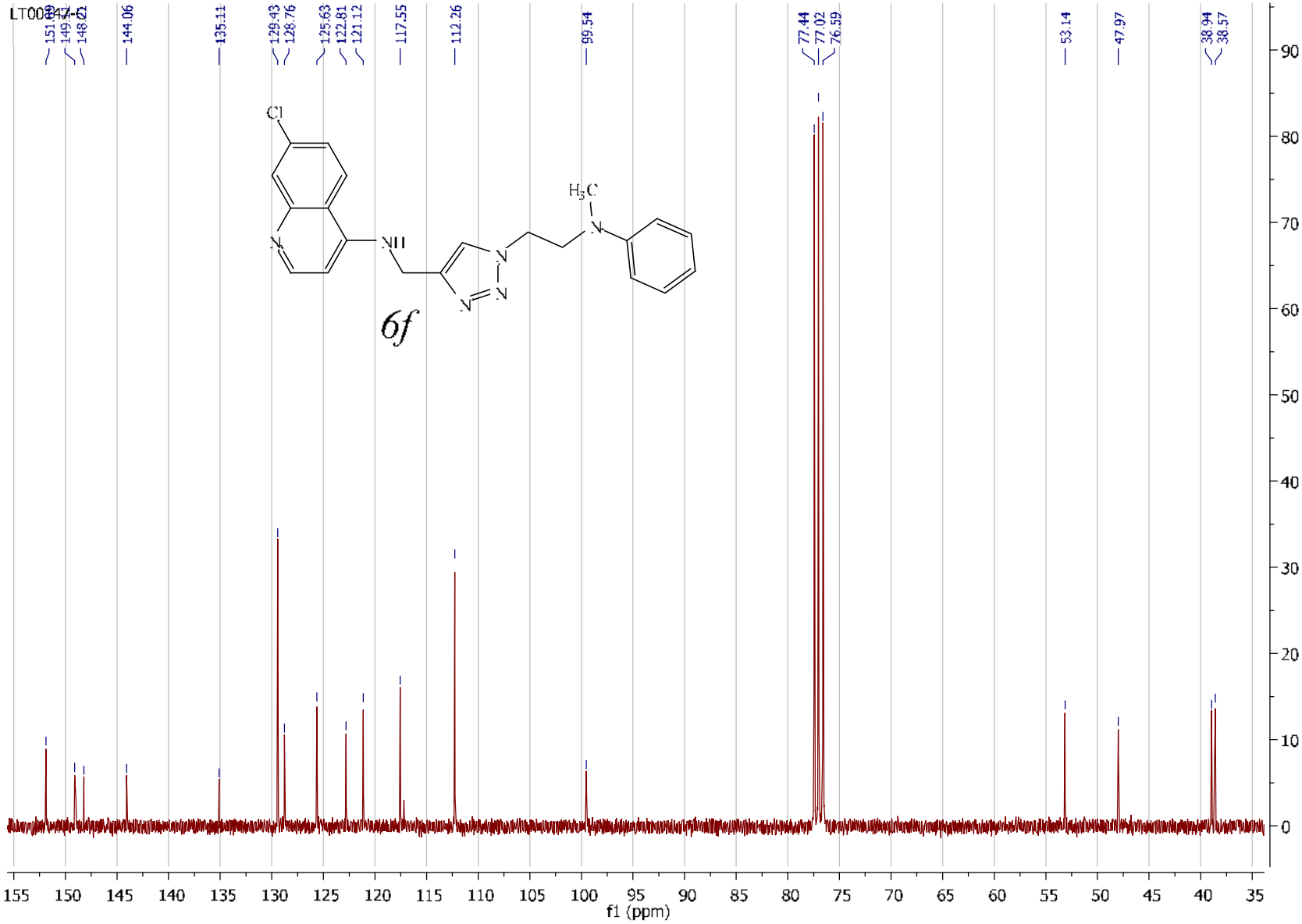
151.64
149.14
148.21
144.06
135.11
129.43
128.76
125.63
122.81
121.12
117.55
112.26
99.54
77.44
77.02
76.59
53.14
47.97
38.94
38.57
Cl
N
NH
N
N
N
N
H3C
N
6f
f1 (ppm)

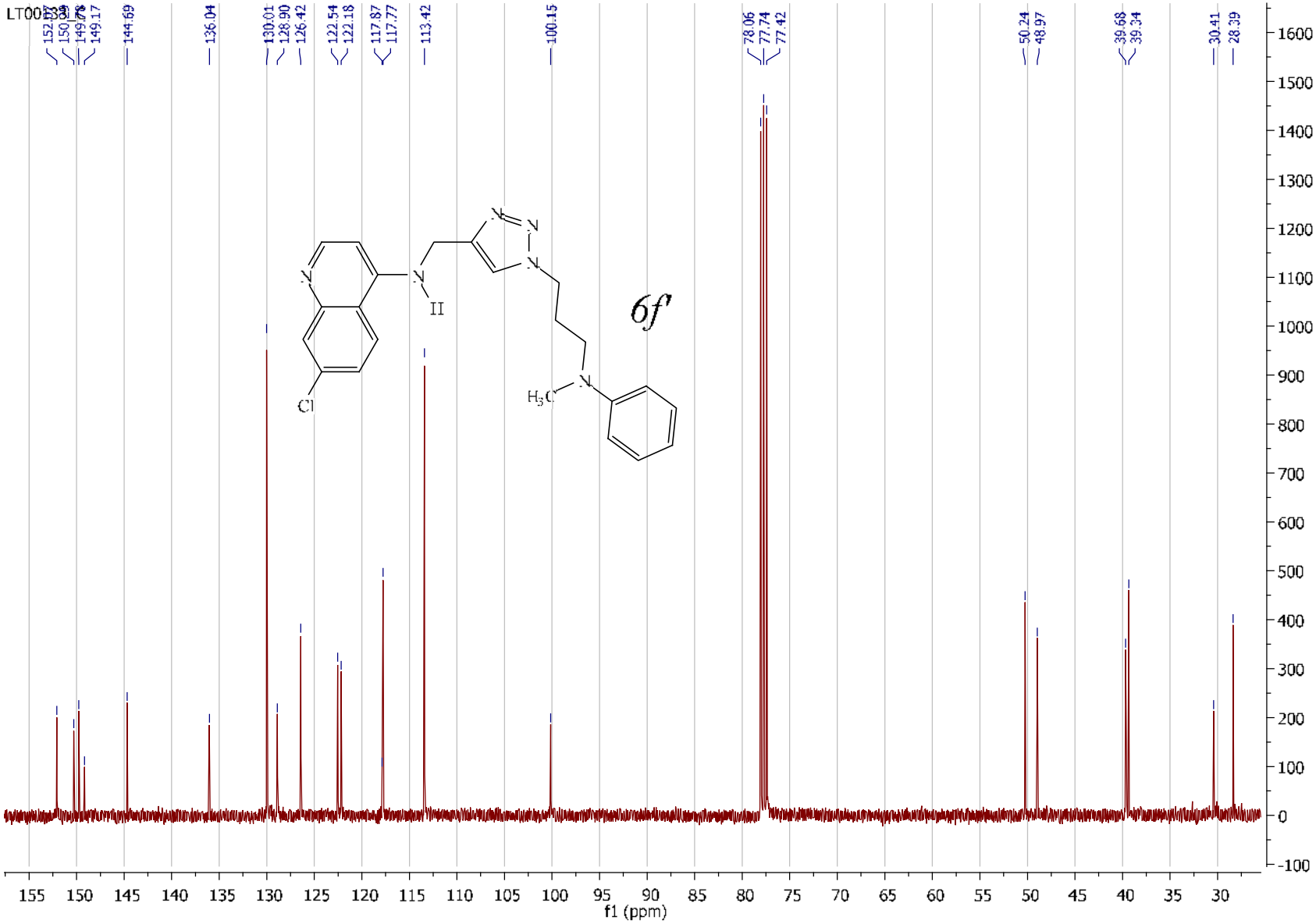
LT0033
152.57
150.34
149.76
149.17
144.69
136.04
130.01
128.90
126.42
122.54
122.18
117.87
117.77
113.42
100.15
78.06
77.74
77.42
50.24
48.97
39.68
39.34
30.41
28.39
6f
Cl
H3C
f1 (ppm)

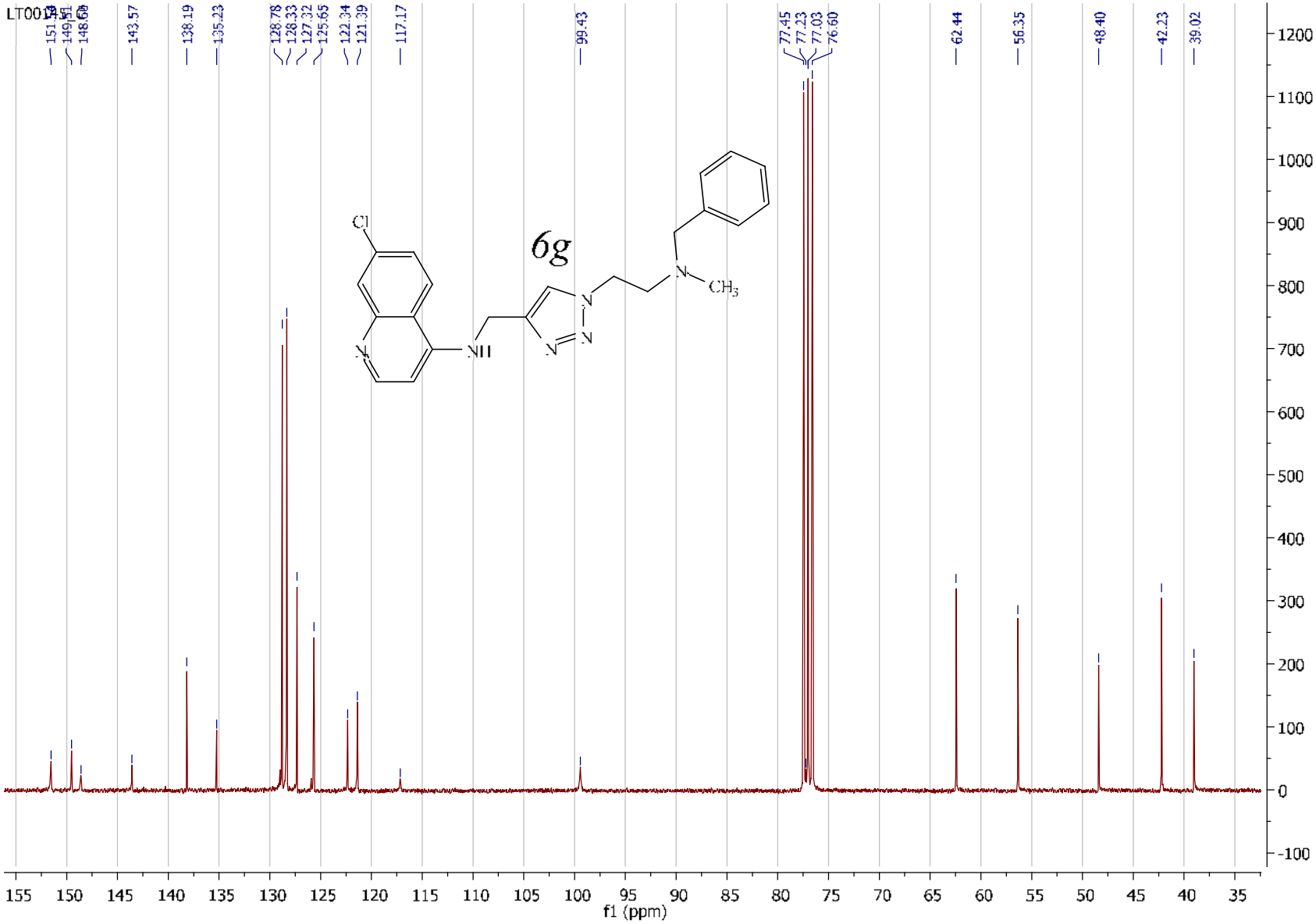
151.51
149.51
148.69
143.57
138.19
135.23
128.78
128.33
127.32
125.65
122.34
121.39
117.17
99.43
77.45
77.23
77.03
76.60
62.44
56.35
48.40
42.23
39.02
6g
Cl
NH
N
CH3
f1 (ppm)

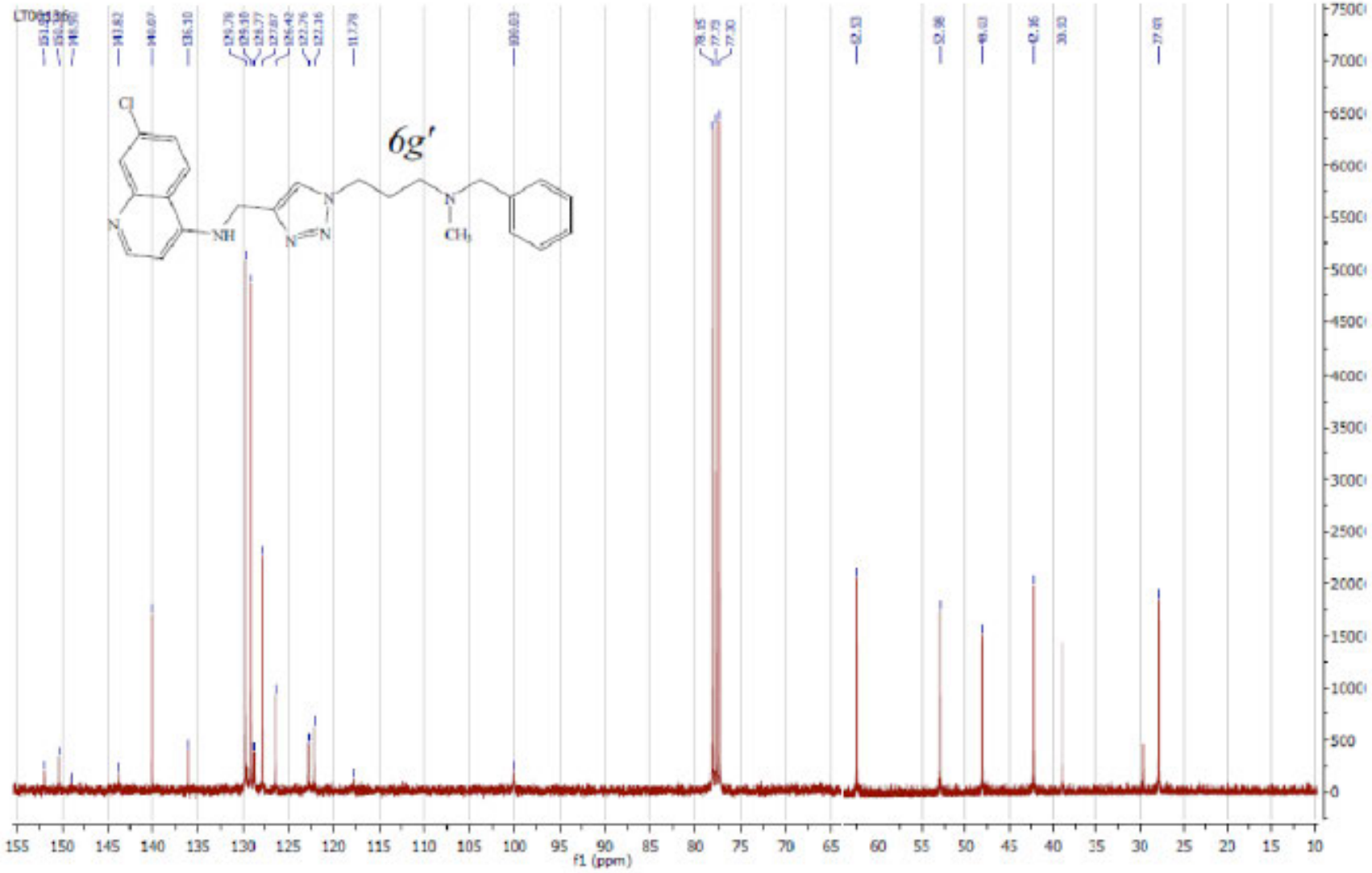
6g'
Cl
NH
N
N
N
CH3
f1 (ppm)

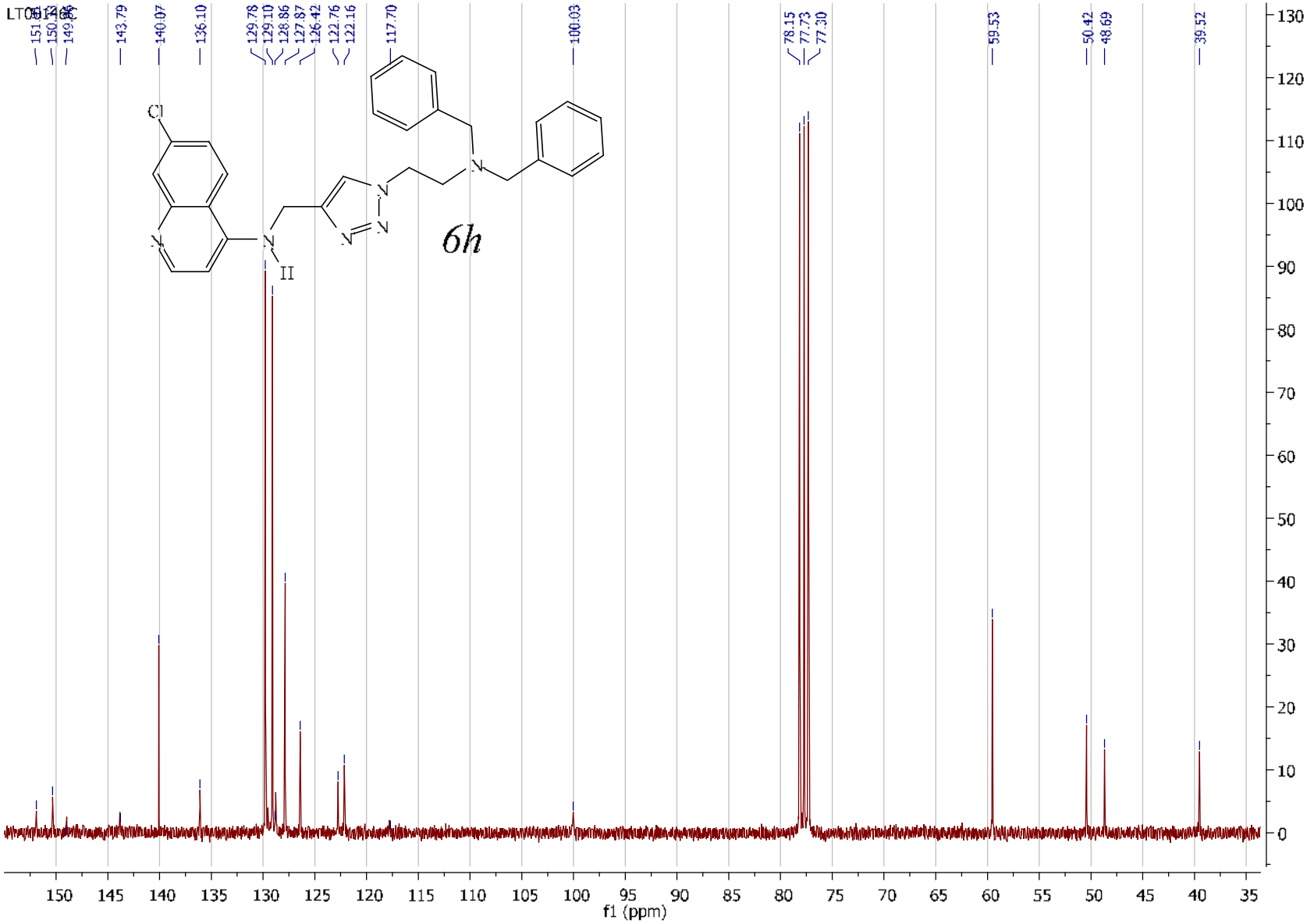
151.61
150.26
149.86
143.79
140.07
136.10
129.78
129.10
128.86
127.87
126.42
122.76
122.16
117.70
100.03
78.15
77.73
77.30
59.53
50.42
48.69
39.52
Cl
N
N
N
N
N
II
6h
f1 (ppm)

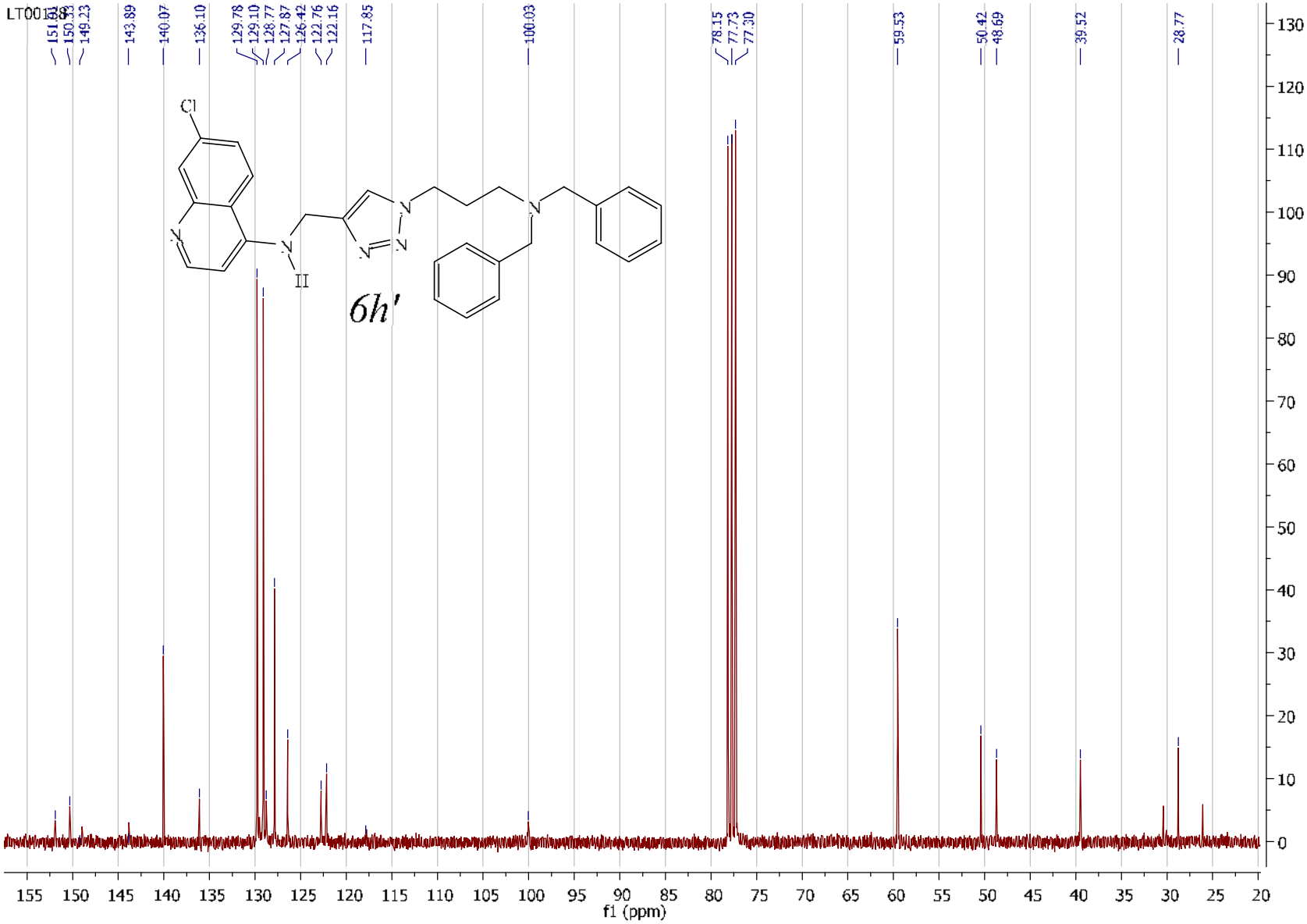
LT00158
151.61
150.83
149.23
143.89
140.07
136.10
129.78
129.10
128.77
127.87
126.42
122.76
122.16
117.85
100.03
78.15
77.73
77.30
59.53
50.42
48.69
39.52
28.77
Cl
II
6h'
f1 (ppm)

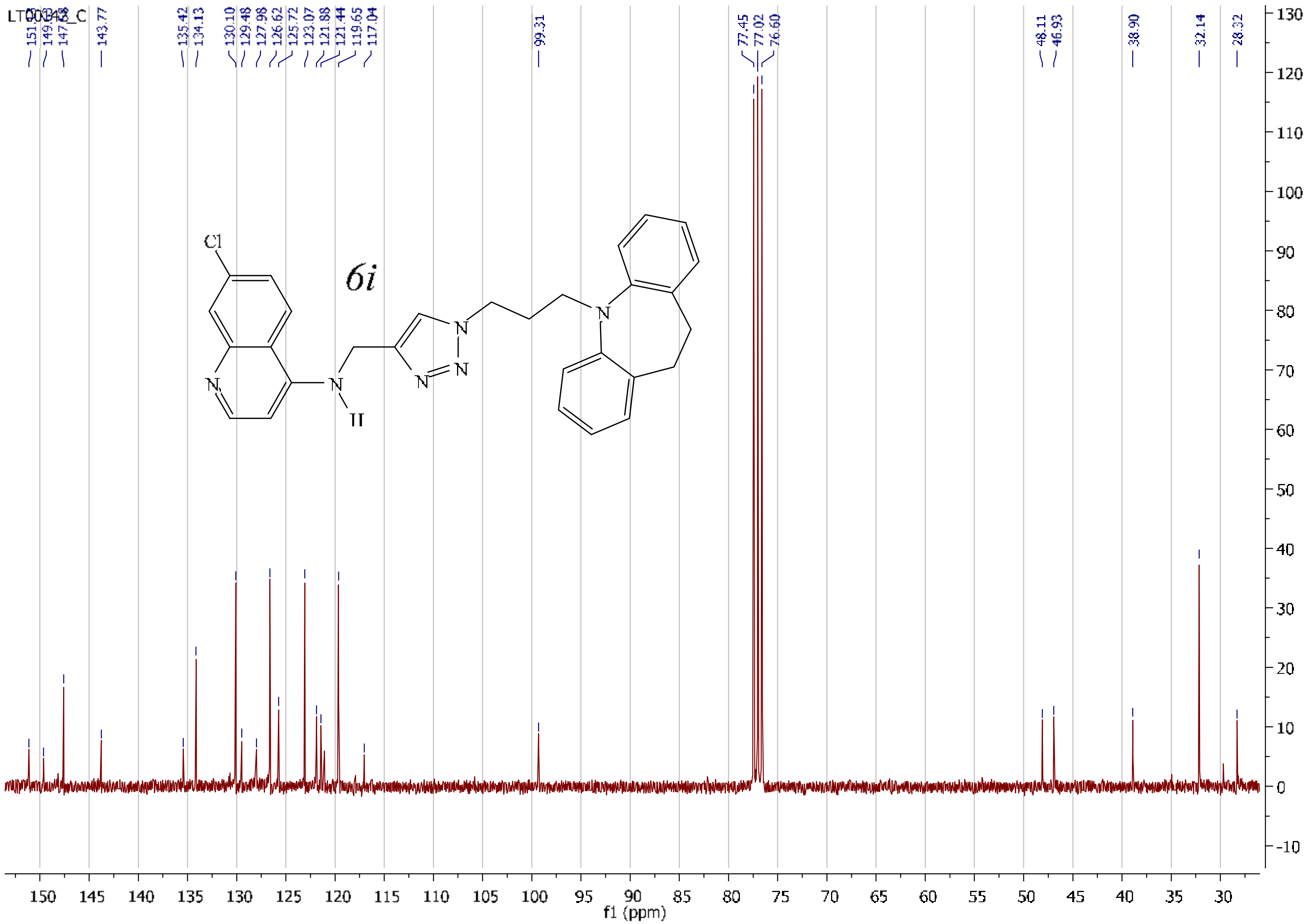
143.77
135.42
134.13
130.10
129.48
127.98
126.62
125.72
123.07
121.88
121.44
119.65
117.04
99.31
77.45
77.02
76.60
48.11
46.93
38.90
32.14
28.32
6i
Cl
N
H
f1 (ppm)

$^{1}H–^{1}H$ Homonuclear correlations

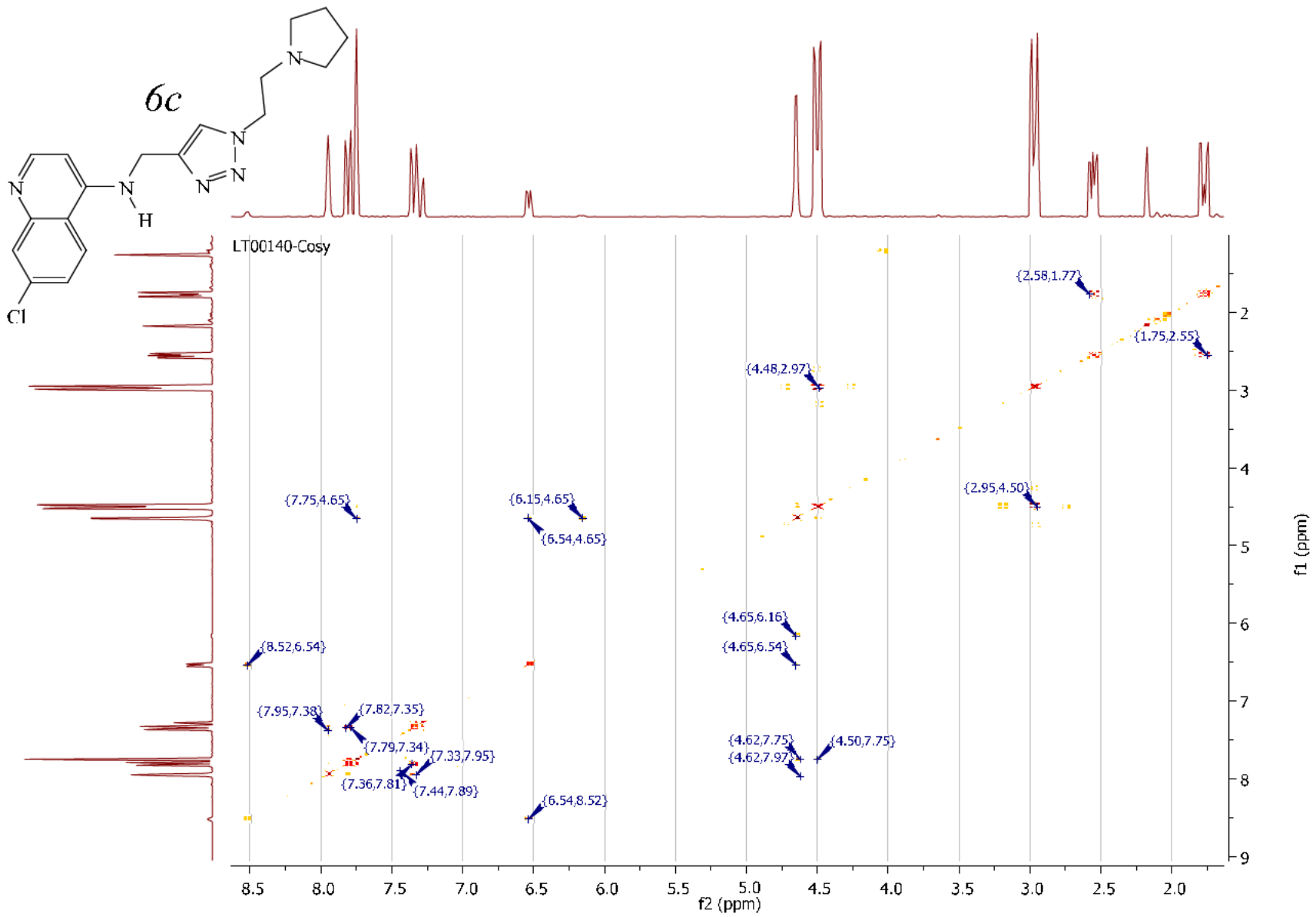
6c
LT00140-Cosy
{2.58,1.77}
{1.75,2.55}
{4.48,2.97}
{2.95,4.50}
{7.75,4.65}
{6.15,4.65}
{6.54,4.65}
{4.65,6.16}
{4.65,6.54}
{8.52,6.54}
{7.95,7.38}
{7.82,7.35}
{7.79,7.34}
{7.33,7.95}
{7.36,7.81}
{7.44,7.89}
{4.62,7.75}
{4.62,7.97}
{4.50,7.75}
{6.54,8.52}
f2 (ppm)
f1 (ppm)

$^{1}H–^{13}C$ Heteronuclear correlations

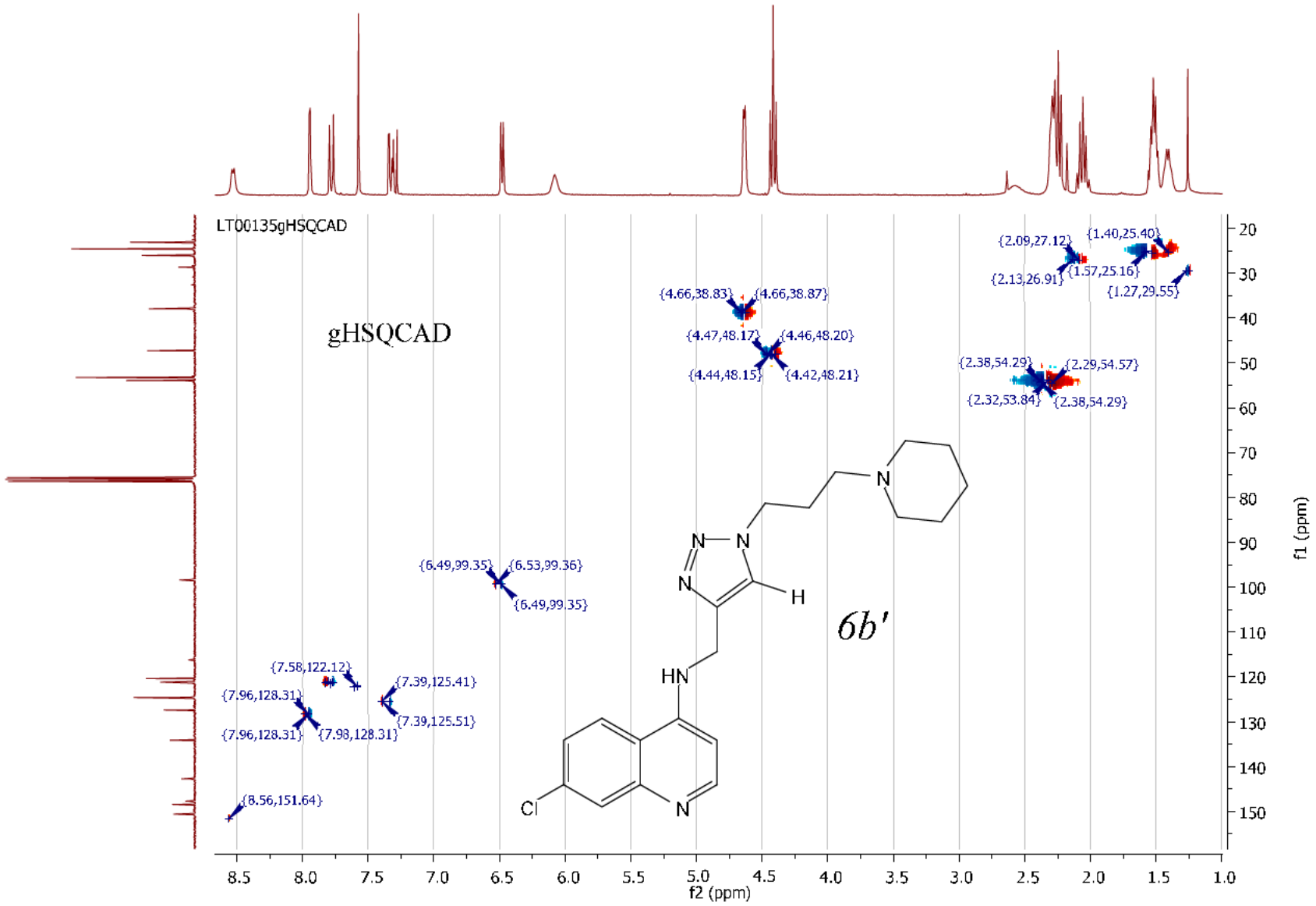
LT00135gHSQCAD
gHSQCAD
{4.66,38.83}
{4.66,38.87}
{4.47,48.17}
{4.46,48.20}
{4.44,48.15}
{4.42,48.21}
{2.09,27.12}
{1.40,25.40}
{2.13,26.91}
{1.57,25.16}
{1.27,29.55}
{2.38,54.29}
{2.29,54.57}
{2.32,53.84}
{2.38,54.29}
{6.49,99.35}
{6.53,99.36}
{6.49,99.35}
{7.58,122.12}
{7.96,128.31}
{7.39,125.41}
{7.39,125.51}
{7.96,128.31}
{7.98,128.31}
{8.56,151.64}
6b'
f2 (ppm)
f1 (ppm)

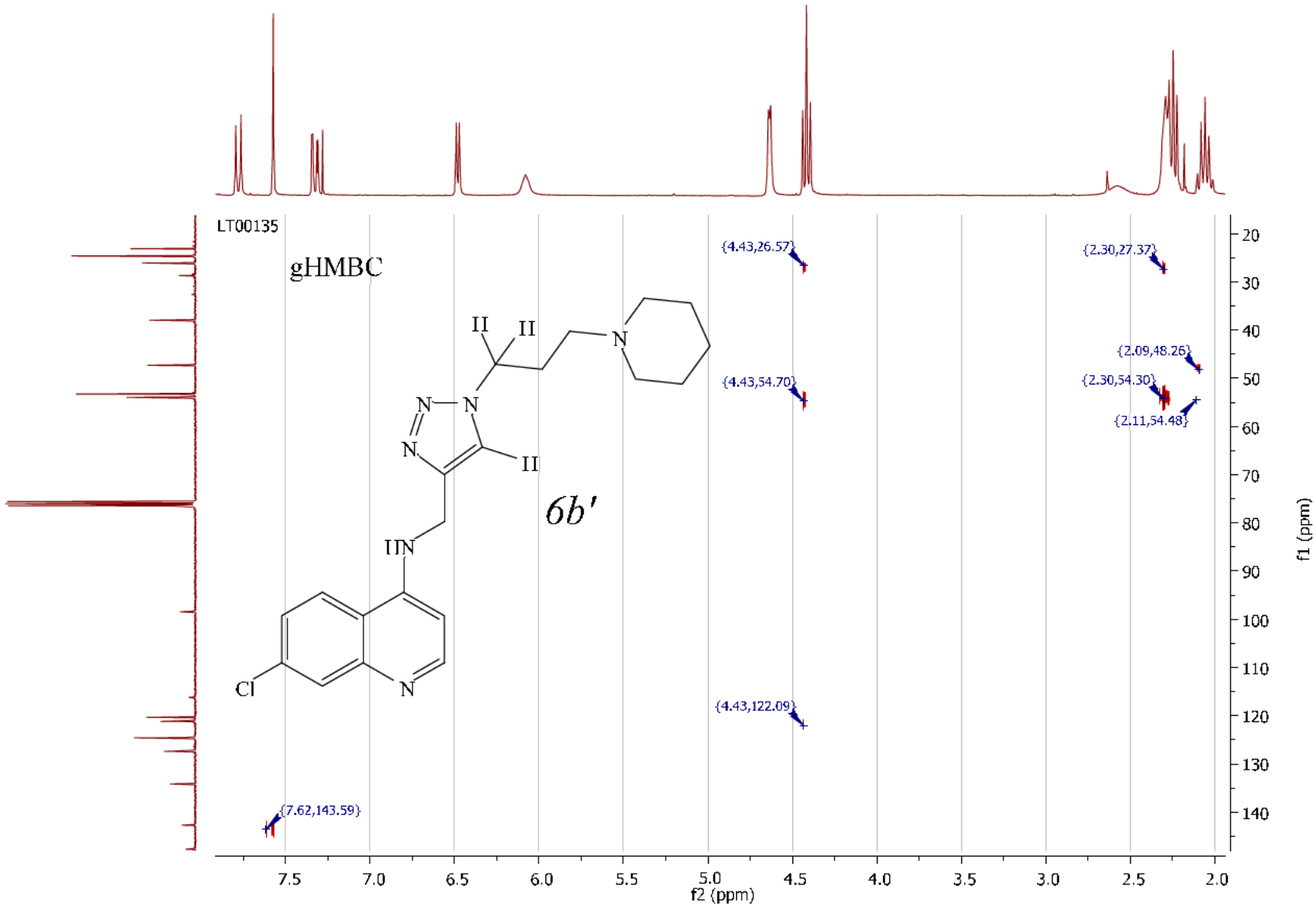
LT00135
gHMBC
6b'
{4.43,26.57}
{2.30,27.37}
{2.09,48.26}
{4.43,54.70}
{2.30,54.30}
{2.11,54.48}
{4.43,122.09}
{7.62,143.59}
f2 (ppm)
f1 (ppm)

(ESI^+) HR MS spectra

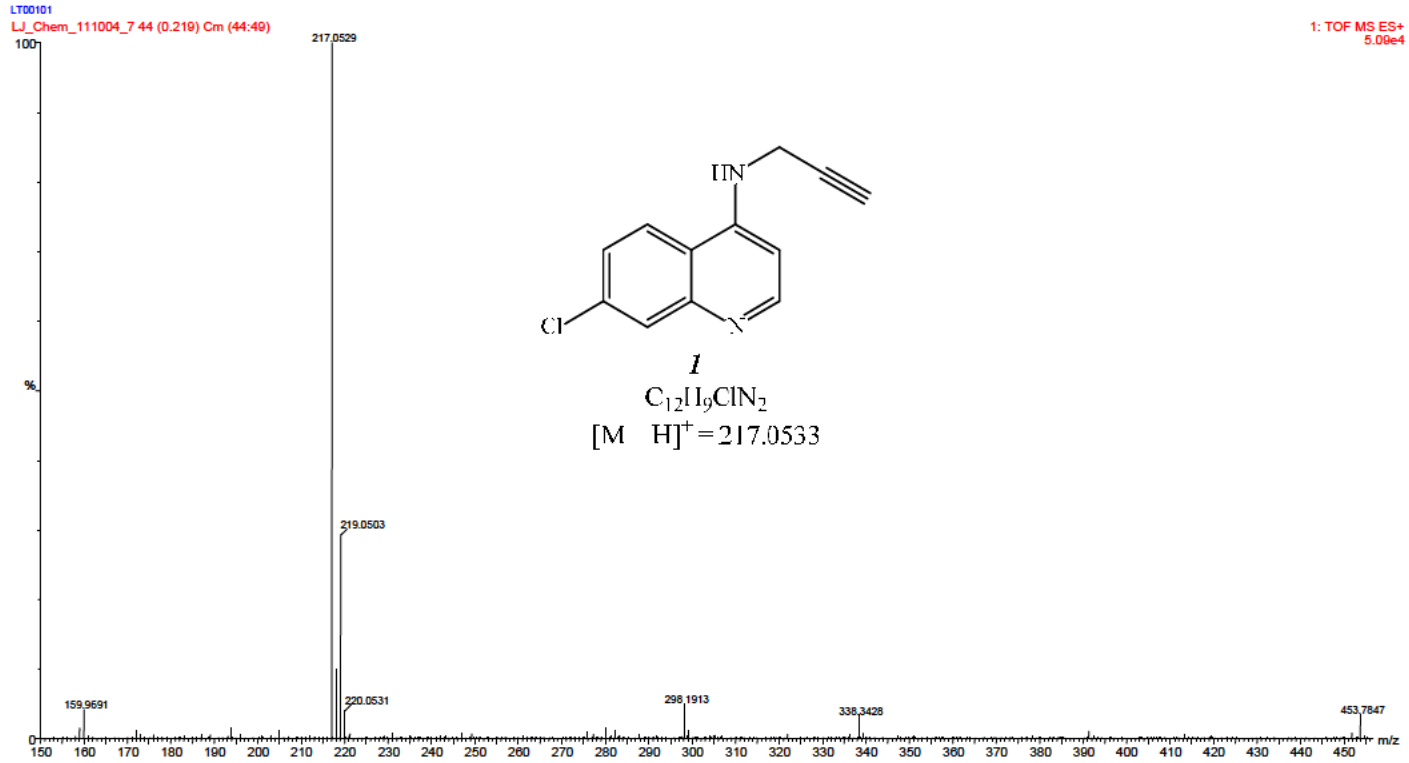

1

$C_{12}H_9ClN_2$

$[M \quad H]^+ = 217.0533$

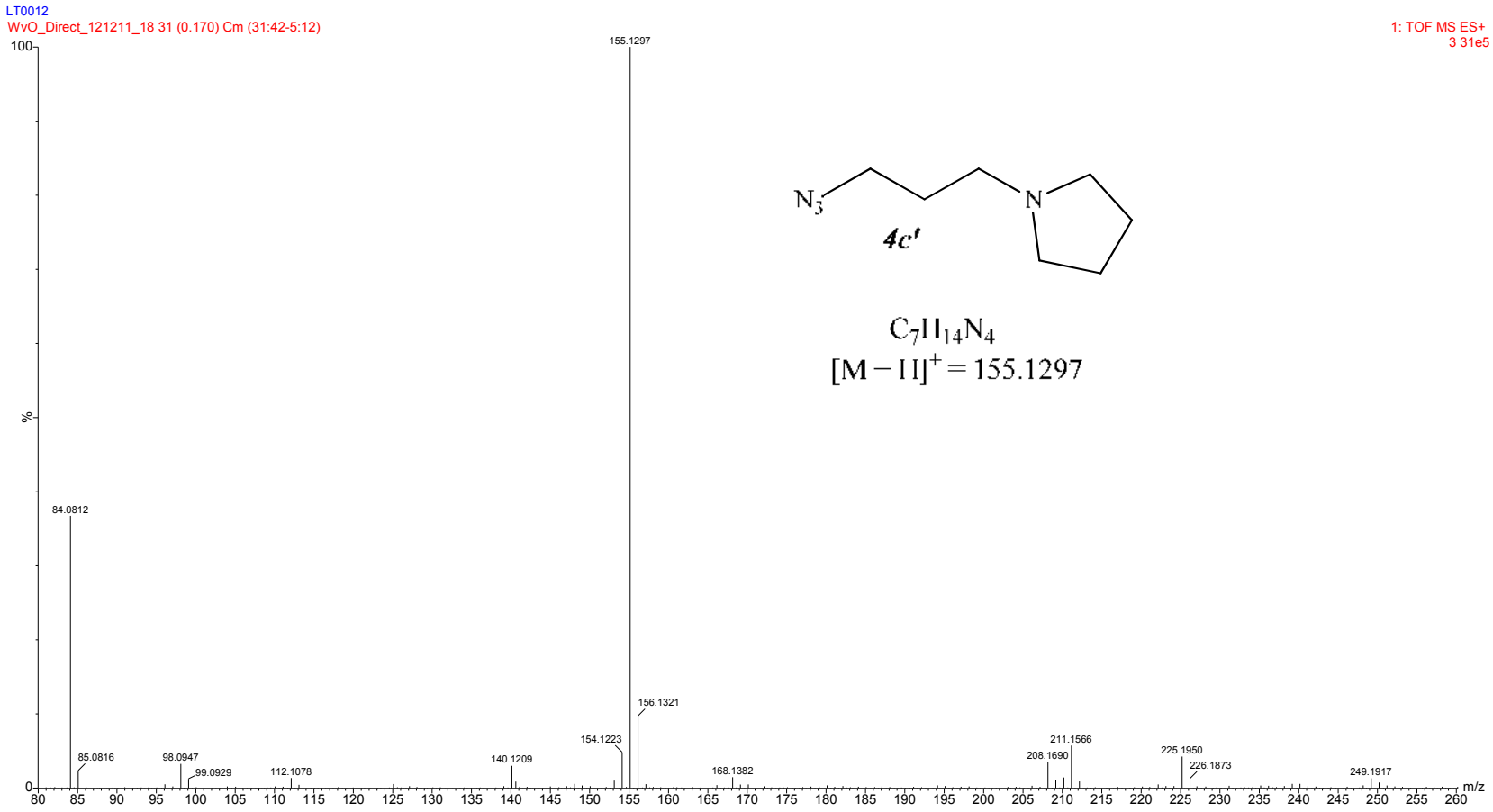

4c'

$C_7H_{14}N_4$

$[M-H]^+ = 155.1297$

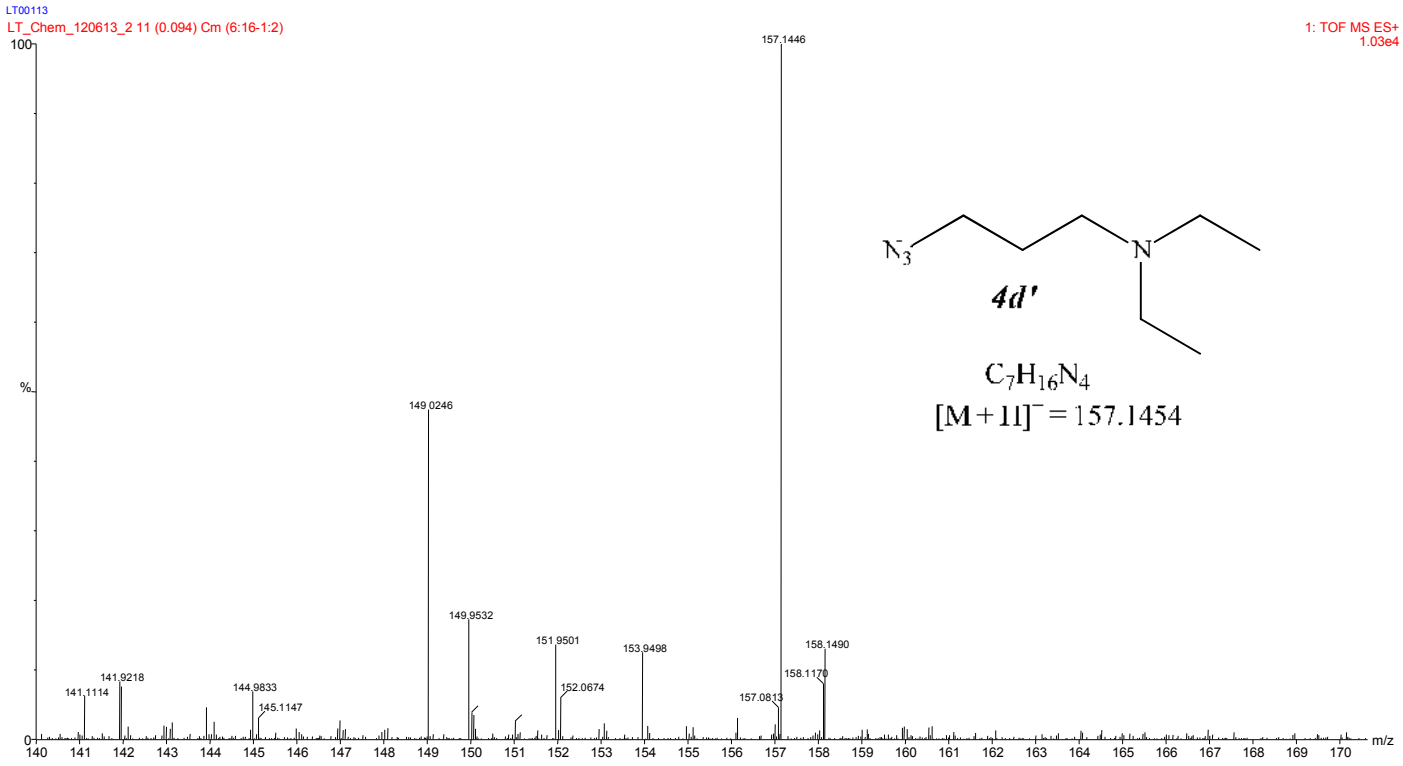
LT00113
LT_Chem_120613_2 11 (0.094) Cm (6:16-1:2)
1: TOF MS ES+
1.03e4
100
%
0
157.1446
149.0246
149.9532
151.9501
153.9498
158.1490
158.1170
141.9218
141.1114
144.9833
145.1147
152.0674
157.0813
m/z
140 141 142 143 144 145 146 147 148 149 150 151 152 153 154 155 156 157 158 159 160 161 162 163 164 165 166 167 168 169 170
N3
N
4d'
C7H16N4
[M+1]+ = 157.1454

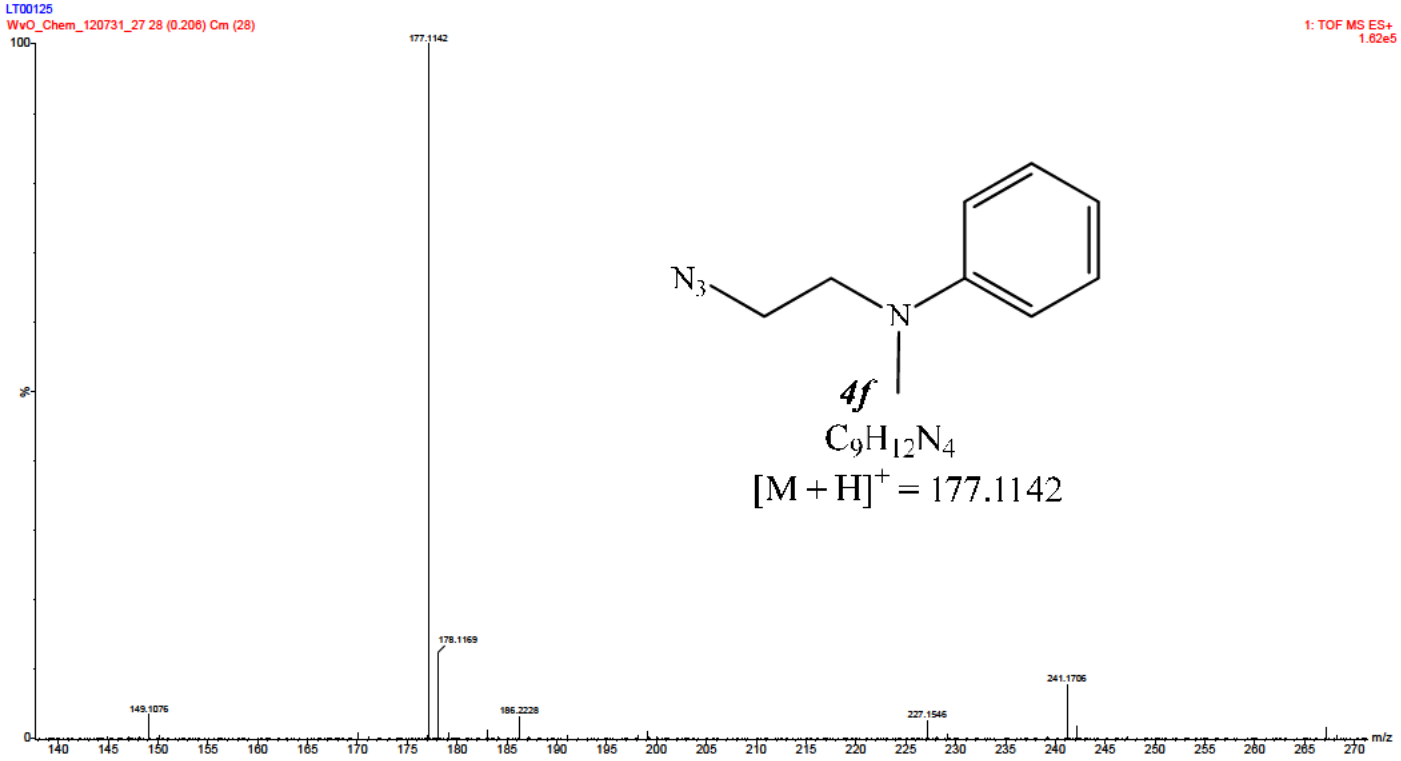

4f

$C_9H_{12}N_4$

$[M+H]^+ = 177.1142$

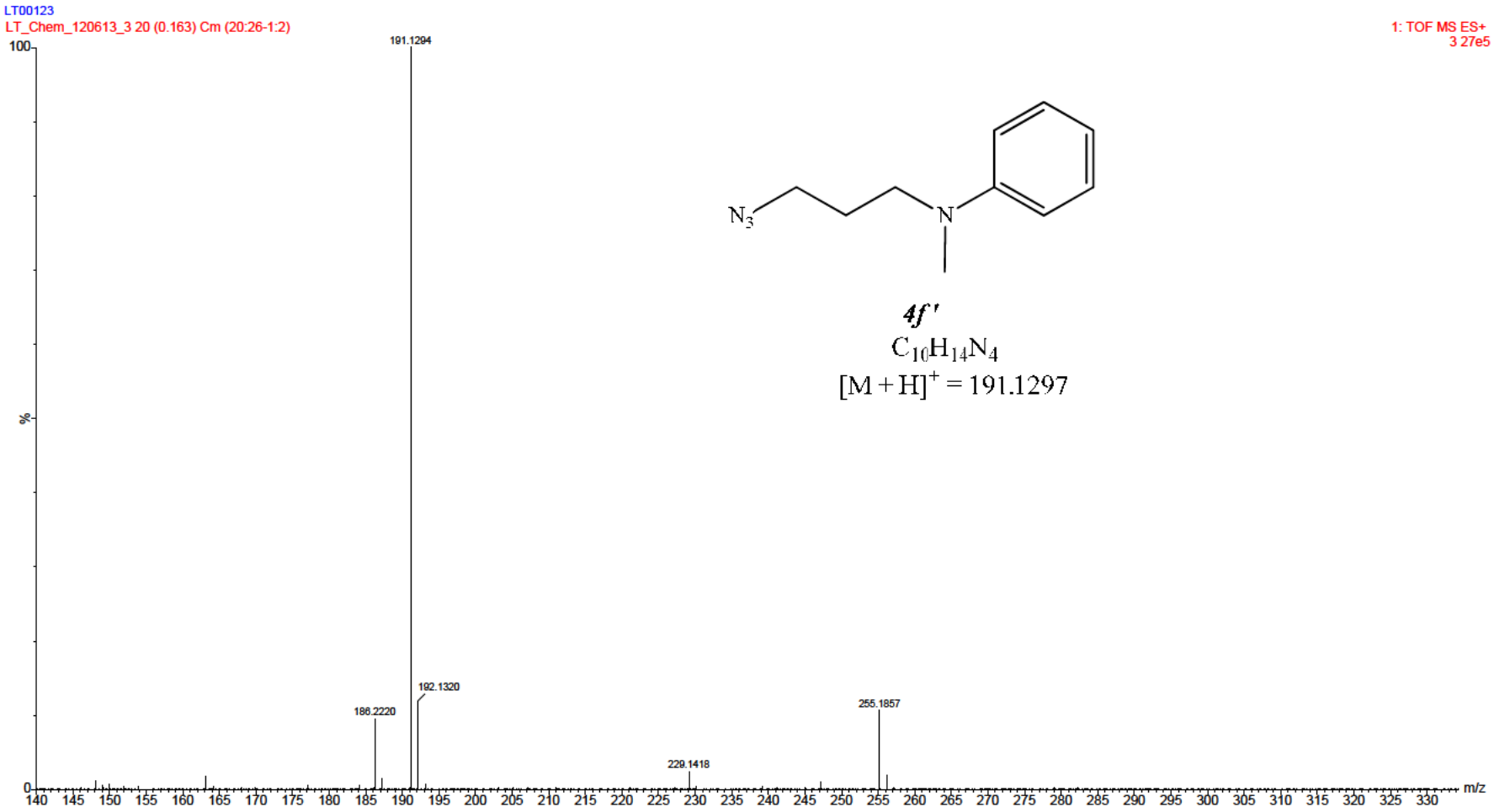

4f'

$C_{10}H_{14}N_4$

$[M+H]^+ = 191.1297$

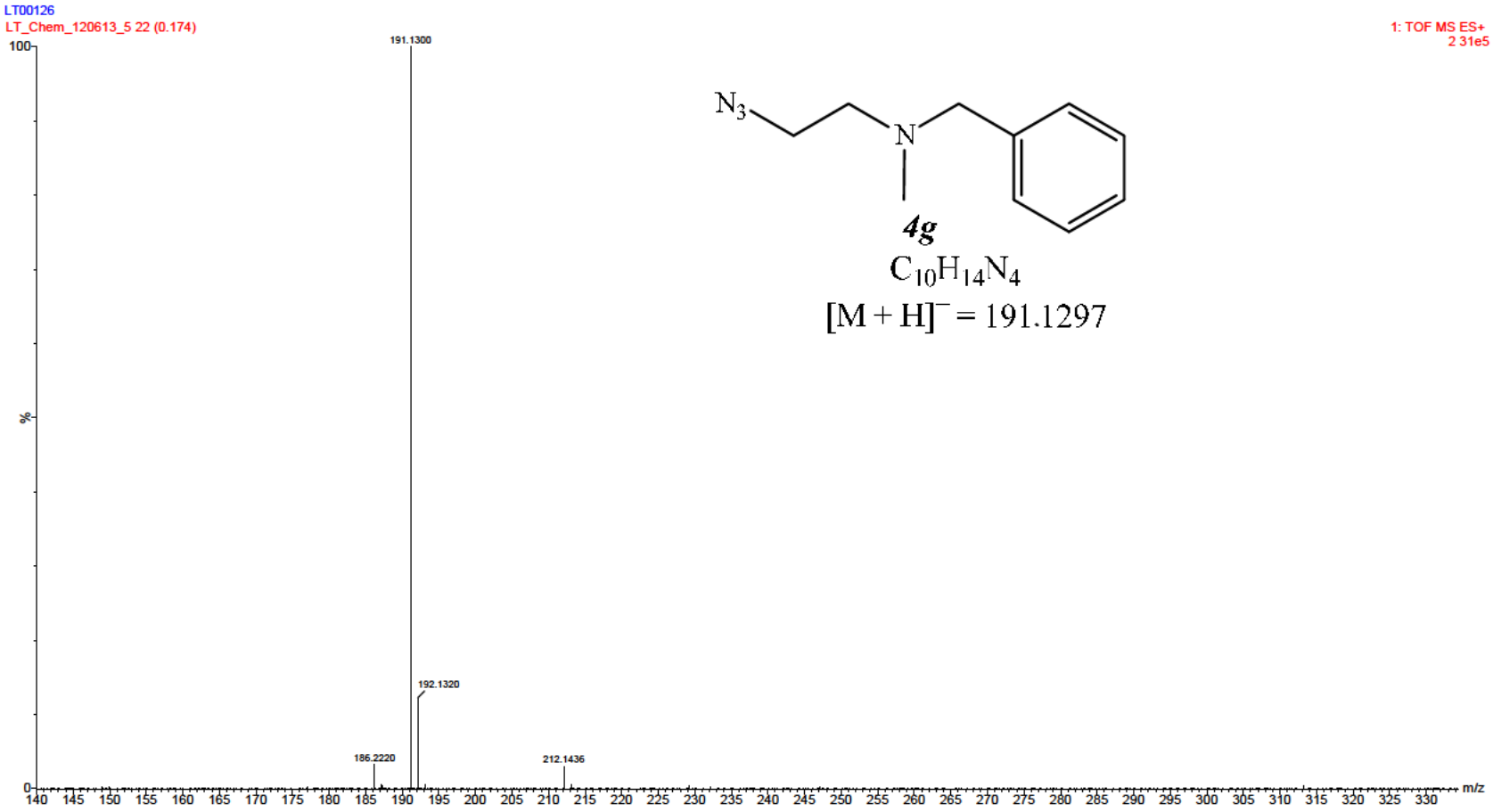

4g

$C_{10}H_{14}N_4$

$[M+H]^- = 191.1297$

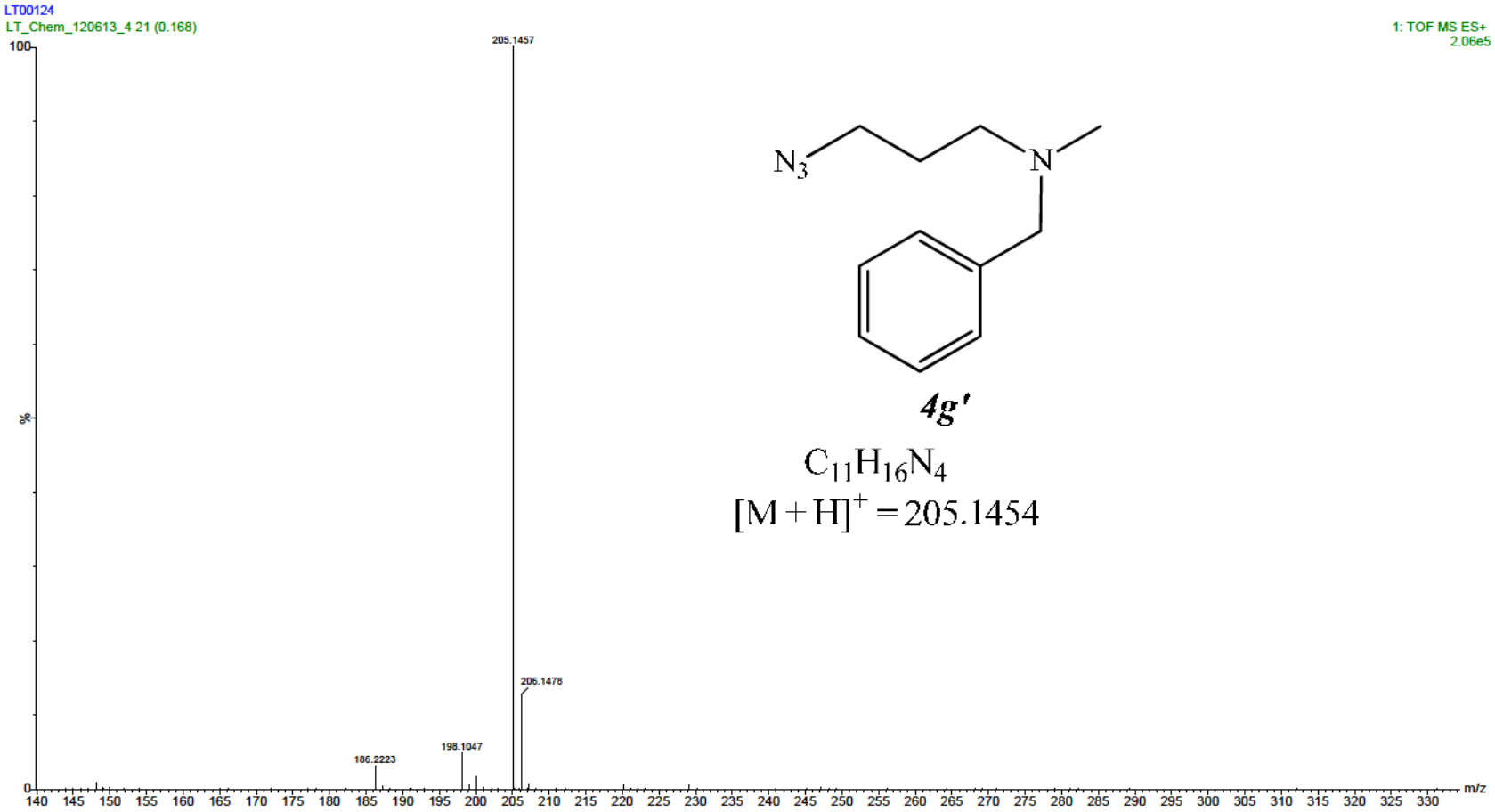

4g'

$C_{11}H_{16}N_4$

$[M+H]^+ = 205.1454$

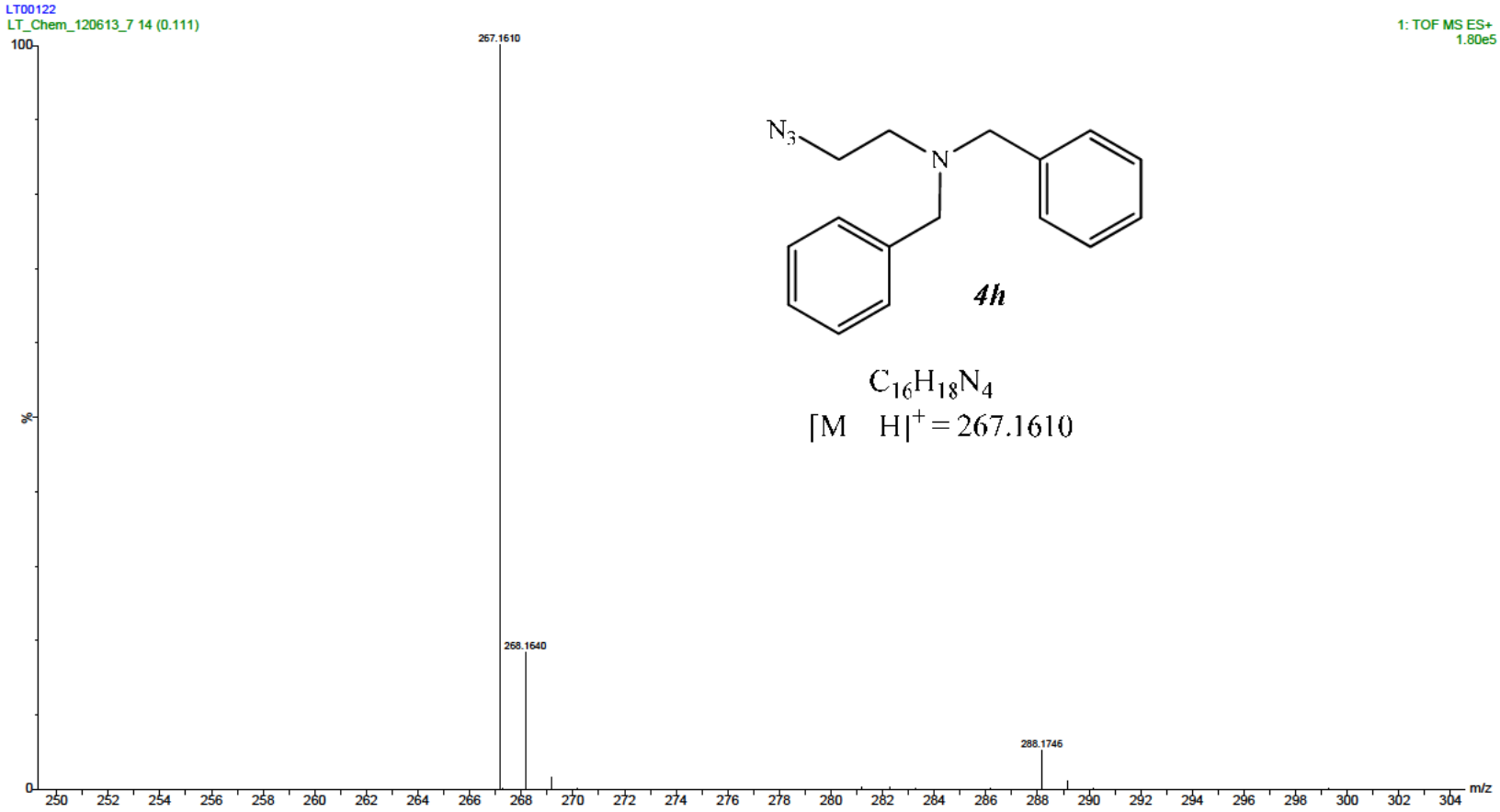

4h

$C_{16}H_{18}N_4$

$[M \quad H]^+ = 267.1610$

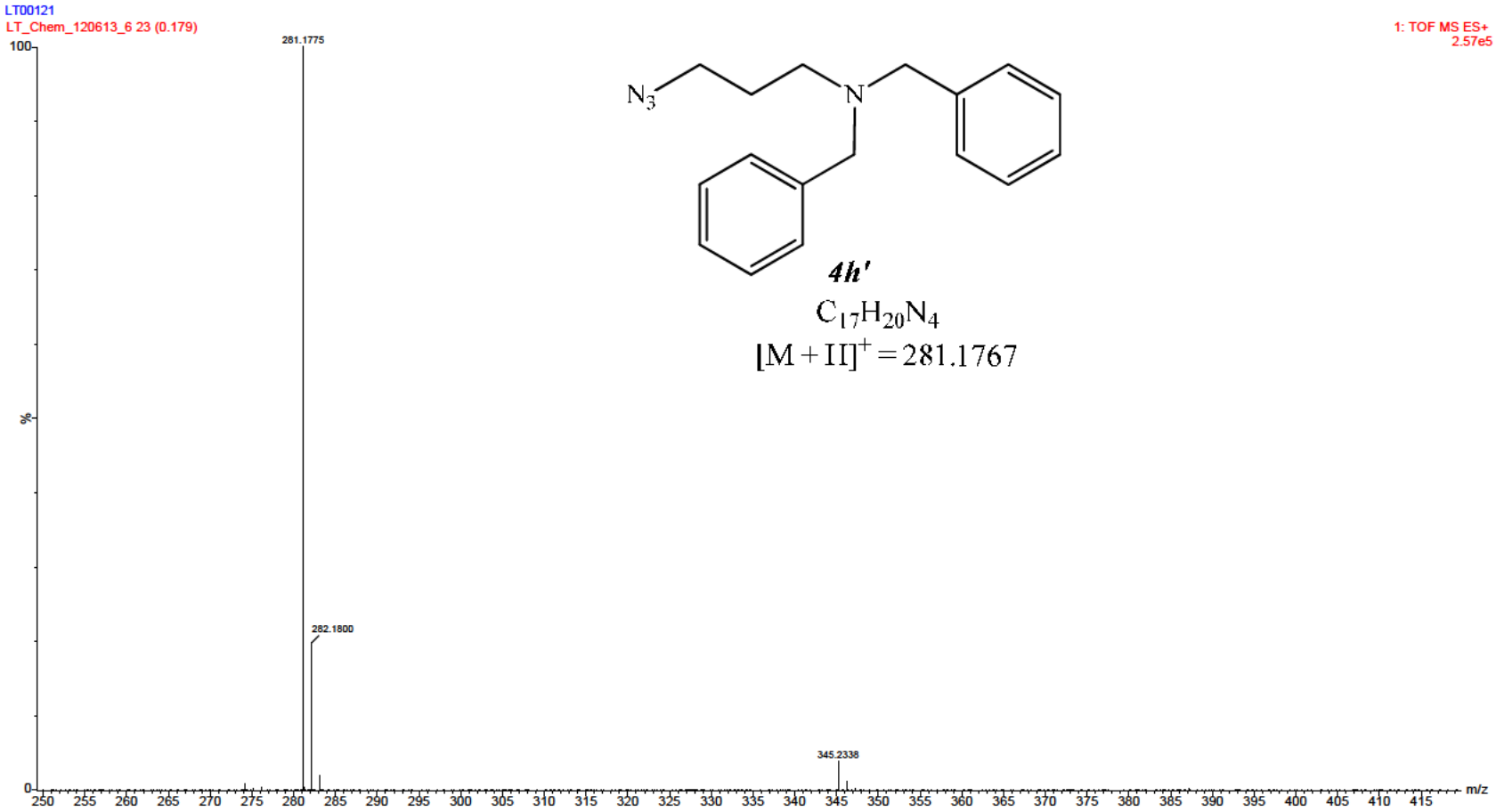

4h'

$C_{17}H_{20}N_4$

$[M+H]^+ = 281.1767$

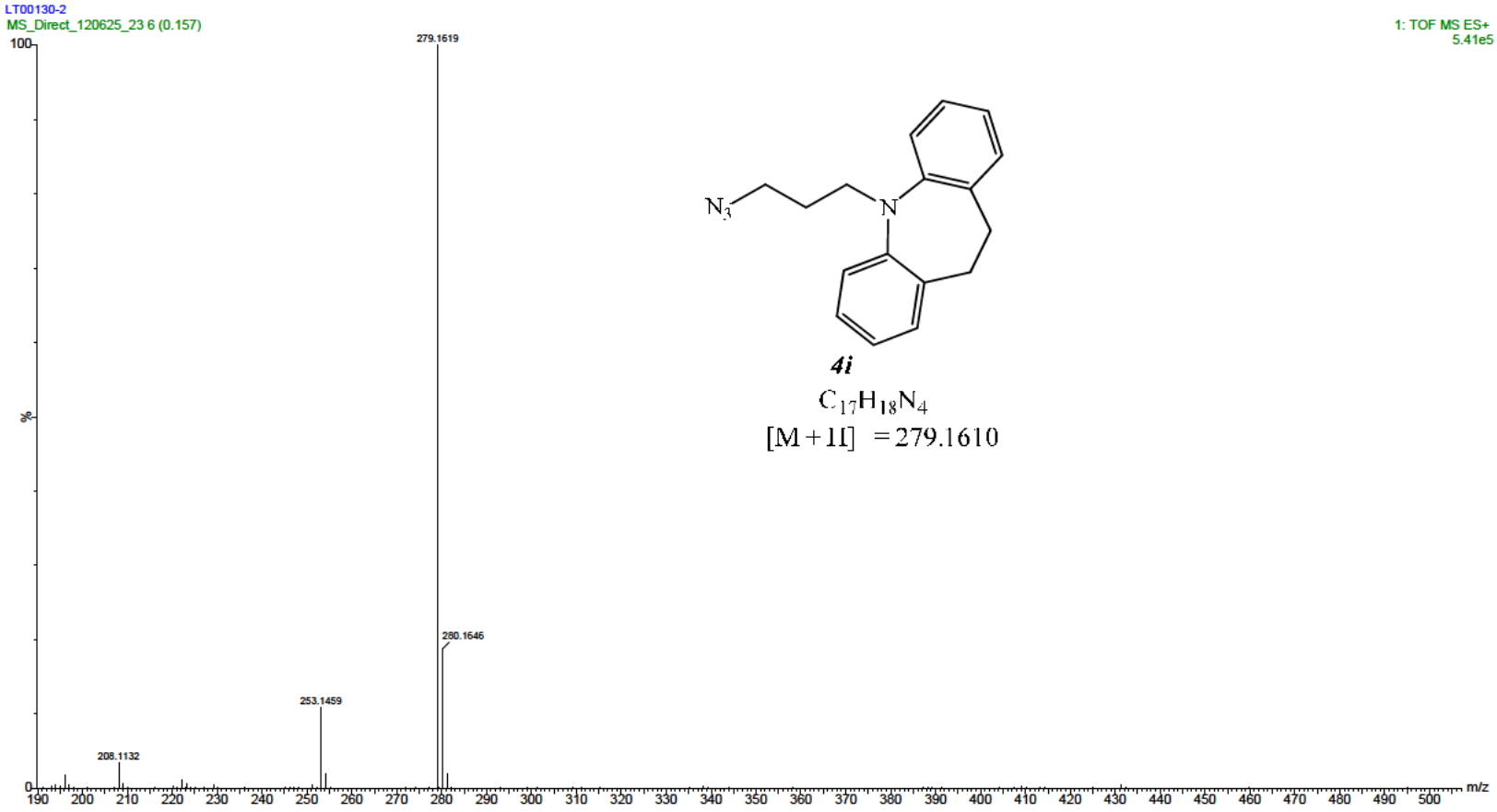

4i

$C_{17}H_{18}N_4$

$[M+1]^+ = 279.1610$

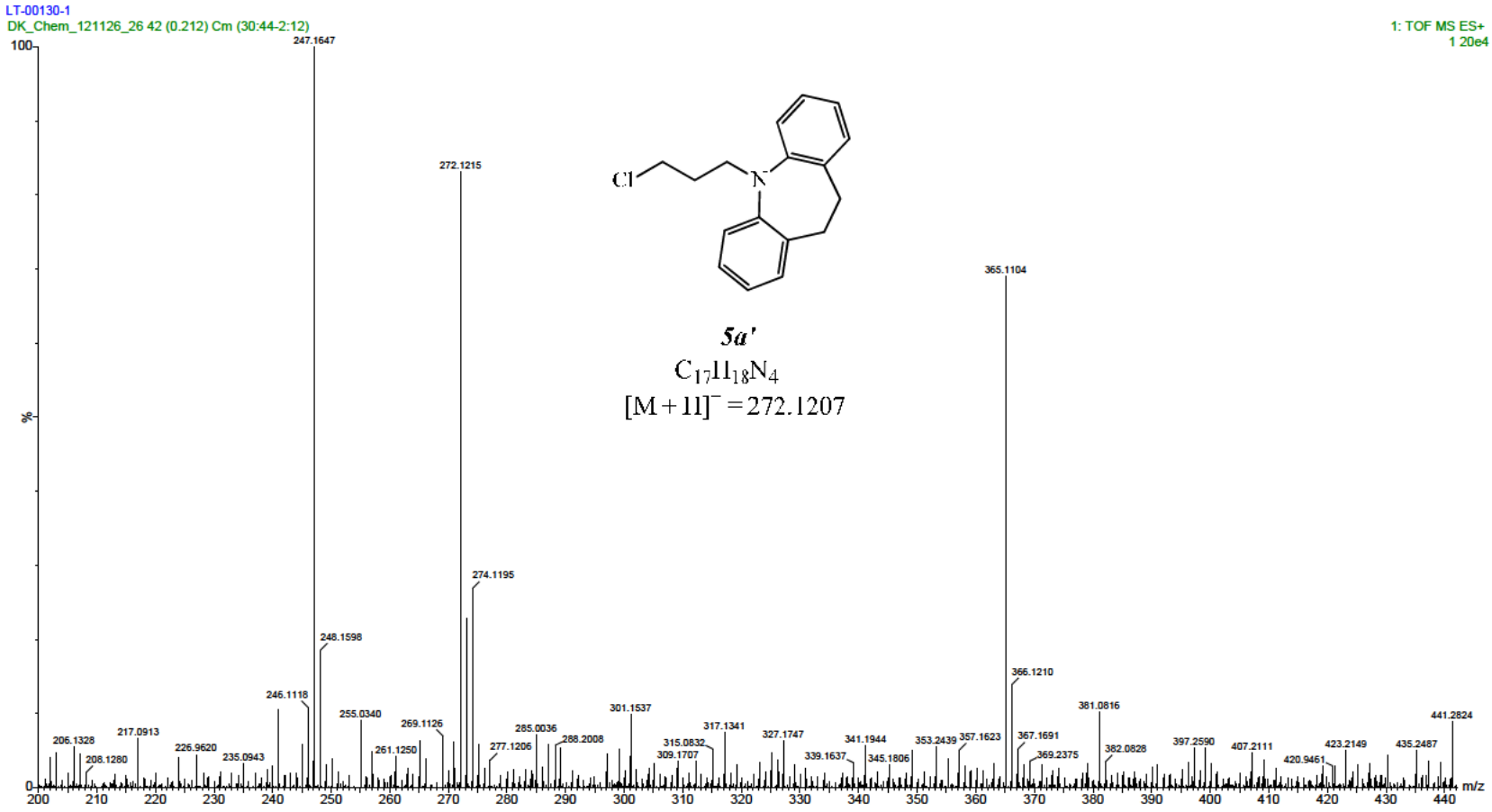
LT-00130-1
DK_Chem_121126_26 42 (0.212) Cm (30:44-2:12)
1: TOF MS ES+
1 20e4
100
%
0
247.1647
272.1215
274.1195
248.1598
246.1118
255.0340
269.1126
365.1104
366.1210
381.0816
441.2824
206.1328
208.1280
217.0913
226.9620
235.0943
261.1250
277.1206
285.0036
288.2008
301.1537
309.1707
315.0832
317.1341
327.1747
339.1637
341.1944
345.1806
353.2439
357.1623
367.1691
369.2375
382.0828
397.2590
407.2111
420.9461
423.2149
435.2487
200
210
220
230
240
250
260
270
280
290
300
310
320
330
340
350
360
370
380
390
400
410
420
430
440
m/z
Cl
N
5a'
C17H18N4
[M+H]+ = 272.1207

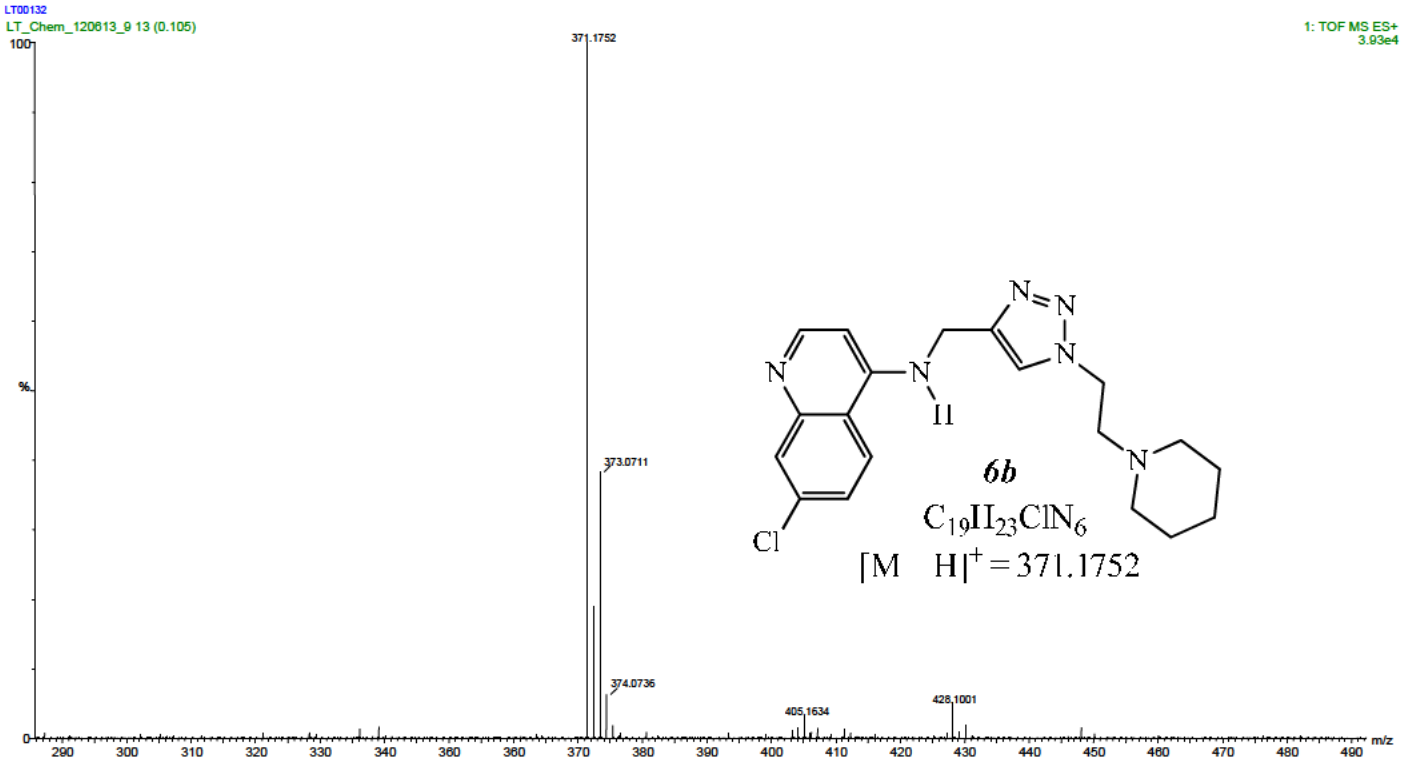
LT00132
LT_Chem_120613_9 13 (0.105)
1: TOF MS ES+
3.93e4
100
%
0
371.1752
373.0711
374.0736
405.1634
428.1001
290 300 310 320 330 340 360 380 370 380 390 400 410 420 430 440 450 460 470 480 490
m/z
N
N
N
N
N
H
Cl
6b
C19H23ClN6
[M H]+ = 371.1752

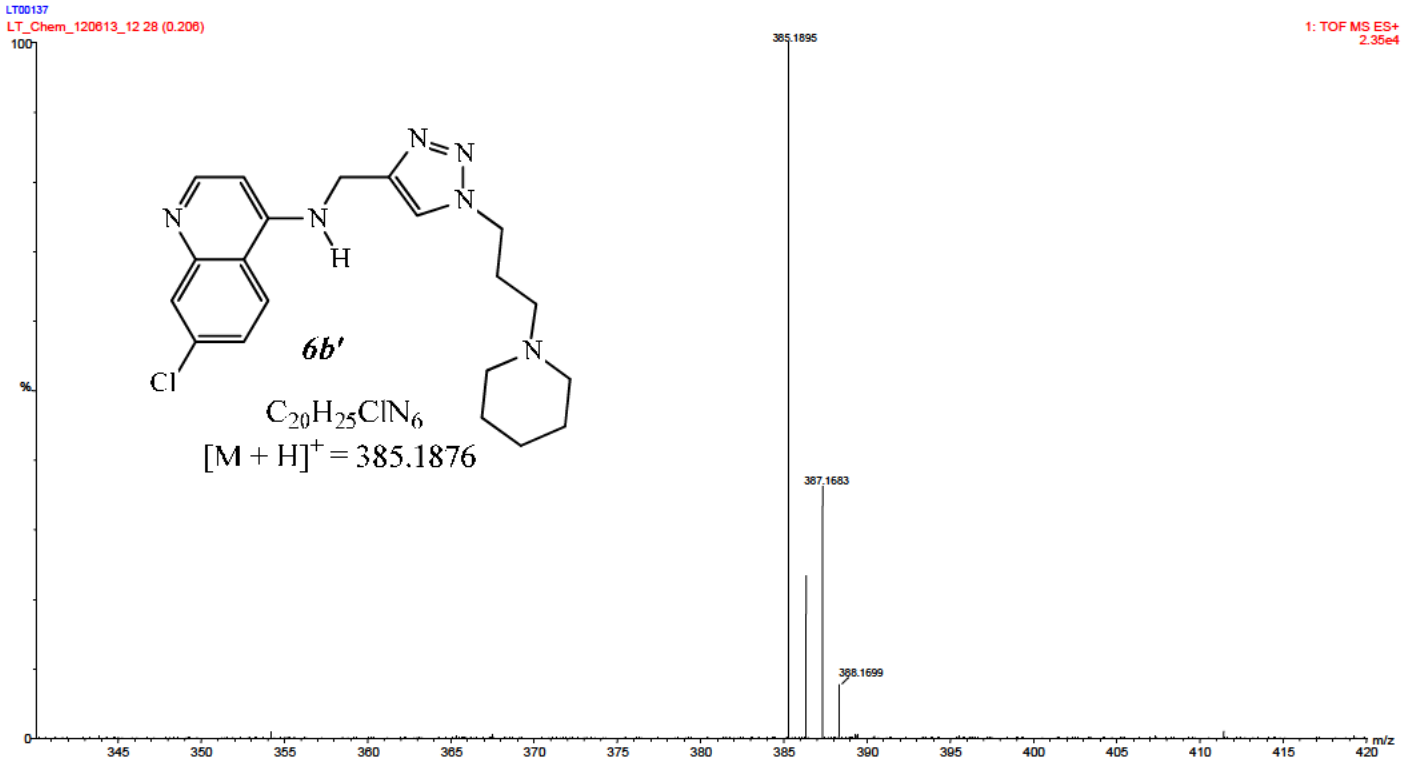
LT00137
LT_Chem_120613_12 28 (0.206)
1: TOF MS ES+
2.35e4
385.1895
387.1683
388.1699
100
%
0
345
350
355
360
365
370
375
380
385
390
395
400
405
410
415
420
m/z
N
N
N
N
H
N
Cl
6b'
$C_{20}H_{25}ClN_6$
$[M + H]^+ = 385.1876$

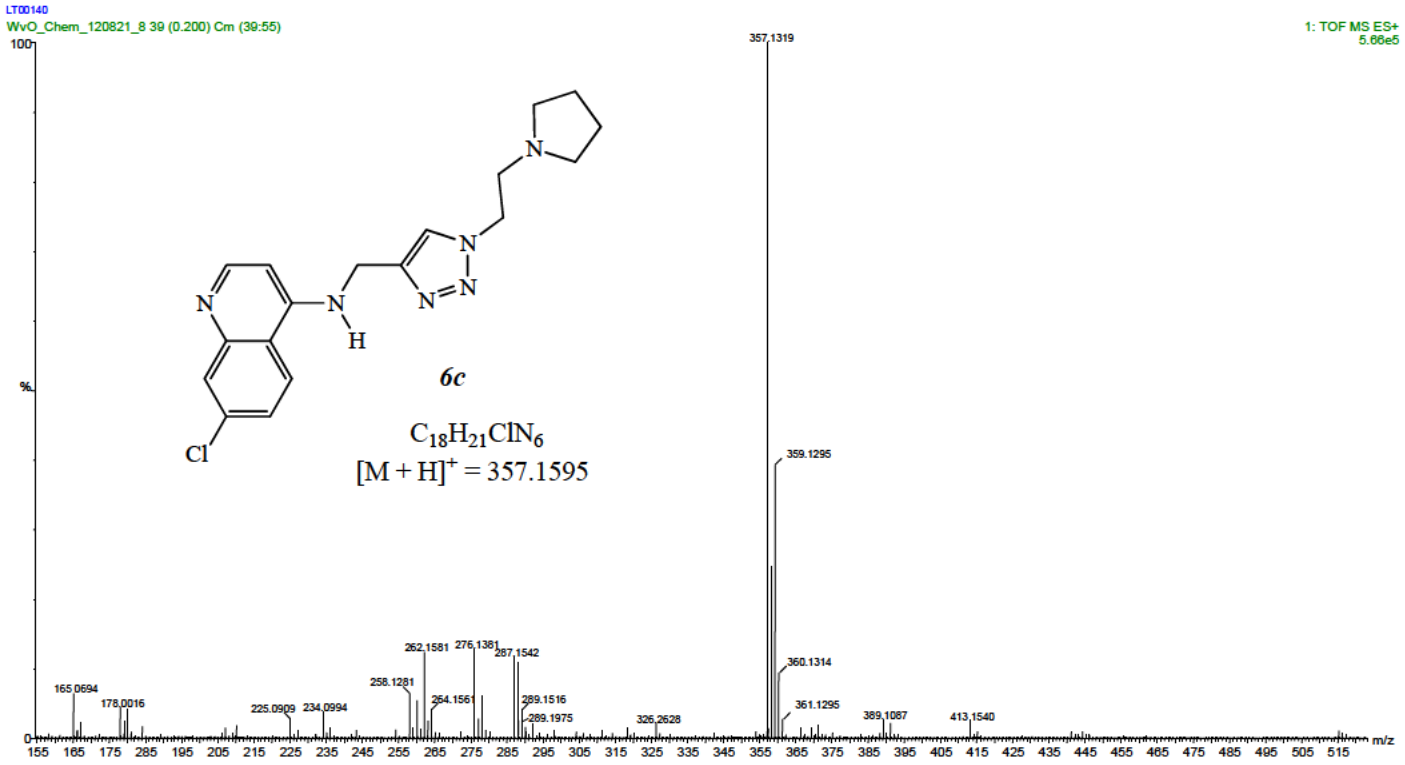
LT00140
WvO_Chem_120821_8 39 (0.200) Cm (39:55)
1: TOF MS ES+
5.66e5
100
%
0
357.1319
359.1295
360.1314
361.1295
389.1087
413.1540
262.1581
276.1381
287.1542
258.1281
264.1561
289.1516
289.1975
326.2628
165.0694
178.0016
225.0909
234.0994
m/z
155 165 175 285 195 205 215 225 235 245 255 265 275 285 295 305 315 325 335 345 355 365 375 385 395 405 415 425 435 445 455 465 475 485 495 505 515
N
N
N
N
N
H
Cl
6c
C18H21ClN6
[M + H]+ = 357.1595

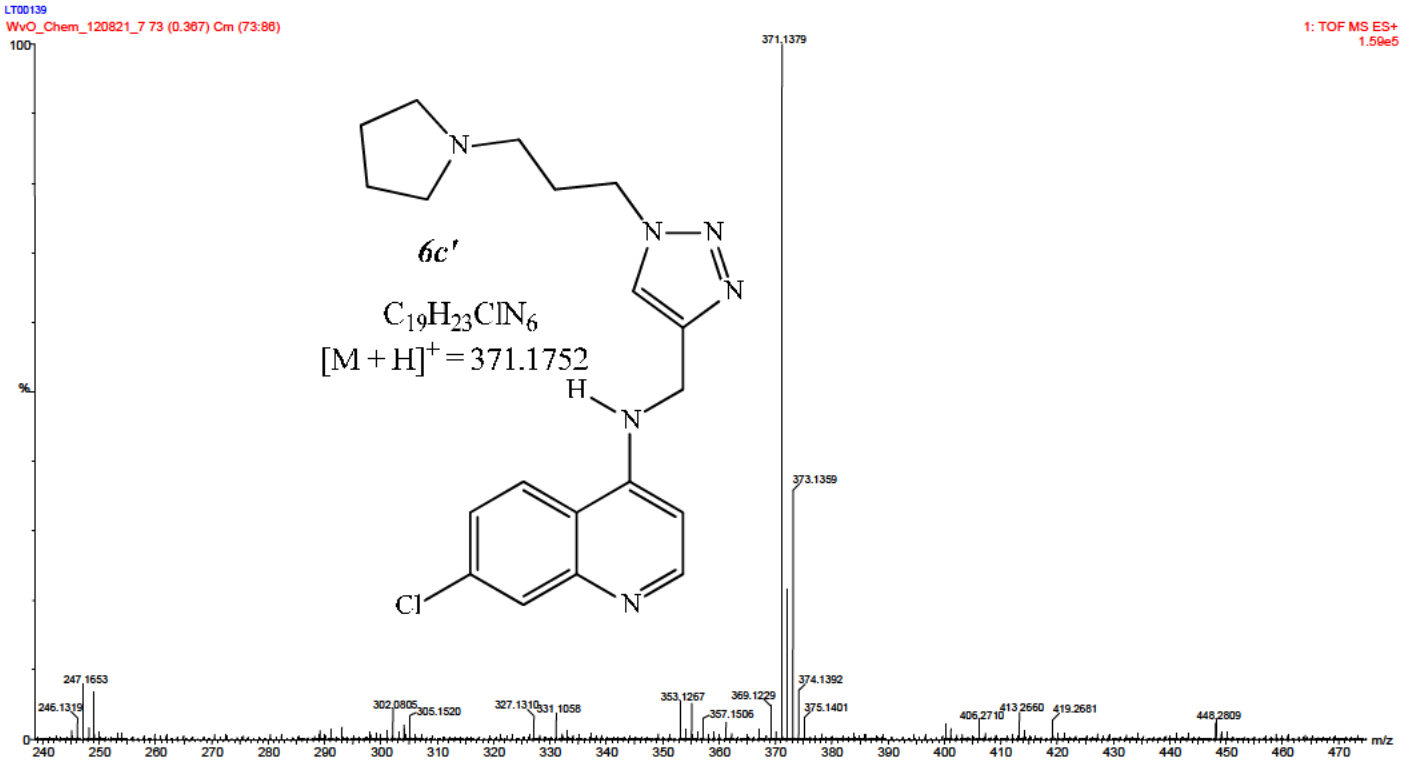
LT00139
WvO_Chem_120821_7 73 (0.367) Cm (73:86)
1: TOF MS ES+
1.59e5
100
%
0
371.1379
373.1359
374.1392
247.1653
246.1319
302.0805
305.1520
327.1310
331.1058
353.1267
357.1506
369.1229
375.1401
406.2710
413.2660
419.2681
448.2809
m/z
240 250 260 270 280 290 300 310 320 330 340 350 360 370 380 390 400 410 420 430 440 450 460 470
6c'
$C_{19}H_{23}ClN_6$
$[M+H]^+ = 371.1752$
N
N
N
N
H
N
Cl
N

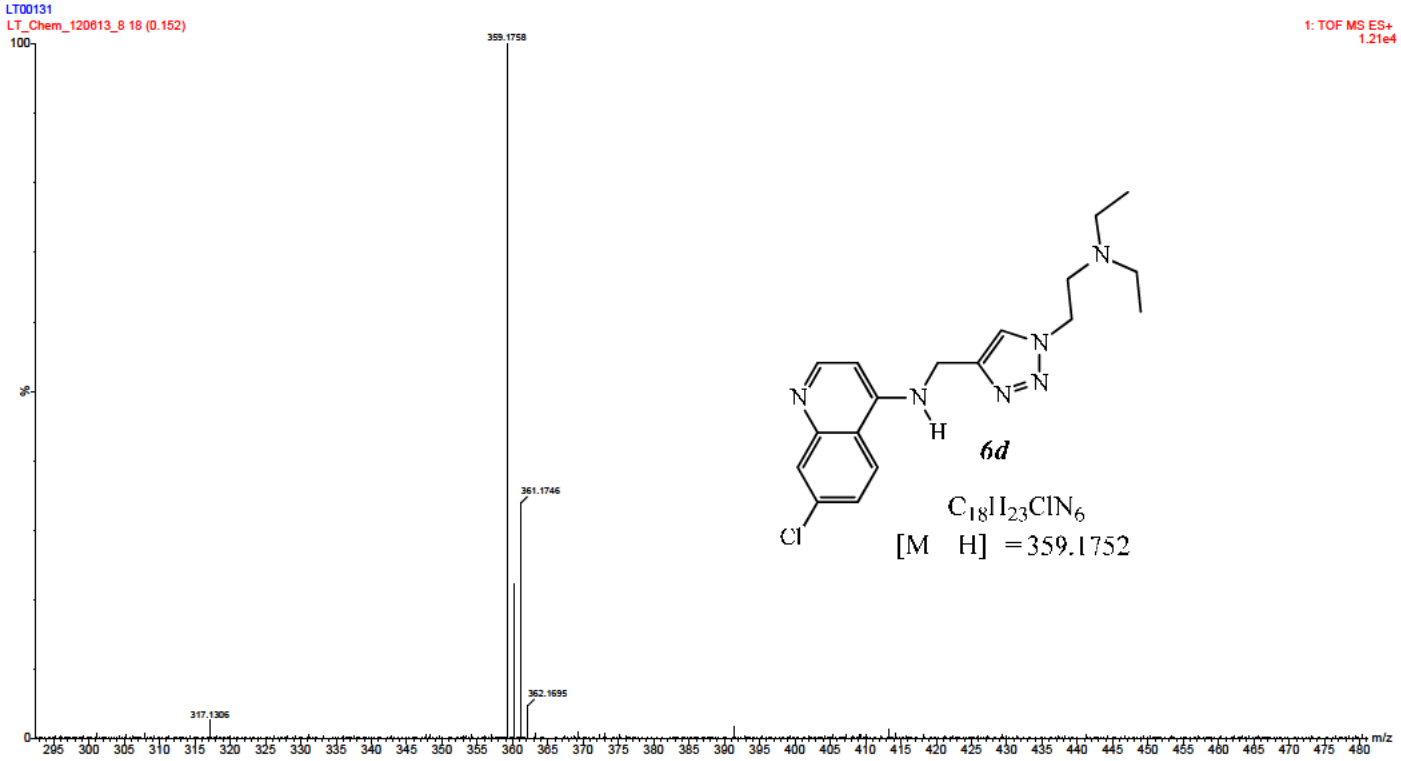
LT00131
LT_Chem_120613_8 18 (0.152)
1: TOF MS ES+
1.21e4
100
%
0
359.1758
361.1746
362.1695
317.1306
295 300 305 310 315 320 325 330 335 340 345 350 355 360 365 370 375 380 385 390 395 400 405 410 415 420 425 430 435 440 445 450 455 460 465 470 475 480
m/z
N
N
H
N
N
N
N
Cl
6d
C18H23ClN6
[M H] =359.1752

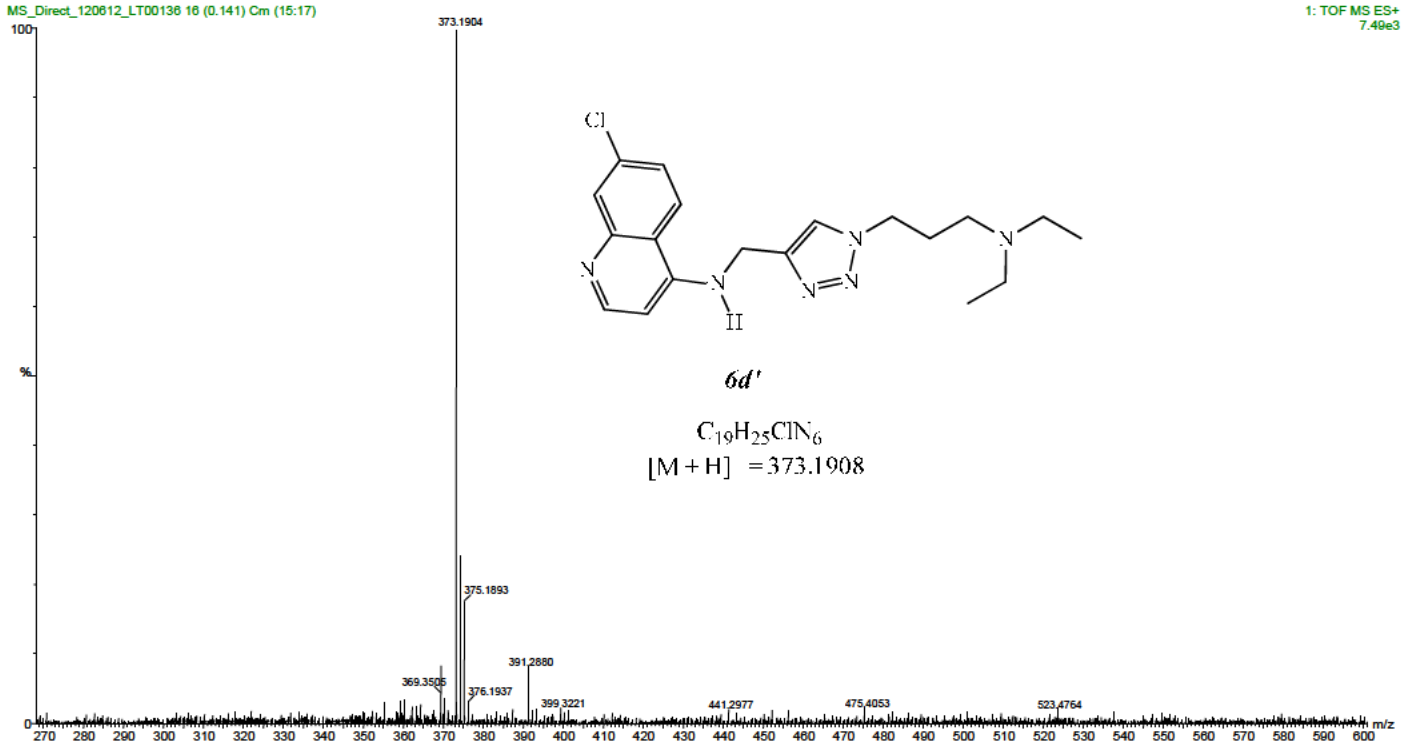

6d'

$C_{19}H_{25}ClN_6$

$[M+H]^+ = 373.1908$

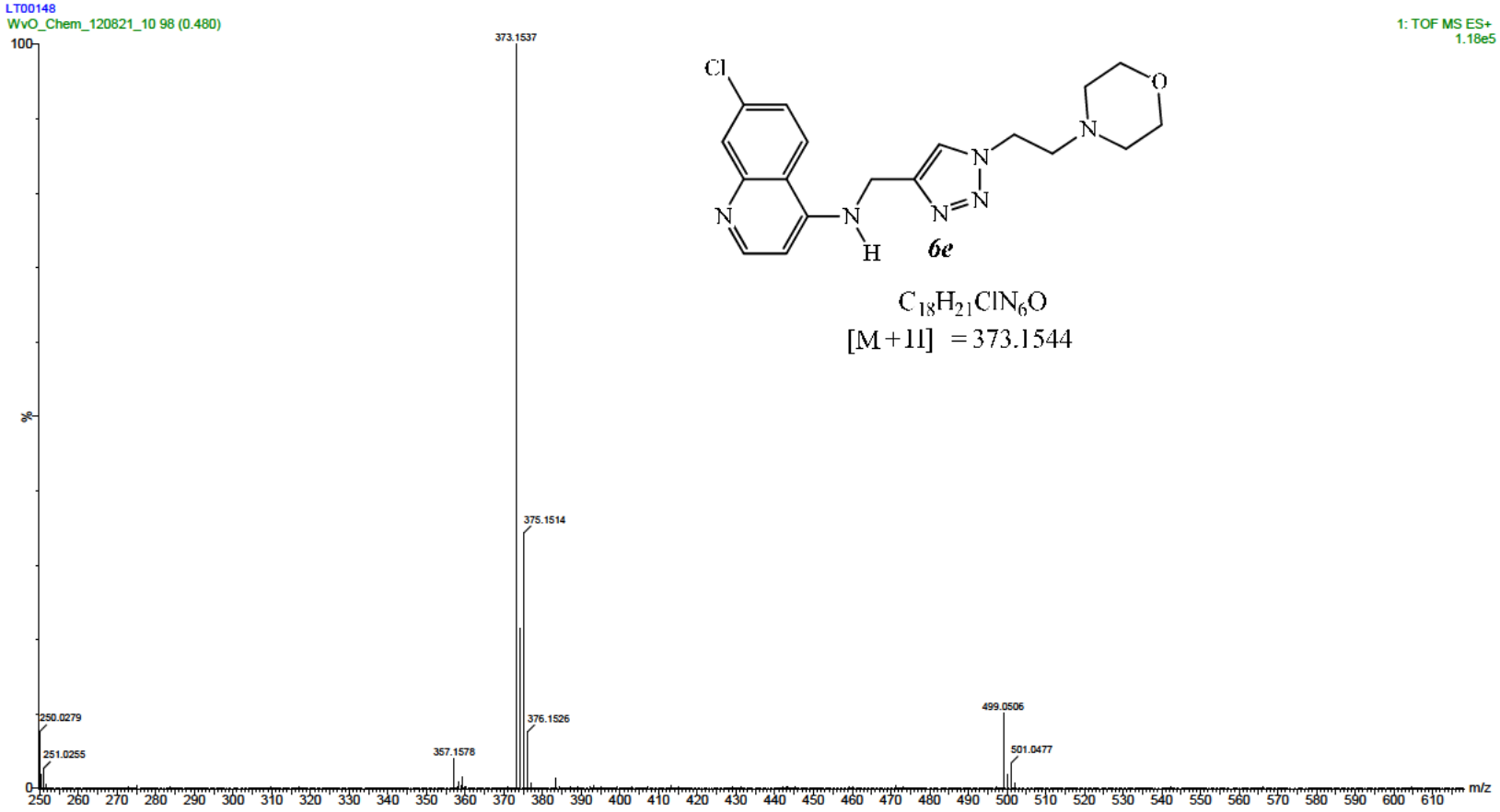
LT00148
WvO_Chem_120821_10 98 (0.480)
1: TOF MS ES+
1.18e5
100
%
0
373.1537
375.1514
376.1526
250.0279
251.0255
357.1578
499.0506
501.0477
m/z
250 260 270 280 290 300 310 320 330 340 350 360 370 380 390 400 410 420 430 440 450 460 470 480 490 500 510 520 530 540 550 560 570 580 590 600 610
Cl
N
N
N
N
N
H
O
6e
C18H21ClN6O
[M+1] =373.1544

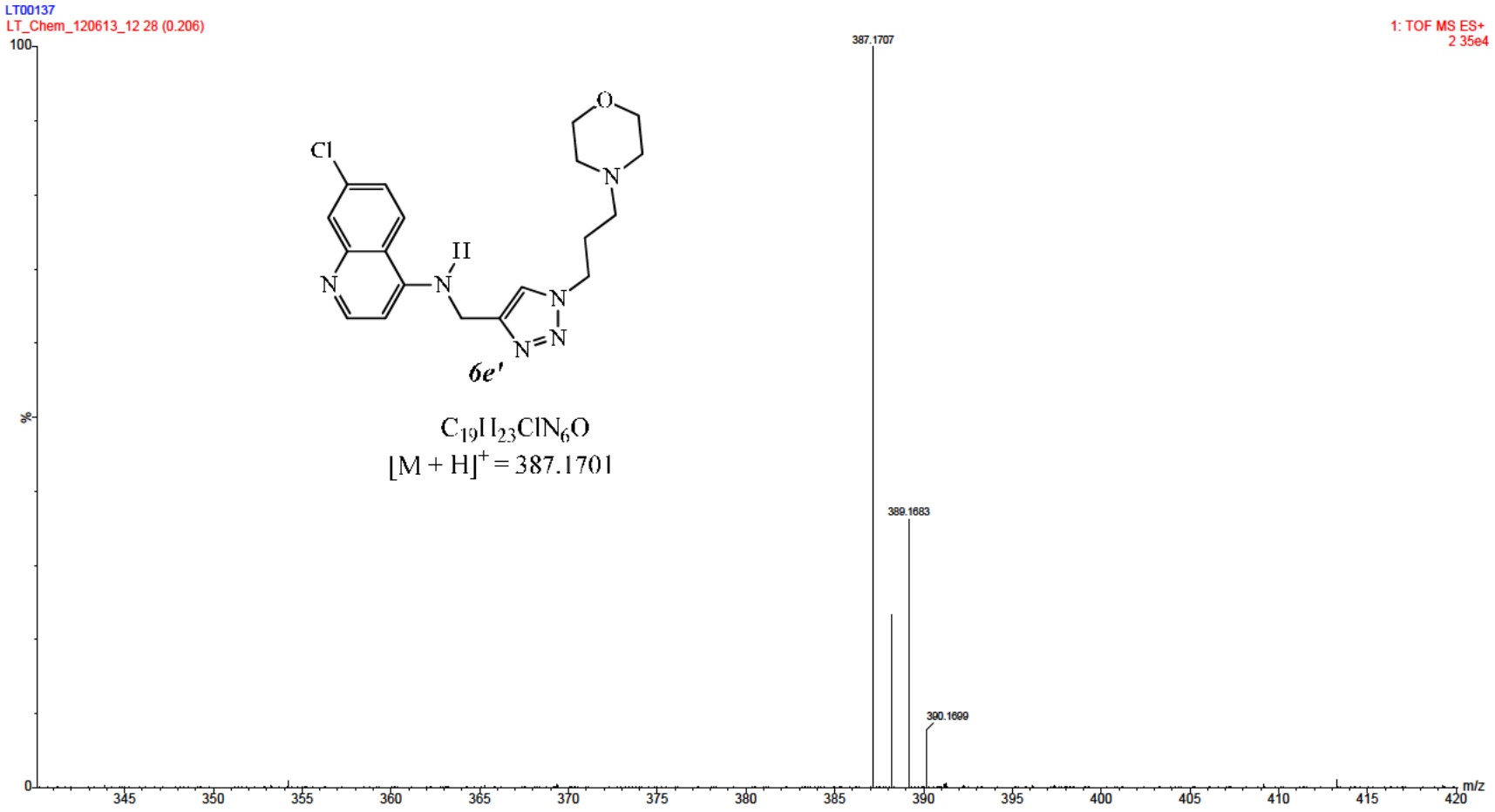
LT00137
LT_Chem_120613_12 28 (0.206)
1: TOF MS ES+
2 35e4
100
%
0
387.1707
389.1683
390.1699
345
350
355
360
365
370
375
380
385
390
395
400
405
410
415
420
m/z
Cl
N
O
N
H
N
N
N
N
6e'
C19H23ClN6O
[M + H]+ = 387.1701

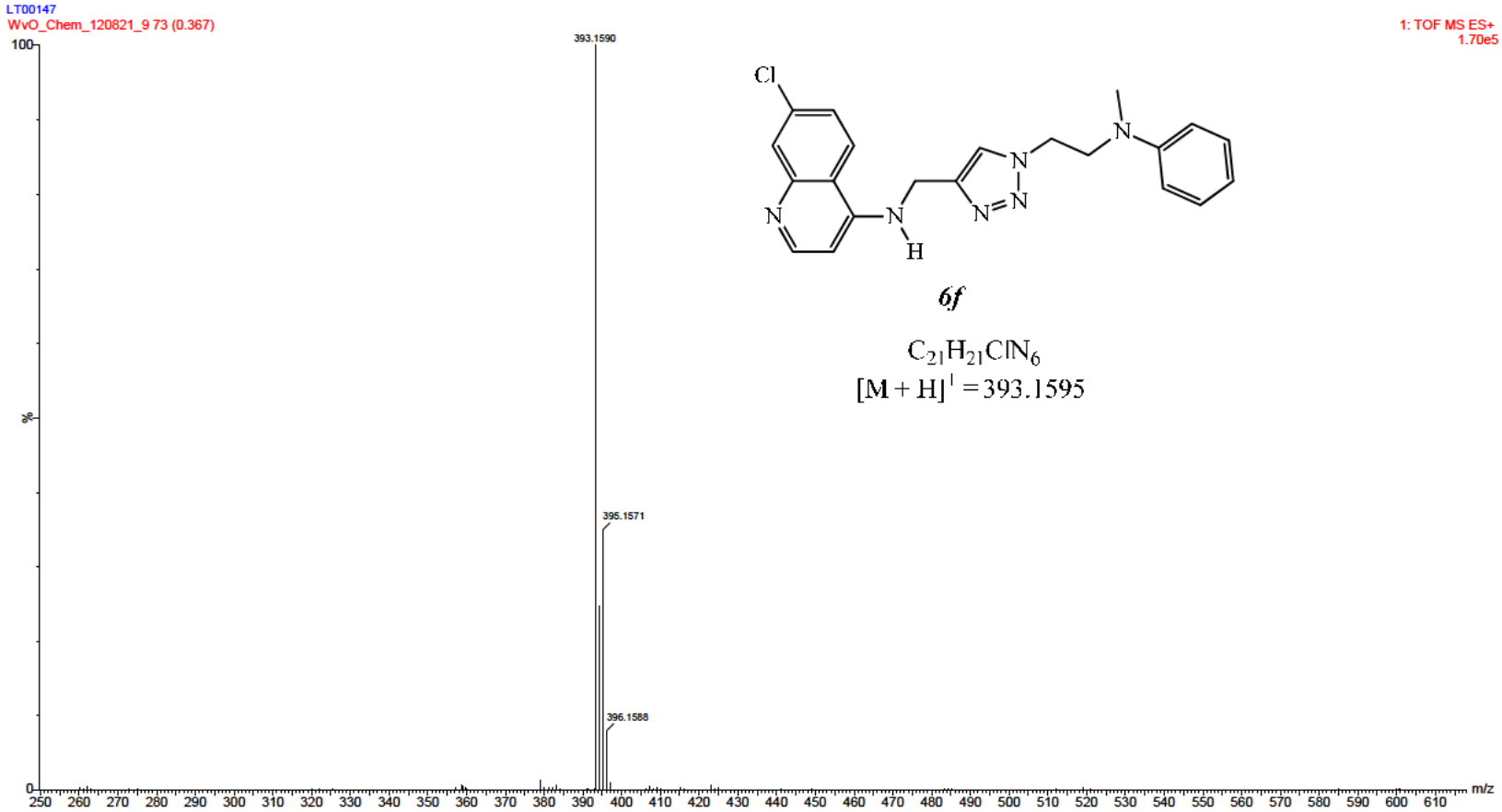

6f

$C_{21}H_{21}ClN_6$

$[M+H]^{+} = 393.1595$

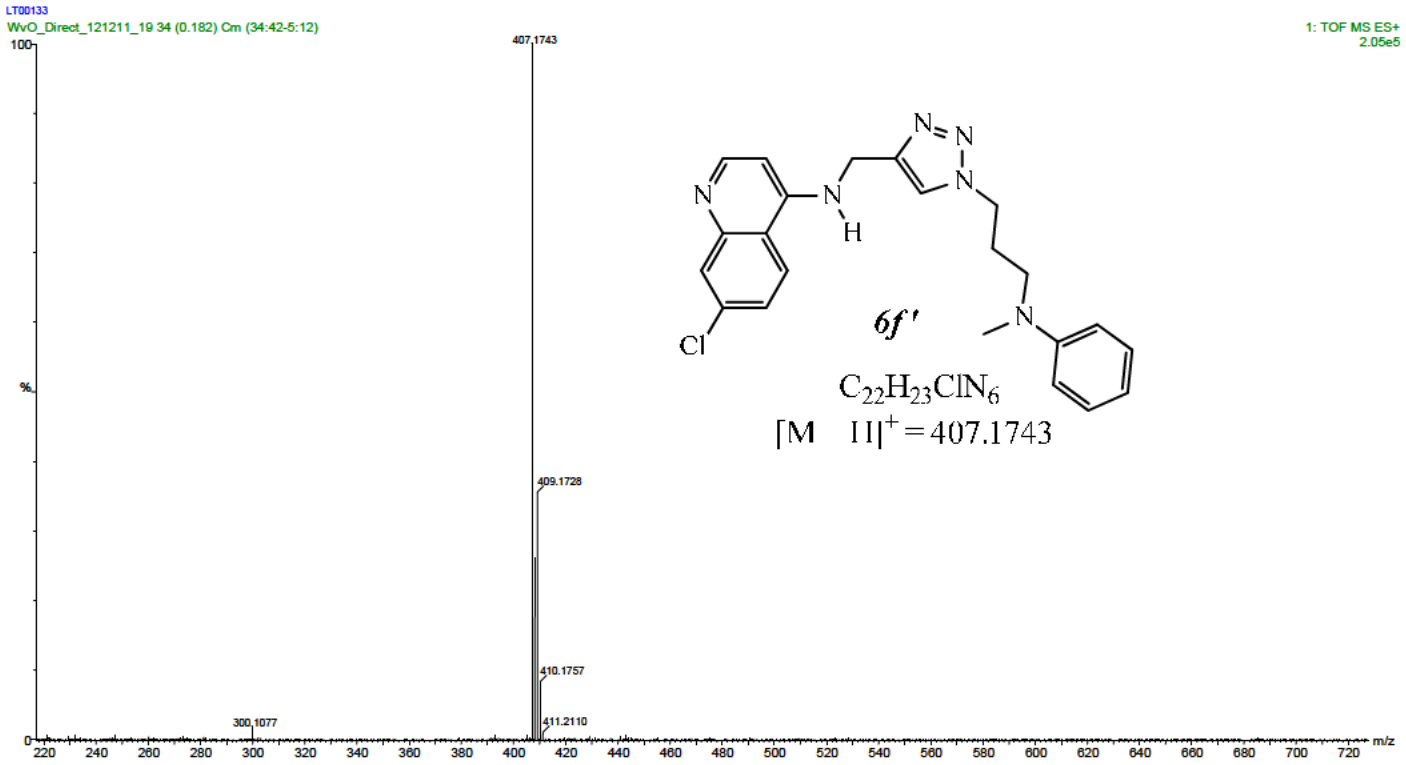
LT00133
WvO_Direct_121211_19 34 (0.182) Cm (34:42-5:12)
1: TOF MS ES+
2.05e5
100
%
0
407.1743
409.1728
410.1757
411.2110
300.1077
220 240 260 280 300 320 340 360 380 400 420 440 460 480 500 520 540 560 580 600 620 640 660 680 700 720
m/z
N
N
H
N
N
N
N
Cl
6f'
C22H23ClN6
[M + H]+ = 407.1743

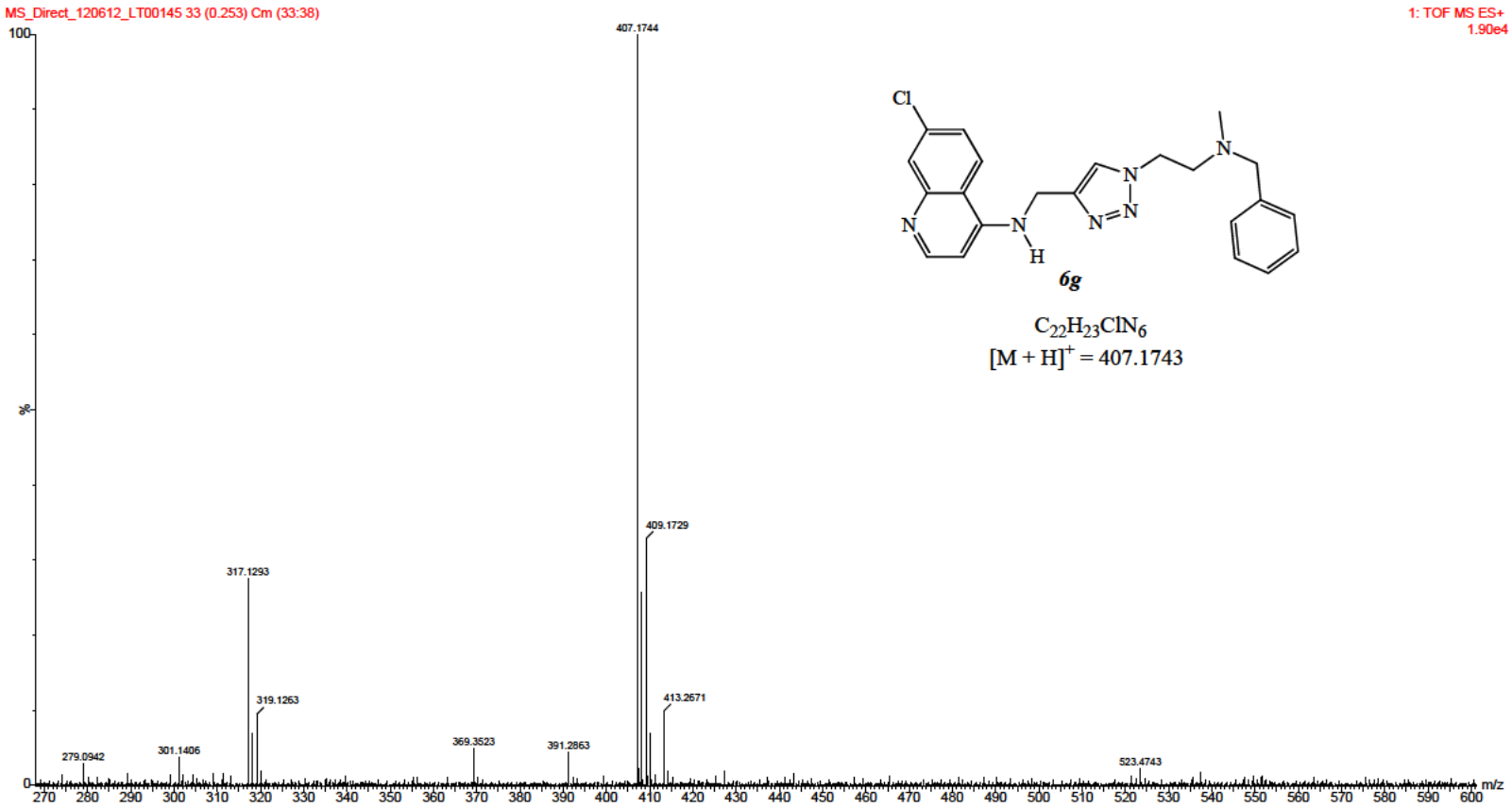

6g

$C_{22}H_{23}ClN_6$

$[M + H]^+ = 407.1743$

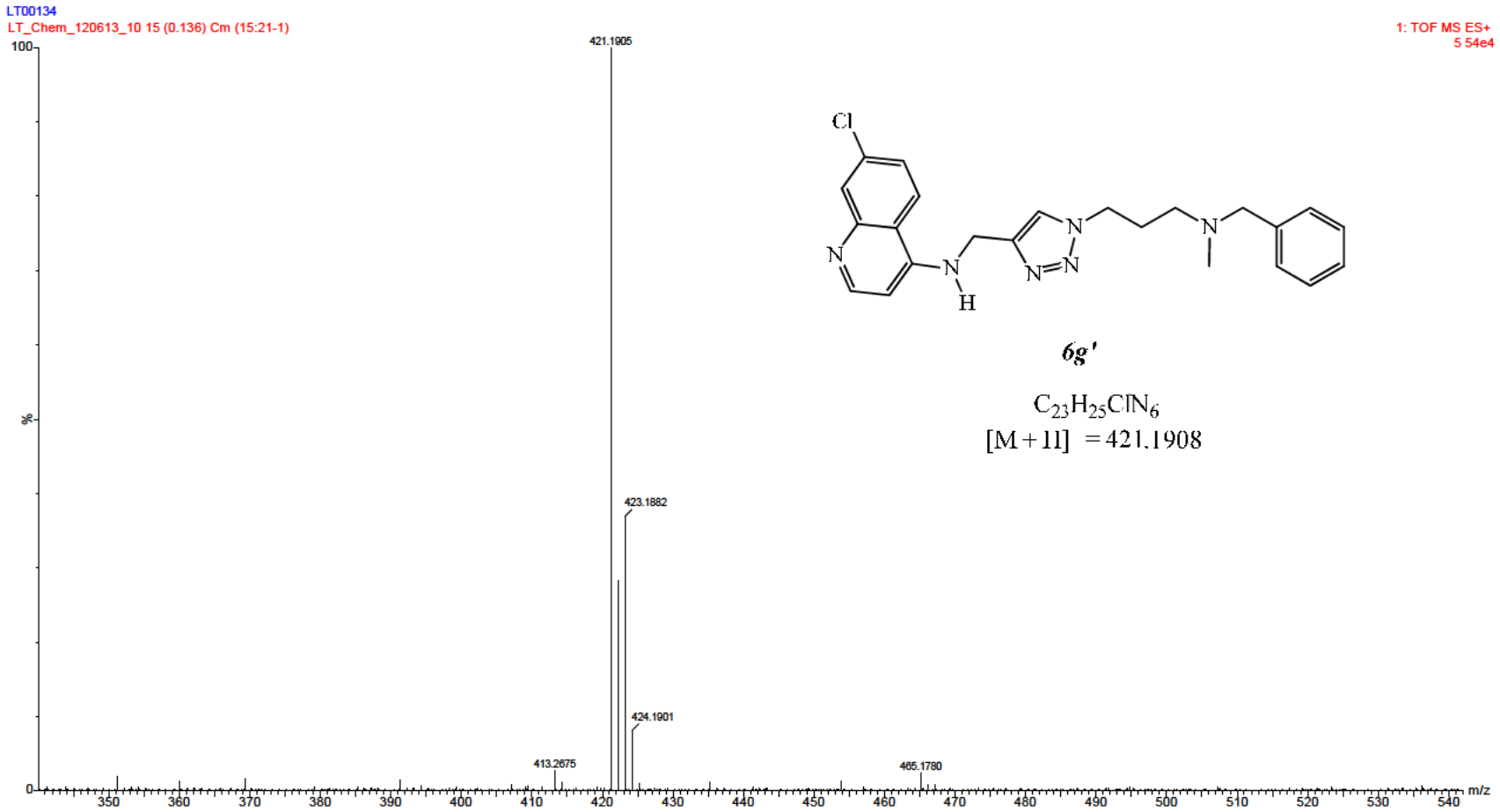

6g'

$C_{23}H_{25}ClN_6$

$[M+1]^+ = 421.1908$

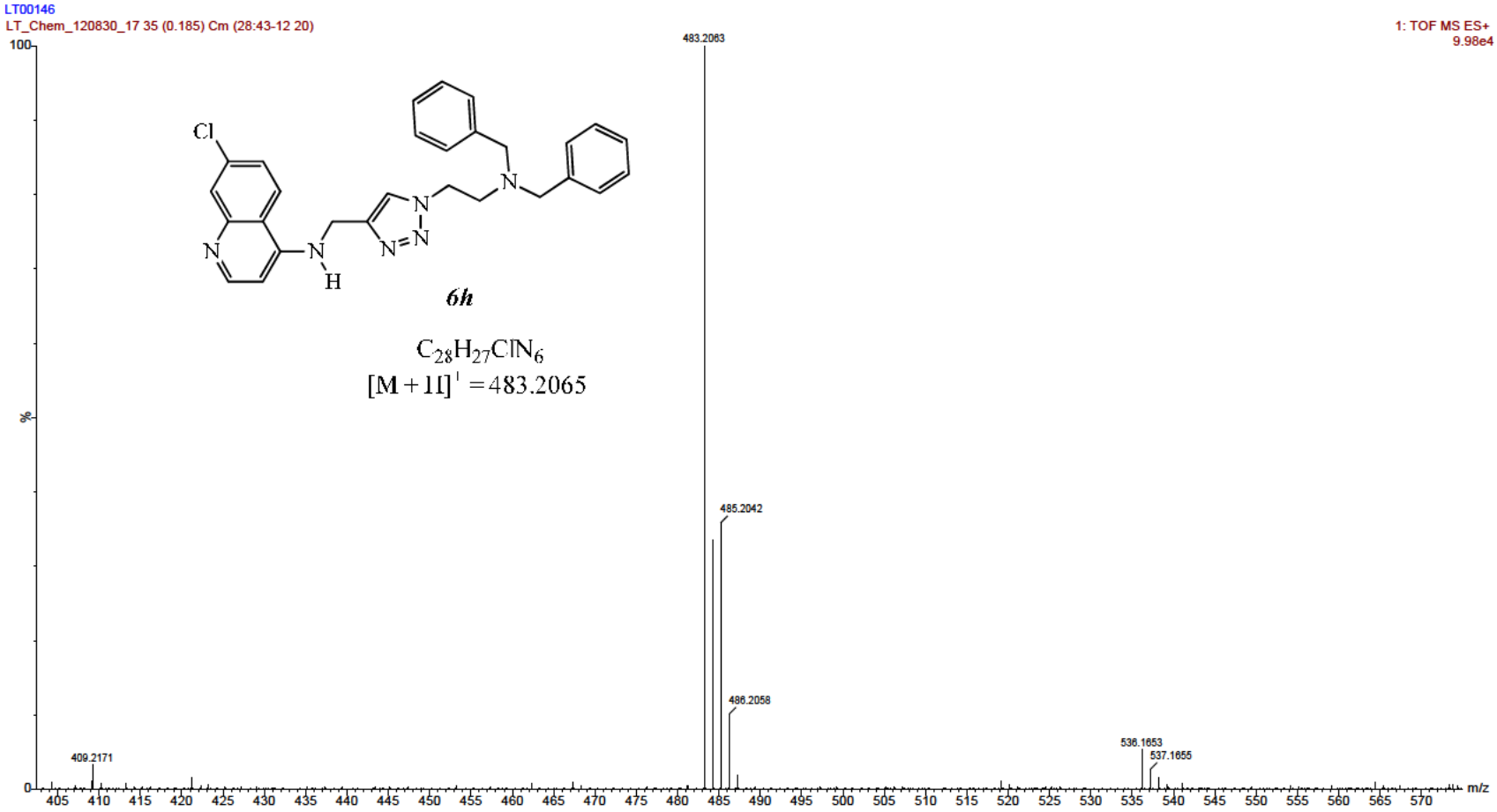
LT00146
LT_Chem_120830_17 35 (0.185) Cm (28:43-12 20)
1: TOF MS ES+
9.98e4
100
%
0
483.2063
485.2042
486.2058
409.2171
536.1653
537.1655
m/z
405 410 415 420 425 430 435 440 445 450 455 460 465 470 475 480 485 490 495 500 505 510 515 520 525 530 535 540 545 550 555 560 565 570
Cl
N
N
H
N
N
N
N
6h
$C_{28}H_{27}ClN_6$
$[M+1]^+ = 483.2065$

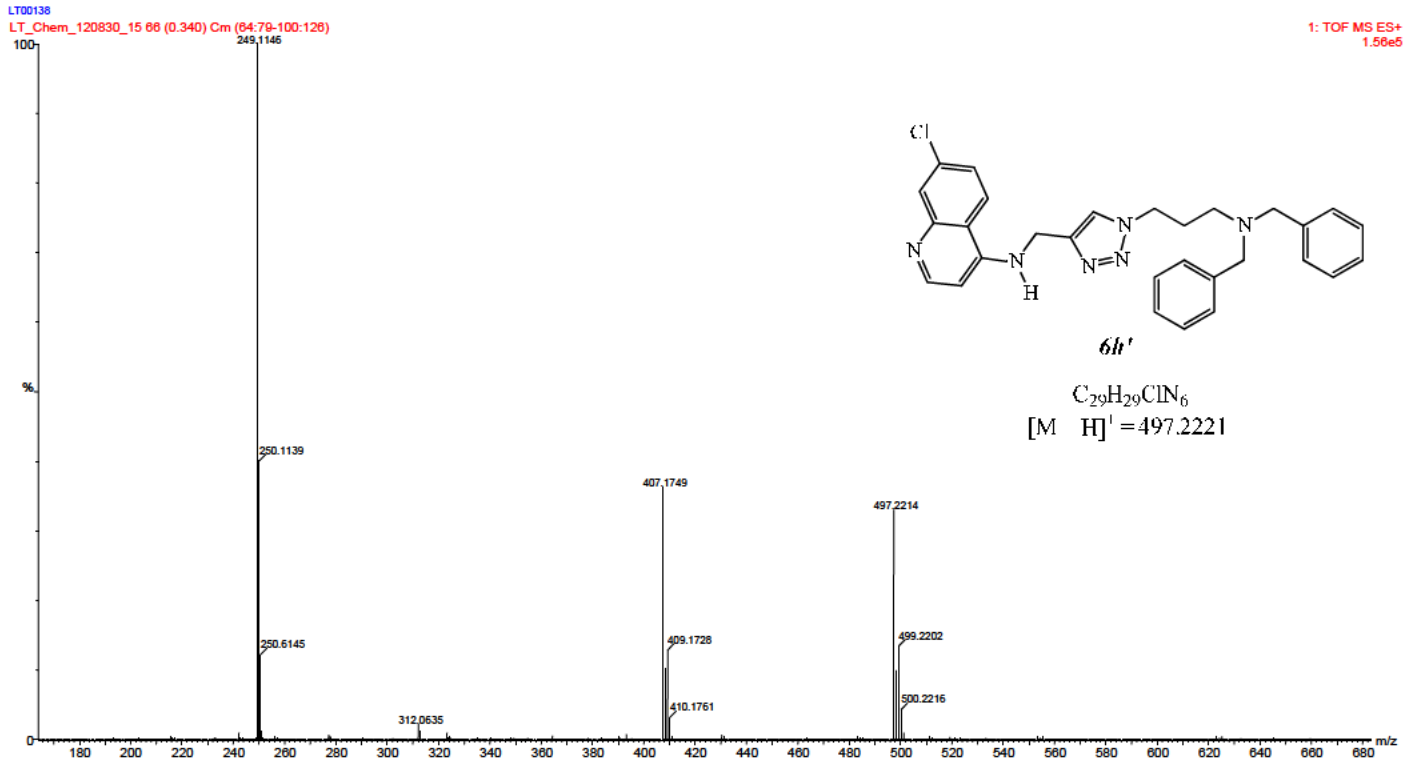
LT00138
LT_Chem_120830_15 66 (0.340) Cm (64:79-100:126)
1: TOF MS ES+
1.56e5
100
%
0
249.1145
250.1139
250.6145
312.0635
407.1749
409.1728
410.1761
497.2214
499.2202
500.2216
180 200 220 240 260 280 300 320 340 360 380 400 420 440 460 480 500 520 540 560 580 600 620 640 660 680
m/z
Cl
N
N
H
N
N
N
N
6h'
C29H29ClN6
[M H]+ =497.2221

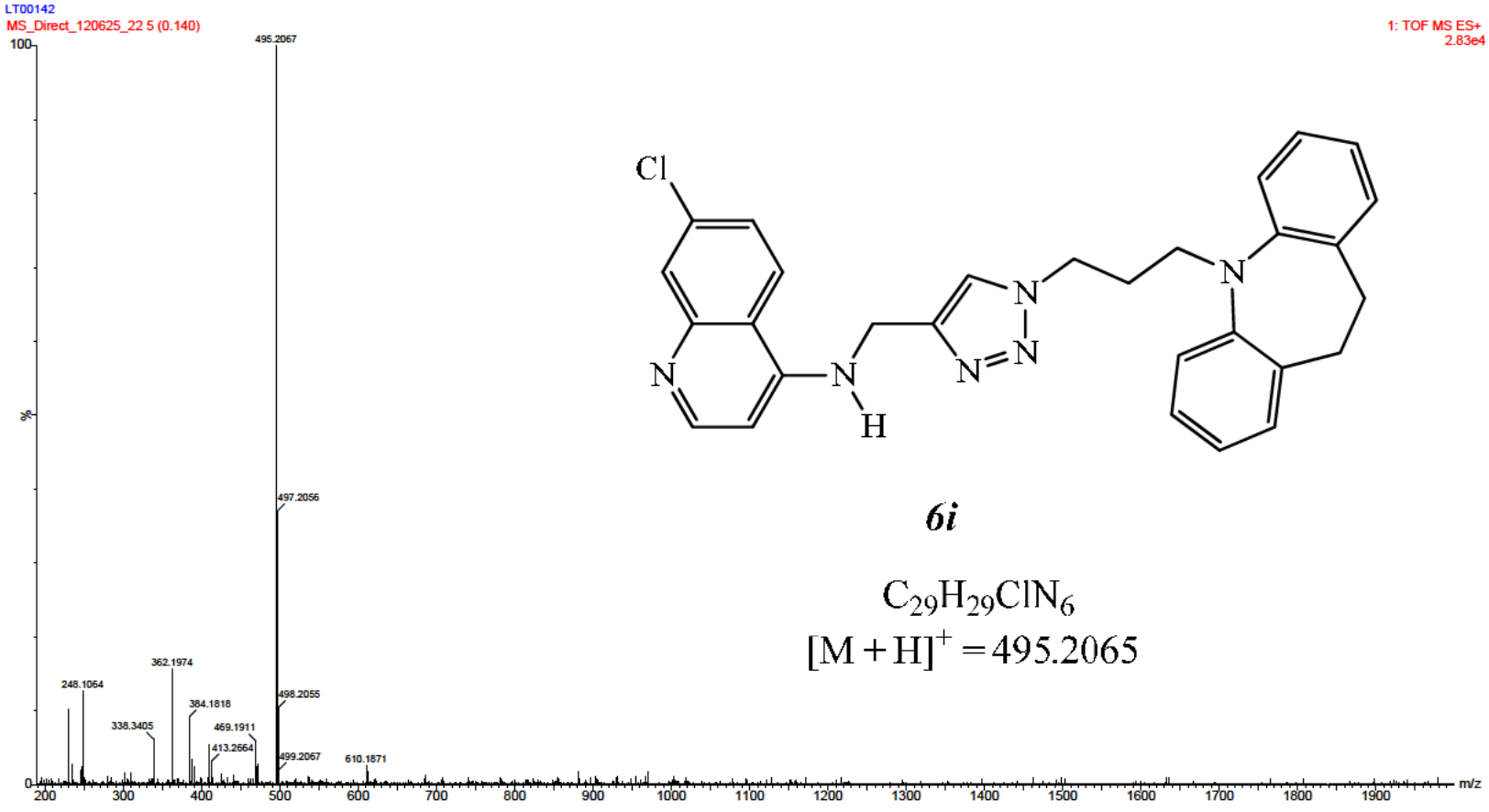

6i

$C_{29}H_{29}ClN_6$

$[M+H]^+ = 495.2065$

IR Spectra

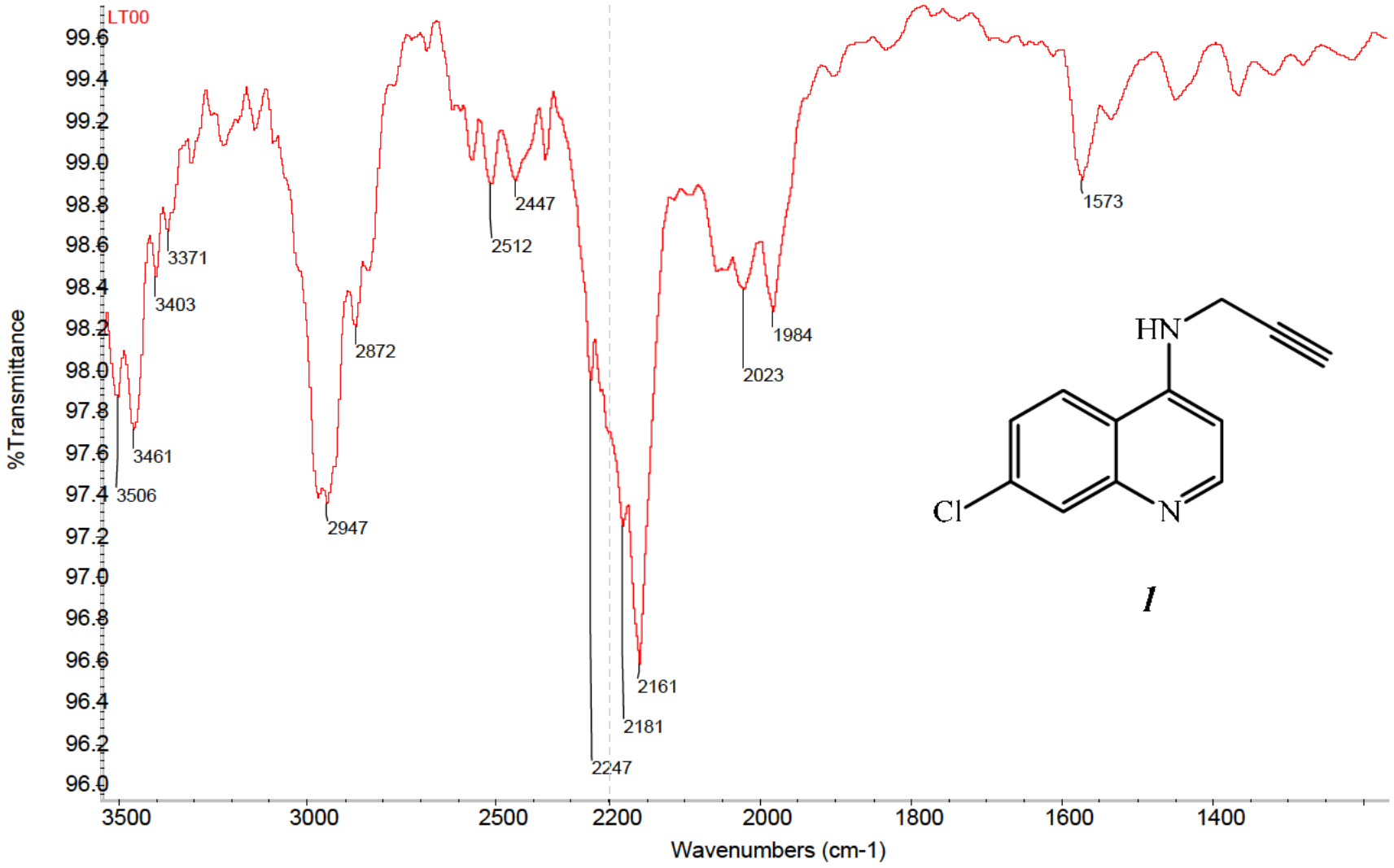
LT00
%Transmittance
99.6
99.4
99.2
99.0
98.8
98.6
98.4
98.2
98.0
97.8
97.6
97.4
97.2
97.0
96.8
96.6
96.4
96.2
96.0
3506
3461
3403
3371
2947
2872
2512
2447
2247
2181
2161
2023
1984
1573
3500
3000
2500
2200
2000
1800
1600
1400
Wavenumbers (cm-1)
HN
Cl
N

1

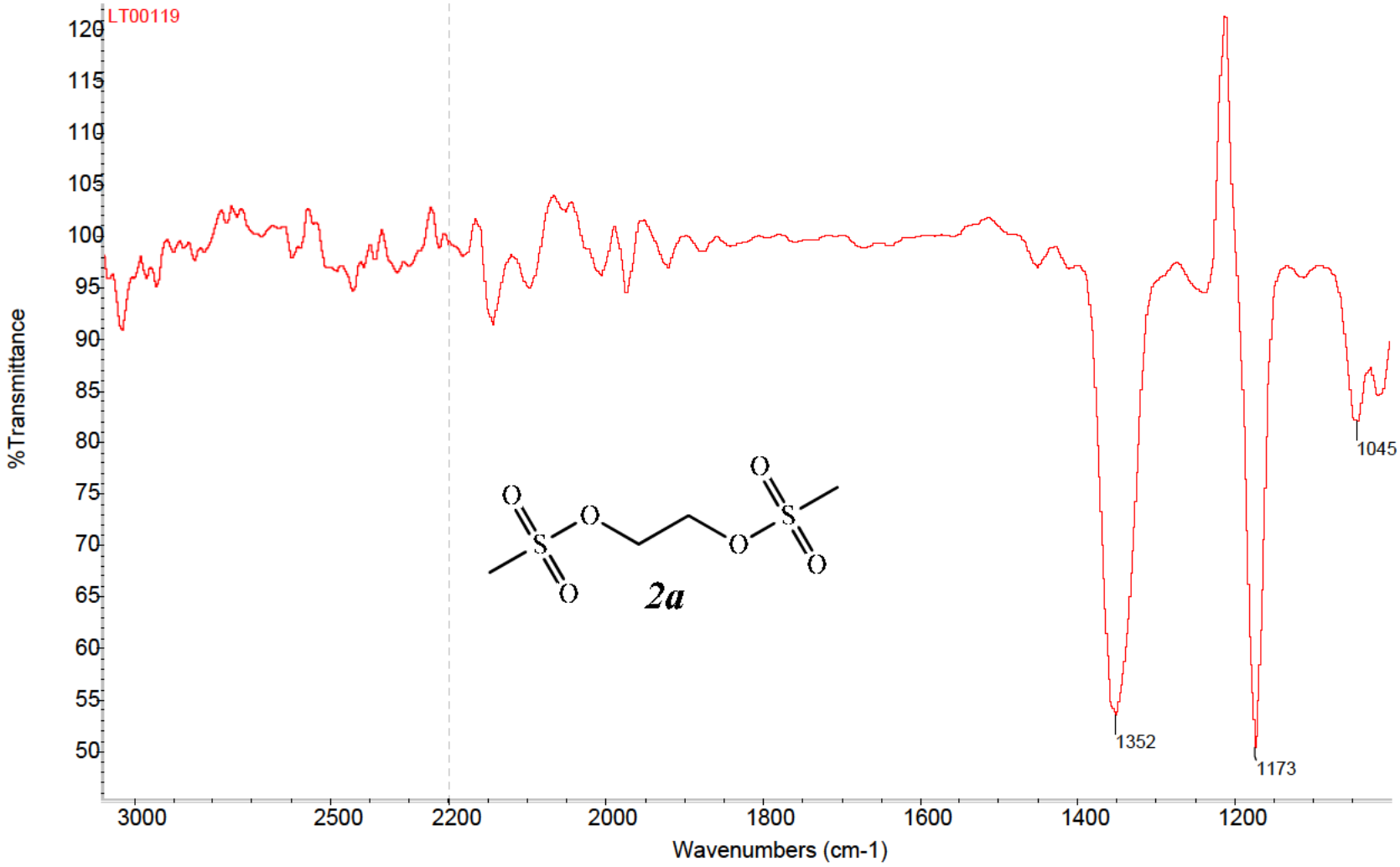
LT00119
%Transmittance
120
115
110
105
100
95
90
85
80
75
70
65
60
55
50
3000
2500
2200
2000
1800
1600
1400
1200
Wavenumbers (cm-1)
1352
1173
1045
O
S
O
O
O
O
S
O
O
2a

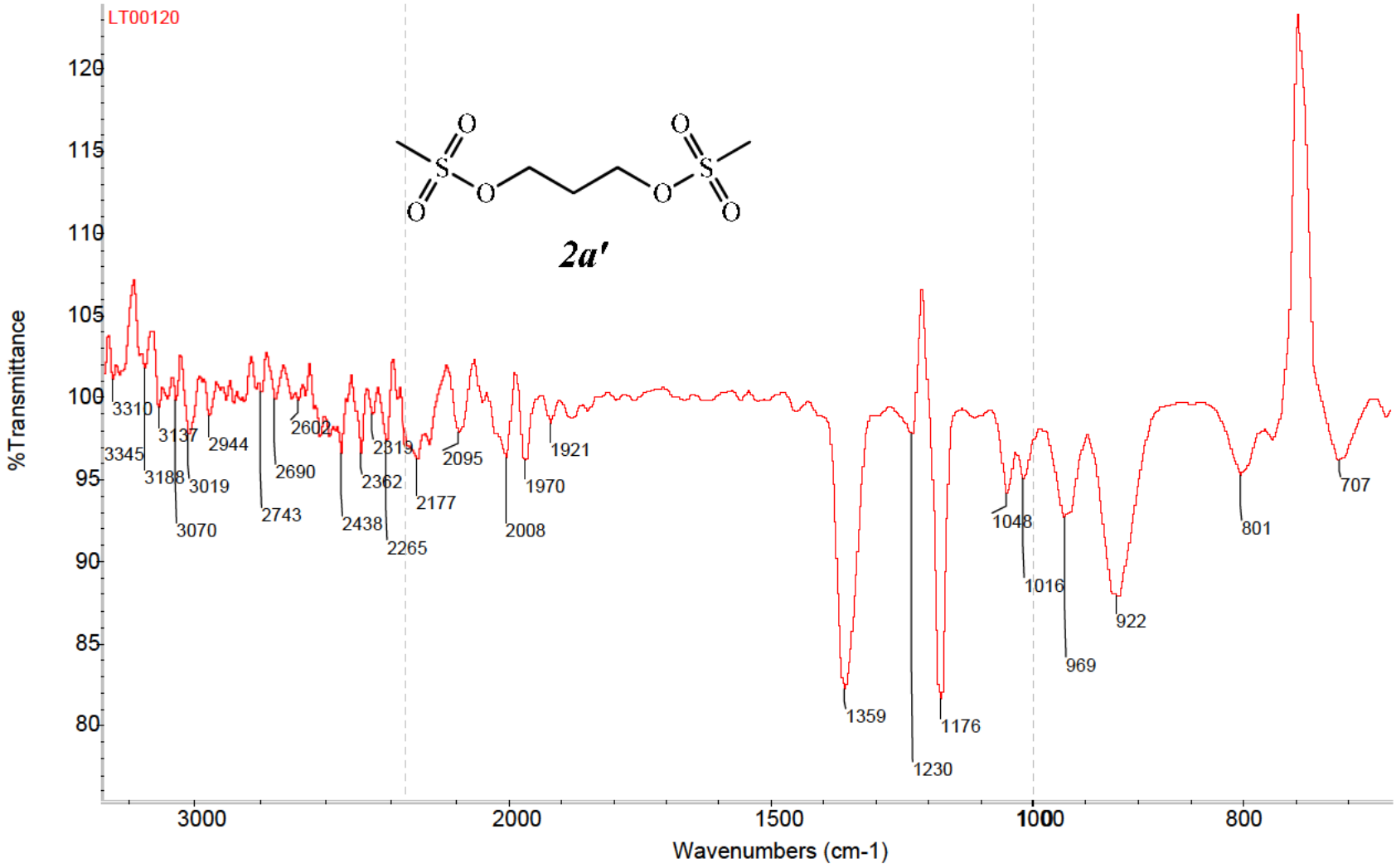
LT00120
2a'
%Transmittance
Wavenumbers (cm-1)
120
115
110
105
100
95
90
85
80
3000
2000
1500
1000
800
3345
3310
3188
3137
3070
3019
2944
2743
2690
2602
2438
2362
2319
2265
2177
2095
2008
1970
1921
1359
1230
1176
1048
1016
969
922
801
707

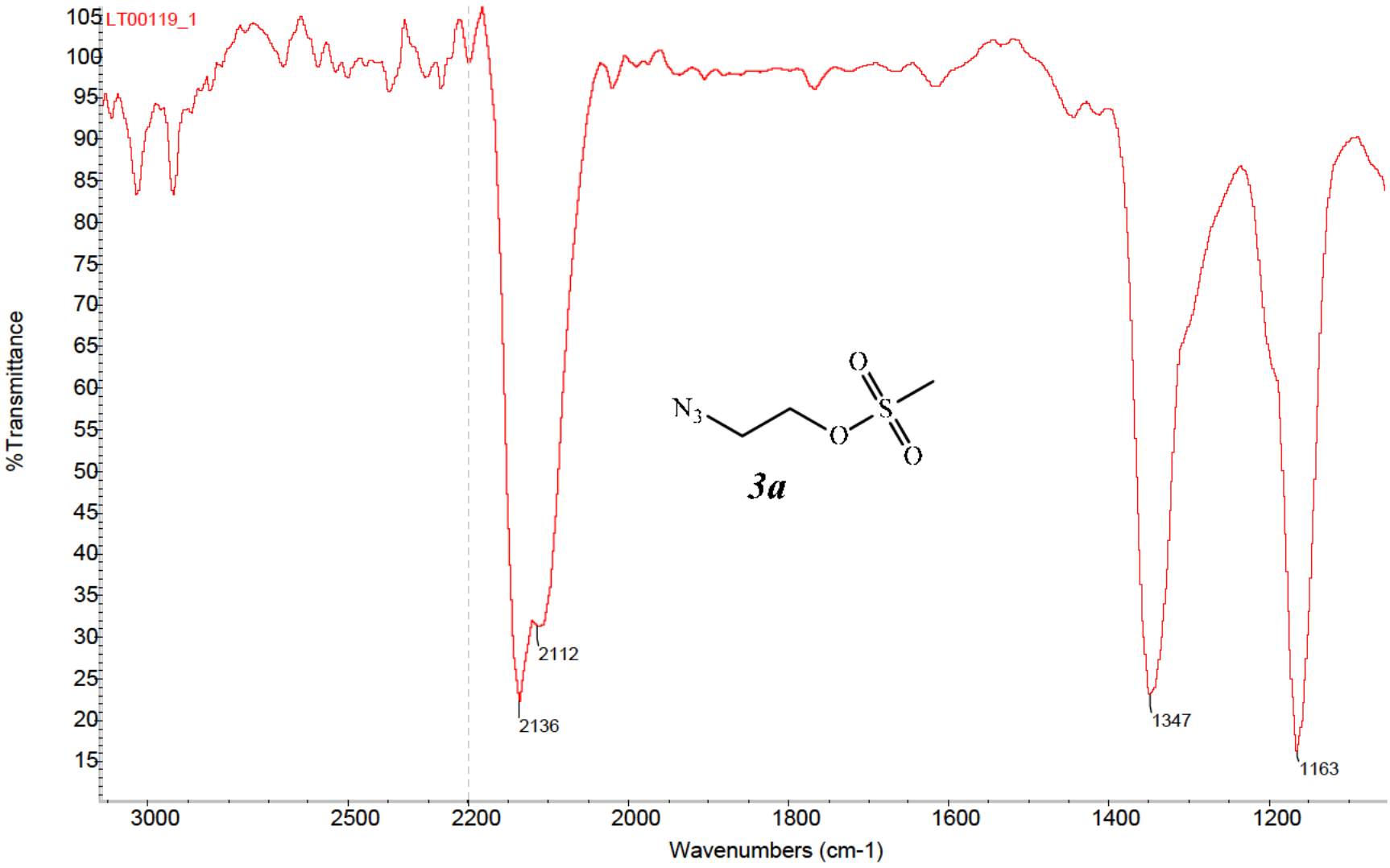
LT00119_1
%Transmittance
Wavenumbers (cm-1)
2112
2136
1347
1163
3a

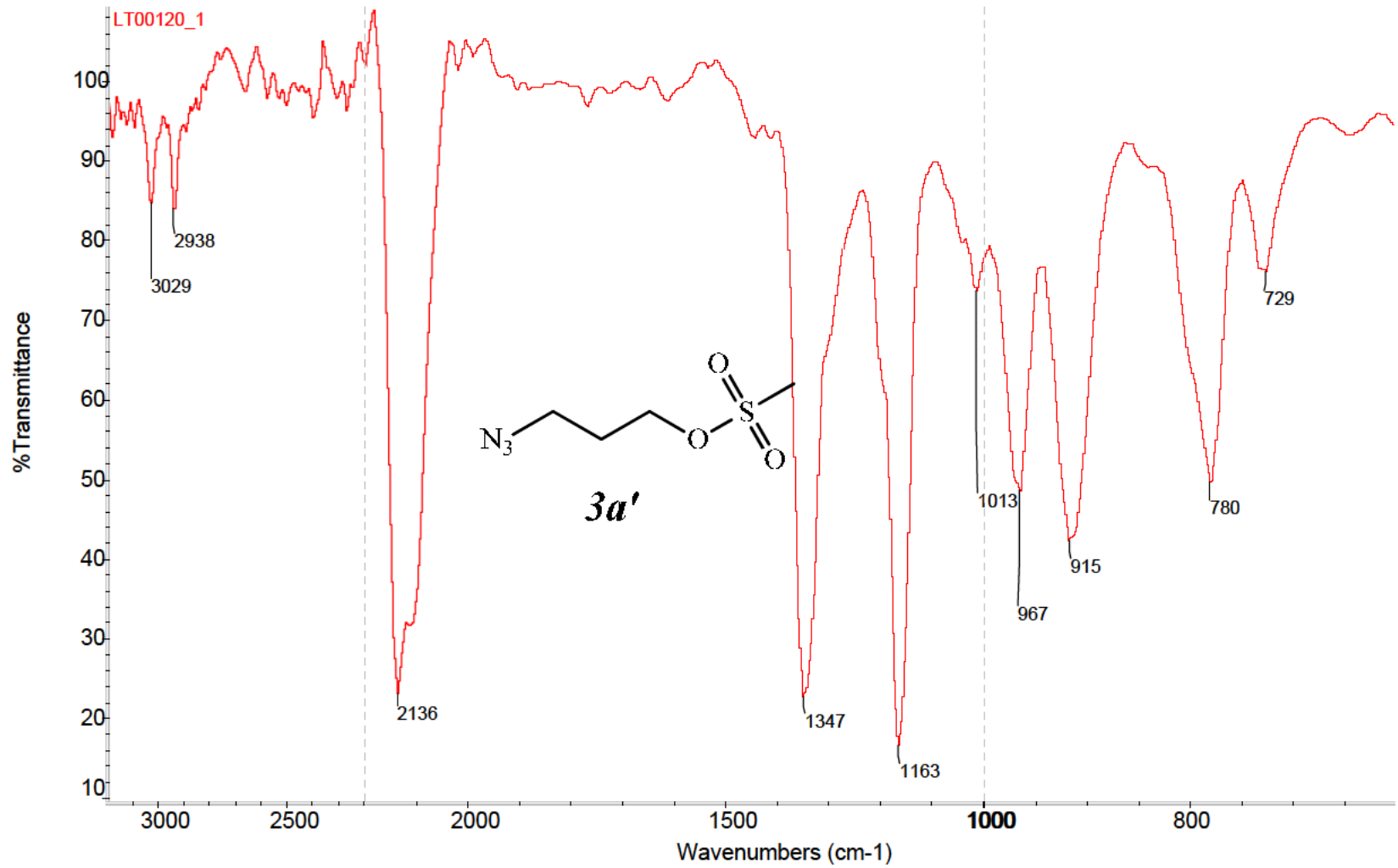
LT00120_1
%Transmittance
100
90
80
70
60
50
40
30
20
10
3000
2500
2000
1500
1000
800
Wavenumbers (cm-1)
3029
2938
2136
1347
1163
1013
967
915
780
729
N3
O
S
O
O
3a'

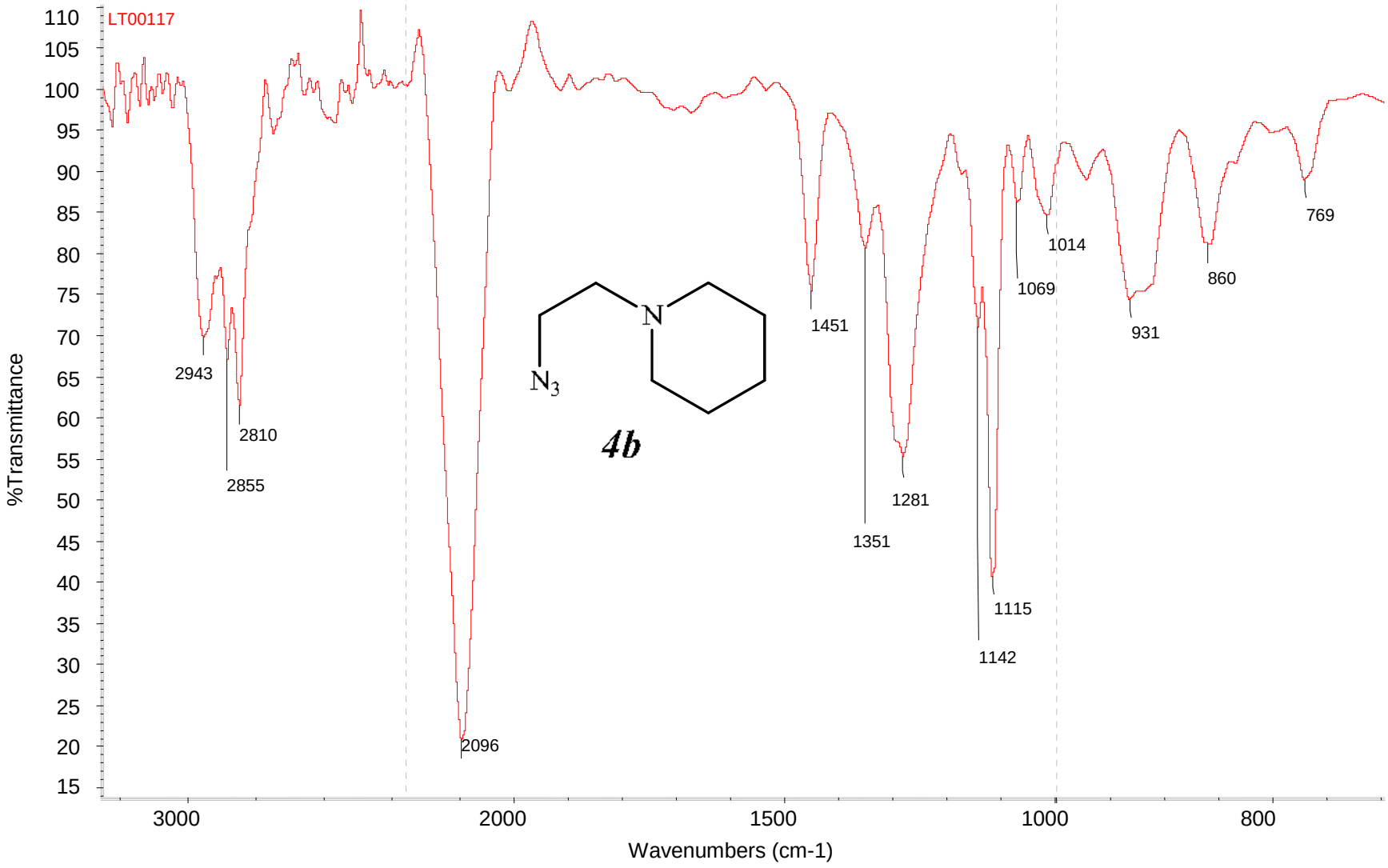
LT00117
%Transmittance
Wavenumbers (cm-1)
3000
2000
1500
1000
800
2943
2855
2810
2096
1451
1351
1281
1142
1115
1069
1014
931
860
769
N
N3
4b

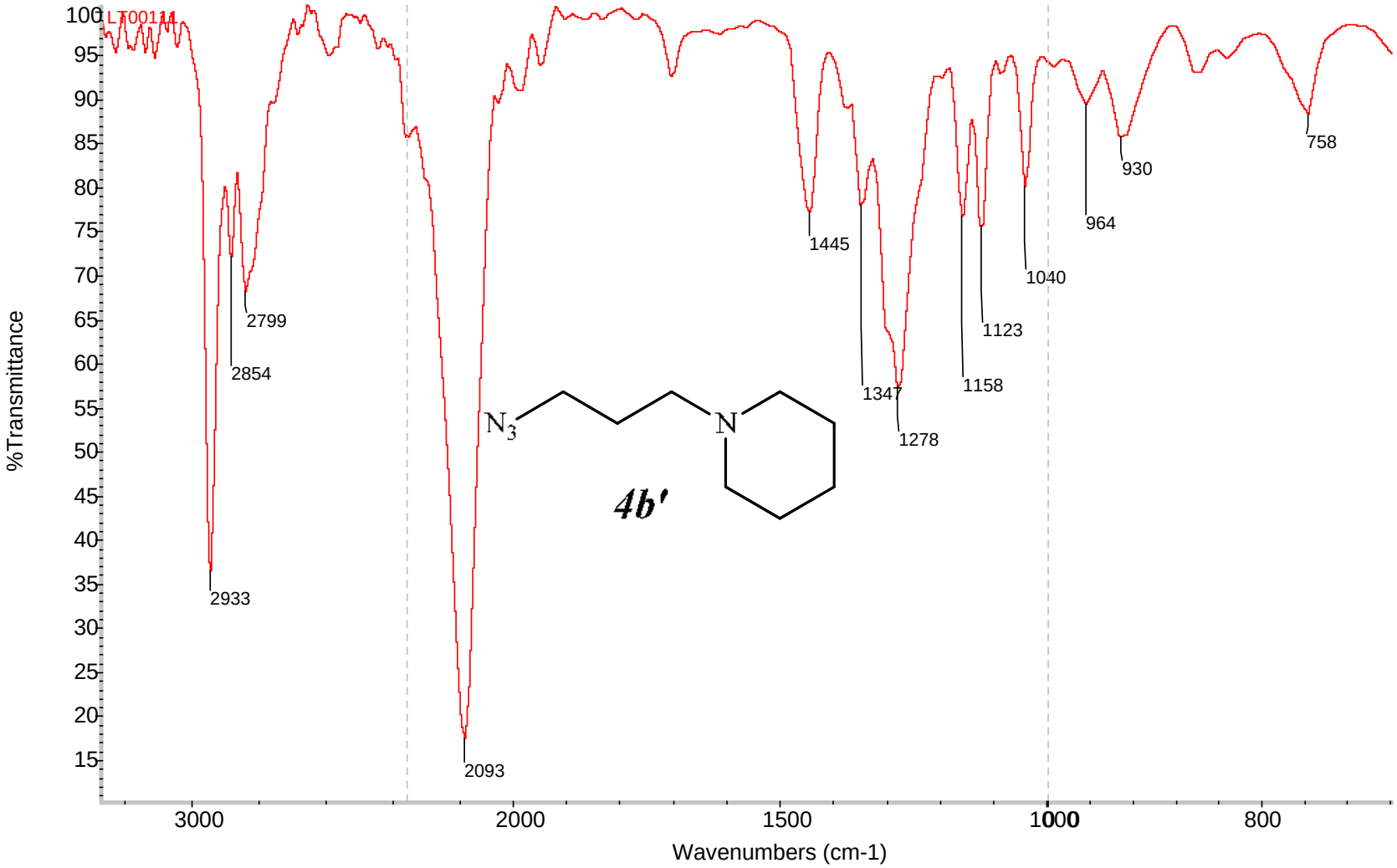
LT00111
%Transmittance
Wavenumbers (cm-1)
3000
2000
1500
1000
800
2933
2854
2799
2093
1445
1347
1278
1158
1123
1040
964
930
758
N3
N
4b'

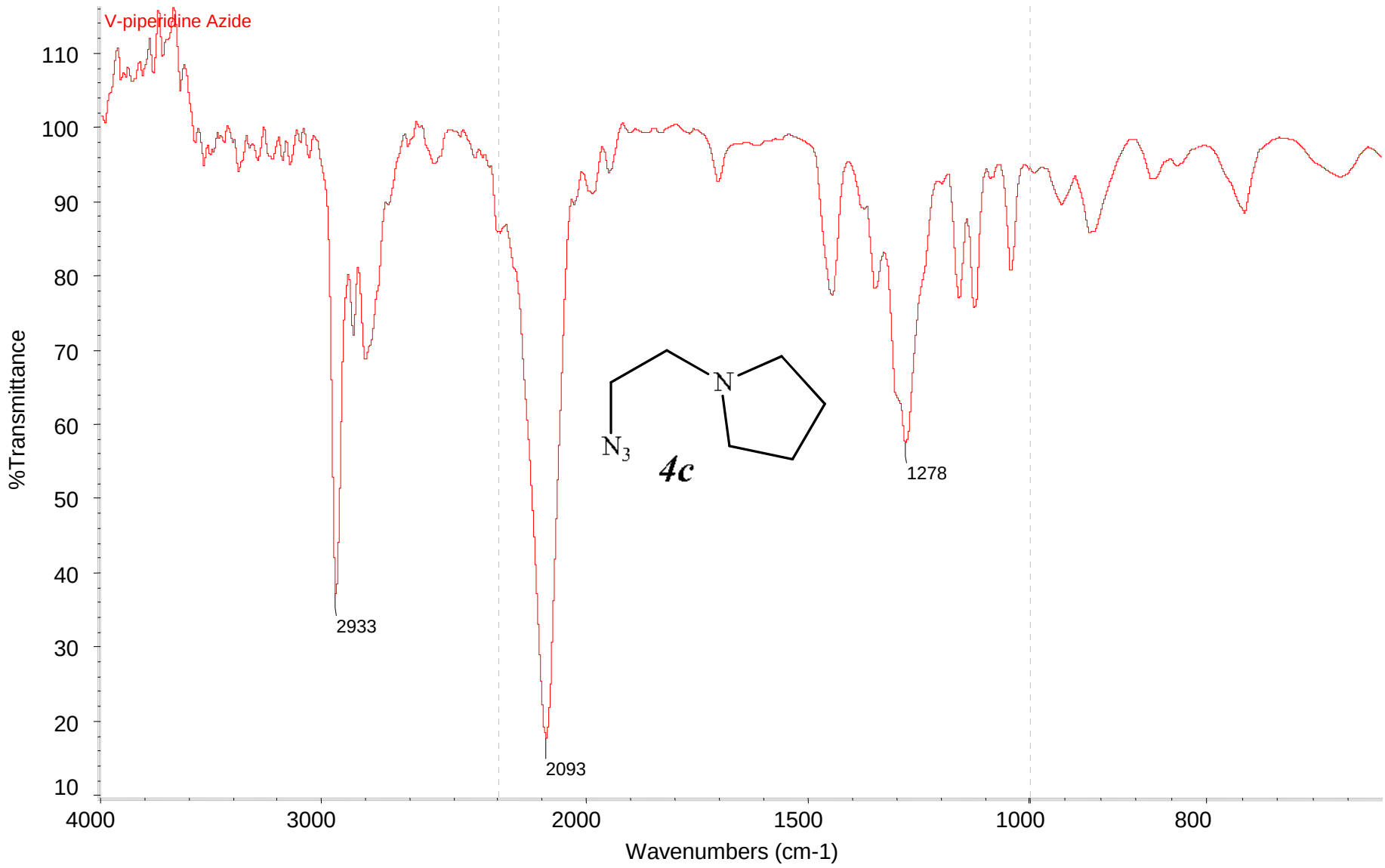
V-piperidine Azide
%Transmittance
110
100
90
80
70
60
50
40
30
20
10
4000
3000
2000
1500
1000
800
Wavenumbers (cm-1)
2933
2093
1278
N
N3
4c

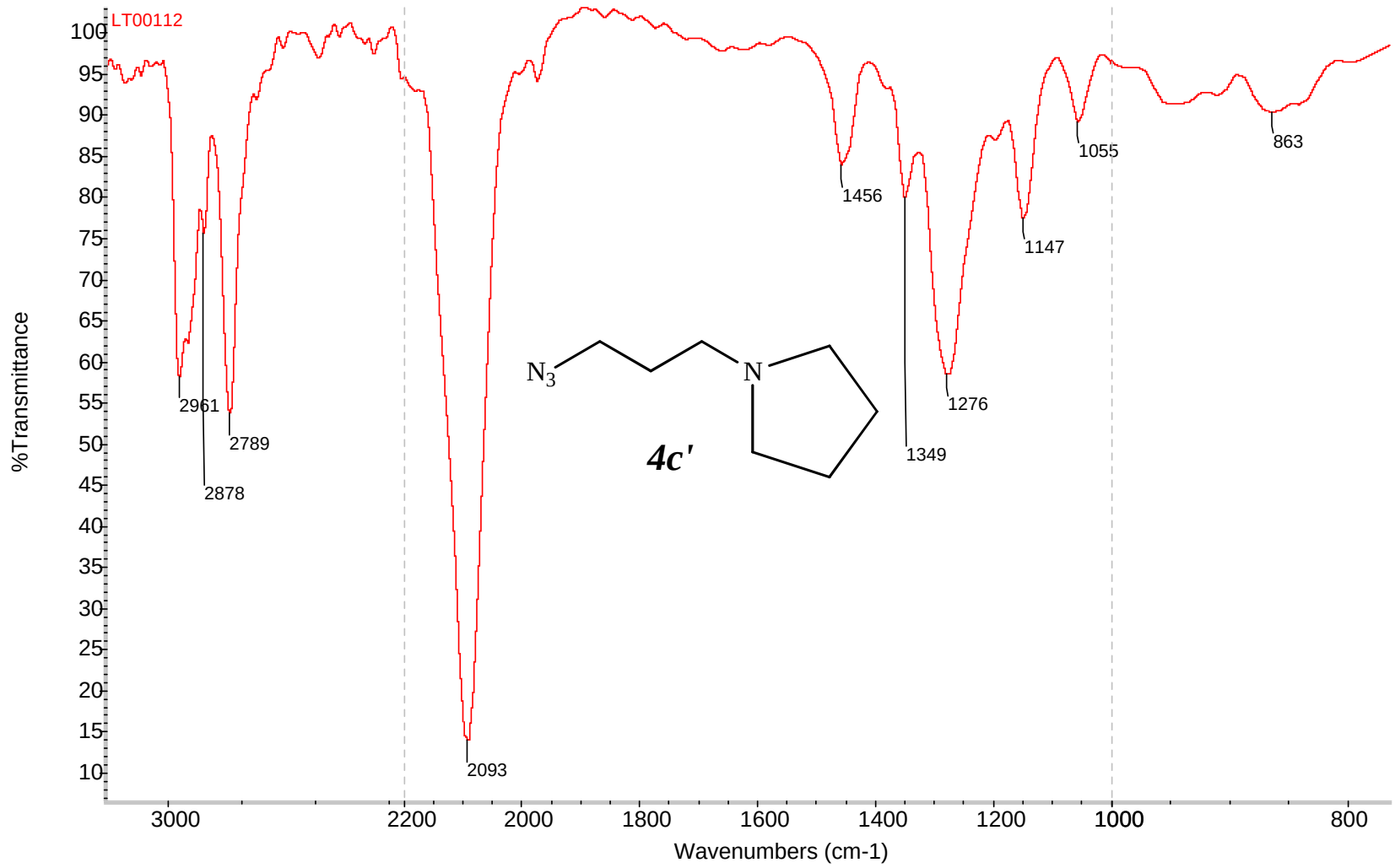
LT00112
%Transmittance
Wavenumbers (cm-1)
2961
2878
2789
2093
1456
1349
1276
1147
1055
863
N3
N
4c'

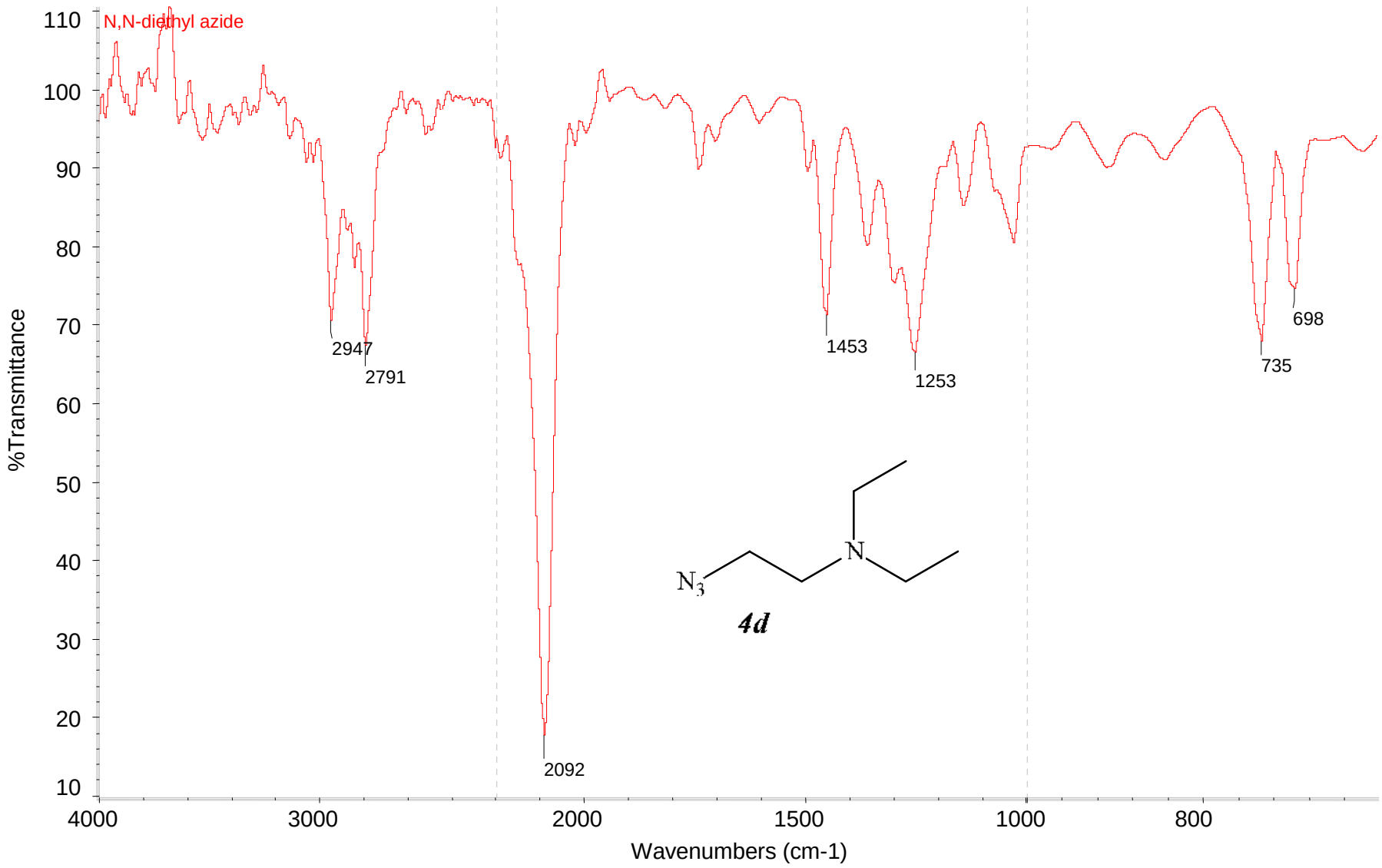
N,N-diethyl azide
%Transmittance
Wavenumbers (cm-1)
110
100
90
80
70
60
50
40
30
20
10
4000
3000
2000
1500
1000
800
2947
2791
2092
1453
1253
735
698
N
N3
4d

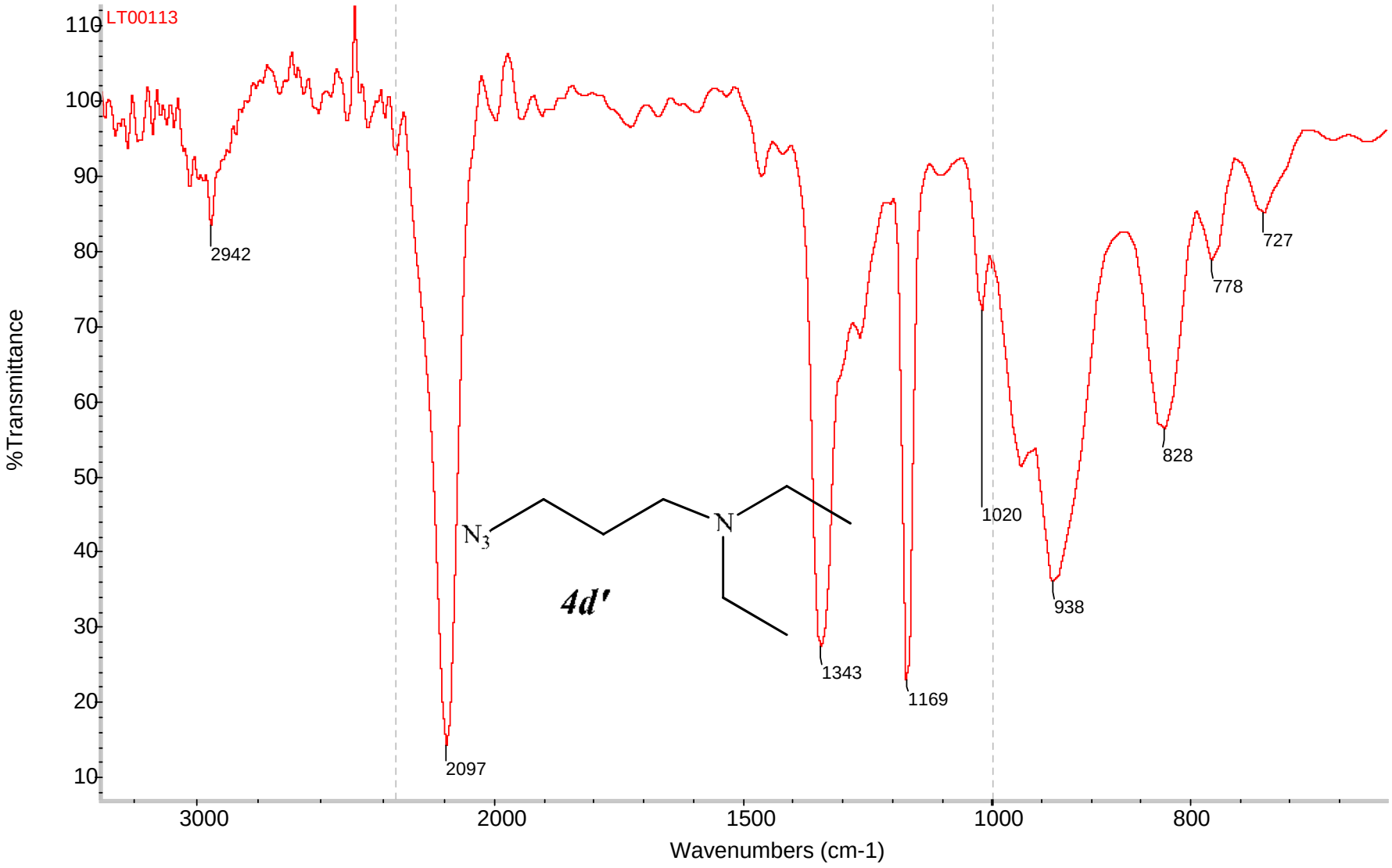
LT00113
%Transmittance
Wavenumbers (cm-1)
2942
2097
1343
1169
1020
938
828
778
727
4d'

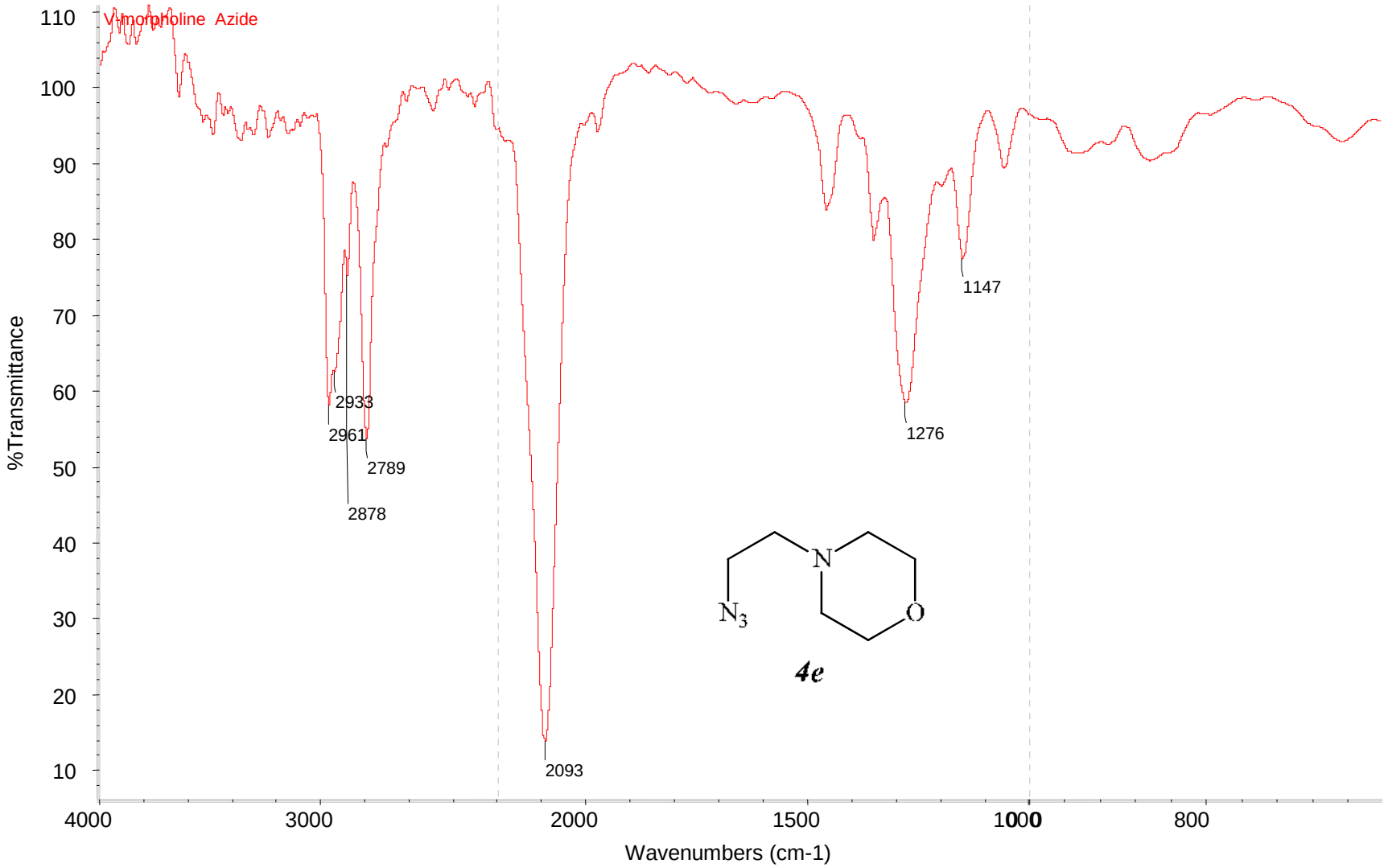
V-morpholine Azide
%Transmittance
Wavenumbers (cm-1)
2933
2961
2789
2878
2093
1276
1147
N
N3
O
4e

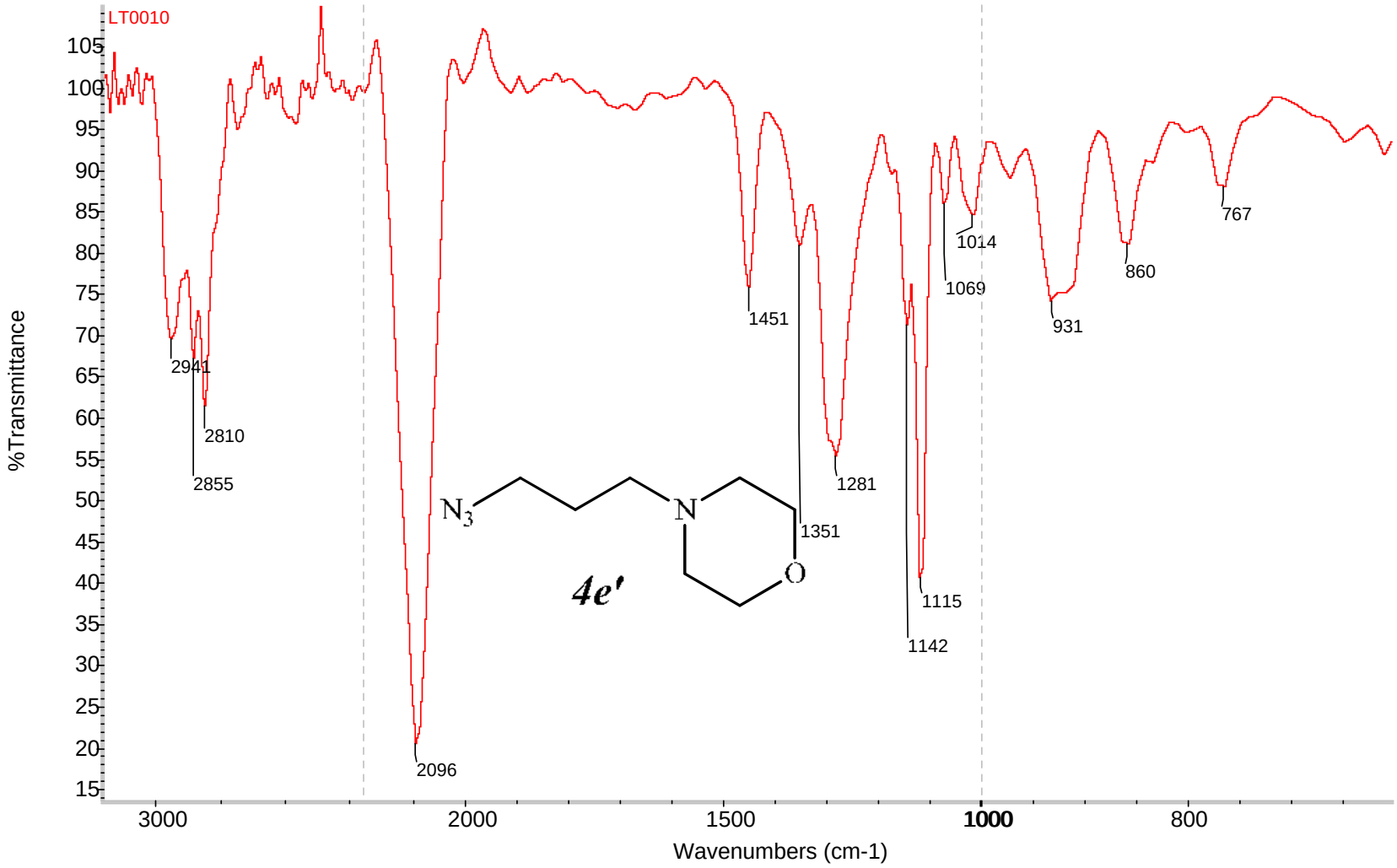
LT0010
%Transmittance
Wavenumbers (cm-1)
3000
2000
1500
1000
800
2941
2810
2855
2096
1451
1351
1281
1142
1115
1069
1014
931
860
767
N3
N
O
4e'

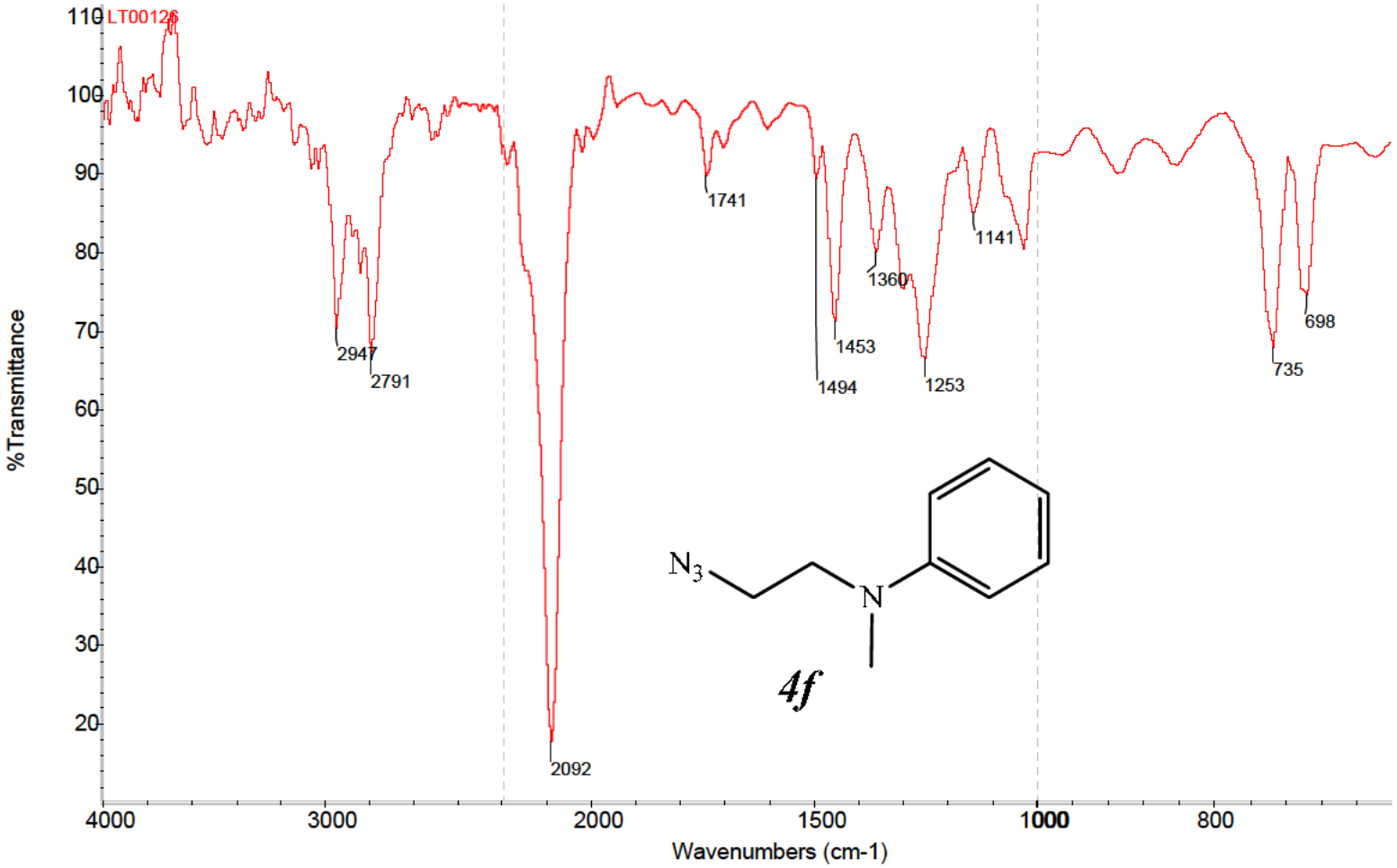
LT00126
%Transmittance
Wavenumbers (cm-1)
2947
2791
2092
1741
1494
1453
1360
1253
1141
735
698
N_3
N
4f

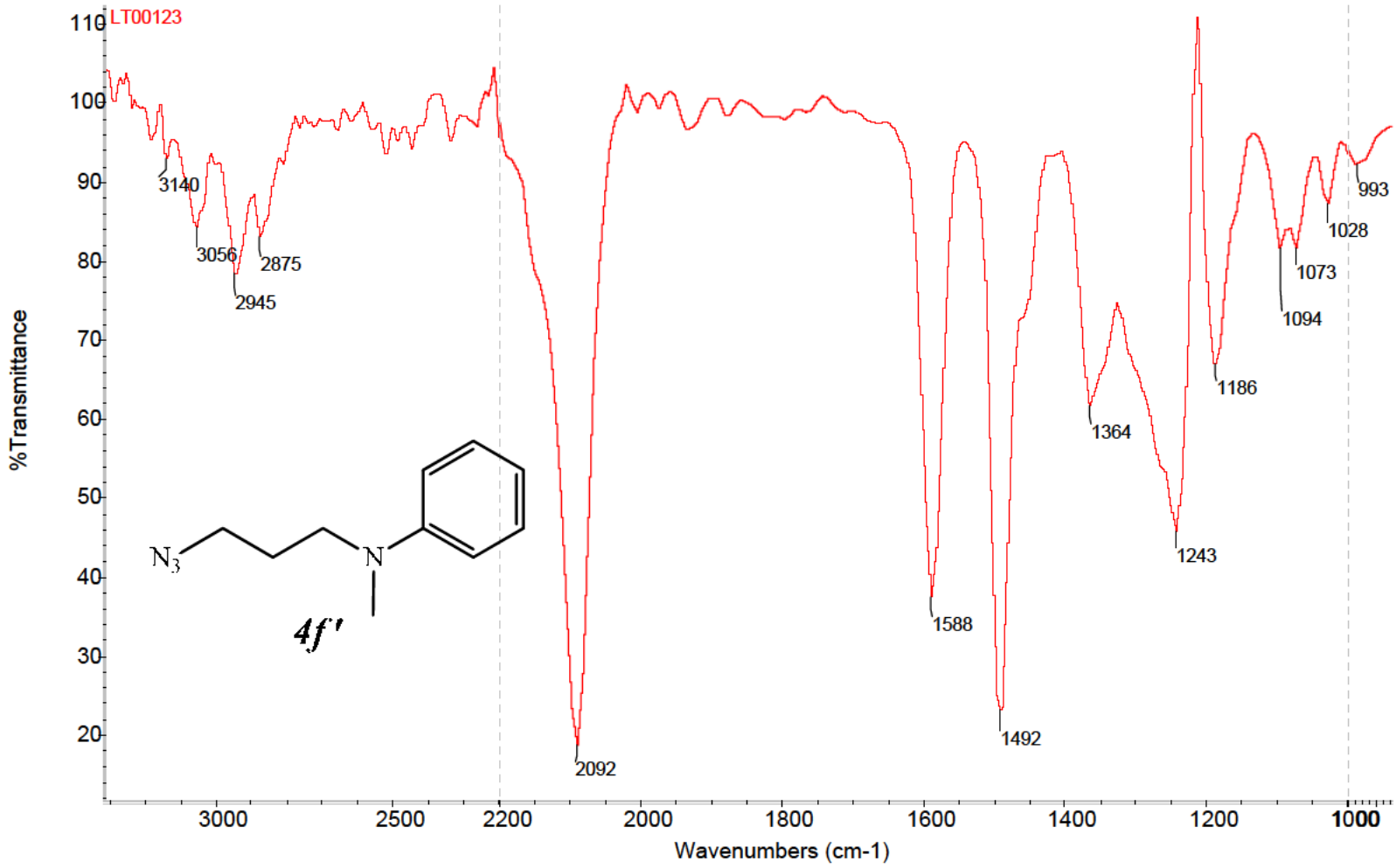
LT00123
%Transmittance
Wavenumbers (cm-1)
3140
3056
2945
2875
2092
1588
1492
1364
1243
1186
1094
1073
1028
993
N3
N
4f'

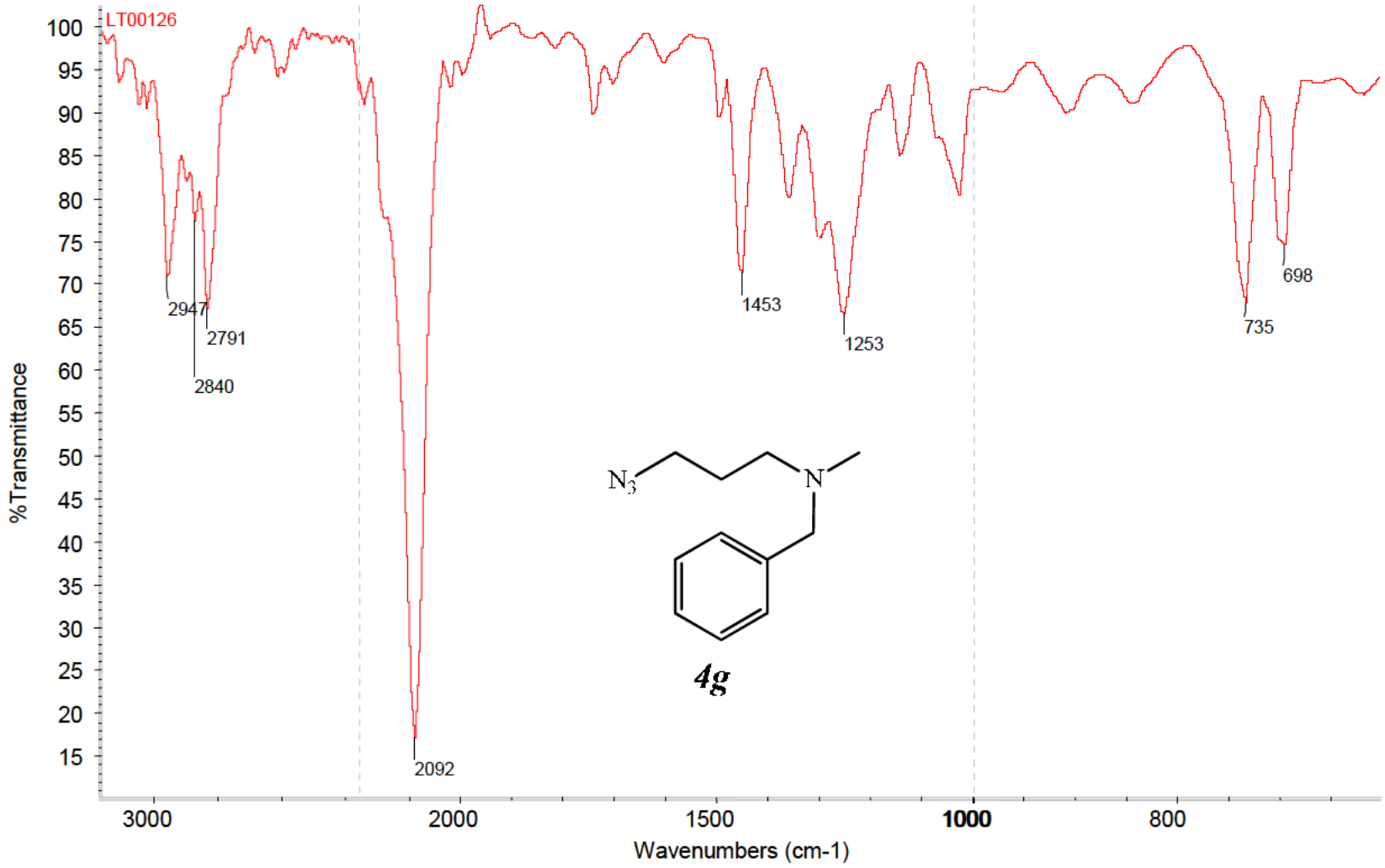
LT00126
%Transmittance
100
95
90
85
80
75
70
65
60
55
50
45
40
35
30
25
20
15
2947
2791
2840
2092
1453
1253
735
698
3000
2000
1500
1000
800
Wavenumbers (cm-1)
N3
N

4g

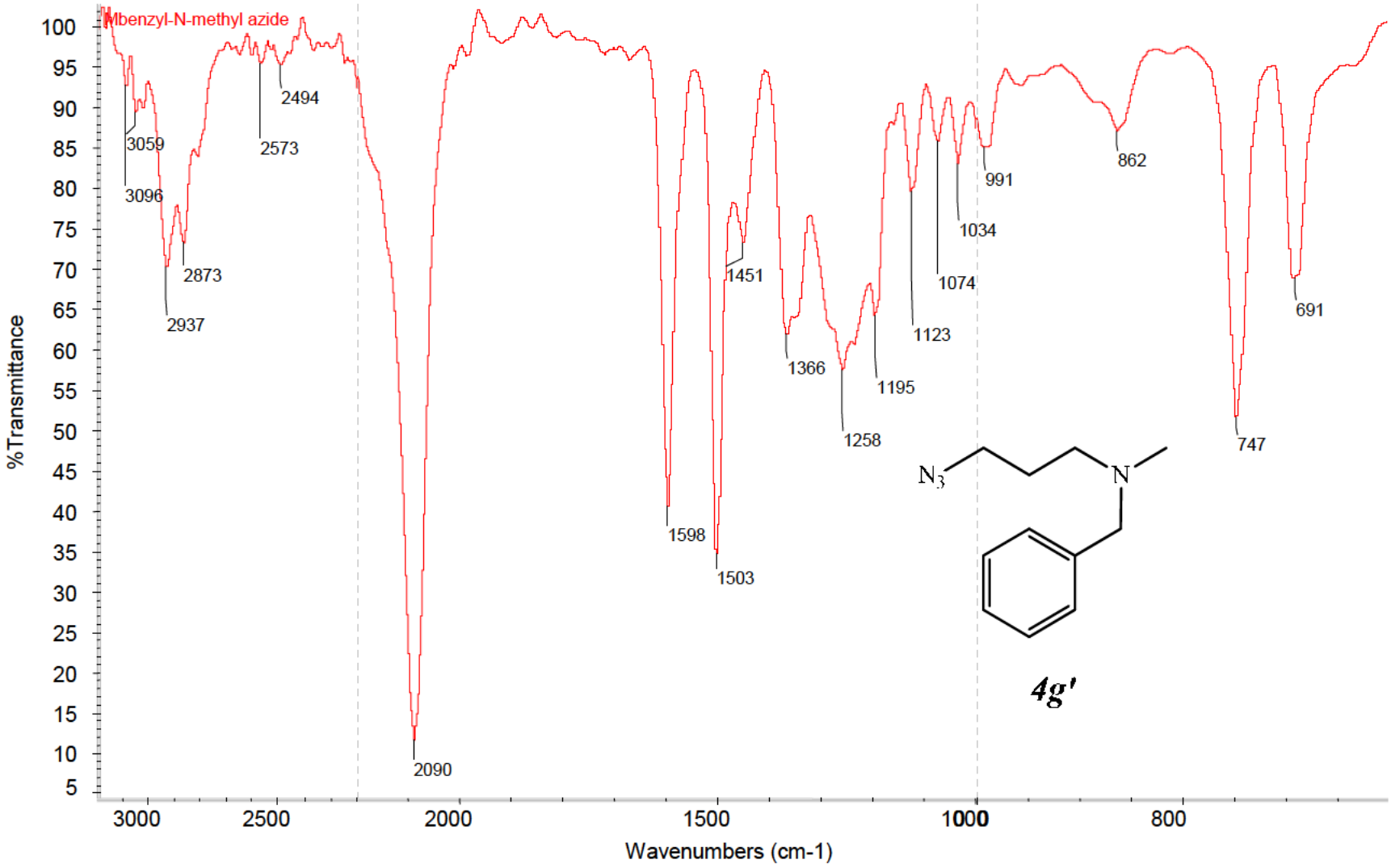
Mbenzyl-N-methyl azide
%Transmittance
Wavenumbers (cm-1)
3096
3059
2937
2873
2573
2494
2090
1598
1503
1451
1366
1258
1195
1123
1074
1034
991
862
747
691
N3
N
4g'

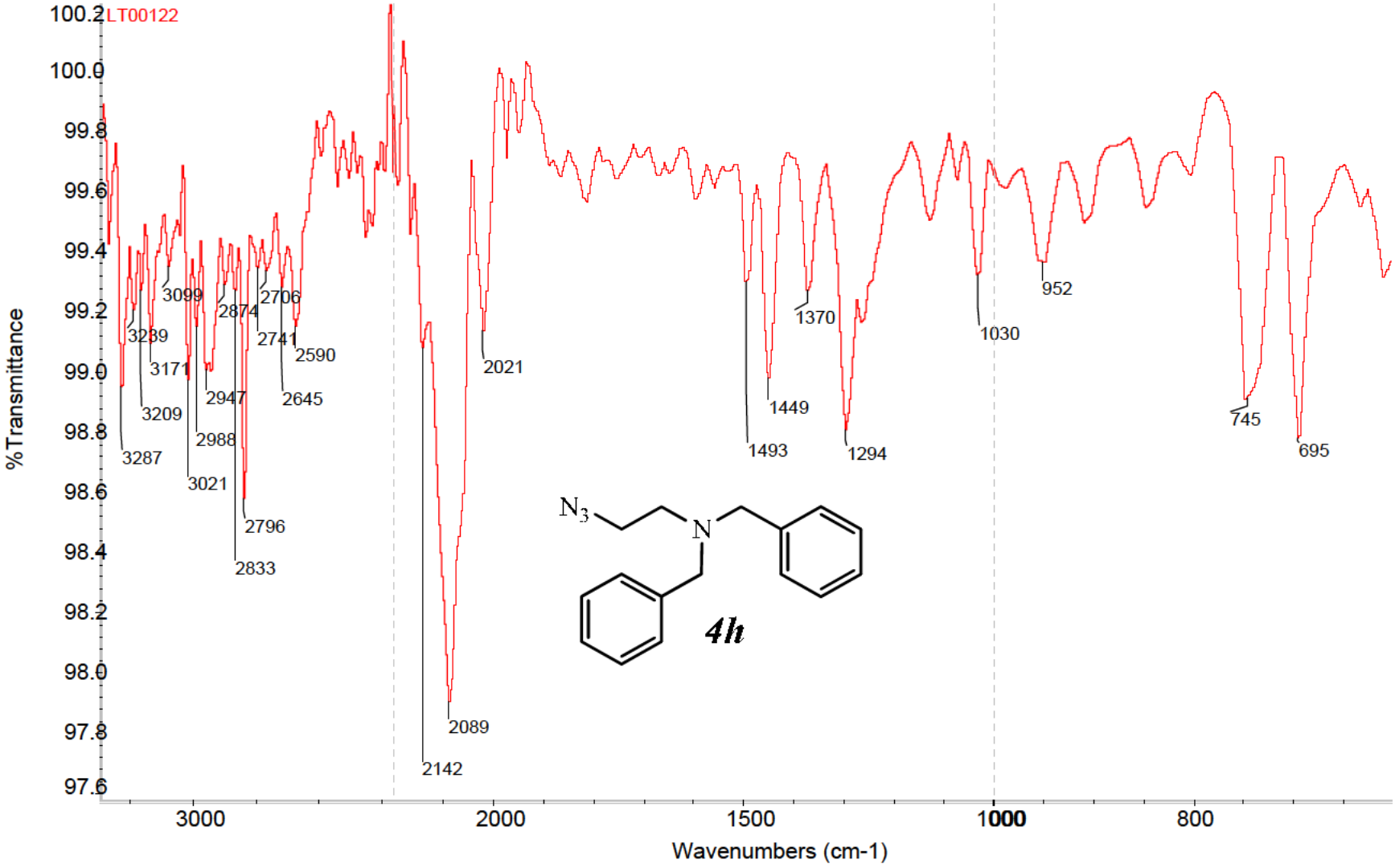
LT00122
100.2
100.0
99.8
99.6
99.4
99.2
99.0
98.8
98.6
98.4
98.2
98.0
97.8
97.6
%Transmittance
3287
3239
3209
3171
3099
3021
2988
2947
2874
2833
2796
2741
2706
2645
2590
2142
2089
2021
1493
1449
1370
1294
1030
952
745
695
3000
2000
1500
1000
800
Wavenumbers (cm-1)
N3
N
4h

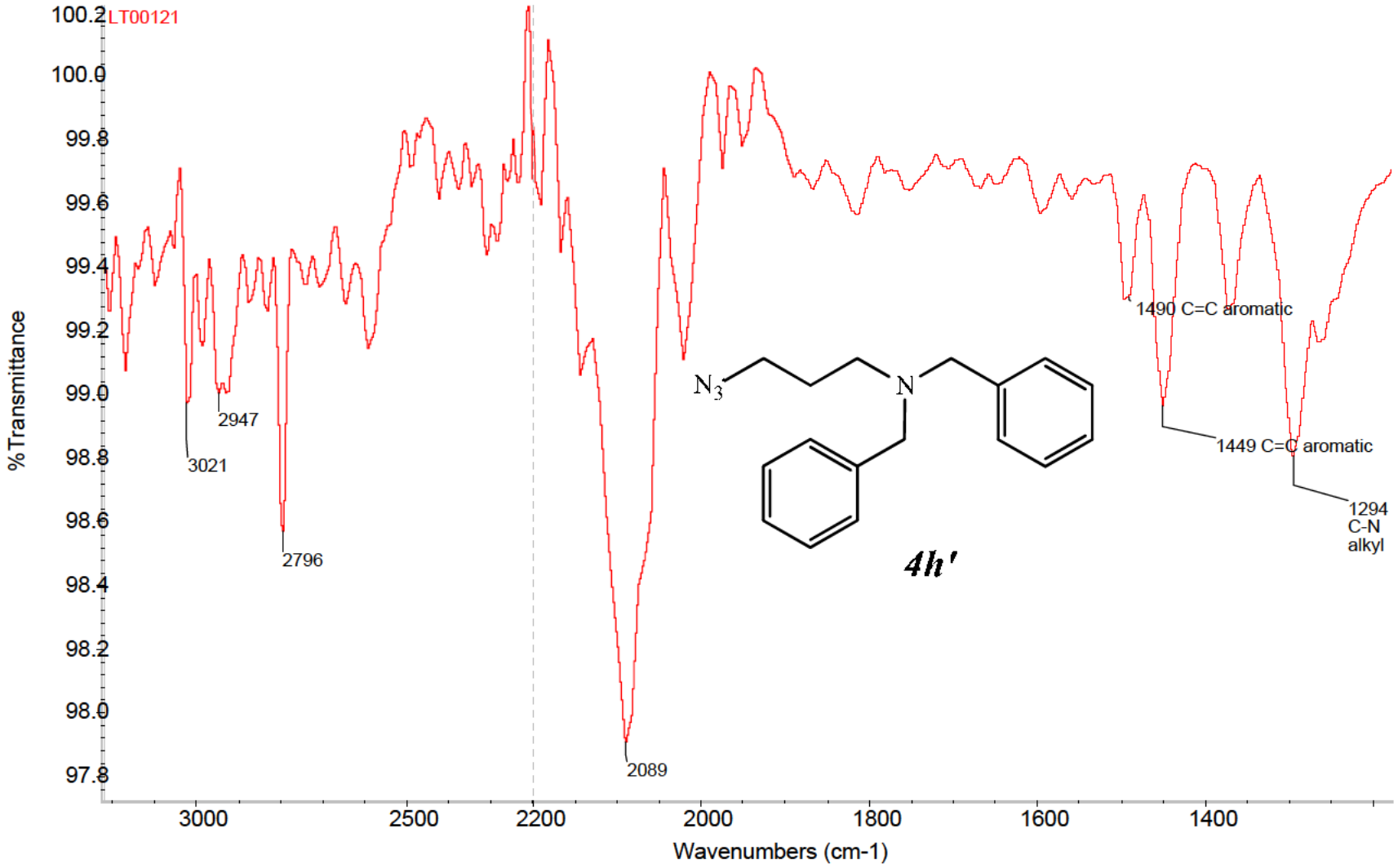
LT00121
100.2
100.0
99.8
99.6
99.4
99.2
99.0
98.8
98.6
98.4
98.2
98.0
97.8
%Transmittance
3021
2947
2796
2089
1490 C=C aromatic
1449 C=C aromatic
1294
C-N
alkyl
N3
N
4h'
3000
2500
2200
2000
1800
1600
1400
Wavenumbers (cm-1)

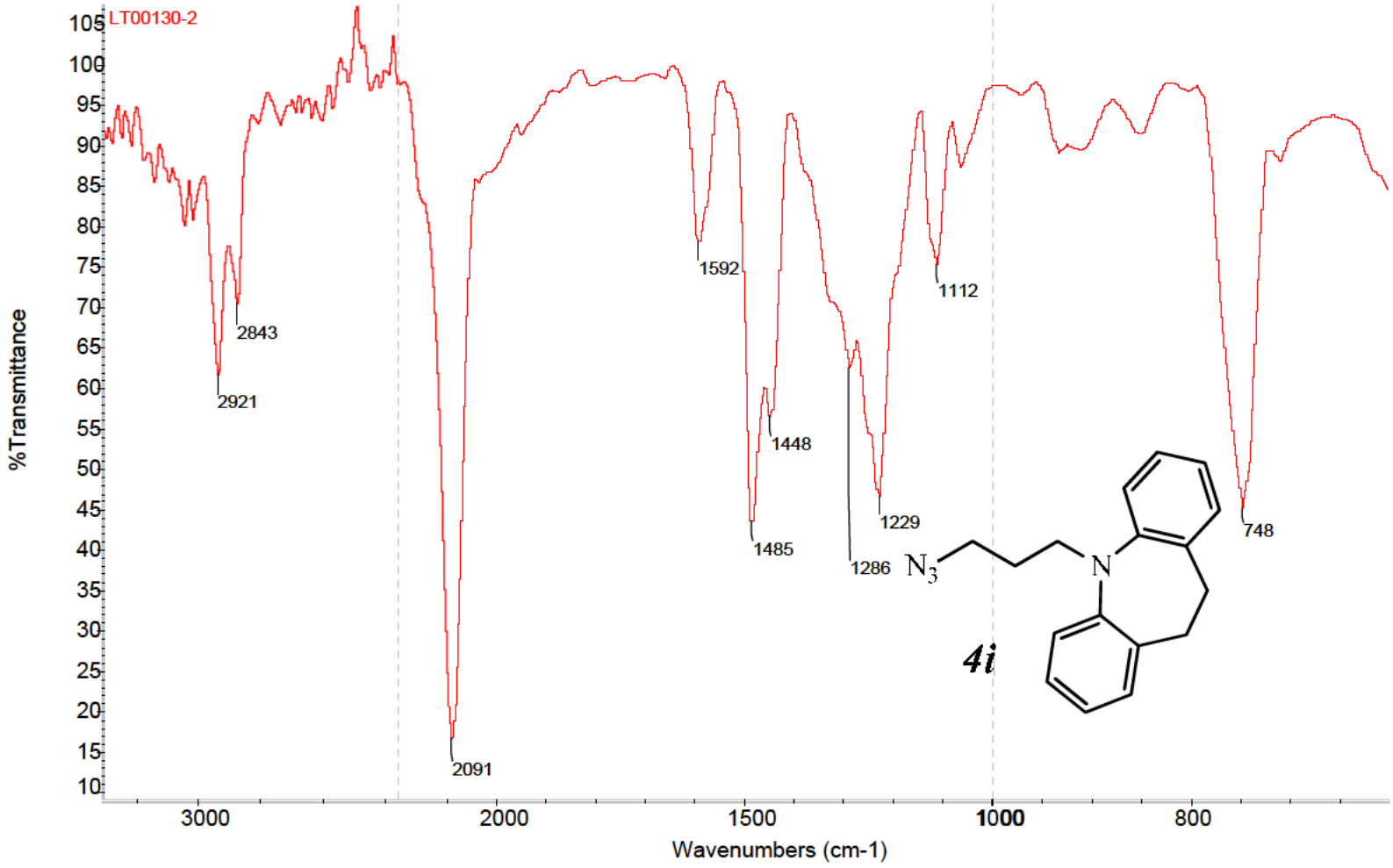
LT00130-2
%Transmittance
Wavenumbers (cm-1)
2921
2843
2091
1592
1485
1448
1286
1229
1112
748
N3
N
4i

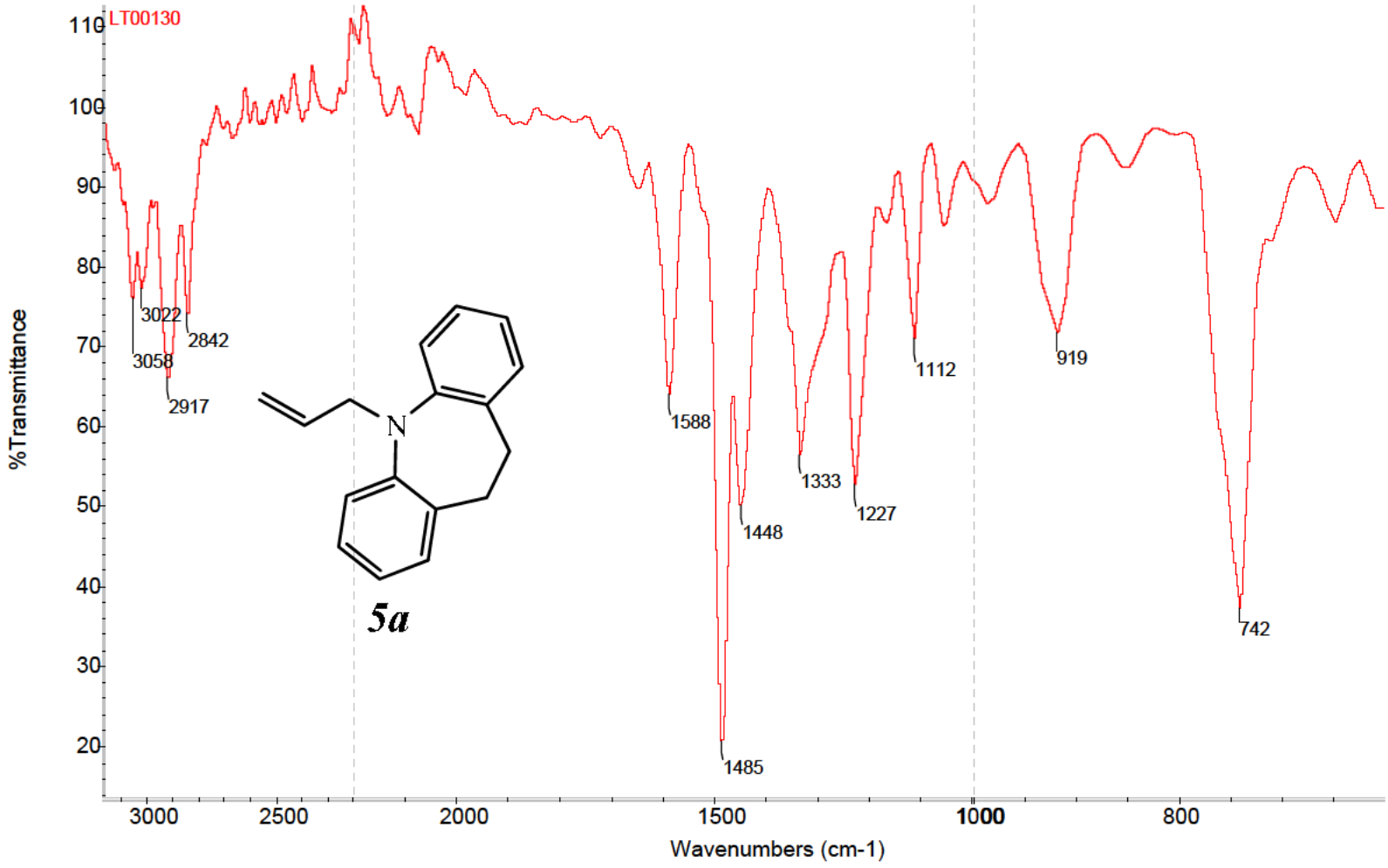
LT00130
%Transmittance
110
100
90
80
70
60
50
40
30
20
3058
3022
2917
2842
1588
1485
1448
1333
1227
1112
919
742
N
5a
3000
2500
2000
1500
1000
800
Wavenumbers (cm-1)

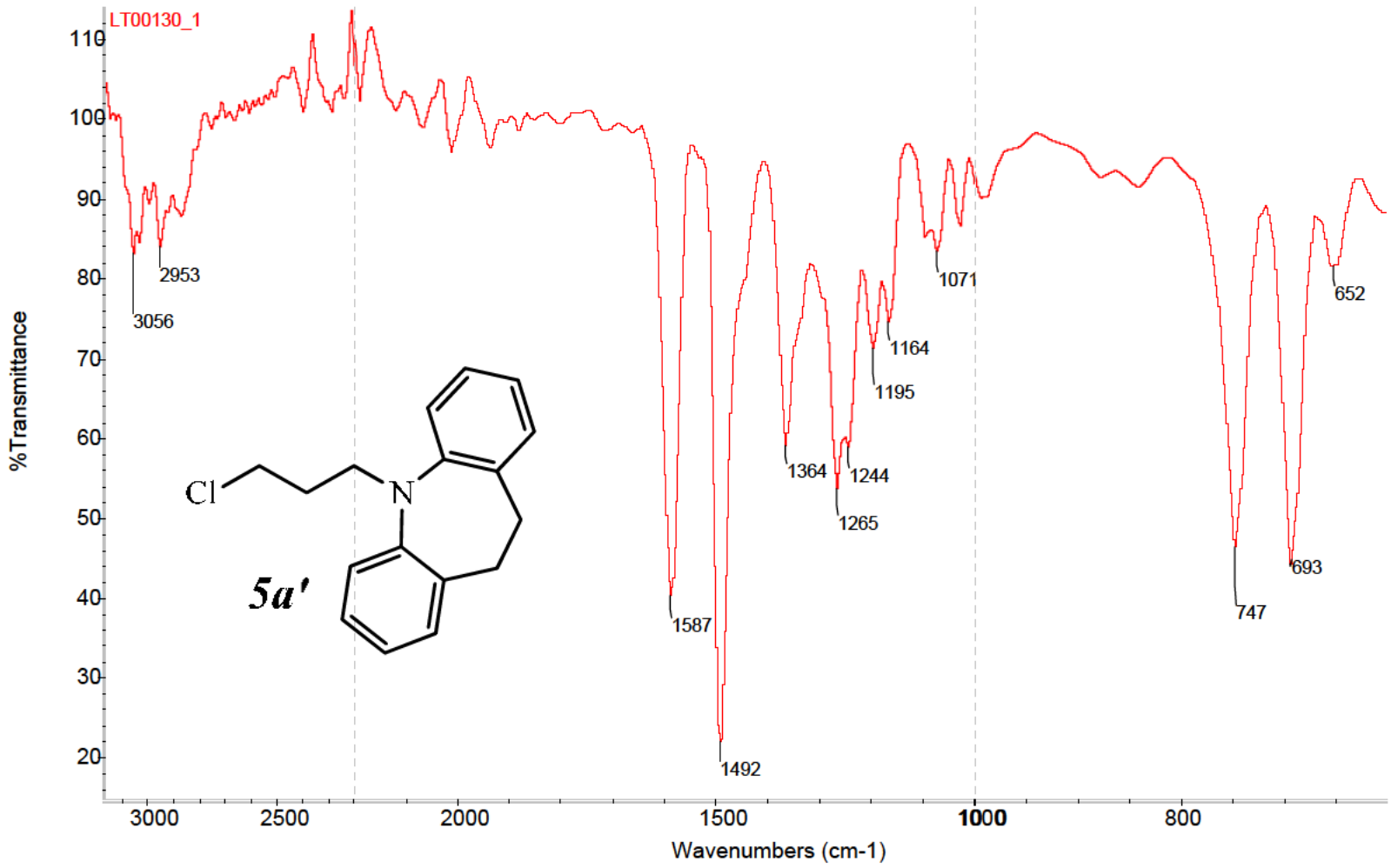
LT00130_1
%Transmittance
Wavenumbers (cm-1)
3056
2953
1587
1492
1364
1265
1244
1195
1164
1071
747
693
652
Cl
N
5a'

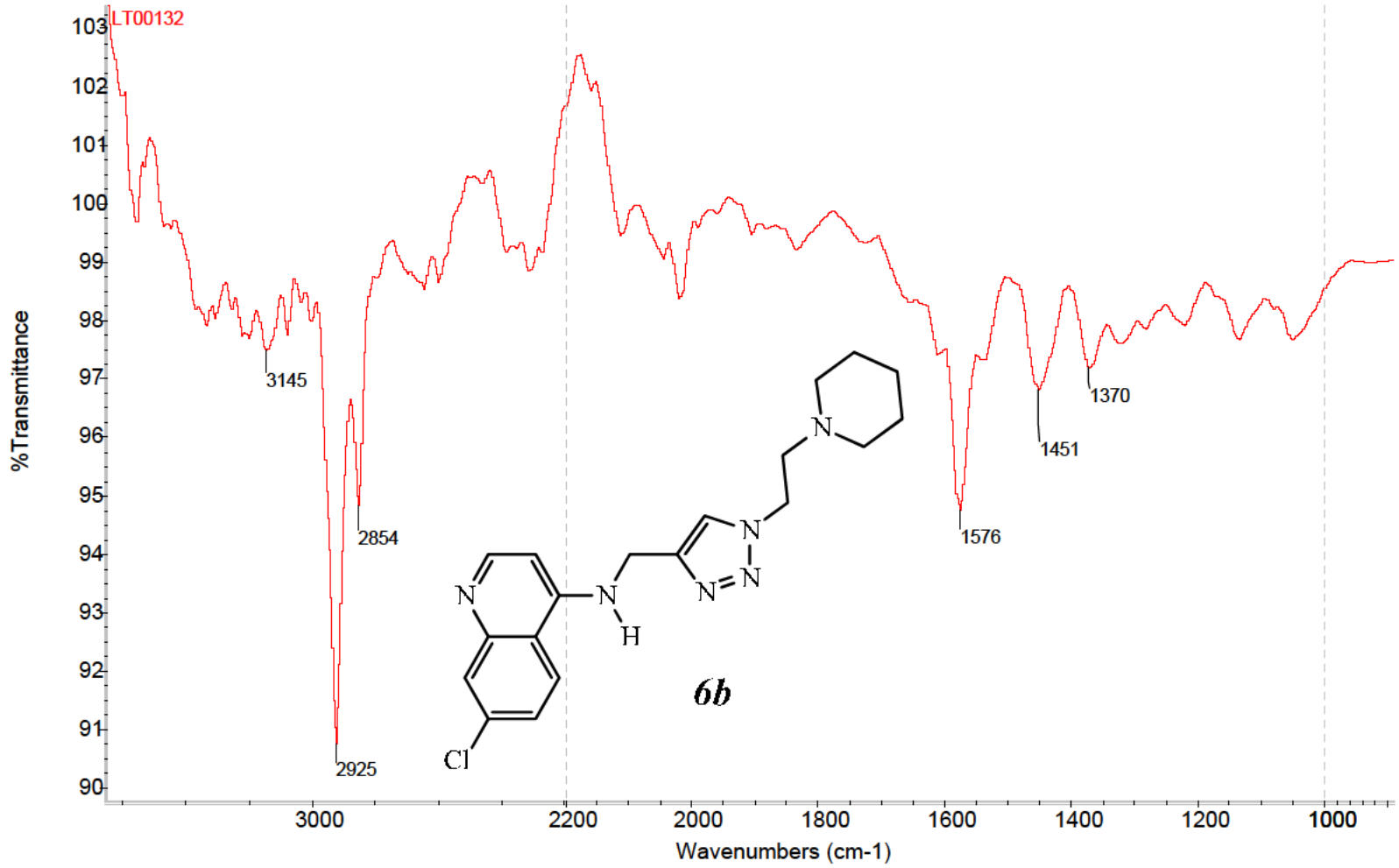
LT00132
%Transmittance
Wavenumbers (cm-1)
3145
2925
2854
1576
1451
1370
6b

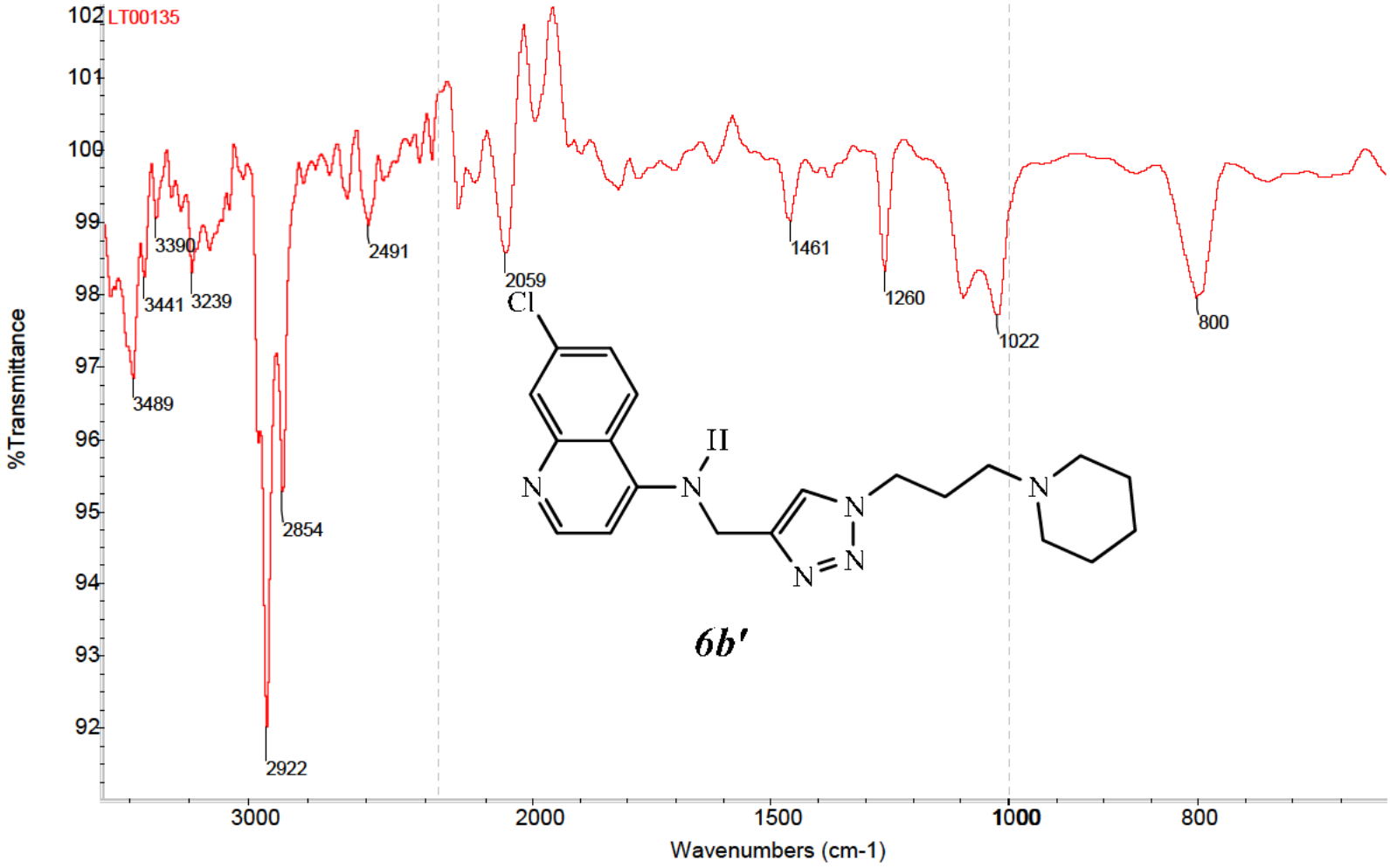
LT00135
%Transmittance
Wavenumbers (cm-1)
3489
3441
3390
3239
2922
2854
2491
2059
1461
1260
1022
800
Cl
N
II
N
N
N
N
N
6b'

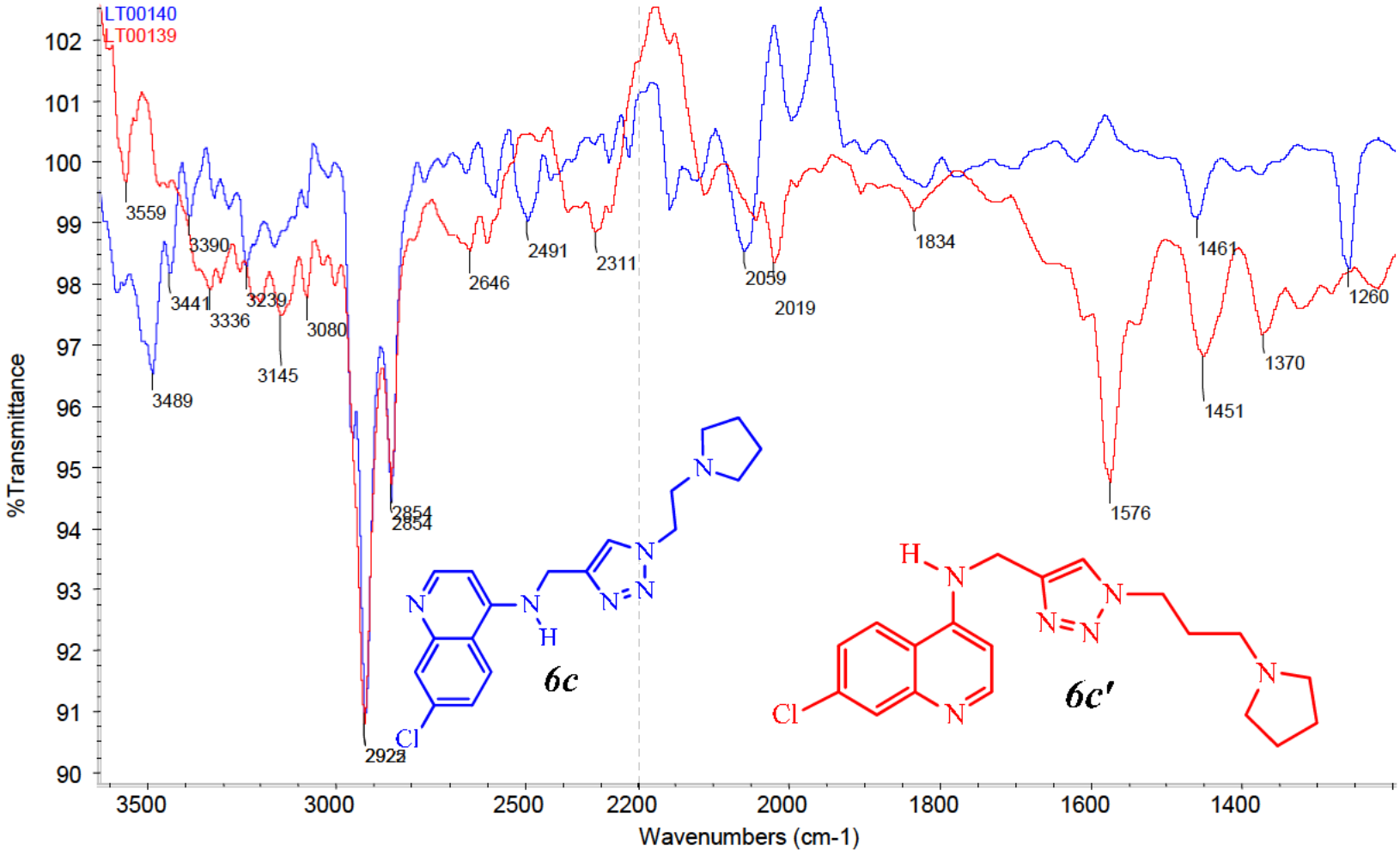
LT00140
LT00139
%Transmittance
Wavenumbers (cm-1)
3559
3441
3390
3336
3239
3145
3080
3489
2923
2854
2854
2646
2491
2311
2059
2019
1834
1576
1461
1451
1370
1260
6c
6c'

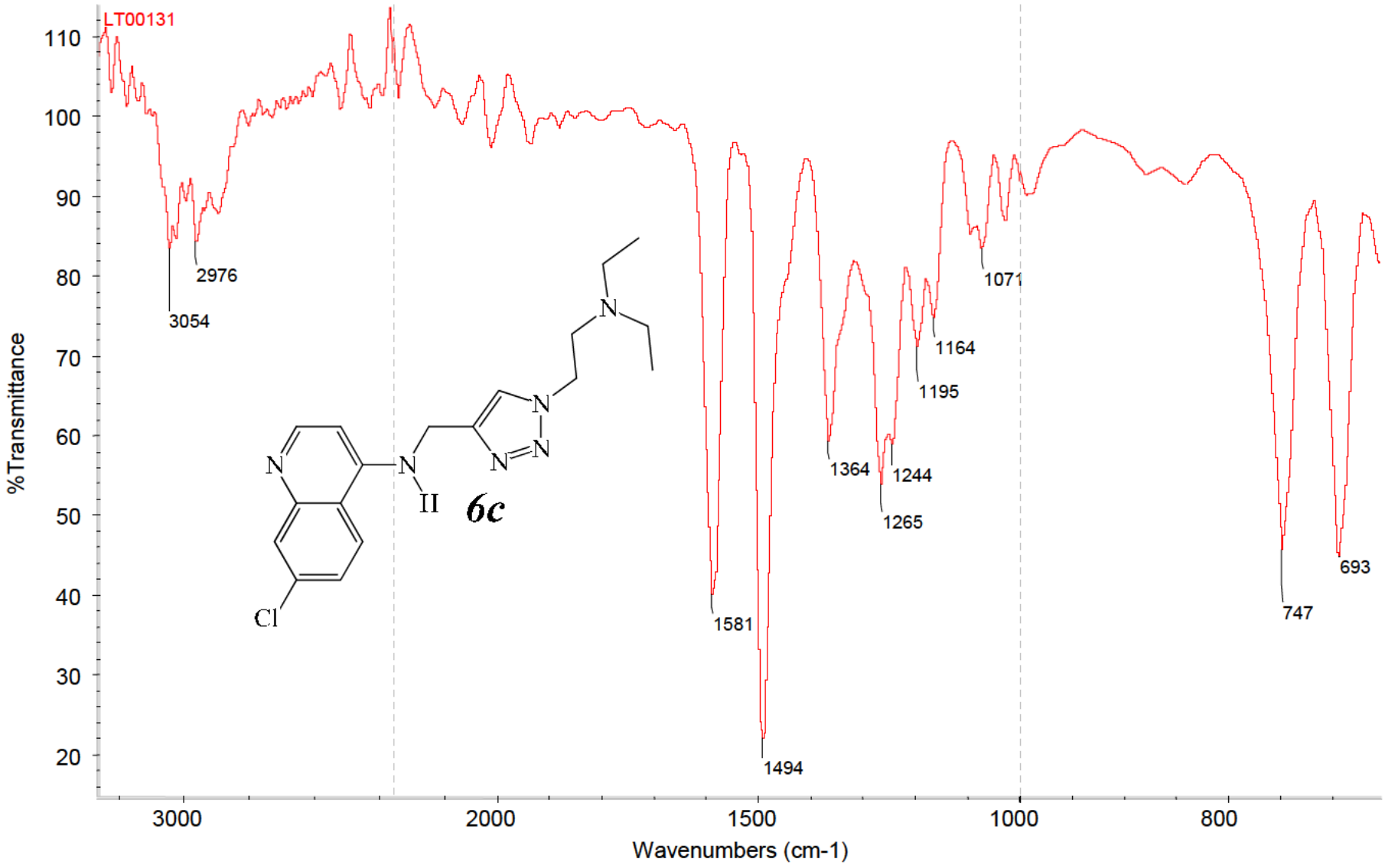
LT00131
%Transmittance
Wavenumbers (cm-1)
3000
2000
1500
1000
800
110
100
90
80
70
60
50
40
30
20
3054
2976
1581
1494
1364
1265
1244
1195
1164
1071
747
693
Cl
6c

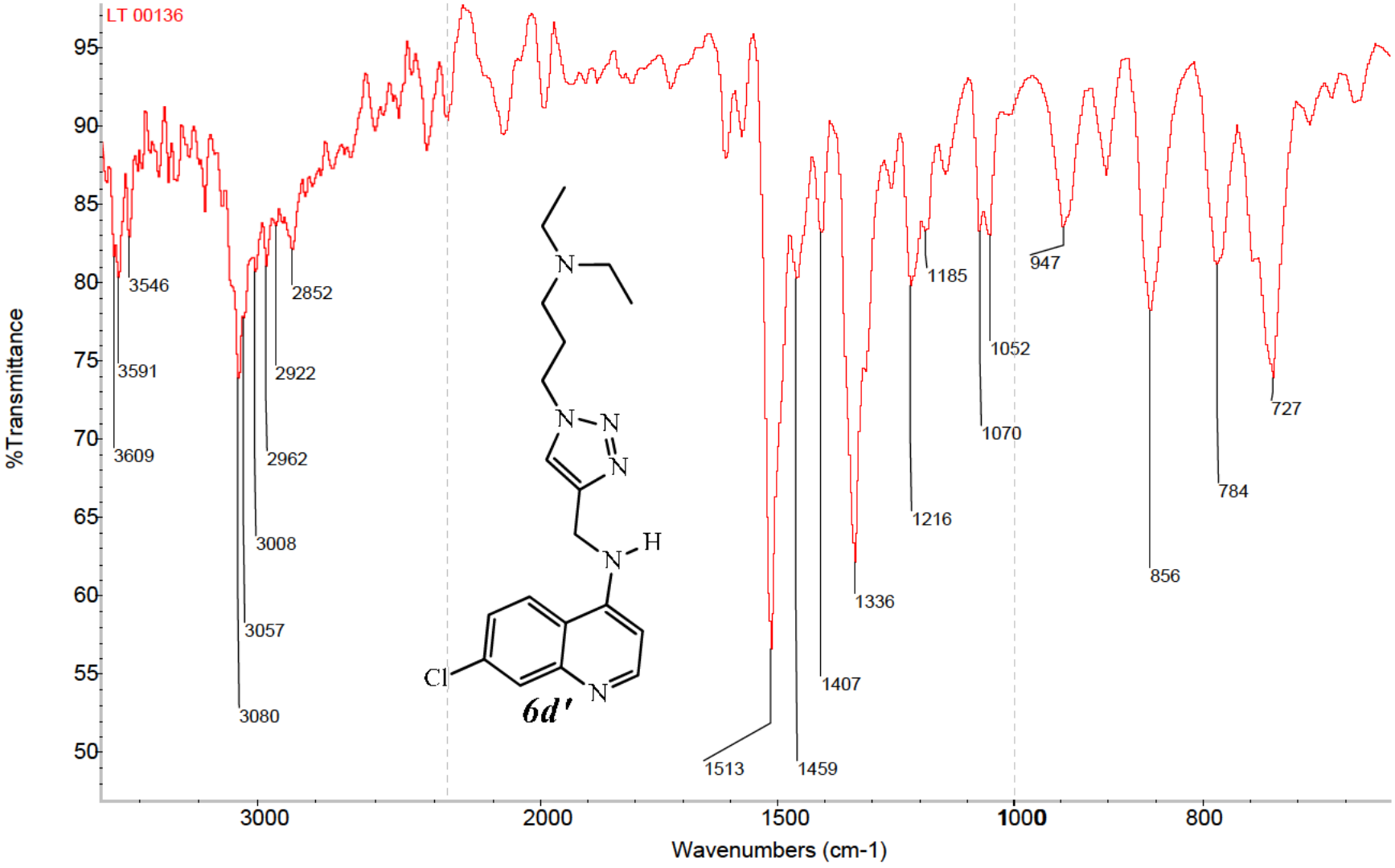
LT 00136
%Transmittance
Wavenumbers (cm-1)
95
90
85
80
75
70
65
60
55
50
3000
2000
1500
1000
800
3609
3591
3546
3080
3057
3008
2962
2922
2852
1513
1459
1407
1336
1216
1185
1070
1052
947
856
784
727
Cl
N
H
6d'

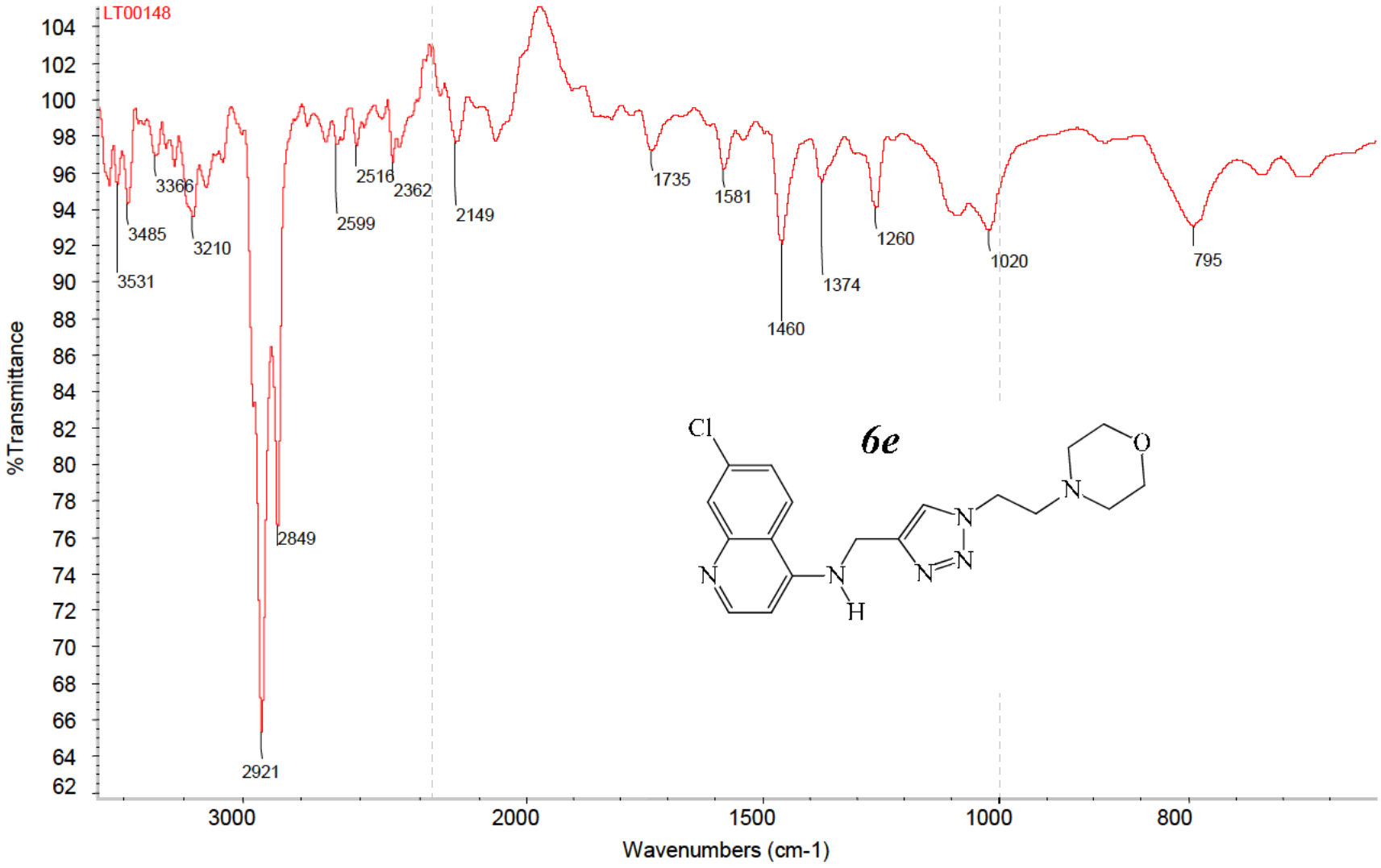
LT00148
%Transmittance
Wavenumbers (cm-1)
3531
3485
3366
3210
2921
2849
2599
2516
2362
2149
1735
1581
1460
1374
1260
1020
795
6e
Cl
N
N
H
N
N
N
O

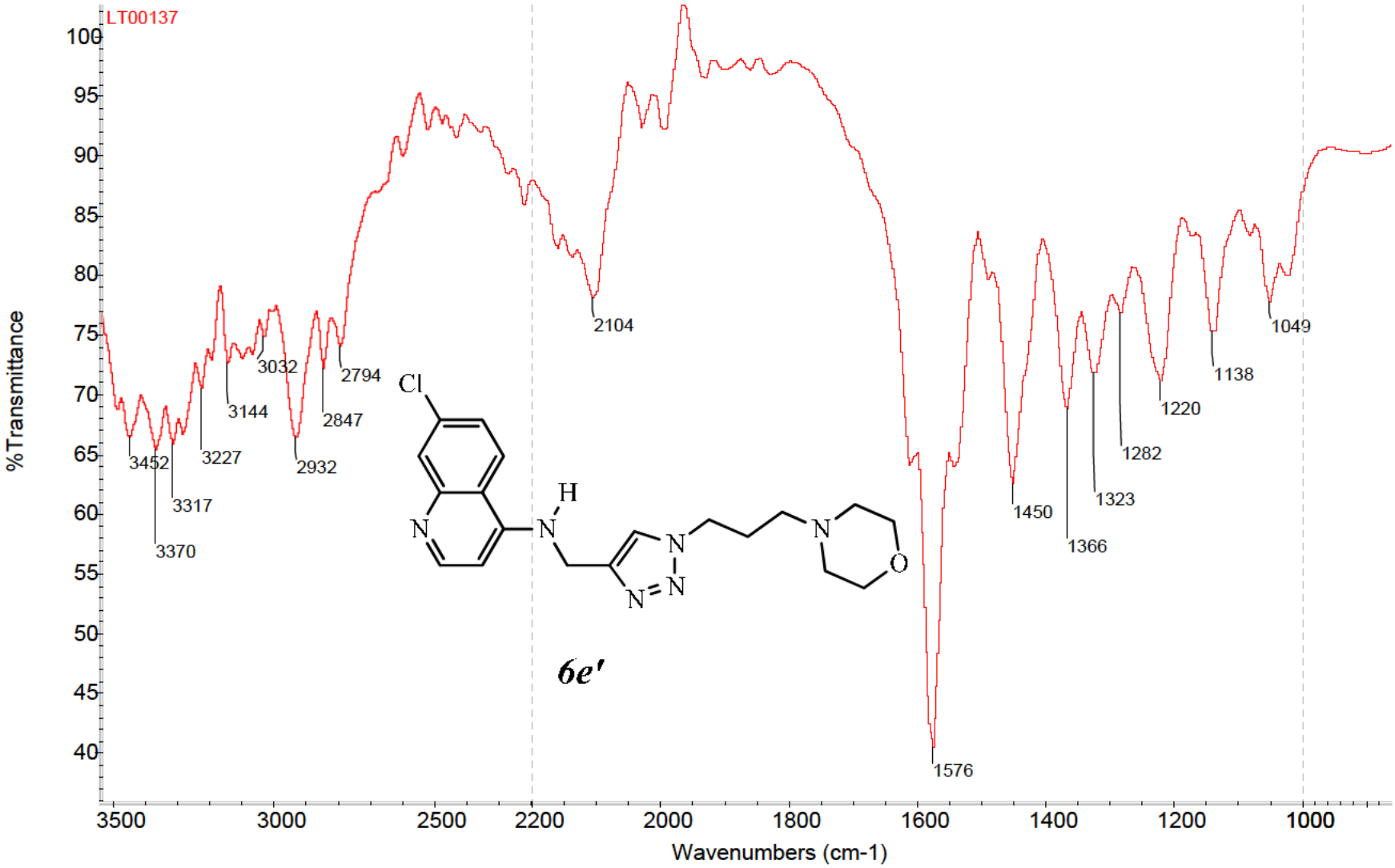
LT00137
%Transmittance
Wavenumbers (cm-1)
3452
3370
3317
3227
3144
3032
2932
2847
2794
2104
1576
1450
1366
1323
1282
1220
1138
1049
Cl
H
N
O
6e'

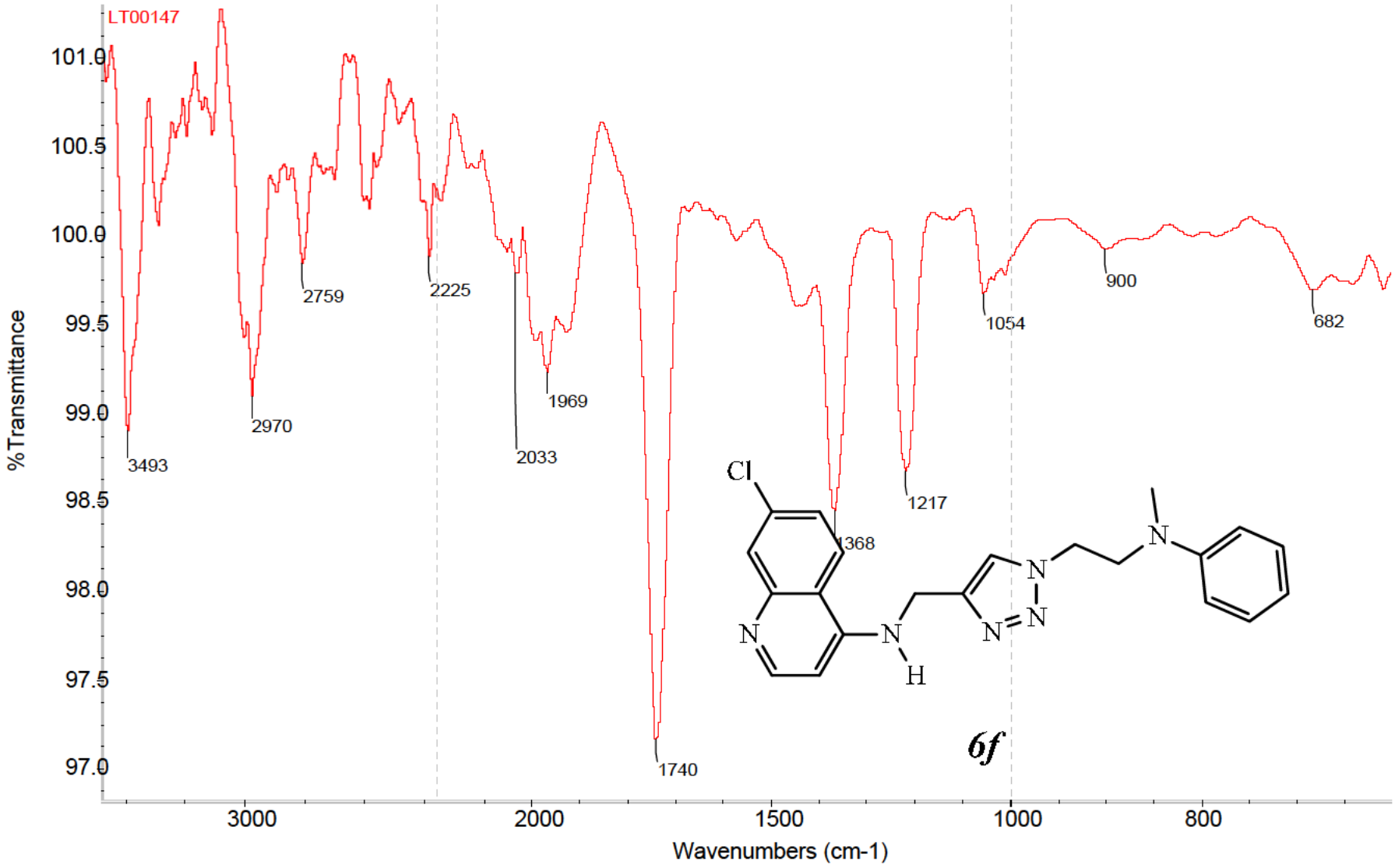
LT00147
%Transmittance
Wavenumbers (cm-1)
3493
2970
2759
2225
2033
1969
1740
1368
1217
1054
900
682
Cl
N
H
6f

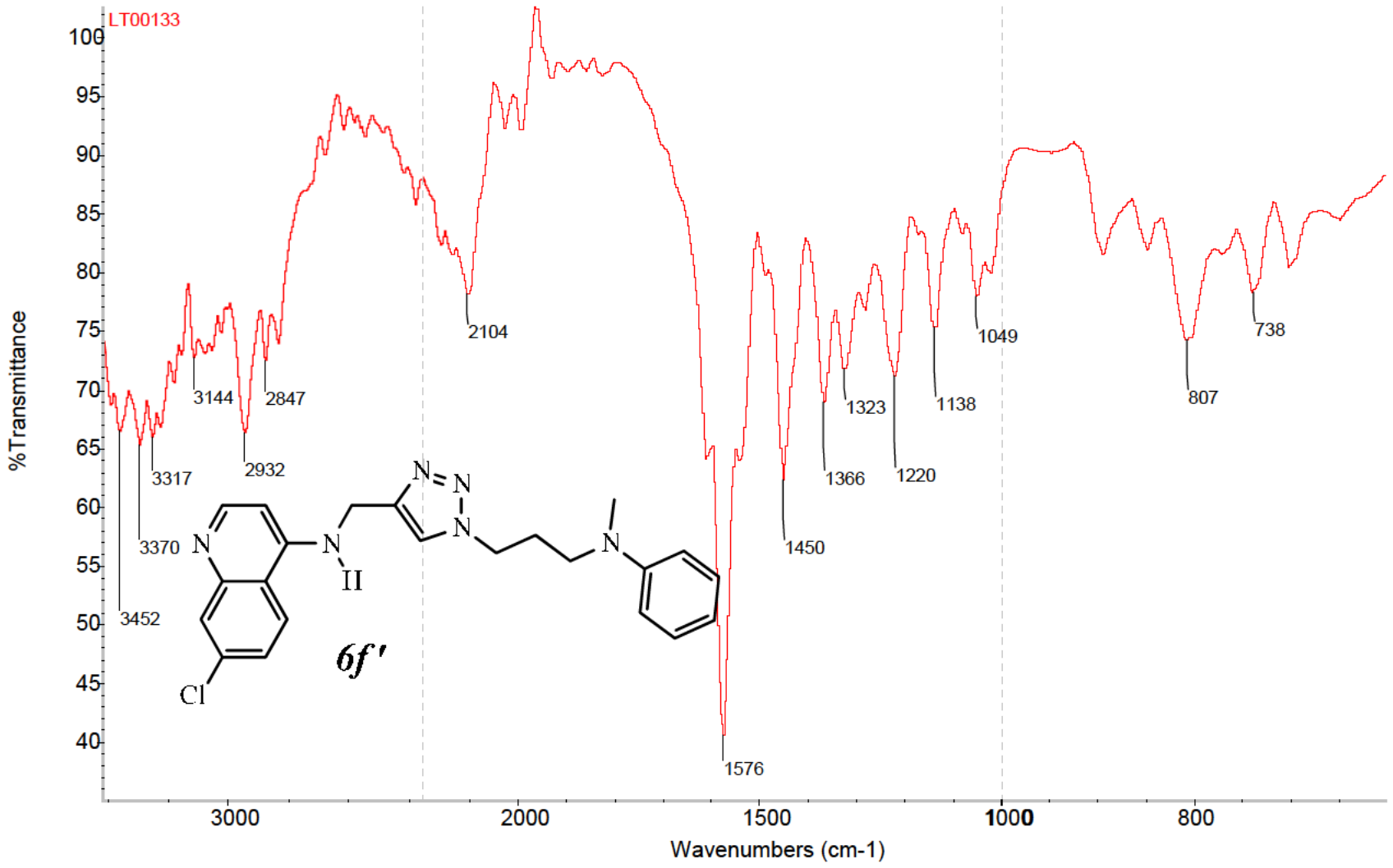
LT00133
%Transmittance
Wavenumbers (cm-1)
3452
3370
3317
3144
2932
2847
2104
1576
1450
1366
1323
1220
1138
1049
807
738
6f'

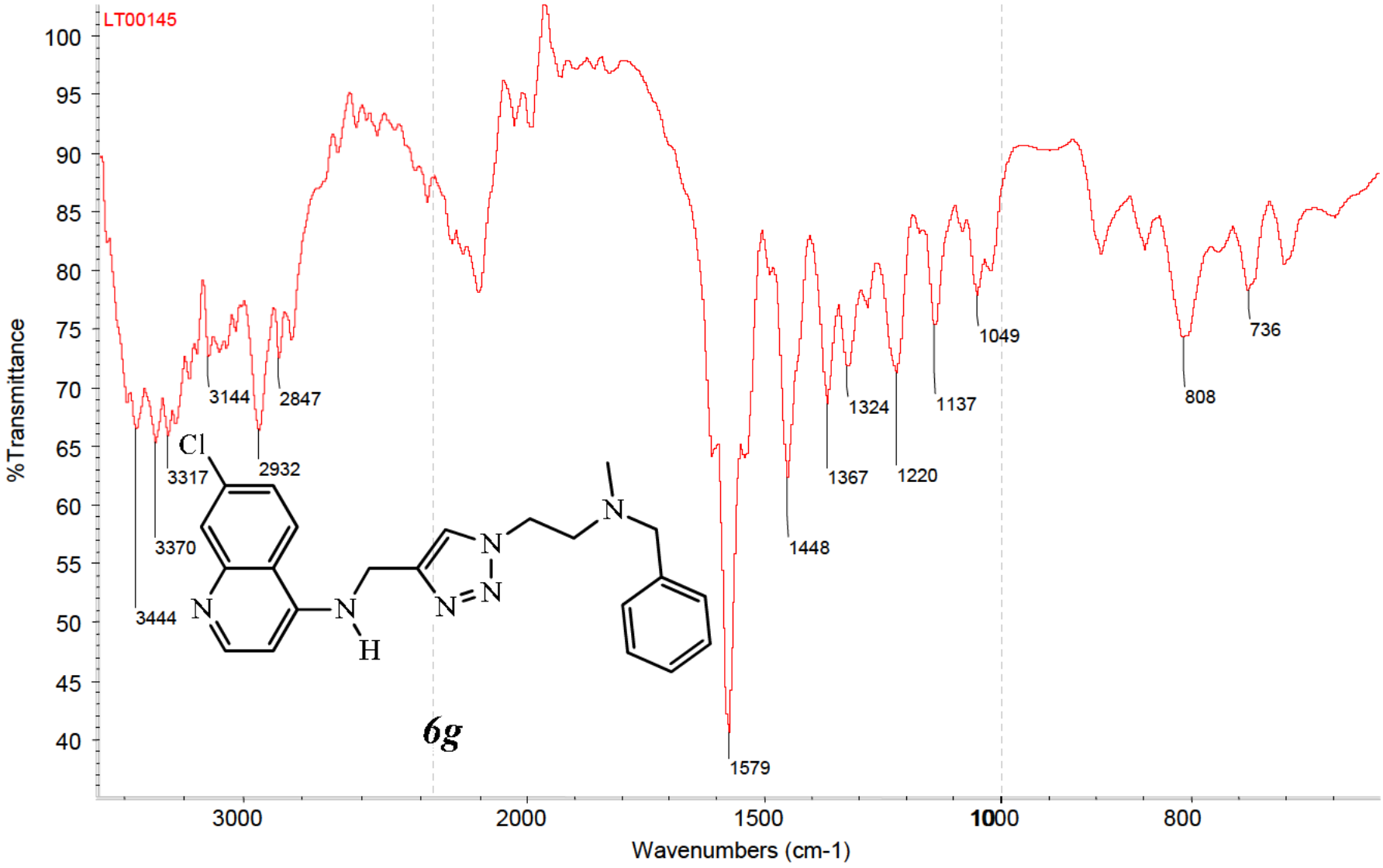
LT00145
%Transmittance
Wavenumbers (cm-1)
3000
2000
1500
1000
800
100
95
90
85
80
75
70
65
60
55
50
45
40
3444
3370
3317
3144
2932
2847
1579
1448
1367
1324
1220
1137
1049
808
736
Cl
N
H
6g

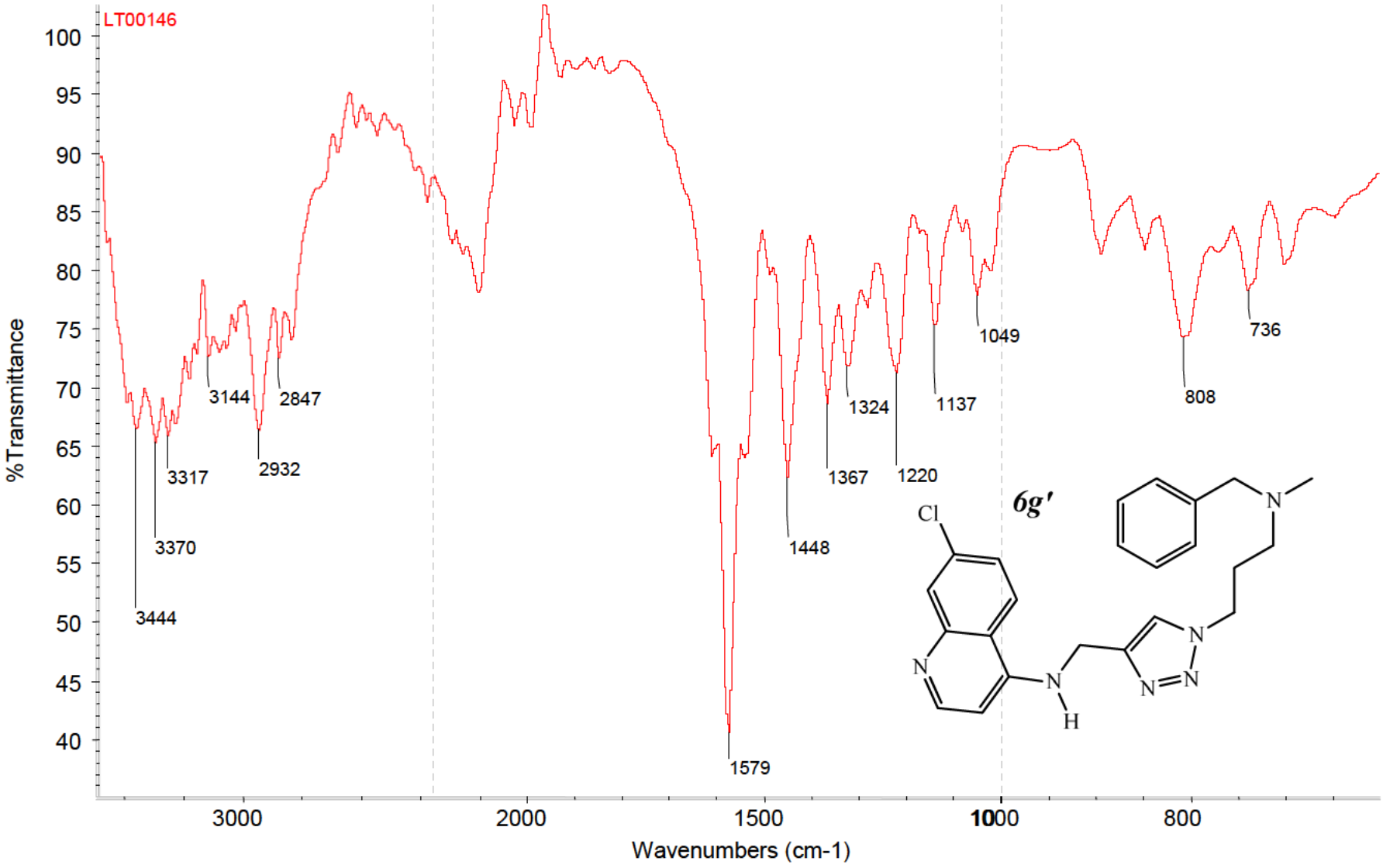
LT00146
%Transmittance
Wavenumbers (cm-1)
3444
3370
3317
3144
2932
2847
1579
1448
1367
1324
1220
1137
1049
808
736
6g'
Cl
N
N
N
N
N
H

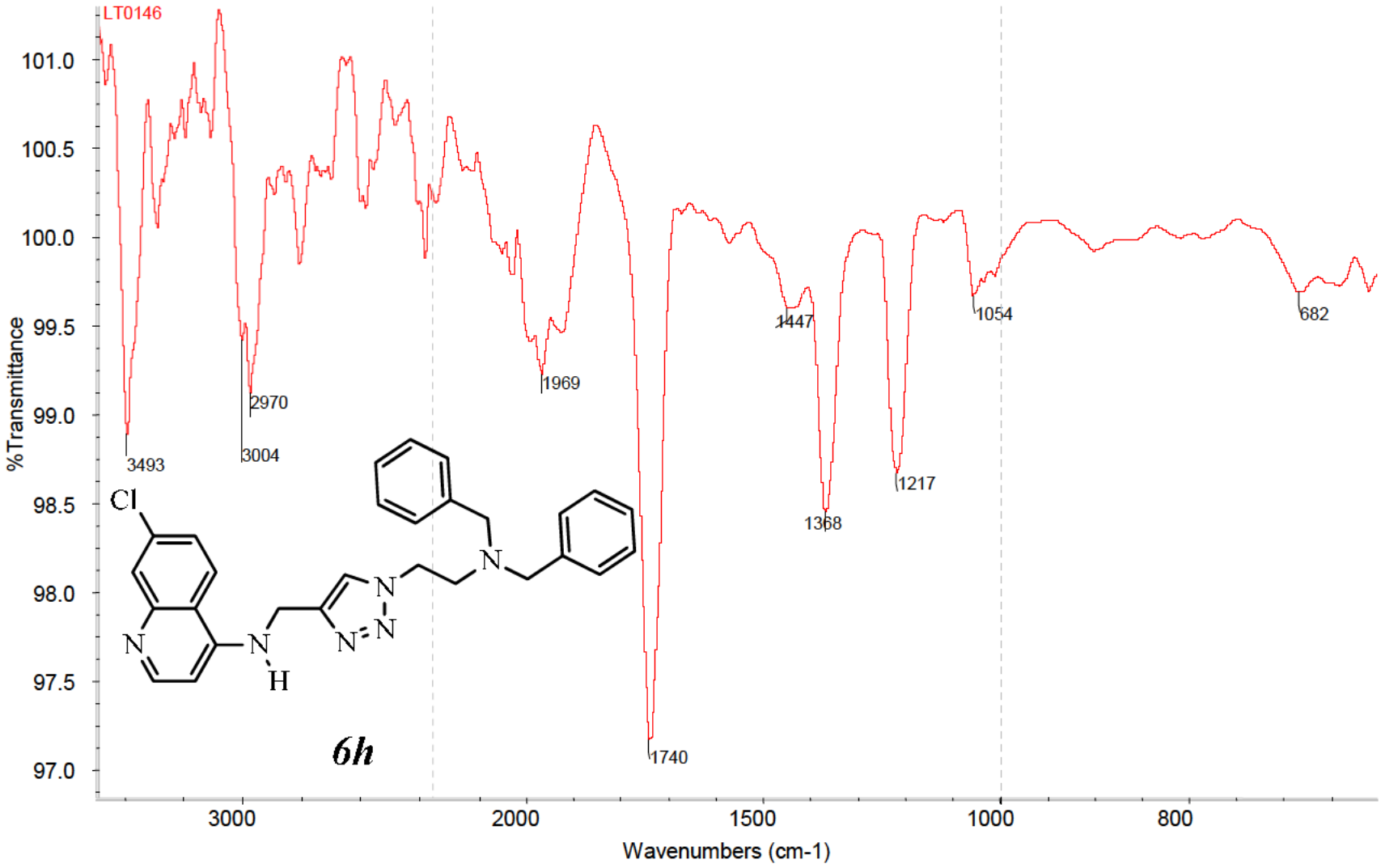
LT0146
%Transmittance
101.0
100.5
100.0
99.5
99.0
98.5
98.0
97.5
97.0
3493
2970
3004
1969
1740
1447
1368
1217
1054
682
Cl
N
N
H
N
N
N
N
N
6h
3000
2000
1500
1000
800
Wavenumbers (cm-1)

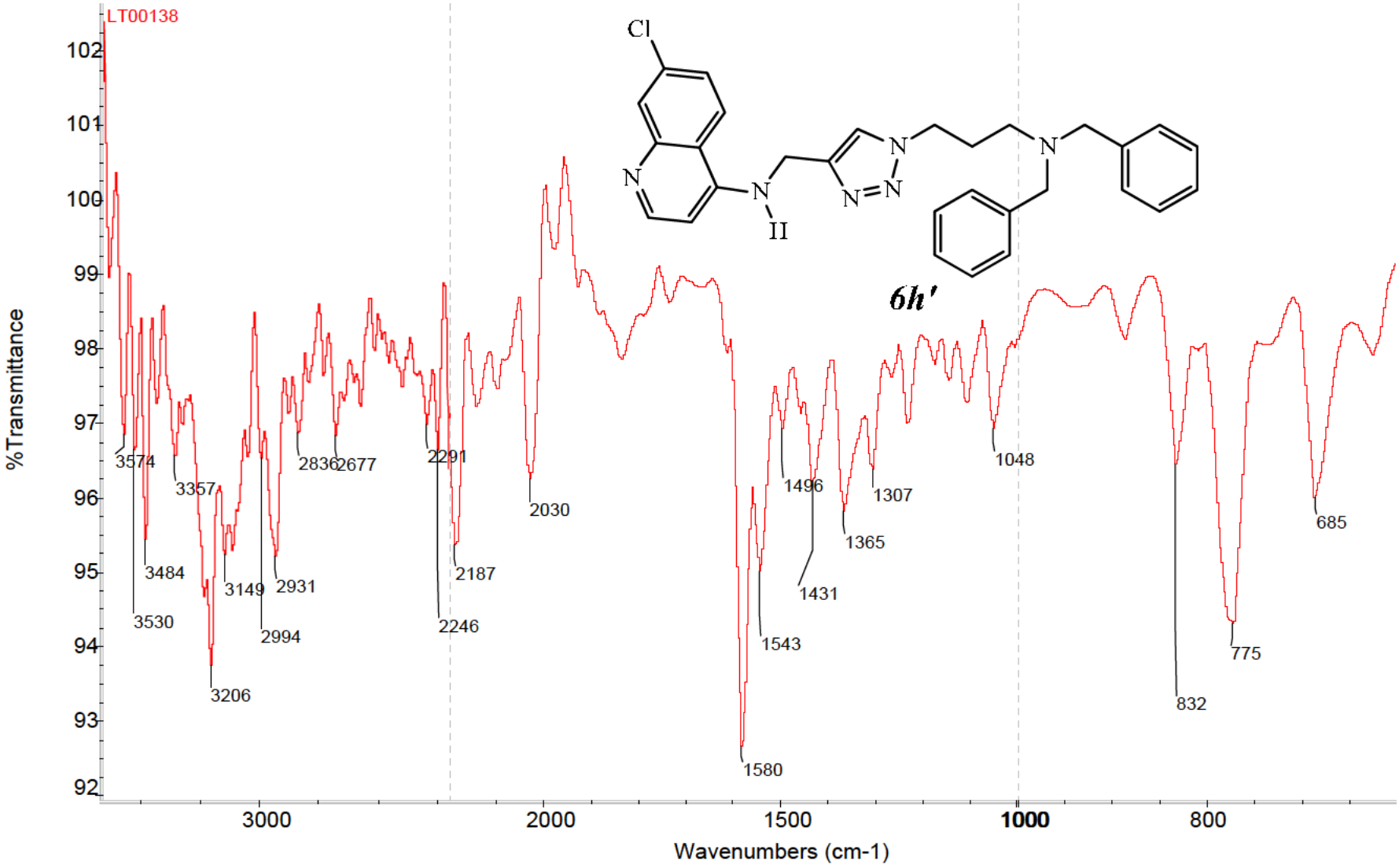
LT00138
Cl
N
N
II
N
N=N
N
N
6h'
%Transmittance
102
101
100
99
98
97
96
95
94
93
92
3574
3530
3484
3357
3206
3149
2994
2931
2836
2677
2291
2246
2187
2030
1580
1543
1496
1431
1365
1307
1048
832
775
685
3000
2000
1500
1000
800
Wavenumbers (cm-1)

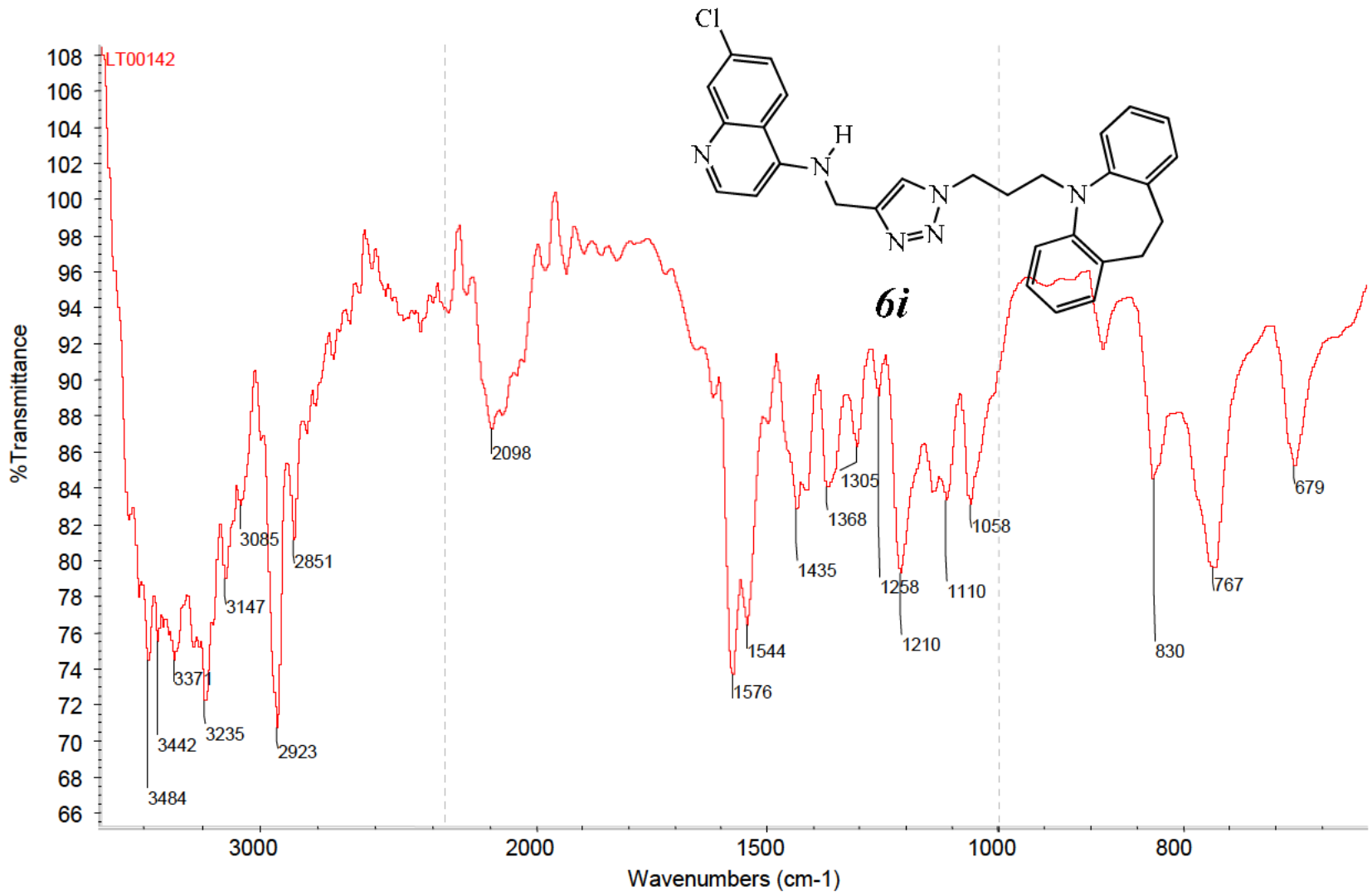
LT00142
%Transmittance
Wavenumbers (cm-1)
3484
3442
3371
3235
3147
3085
2923
2851
2098
1576
1544
1435
1368
1305
1258
1210
1110
1058
830
767
679
Cl
N
H
N
N
N
N
N
6i